Facultad de Farmacia
Departamento de Farmacia y Tecnología Farmacéutica
Programa de doctorado en Medicina Clínica y Salud Pública

NANOCOMPOSITES DE QUITOSANO Y MONTMORILLONITA COMO PROMOTORES DE LA PERMEABILIDAD CELULAR DE OXITETRACICLINA

Chitosan/Montmorillonite nanocomposites as enhancers of Oxytetracycline cellular permeability

Memoria de Tesis presentada por la Licenciada en Farmacia Doña Inmaculada Salcedo Bellido para optar al grado de Doctor por la Universidad de Granada, con mención de Doctorado Internacional.

Esta Tesis Doctoral ha sido dirigida por los Doctores Carola Aguzzi, Pilar Cerezo González y César Viseras Iborra, Profesores del Departamento de Farmacia y Tecnología Farmacéutica de la Universidad de Granada.

Granada, Junio 2013

VºBº de los Directores

Carola Aguzzi Pilar Cerezo González César Viseras Iborra

La Doctoranda

Inmaculada Salcedo Bellido

Editor: Editorial de la Universidad de Granada
Autor: Inmaculada Salcedo Bellido
D.L.: GR 356-2014
ISBN: 978-84-9028-761-3

El doctorando INMACULADA SALCEDO BELLIDO y los directores de la tesis CAROLA AGUZZI, PILAR CEREZO GONZÁLEZ, CÉSAR VISERAS IBORRA Garantizamos, al firmar esta tesis doctoral, que el trabajo ha sido realizado por el doctorando bajo la dirección de los directores de la tesis y hasta donde nuestro conocimiento alcanza, en la realización del trabajo, se han respetado los derechos de otros autores a ser citados, cuando se han utilizado sus resultados o publicaciones.

En GRANADA, 10 de JUNIO de 2013.

Director/es de la Tesis

Fdo.: CAROLA AGUZZI PILAR CEREZO GONZALEZ CESAR VISERAS IBORRA

Doctoranda

Fdo..: INMACULADA SALCEDO BELLIDO

La presente Tesis Doctoral ha sido financiada por el proyecto del Plan Nacional de I+D+i CGL2010-16369 y por el Grupo de Investigación CTS-946 de la Junta de Andalucía. La doctoranda ha disfrutado de una beca de Formación de Personal Docente e Investigador de la Junta de Andalucía. El trabajo ha sido desarrollado en los laboratorios del Departamento de Farmacia y Tecnología Farmacéutica de la Universidad de Granada, del Instituto Andaluz de Ciencias de la Tierra (CSIC-Universidad de Granada) y del Dipartimento di Scienze del Fármaco de la Universitá degli Studi di Pavia (Italia).

Índice

ABSTRACT

Abstract

This thesis has been carried out in the Andalusian research group CTS-946 "Pharmaceutical development of natural resources". Pharmaceutical development of new materials based on nanoscale interactions between natural occurring excipients is one of the research lines of the group. This is the research area in which this thesis work was focused, and in particular, in the preparation, and characterization of chitosan/montmorillonite nanocomposites to be used as nanocarriers of oxytetracycline. With this aim, it was firstly reviewed the possibility of obtaining hybrid nanostructures materials with the selected polysaccharide and phyllosilicate and their expected biopharmaceutical and technological features. Then, we proceed to prepare nanocomposites by solid-liquid contact of the components and to evaluate the resulting structure and possible interaction mechanism. The obtained results showed that chitosan was effectively retained by montmorillonite particles through cation exchange. The new material showed good biocompatibility in the range 5–500 μg/ml, being also able to effectively stimulate cell proliferation over Caco-2 cell cultures. The nanocomposite also possessed mucoadhesive properties and low solubility in acidic environment compared to chitosan alone. These properties led to consider the nanocomposite as a functional excipient able to be coupled with drugs with limited bioavailability due to poor adhesion and deficient transport across the gastrointestinal tract. Oxytetracycline was selected as model drug to evaluate this possibility. The drug was loaded into the nanocomposite and the resulting structure characterized by means of X-Ray diffraction, thermal analysis and FTIR. The results demonstrated that the antibiotic was effectively retained into the nanocomposite structure. The loaded nanocomposite maintained its biocompatibility and overcame the bioavailability uncertainties of the drug. The amount of drug permeated across the cellular substrates also increased as a result of the interaction with the nanocomposite. It can be concluded that by interaction between chitosan and montmorillonite it was possible to obtain a new material that could be use to improve the transport of oxytetracycline across gastrointestinal epithelial cells.

CAPÍTULO I.

Introducción

I.1- NANOTECNOLOGÍA Y NANOMEDICINA

La nanotecnología puede definirse como la investigación y desarrollo tecnológico a escala atómica, molecular o macromolecular (1-100 nm) con el objetivo de proporcionar un conocimiento fundamental de los fenómenos y materiales a esta escala (nanoescala) así como de crear y utilizar estructuras, dispositivos y sistemas con propiedades y funcionalidades novedosas que aparecen asociadas a estos tamaños. La nanomedicina es una rama de la nanotecnología centrada en las aplicaciones en salud, incluyendo nanodiagnóstico, nanoterapéutica y nanomateriales para aplicaciones farmacéuticas (NIH, 2006). Los sistemas nanotecnológicos de interés farmacéutico que han sido desarrollados hasta ahora aparecen resumidos en la Tabla I.1.

Tabla I.1. Sistemas nanotecnológicos de liberación de fármacos (modificado de Devadasu et al., 2013).

Sistemas de liberación	**Descripción**
Micelas	Disposición en monocapas esféricas de moléculas polares
Vesículas	Estructura en bicapas cerradas uni o multilaminares
Dendrímeros	Moléculas en ramificaciones esféricas
Nanocristales	Cristales de fármacos con o sin excipientes funcionales
Nanopartículas	Huecas o rellenas. Naturaleza inorgánica, polimérica, lipídica,…
Nanoemulsiones	Normalmente de fase externa acuosa
SNEDDS	Sistemas de liberación de fármacos auto nanoemulsionables
Liposomas	Vesículas lipídicas
Niosomas	Vesículas formadas por lípidos no iónicos
Esfingosomas	Vesículas formadas por lípidos basadas en esfingosina
Polimerosomas	Vesículas de dendrímeros
Conjugados de polímero-fármaco	Fármaco unido covalentemente a un polímero o transportador peptídico o nutriente/antígeno/anticuerpo
Nanopartículas basadas en proteínas	Fármacos unidos a proteinas de tamaño nanométrico
Nanopartículas sólido-lipídicas	Nanopartículas lipídicas
Virosomas	Vacuna formada por cápsulas virales y lipídicas

Entre los materiales usados para el desarrollo de los sistemas de liberación descritos destacan cuatro grupos de excipientes (Figura I.1).

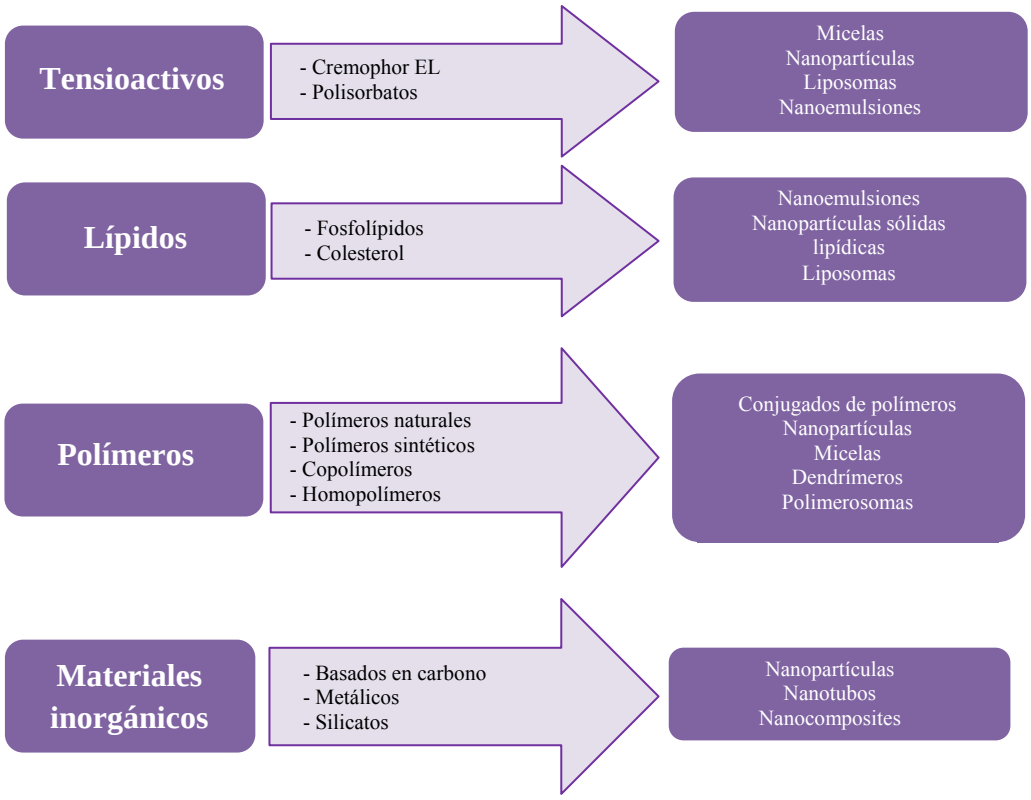

Figura I. 1. Materiales y sistemas nanotecnológicos de empleo en liberación modificada (modificado de Devadasu et al., 2013).

Entre los materiales utilizados, destacan los polímeros naturales y sintéticos, empleados para la obtención de nanopartículas y nanoconjugados con fármacos, entre otras aplicaciones, así como los materiales inorgánicos naturales y sintéticos para la elaboración de nanocomposites, nanopartículas y nanotubos. Estos son precisamente los materiales usados en esta tesis, por lo que centraremos en ellos nuestra atención.

I.1.1- NANOCOMPOSITES POLÍMERO/ARCILLA

Tanto los polímeros como las arcillas son excipientes usados con frecuencia en la elaboración de medicamentos (Aguzzi et al., 2007; López-Galindo et al., 2007, 2011; Viseras et al., 2007). Su uso en la elaboración de nanocomposites ha sido asimismo propuesto por distintos autores (LeBaron et al., 1999; Sinha Ray y Okamoto, 2003; Sinha Ray y Bousmina, 2005; Paul y Roberson, 2008; Pavlidou y Papaspyrides, 2008; Viseras et al., 2008a, 2010). Los nanocomposites pueden definirse como materiales

"híbridos" (orgánico/inorgánico) en los cuales al menos una de las dimensiones de los componentes es de tamaño nanométrico (Giannelis, 1996). En el caso de los nanocomposites polímero/arcilla (NCPA), las partículas de arcilla o las capas que las forman presentan una dimensión nanométrica y se encuentran dispersas en el seno de una matriz polimérica. Los polímeros usados para obtener estos nanocomposites incluyen homopolímeros, copolímeros, polímeros ramificados, reticulados y mezclas de dos o más tipos. Cuando el nanocomposite que se desarrolla está destinado al uso en nanomedicina, resultan particularmente interesantes los polímeros biodegradables, tales como alcohol polivinílico, poli (ε-caprolactona), polilacticidas, poli(3-hidroxi butirato), poli(butilensuccionato), poliésteres alifáticos, derivados de la celulosa como hidroxipropil-metil-celulosa y etilcelulosa, polisacáridos como amidas, alginatos, quitosano y gelatina, etc. Respecto del componente inorgánico, han sido propuestos tanto arcillas naturales (como la hectorita, montmorillonita, saponita y otras esmectitas), o modificadas (órgano-esmectitas y esmectitas pilareadas) como "arcillas" sintéticas (fluorohectorita, fluoromica, hidrotalcita.…). En todos los casos, el desarrollo de un nanocomposite polímero/arcilla tiene como objetivo la obtención de un producto con propiedades "especiales", como resultado de los cambios significativos ("nanoefectos") que aparecen respecto de las propiedades que presentan los componentes por separado. Cabe destacar los cambios inducidos en las propiedades mecánicas (Okada et al., 1988, 1990; Kojima et al., 1993; Giannelis, 1996; Giannelis et al., 1998; Le Baron et al., 1999; Vaia et al., 1999; Biswas e Sinha Ray, 2001; Kawasumi, 2004; Huang et al., 2012; Mahmoudian et al., 2012; Chieruzzi et al., 2013), térmicas (Dabrowski et al., 1993; Yano et al., 1993; Messersmith y Giannelis, 1995; Giannelis, 1998; Gilman et al., 1998a, 2000; Gilman, 1999; Bharadwj, 2001; Xu et al., 2001; Chrissafis y Bikiaris, 2011; Silvestre et al., 2011; Nafaji et al., 2012; Naguib et al., 2012; Qian et al., 2012) y aquellas relativas a la biodegradabilidad del polímero (Sinha Ray et al., 2002).

I.1.1.1- PREPARACIÓN DE NCPA

Hasta el momento se han desarrollado cuatro métodos principales para producir nanocomposites polímero/arcilla: (1) síntesis *in situ,* (2) intercalación de polímeros en solución, (3) intercalación por polimerización *in situ* y (4) intercalación por fusión (Alexandre y Dubois, 2000; Dennis et al., 2001; Fornes et al., 2001; Kim et al., 2001;

Beyer, 2002). Otros métodos han sido propuestos, pero su empleo no se ha generalizado, tal como la posibilidad de obtener nanocomposites polímero/arcilla mediante irradiación con microondas (Kabiri et al., 2007; El-Sherif y El-Masry, 2011). Centraremos nuestra atención en los cuatro métodos más usuales.

SÍNTESIS *IN SITU*

En esta técnica la arcilla es sintetizada directamente en la matriz polimérica, utilizando una solución polimérica que contiene un precursor de la arcilla (por ejemplo óxido de magnesio, fluoruro de litio, etc). Presenta la limitación de que la arcilla debe formarse a temperaturas relativamente bajas, para evitar la degradación de la matriz polimérica, lo que limita el número de arcillas sintéticas que pueden formarse (hectorita). Asimismo, se produce una tendencia al colapso de las capas de arcilla durante el crecimiento de los cristales (Pavlidou y Papaspyrides, 2008).

INTERCALACIÓN DE POLÍMEROS EN SOLUCIÓN

Este método implica la puesta en contacto en un medio liquido de las cadenas de polímero disueltas y las partículas de arcilla en suspensión (Figura I.2), de tal manera que las cadenas poliméricas penetran en los estratos de la arcilla desplazando el medio. Cuando se elimina el solvente, la estructura del silicato se mantiene y da lugar a un híbrido polímero/arcilla (Sinha Ray y Okamoto, 2003).

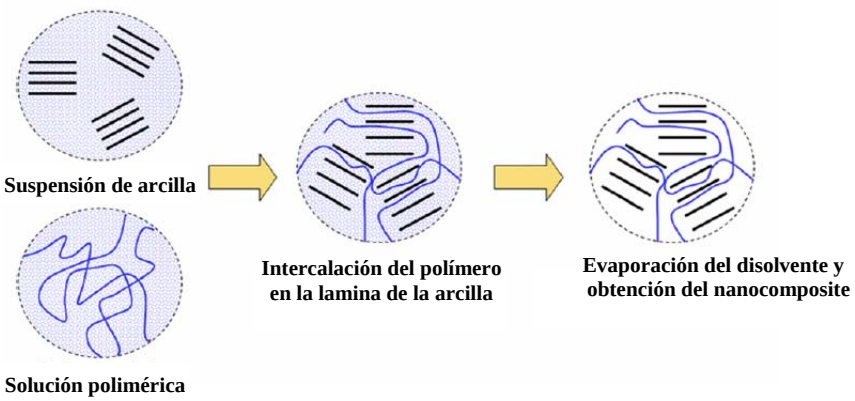

Figura I.2. Proceso de intercalación en solución (modificada de Pavlidou y Papaspyrides, 2008).

INTERCALACIÓN POR POLIMERIZACIÓN *IN SITU*

En este caso las partículas de arcilla son hidratadas en soluciones del monómero (o directamente en un monómero líquido) de modo que la formación del polímero tiene lugar en los espacios interlaminares de arcilla. La polimerización se puede inducir por calor, radiaciones o presencia de un iniciador (Sinha Ray y Okamoto, 2003).

INTERCALACIÓN POR FUSIÓN

Este método consiste en la mezcla de la arcilla con una matriz polimérica y posterior fusión de la matriz (Figura I. 3). En tales condiciones, si la afinidad de los componentes es adecuada, las cadenas poliméricas difunden en el espacio interlaminar para formar un nanocomposite (Alexandre y Dubois, 2000; Solomon et al., 2001; Beyer, 2002).

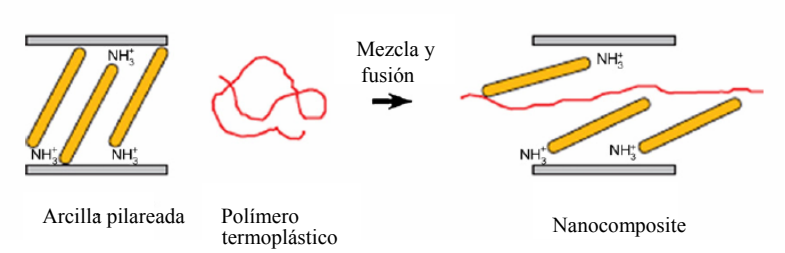

Figura I.3. Proceso de intercalación por fusión (modificada de Beyer, 2002).

Respecto de los métodos anteriores, permite evitar el uso de disolventes, habiendo sido usado para la intercalación de polímeros que no permitían la polimerización *in situ* o mediante solución (Sinha Ray y Okamoto, 2003), no obstante tiene la limitación de que el polímero debe resistir la temperatura de fusión sin degradarse.

I.1.1.2- ESTRUCTURA DE NCPA

Cualquier mezcla polímero/arcilla no da lugar a un nanocomposite, como es obvio, siendo necesario que en el compuesto resultante, los estratos de arcilla se encuentren dispersos uniformemente en la matriz polimérica (Figura I.4). En mezclas físicas convencionales entre los componentes orgánicos e inorgánicos no se produce un cambio significativo de las propiedades, e incluso disminuye la resistencia mecánica como resultado de la tendencia de las partículas de arcilla a formar agregados (Giannelis, 1996). Podemos decir que en ausencia nanoefectos, el compuesto presenta propiedades

análogas o incluso inferiores a las de los componentes por separado (Alexandre y Dubois, 2000; Beyer, 2002). Cuando, en cambio, se forma un nanocomposite, cabe distinguir dos situaciones; nanocomposites intercalados y exfoliados, en función del método de preparación y de los componentes utilizados (Alexandre y Dubois, 2000; Beyer, 2002).

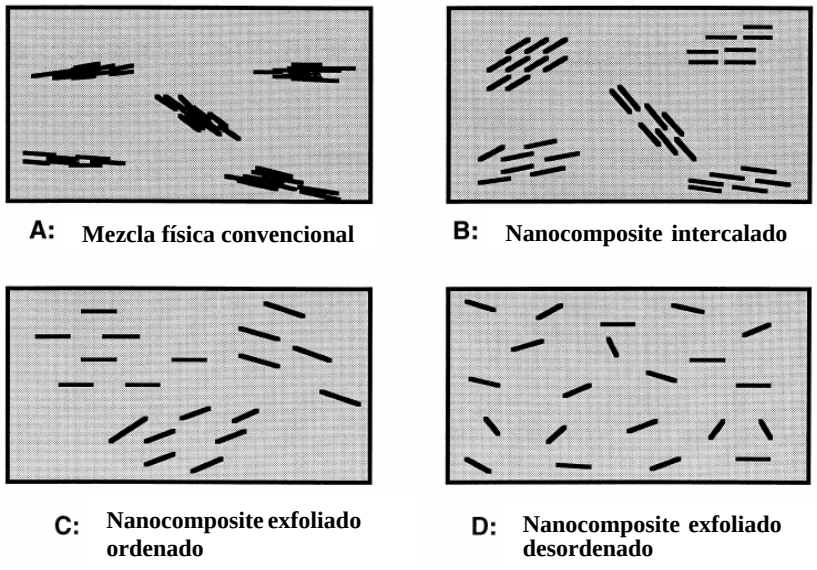

Figura I.4. Tipos de mezclas polímero/arcilla (modificado de Le Baron, 1999).

La estructura intercalada (Figura I.5) aparece cuando una o varias cadenas poliméricas se encuentran interpuestas entre las capas de arcilla, dando como resultado una estructura ordenada en capas alternas de polímero y arcilla, con una distancia definida y repetitiva entre ellas, lo que permite su evaluación por difracción de rayos X (Giannelis, 1996; Alexandre y Dubois, 2000; Chin et al. 2001; Dennis et al., 2001; Kim et al., 2001; Beyer, 2002).

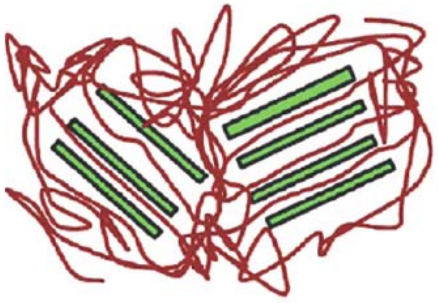

Figura I.5. Esquema de un nanocomposite intercalado (verde: arcilla; rojo: cadenas poliméricas) (modificado de Pavlidou e Papaspyrides, 2008).

Cuando, en cambio la intercalación de las cadenas de polímero da lugar a la separación o exfoliación de las capas de arcilla, el nanocomposite obtenido se dice que es exfoliado (Figura I.6) (Dennis et al., 2001).

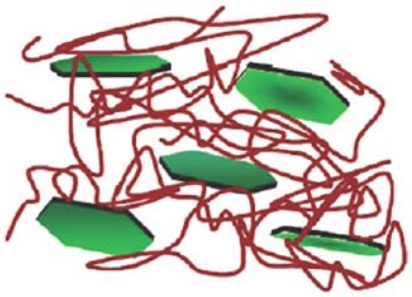

Figura I.6. Esquema de un nanocomposite exfoliado (verde: arcilla; rojo :cadenas poliméricas) (modificado de Pavlidou y Papaspyrides, 2008).

Los nanocomposites exfoliados poseen propiedades únicas debidas al tamaño de las partículas de arcilla dispersas (en orden de nanómetros) y elevada área superficial. Sin embargo, no siempre es posible obtener esta morfología ideal, por la tendencia de las arcillas a formar estructuras en emparedado. La mayor parte de los nanocomposites poliméricos encontrados en la literatura presenta estructuras intercaladas o intercaladas-exfoliadas (Chin et al., 2001). Dado que las partículas de arcilla son muy anisotrópas se puede esperar que tiendan a ordenarse en direcciones preferenciales dentro de la matriz polimérica.

Las distintas estructuras que aparecen cuando una arcilla y un polímero se interponen pueden apreciarse con microscopía electrónica de transmisión y los espaciados entre las láminas que constituyen las arcillas determinarse por difracción de rayos X (Figura I.7) (LeBaron et al., 1999; Pinnavaia y Beall, 2000; Dennis et al., 2001; Yariv y Cross, 2002; Sinha Ra.y y Okamoto, 2003; Hussain et al., 2006; Mai y Yu, 2006). De esta forma, una mezcla física en la que no se ha formado un nanocomposite presentará agregados de partículas y patrones de difracción de rayos X similares a los correspondientes a la arcilla pura. Cuando las partículas se encuentran exfoliadas, la imagen de microscopía revela la presencia de partículas individuales sin una orientación preferente y en el patrón de difracción de rayos X el pico de la arcilla que nos informa de la distancia entre láminas desaparece, dado que el ángulo 2θ es demasiado bajo, para poder ser registrado. A pesar de esto, en la mayor parte de los casos los nanocomposites

muestran el pico característico del espacio basal de la arcilla (d_{001}), aunque desplazado hacia valores menores de 2θ en comparación con el mineral puro. Esto indica que el espacio basal se incrementa después de la intercalación de las cadenas poliméricas en el espacio interlaminar de la arcilla. Hasta hace unos años se creía que la intercalación era una etapa intermedia a la exfoliación, aunque estudios recientes plantean que la formación de un tipo u otro de nanocomposite son independientes (Cho y Paul, 2001; Fornes et al., 2001; Krishnamoorti, 2007).

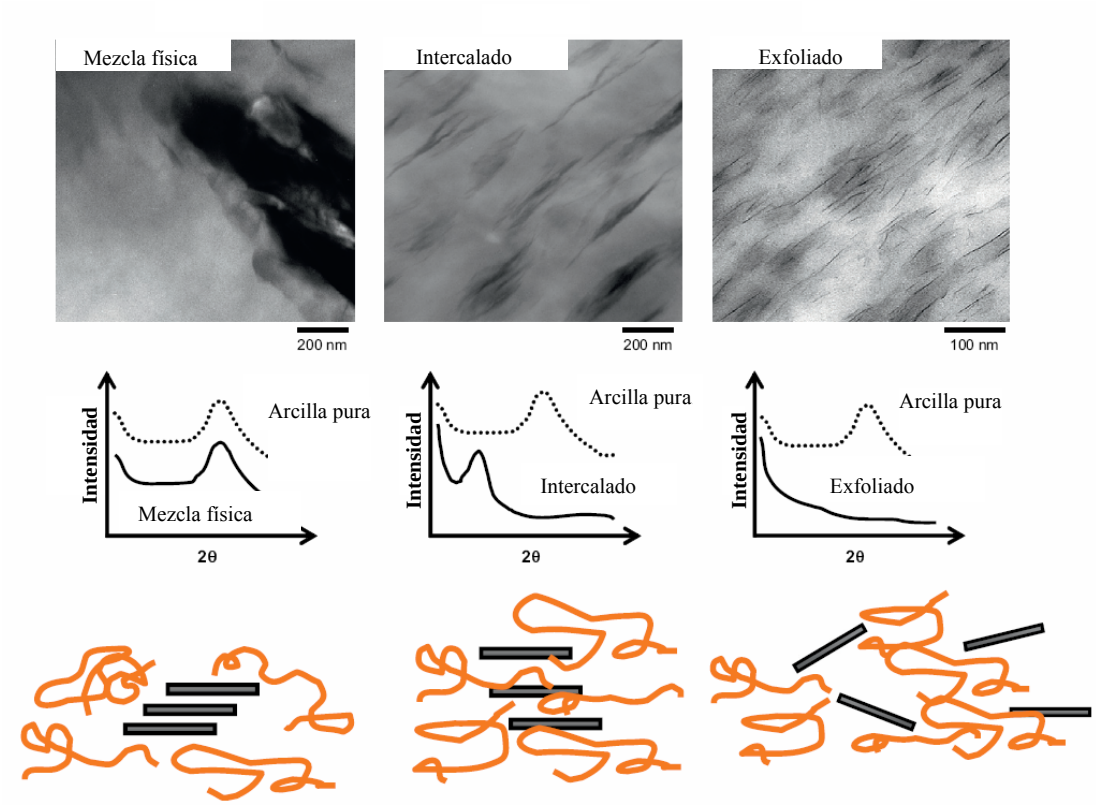

Figura I.7. Esquema de tipos de mezclas polímero/arcilla, con sus correspondientes patrones de difracción e imágenes de TEM (modificado de Paul y Robeson, 2008).

I.1.1.3- PROPIEDADES DE NCPA

Como resultado de la interacciones a escala nanométrica entre las partículas de arcilla y las cadenas poliméricas, los nanocomposites muestran propiedades mejoradas en comparación con los componentes individuales puros, incluso con poca cantidad de arcilla dispersa (Sinha Ray y Okamoto, 2003). En particular, han sido estudiados los efectos mecánicos, térmicos, de inflamabilidad y de biodegradabilidad de estos nanocomposites.

La interposición de las partículas de arcilla en la matriz polimérica aumenta su resistencia mecánica (módulo de Young). Esto sucede también en mezclas físicas convencionales, pero mientras que en ellas el aumento de la resistencia mecánica es lineal con la cantidad de partículas incorporadas, en los nanocomposites, una pequeña presencia de arcilla induce un gran aumento en la resistencia (Sinha Ray y Okamoto, 2003). Por ejemplo, en un nanocomposite de montmorillonita al 6% en peso con celulosa el módulo de Young aumenta un 40% (Mahmoudian et al., 2012). Esta tendencia general presenta, no obstante, alguna excepción como muestra la Figura I.8, en la que la intercalación de la arcilla reduce la reticulación del polímero, reduciendo con ello el módulo de Young (Bharadwaj et al., 2002).

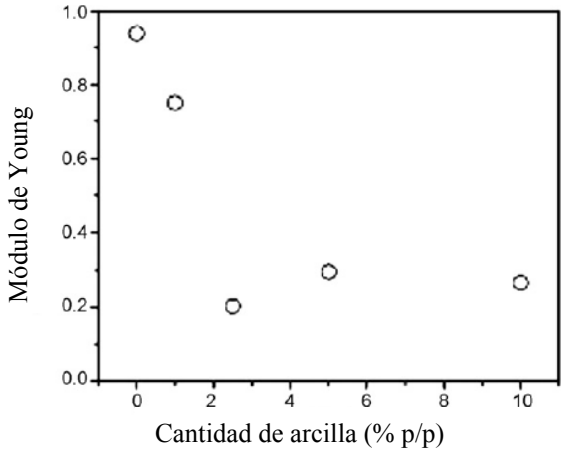

Figura I.8. Efecto de la intercalación de arcilla en el módulo de Young de una matriz de polímero reticulado (modificado de Bharadwaj et al., 2002).

La formación de un nanocomposite de polímero y arcilla hace asimismo aumentar la resistencia a la tracción, en comparación con el polímero puro (Pongjanyakul et al., 2005a), aunque este efecto no siempre se produce (Pavlidou y Papaspyrides, 2008).

Por otra parte, la incorporación de partículas de arcilla a una matriz polimérica produce un aumento de la estabilidad térmica del polímero (Zhu et al., 2001; Sinha Ray y Okamoto, 2003; Sinha Ray y Bousima, 2005; Fukushima et al., 2012a; Mahmoudian et al., 2012) y una disminución de la inflamabilidad (Porter et al., 2000; Beyer, 2002; Tai et al., 2012). En ambos casos, la baja capacidad calorífica de la arcilla produce una disminución de la transferencia de energía del nanocomposite, respecto del polímero puro (Gilman et al., 1998b; Porter et al., 2000; Beyer, 2002; Kashiwagi et al., 2004; Preston et al., 2004). Son también numerosos los estudios en los que se ha puesto de manifiesto el interés que presentan los nanocomposites de polímero y arcilla para

reducir la permeabilidad a los gases de las matrices poliméricas. Aparentemente, la presencia de las partículas de arcilla aumenta la tortuosidad del camino que debe atravesar el gas, retrasando el progreso de las moléculas a través de la matriz (Figura I.9) (Burnside y Giannelis, 1995; Messersmith y Giannelis, 1995; Giannelis, 1996; Fredrickson y Bicerano, 1999; LeBaron et al., 1999; Lange y Wyser, 2003; Sinha Ray et al., 2003a; Sinha Ray y Okamoto, 2003; Cushen et al., 2012; Huang et al., 2012; Scarfato et al., 2012).

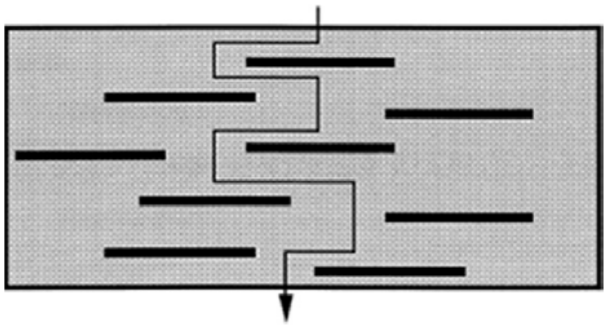

Figura I.9. Modelo de paso de una molécula de gas a través de una matriz de nanocomposite polímero/arcilla.

Mientras que las propiedades anteriores no parecen de interés inmediato para el empleo en salud de los nanocomposites polímero/arcilla, si tiene una importancia evidente el efecto que sobre la biodegradabilidad de las matrices poliméricas tiene la incorporación de partículas de arcilla. En efecto, los nanocomposites polímero/arcilla presentan, en general, una biodegradación más rápida que los polímeros de partida (Tetto et al., 1999). Para explicar este efecto se han propuesto distintos mecanismos, tales como el efecto catalítico de los grupos silanoles presentes en la arcilla (Sinha Ray et al., 2003b), el mayor tiempo de retención de oxígeno en la matriz como resultado de su tortuosidad, y la consiguiente oxidación (Pandey et al., 2005) o la entrada de agua atraída por las partículas hidrófilicas de arcilla y la hidrólisis consiguiente del polímero (Fukushima et al., 2012b). Algunos autores han puesto de manifiesto que en ocasiones el nanocomposite presenta una menor biodegradabilidad (Lee et al., 2002) y de nuevo, la tortuosidad impuesta por las partículas de arcilla ha sido usada para explicar en este caso que la difusión de microorganismos responsables de la degradación se vea dificultada. Otros autores explican la disminución de la biodegradabilidad como resultado del aumento del efecto barrera al incorporar la arcilla (Maiti et al., 2003). Esta explicación parece estar en contraste con los resultados de Sinha Ray y colaboradores

(Sinha Ray et al., 2003b), que han revelado una relación entre la biodegradabilidad y la propiedad de barrera. De los resultados contradictorios citados, es evidente que un aumento o una reducción de la biodegradabilidad de los nanocomposites sigue siendo objeto de debate y que, hasta la fecha no podemos aceptar las conclusiones sobre los mecanismos que regulan estos procesos, en base a los datos de la literatura (Pandey et al., 2005).

Si interesante resulta el estudio de biodegradabilidad de los nanocomposites, no menos lo es el efecto en las propiedades reológicas de sistemas poliméricos fluidos (Sinha Ray y Okamoto, 2003; Sinha Ray y Bousima, 2005; Yilmaz et al., 2011). La incorporación de arcillas a los geles poliméricos modifica las propiedades reológicas a través de diversos mecanismos que dependen de las características fisicoquímicas del polímero y de la arcilla (Khunawattanakul et al., 2008). Generalmente es aceptado que, cuando se forma un nanocomposite, la viscosidad aumenta al aumentar la concentración de la arcilla (Cho y Paul, 2001). En general, el tipo de interacción entre las cadenas poliméricas y las partículas de arcilla ha sido usado para explicar los cambios en la reología observados. Así, la incorporación de arcilla a geles de alginato sódico (polímero aniónico) o quitosano (polímero catiónico) aumenta la viscosidad y determina cambios en el comportamiento, que pasa de newtoniano a pseudoplastico con tixotropía, mientras que cuando el gel polimérico es de hidroxipropilmetilcelulosa o de poloxámero 407 (ambos no iónicos) el efecto es mucho menos intenso (Pongjanyakul et al., 2005b; Khunawattanakul et al., 2008). La sinergia entre los polímeros iónicos y las partículas de arcilla ha sido explicada como consecuencia de las interacciones entre los grupos silanóles de la arcilla y grupos cargados del polímero, e incluso de enlaces de tipo "cross-linking" entre el ácido glucónico del alginato y los cationes de intercambio de la arcilla (Pongjanyakul et al., 2005b).

I.1.1.4- INTERÉS DE LOS NCPA EN LIBERACIÓN MODIFICADA DE FÁRMACOS

Tanto las arcillas como los polímeros son materiales frecuentemente usados en el campo farmacéutico (Peppas et al., 2001; Aguzzi et al., 2007; López-Galindo et al., 2007, 2011; Viseras et al., 2007), aunque en la mayoría de los casos su empleo requiere de alguna modificación para mejorar sus prestaciones. En este sentido, la preparación de

nanocomposites puede mejorar las propiedades de la arcilla (estabilidad en sistemas dispersos, propiedad de intercambio iónico) y del polímero (propiedades mecánicas, reológicas, capacidad de hinchamiento, formación de películas, bioadhesión y permeabilidad celular, etc.) (Viseras et al., 2008a, 2010).

La estabilidad de sistemas dispersos de arcillas aumenta en presencia de polímeros, a través de distintos mecanismos que incluyen la disminución del potencial electrocinético de las partículas de sólido arcilloso, la formación de barreras físicas en torno a las partículas, evitando su contacto o incluso atrapándolas en el seno del gel polimérico. Estos efectos, que aparecen incluso con mezclas convencionales, se expresan de forma muy intensa en nanocomposites, como ha sido estudiado con sistemas híbridos de laponita (una arcilla sintética) y copolímeros de polietilenglicol y poliamina (Takahashi et al., 2005). Asimismo, la formación de nanocomposites aumenta la afinidad de las arcillas por moléculas neutras o aniónicas, que a priori no son retenidas por el sólido inorgánico dada su carga neta negativa (An y Dultz, 2007). Es inherente a este efecto, el interés de los nanocomposites de polímeros y arcillas en la retención y posterior liberación de fármacos aniónicos o neutros, aun cuando hasta la fecha hayan sido usados fundamentalmente para retención de contaminantes presentes en suelos o agua (Chatterjee et al., 2010; Futalan et al., 2011; Celis et al., 2012; Lertsutthiwong et al., 2012; Peng et al., 2012). También resulta evidente que el aumento de la tortuosidad de las matrices poliméricas como resultado de la presencia de partículas de arcilla puede resultar de gran interés como mecanismo de control de la liberación de fármacos (Cojocariu et al., 2012). No es de extrañar, por tanto, que de forma específica distintos autores hayan puesto de manifiesto las posibilidades que presentan los nanocomposites en liberación modificada de fármacos, siendo objeto de revisiones detalladas (Viseras et al., 2008a, 2010; De Sousa Rodrigues et al., 2013).

Con mucha diferencia, la montmorillonita ha sido el mineral de la arcilla más usado para obtener nanocomposites en vistas a la liberación modificada de fármacos. Con este mineral se han preparado nanocomposites con polímeros como el quitosano y ácido poliláctico (Nanda et al., 2011), ácido poli (D, L-láctico-co-ácido glicólico) (Dong y Feng, 2005; Sun et al., 2008; Si-Shen et al., 2009), poliuretano (Silva et al., 2009), entre otros. Entre los fármacos estudiados se incluyen agentes antitumorales como el paclitaxel y docetaxel (Dong y Feng, 2005; Sun et al., 2008; Feng et al., 2009) o el 5-fluorouracilo (Pradosh et al., 2011), corticoides como la dexametasona (Silva et al.,

2009), antiinflamatorios como el diclofenaco (Kevadiya et al., 2011), beta-bloqueantes como el propranolol (Pongjanyakul y Rongthon, 2010), opioides como el fentanilo (Forsgren et al., 2010) o incluso fármacos polipeptídicos (Wang et al., 2010; Li et al., 2012; Li et al., 2012). En general, los perfiles de liberación de los fármacos cargados en dichos nanocomposites presentan patrones que permiten hablar de liberación prolongada y en ocasiones una reducción del efecto "Burst" inicial (Pongjanyakul y Rongthon, 2010). Junto con estas mejoras biofarmacéuticas, los nanocomposites polímero/montmorillonita confieren a los sistemas propiedades añadidas como una reducción de daños en el ADN y disminución de la toxicidad asociada a la quimioterapia (Kevadiya et al., 2011; Pradosh et al., 2011) o un aumento de la captación celular (Dong y Feng, 2005) que puede ser explicado por la interacciones específicas entre los cationes presentes en las partículas de arcilla y los grupos hidroxilos de las proteínas de membrana (Lavie y Stotzky, 1986). Algunos autores han desarrollado nanocomposites de quitosano y montmorillonita en presencia de un polianión (tripolifosfato) que induce el entrecruzamiento de las cadenas poliméricas dando lugar a formas esféricas tipo "beads" estables y capaces de retener de forma efectiva el fármaco estudiado (oxofloxacina) (Hua et al., 2010).

En el grupo de investigación CTS-946, del que formo parte, se han desarrollado nanocomposites con quitosano y distintas arcillas capaces de retener el ácido 5-amino salicílico, de empleo en el tratamiento de la enfermedad inflamatoria intestinal, encontrando un efecto sinérgico entre los componentes mineral y polisacarídico de tal manera que aumenta la capacidad de retener moléculas de fármaco y el control de la liberación en un medio ácido (Aguzzi et al., 2010).

Junto con el desarrollo de matrices de liberación modificada basadas en nanocomposites polímero/arcilla, son numerosos los estudios en los que estos sistemas han sido desarrollados para el recubrimiento pelicular de formas sólidas en vistas a la modificación de la liberación del fármaco, usando polisacáridos como el quitosano o el alginato y arcillas naturales (Pongjanyakul y Puttipipatkhachom, 2007, 2009; Depan et al., 2009; Pongjanyakul, 2009; Pongjanyakul y Suksri, 2009; Ward et al., 2010; Khunawattanakul et al., 2010, 2011).

En numerosas ocasiones, la arcilla natural se modifica antes de ser incorporada al nanocomposite (Lee y Chen, 2004; Shaikh et al., 2007; Martin et al., 2011), con objeto de mejorar las prestaciones del sistema (carga de polímero, dosis de fármaco retenido,

propiedades mecánicas, de adhesión y de liberación). Otras veces la arcilla natural se sustituye por una sintética, como la Cloisita 20A (Campbell et al., 2008) o las denominadas "arcillas aniónicas" o "layered double hydroxides" (Tammaro et al., 2009; Cao et al., 2011). Estas arcillas sintéticas han sido usadas tanto para el desarrollo de matrices de liberación modificada, como para la obtención de películas de recubrimiento (Wang et al., 2007) o el aumento de la solubilidad de fármacos poco solubles (Ha y Xanthos, 2011).

I.2.- QUITOSANO

I.2.1.- ESTRUCTURA Y PROPIEDADES

El quitosano (Figura I.10) o poli-b(1,4)-2-amino-2-deoxi-D-glucósido, es una sustancia obtenida a partir de la quitina, poli(N-acetil-D-glucosamina), un polisacárido natural que se encuentra en el esqueleto de crustáceos y de insectos y en la pared celular de hongos y microorganismos (Muzzarelli et al., 2012). Descubierto en 1859 por Rouget, al poner en contacto la quitina con una solución caliente de hidróxido de potasio que daba lugar a una sustancia soluble en ácidos inorgánicos, fue inicialmente denominada "quitina modificada". Su denominación actual (quitosano) fue propuesta años más tarde (1894) por Hoppe-Seyler, como recogen distintas revisiones de esta sustancia (Díaz Crespín, 2002).

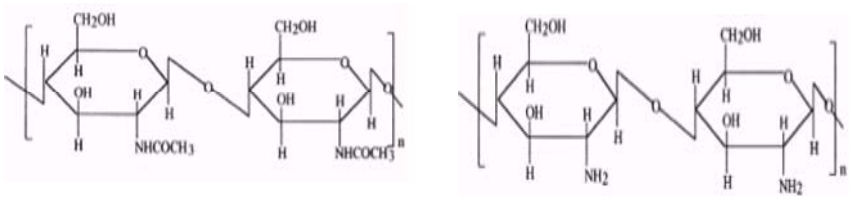

Figura I.10. Estructura química de la quitina (izquierda) y del quitosano (derecha).

La quitina es tratada con soluciones alcalinas y ácidas para eliminar distintas impurezas y finalmente se procede a su desacetilación para obtener quitosano (Figura I.11) (Felt et al., 1998). Las condiciones usadas para la desacetilación son las que van a determinar el peso molecular del quitosano que varía entre 10 y 1000 KDa, así como el grado de desacetilación que suele encontrarse en el intervalo 70-90% (Sonia y Sharma et al., 2011). Los grupos funcionales en la estructura del quitosano son los grupos hidroxilos y las aminas libres en posición C_2 de los residuos de glucosa de la cadena polisacarídica. Dependiendo del grado de desacetilación resulta posible controlar el número de grupos amínicos responsables de la elevada reactividad del quitosano (Arizmendi-Morquecho et al., 2013).

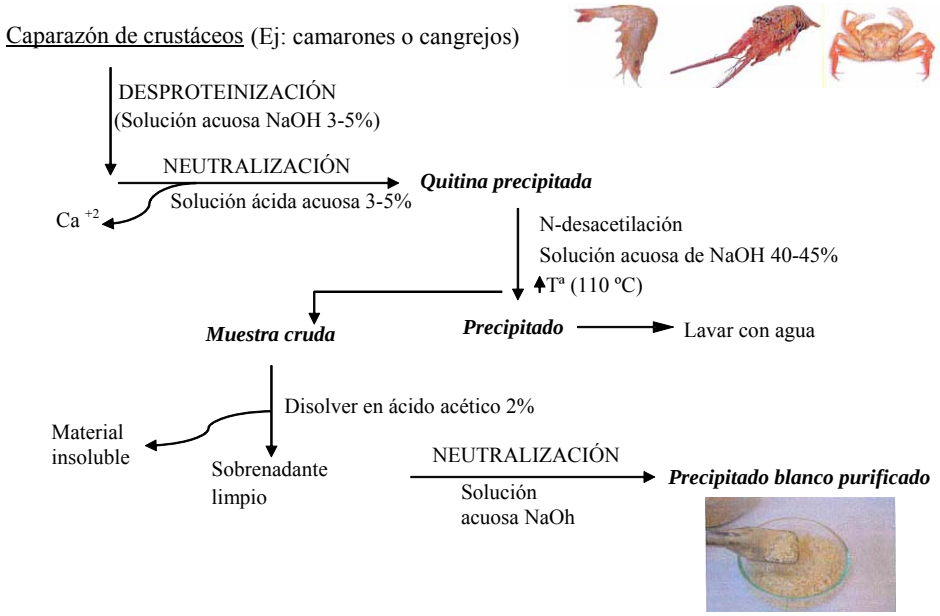

Figura I.11. Esquema de obtención del quitosano.

El quitosano es insoluble en disolventes orgánicos y soluciones acuosas neutras o alcalinas, siendo soluble en soluciones acuosas débilmente ácidas, donde los grupos amínicos libres están protonados (Chandy y Sharma, 1990). A diferencia de la quitina, forma sales con ácidos orgánicos como el acético, láctico o glutámico e inorgánicos diluidos como el ácido clorhídrico. La solubilidad acuosa del quitosano depende de su grado de desacetilación, así como del pK_a, pH y fuerza iónica del medio (Illum, 1998).

La administración oral de quitosano no produce efectos adversos (Hirano et al., 1990; Dornish et al., 1997; Kim et al., 2001; Gades y Stern, 2003; Naito et al., 2007; Tapola et al., 2008), no obstante se haya puesto de manifiesto que su administración oral prolongada puede dar lugar a algunos efectos secundarios leves como náuseas y estreñimiento (Ylitalo et al., 2002). El quitosano no presenta potencial carcinogénico (Takashashi et al., 2009) ni genotóxico (Ishiara et al., 2002; Lee et al., 2004). Algunos autores han planteado posibles efectos citotóxicos relacionados con el tipo de sal y peso molecular del polímero (Carreño-Gómez y Duncan, 1997; Chae et al., 2005; Opanasopit et al., 2007). Su uso en implantes no da lugar a reacciones adversas específicas (Aspden et al., 1997; Calvo et al., 1997; Rao y Sharma, 1997; Tomihata e Ikada, 1997; Haffejee et al., 2001; VandeVord et al. 2002; Azab et al., 2007).

El quitosano es biocompatible, dado que tanto la N-acetilglucosamina como la glucosamina que constituyen su estructura están presentes en la mayoría de las

macromoléculas de los órganos y tejidos del cuerpo humano (Peh et al., 2000; Chatelet et al., 2001). En el organismo, el quitosano se biodegrada por hidrólisis de los enlaces glucosídicos que unen las unidades de N-acetilglucosamina y glucosamina (Chae et al., 2005) para dar lugar a productos de degradación no tóxicos que son eliminados (Nordtveit et al., 1996). La velocidad de degradación disminuye al aumentar el grado de desacetilación (Baxter et al., 1992; Paradossi et al., 1992; Raymond et al., 1993; Lee y Ha, 1995; Kamiyama et al., 1999). Tras su administración oral es degradado por las enzimas de la flora bacteriana presente en el colon (Illum et al., 1998).

El quitosano muestra actividad antibacteriana frente a determinados microorganismos tales como *Escherichia coli* entre otros (Muzzarelli et al., 1990; Bowler et al., 2001; Morimoto et al., 2002) debida a la interacción de los grupos aminos protonados del polímero con las cargas negativas presentes en las paredes celulares bacterianas que dan lugar a cambios en la permeabilidad de membrana (acción bactericida) junto con la inhibición de la síntesis de ARNm y proteínas por la unión del quitosano al ADN (acción bacteriostática) (Sudarshan et al., 1992; Chung et al., 2008). Asimismo, es capaz de inhibir el crecimiento de una gran variedad de hongos y levaduras (Aimin et al., 1999).

I.2.2.- INTERÉS EN TECNOLOGÍA FARMACÉUTICA

Como hemos indicado, el quitosano es biodegradable, biocompatible y presenta baja toxicidad. A estas propiedades, comunes con otros polisacáridos, se une la presencia de grupos amino protonables en su estructura capaces de interaccionar tanto con el sistema biológico en contacto con el medicamento al que aporta su capacidad mucoadhesiva, como con otros componentes del medicamento para obtener complejos fármaco-quitosano. Ambas propiedades tienen interés en el desarrollo de sistemas de liberación modificada de fármacos.

El quitosano posee buenas propiedades mucoadhesivas (Lehr et al., 1992; Needleman y Smales, 1995; Rillosi y Buckton, 1995; He et al., 1998; Shimoda et al., 2001; Kockisch et al., 2003). Ésta característica hace que sea un candidato excelente para liberación prolongada de fármacos ya que, aumenta el tiempo de permanencia del principio activo en la mucosa (Soane et al., 1999), disminuyendo la necesidad de administrar varias dosis. La propiedades mucoadhesivas del quitosano se deben a la interacción entre sus grupos aminos protonados y la capa de mucus, constituida por una glicoproteína

llamada mucina, que presenta cargas negativas debido a la presencia de residuos del ácido siálico (Figura I.12) (Bernkop-Schnürch y Dünnhaupt, 2012). En la mucoadhesion influyen una serie de factores relacionados con el quitosano como la formación de puentes de hidrógeno (Shipper et al., 1997), la elevada densidad de carga (Dodane et al., 1999), la longitud de las cadenas poliméricas y su penetración en la mucina (Schipper et al., 1996; Kotzé et al., 1998), la flexibilidad de las cadenas (He et al., 1998) o la baja capacidad de difusión del polímero a través de la mucosa (Lueβen et al., 1994). El pH también influye en las propiedades mucoadhesivas del quitosano, ya que a pH ácido se encuentra cargado positivamente y, por tanto, es capaz de interaccionar con el mucus. También se ha descrito que un elevado peso molecular favorece la mucoadhesión ya que cuanto más largas son las cadenas poliméricas, más penetran en la capa de mucina (Borchard et al., 1996 ; Majithiya et al., 2005). Se puede concluir que un quitosano de elevado peso molecular y grado de desacetilación favorece la mucoadhesión. No obstante, el quitosano presenta una baja cohesividad que limita su mucoadhesion, que puede mejorarse aumentando su carácter catiónico mediante trimetilación de los grupos amino (Jintapattanakit et al., 2009) o tiolación que induce la formación de enlaces disulfuros entre las cadenas del polímero y las glicoproteínas del mucus mejorando tanto sus propiedades mucoadhesivas como (Werle et al., 2008).

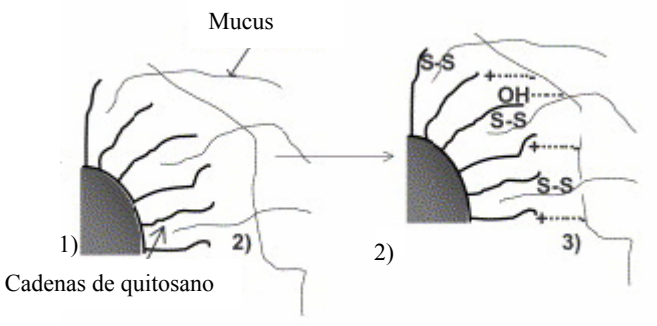

Figura I.12. Mecanismos de interacción con mucina: 1) penetración de cadenas; 2) no covalente (iónica y puentes de hidrógeno) y covalente (enlaces disulfuro)(de Bravo-Osuna et al., 2007).

La liberación modificada de fármacos ionizables puede lograrse mediante interacción electrostática con excipientes que se comporten como polielectrolitos. De esta forma, se plantea la interacción de fármacos catiónicos con polímeros aniónicos (poliacrilatos, carboximetilcelulosa sódica o alginato) o bien de fármacos aniónicos con polímeros catiónicos, entre los que destaca el quitosano. Con esta premisa, el quitosano ha sido empleado para modificar la liberación de naproxeno (Bhise et al., 2008). La interacción

se hace incluso muy fuerte cuando el fármaco tiene carácter polianiónico, como el enoxaparin (Sun et al., 2010). Como resultado de la interacción se obtienen sistemas que, no obstante, presentan deficiencias mecánicas. Para evitarlo, algunos autores han planteado la formación de complejos de quitosano con polímeros aniónicos (alginato, pectina, carragenano, etc) para obtener matrices estables de elevada densidad desde las que el fármaco se libera por mecanismos de difusión y/o erosión (Tapia et al., 2005). Otros autores, en lugar de usar polímeros aniónicos, emplean aniones inorgánicos multivalentes como el tripolifosfato (Figura I.13) para conseguir matrices estables (Shavi et al., 2011).

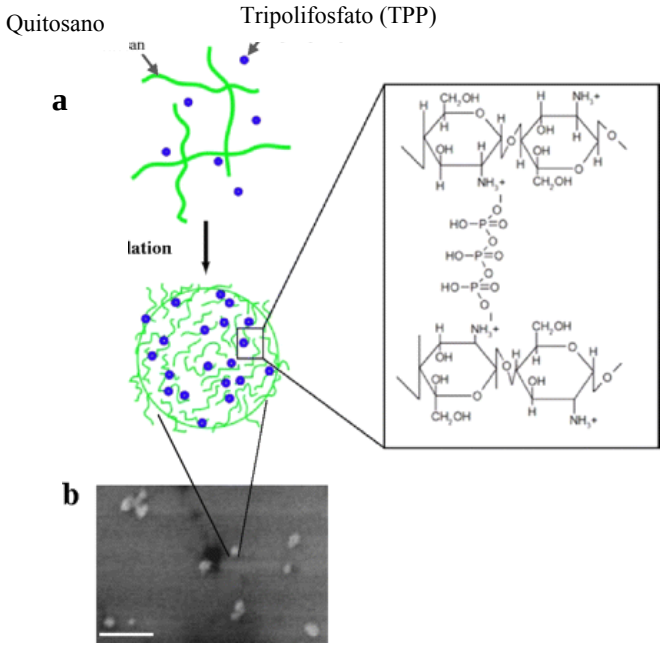

Figura I.13. (a) Formación del complejo quitosano-tripolifosfato mediante gelificación ionotrópica y (b) Imagen SEM. Bar, 200nm (Chávez de Paz et al., 2011).

En virtud de estas interacciones el quitosano ha sido empleado para el desarrollo de sistemas de liberación modificada de fármacos administrados por distintas vías. La administración de fármacos a través de la mucosa bucal proporciona ventajas con respecto a la vía oral ya que se evita el efecto de primer paso hepático, el medio ácido del estómago y la actividad proteolítica del resto del tracto gastrointestinal (Punitha y Girish, 2010). Un sistema ideal de administración bucal debe permanecer en la boca durante el tiempo suficiente para que el fármaco se libere de forma controlada. El desarrollo de estos sistemas para el tratamiento de patologías como la periodontitis, estomatitis, infecciones fúngicas y virales, entre otras, implica el uso de polímeros como

el quitosano y sus derivados, que son candidatos excelentes, dadas sus propiedades mucoadhesivas (comunes con otros polisacáridos) y capacidad de favorecer la penetración de fármacos (Aiedeh y Taha, 2001). Con estas premisas, se han desarrollado comprimidos bucales de quitosano con diacetato de clorhexidina capaces de liberar el fármaco de forma prolongada (Sinha et al., 2004). Asimismo, se han preparado películas de quitosano entrecruzado con tripolifosfato para el control de la liberación de gluconato de clorhexidina (Patel y Amiji, 1996). El quitosano de bajo peso molecular ha sido usado con éxito para la administración parenteral de distintos principios activos (Kamiyama et al., 1996; Vasishtha et al., 1997; Richardson et al., 1999). Uno de los principales inconvenientes de la administración de gotas oftálmicas es su escaso tiempo de permanencia en el ojo. Para subsanar este problema, se han diseñado distintos hidrogeles, microesferas y nanopartículas empleando quitosano (Genta et al., 1997; Fernández-Urrusuno et al., 1999; De Campos et al., 2001; Fisher et al., 2010; Gupta y Vyas 2010; Gupta et al., 2010) para la administración ocular de diferentes principios activos. Con objeto de aumentar la biodisponibilidad de los principios activos administrados por vía nasal se han diseñado asimismo, sistemas mucoadhesivos basados en quitosano (Illum et al., 1998; Soane et al., 1999). El entrecruzamiento de quitosano con glutaraldehido (El-Kamel et al., 2002) y el uso de derivados del polímero (Sandri et al., 2004) han sido planteados para aumentar la biodisponibilidad de fármacos administrados por vía vaginal. Se han propuesto microsferas de quitosano incorporadas a un hidrogel de hidroxipropilmetilcelulosa y carbopol para vía rectal (El-Leithy et al., 2010). Asimismo, se han propuesto hidrogeles para el control de la liberación por vía transdérmica (Tapan Kumar et al., 2012) y parches transdérmicos (Thein-Han y Stevens, 2004; Viyoch et al., 2005). Con el objetivo de conseguir una liberación colon-específica, se han usado polisacáridos biodegradables como el quitosano en películas de recubrimiento de comprimidos y otras formas de administración susceptibles de ser degradadas por las bacterias del colon (Tozaki et al., 1997, 1999; Macleod et al., 1999; Chourasia y Jain, 2004; Thakral et al., 2010). Dada la capacidad del quitosano para estimular la producción de inmunoglobulinas (Maeda et al., 1992) ha sido usado en vacunas contra *Bordetella pertussis* (Jabbal-Gill et al., 1998), *Bacillus anthracis* (Bivas-Benita et al., 2003), diphtheria (Xie et al., 2007) y virus de la gripe (Hasegawa et al., 2007) que se administran por distintas vías (Van der Lubben et al., 2001; Flood et al., 2010) en forma

de geles o de nanopartículas cargadas con el antígeno (Sieval et al., 1998; Des Rieux et al., 2006, 2007). Para asegurar que mantenga su capacidad mucoadhesiva en el intervalo de pH del intestino, se emplea el quitosano trimetilado el cual al estar cargado positivamente independientemente del pH, aumenta el tiempo de contacto del antígeno con el intestino incrementando su penetración (Van der Lubben et al., 2001; Van der Merwe et al., 2004; Sandri et al., 2007; Zhou et al., 2007; Chen et al., 2008;). Asimismo, el polímero ha sido usado en sistemas de liberación de plásmidos (MacLaughlin et al., 1998). Su capacidad para transportar genes se debe a las interacciones electroestáticas que se establecen entre sus grupos protonados y los grupos fosfatos del ADN (Figura I.14) (Duceppe y Tabrizian, 2010) presentando además las ventajas de ser biocompatible y biodegradable (Prabaharan y Mano, 2005) y tener una baja toxicidad celular (Murata et al., 1997; Roy et al., 1997). Para mejorar su eficacia de transfección de los genes transportados se han llevado a cabo distintas modificaciones del polímero que incluyen su cuaternización (Germershaus et al., 2008), tiolación (Zhao et al., 2010) y galactosilación (Jiang et al., 2010).

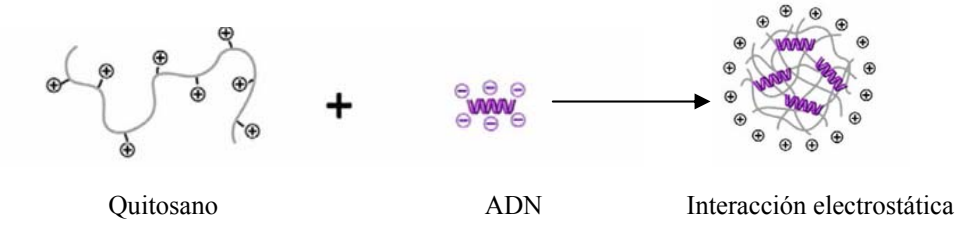

Figura I.14. Interacción del quitosano con el ADN (de Liu et al., 2011).

I.3. MONTMORILLONITA

La montmorillonita es un mineral que constituye el componente mayoritario de un tipo de materiales de interés farmacéutico; las arcillas. Las arcillas han sido usadas en la elaboración de medicamentos desde el origen de la Farmacia y siguen siendo un material de elevado interés en la actualidad.

I.3.1- ARCILLAS

El término "arcilla" deriva del griego "argilos", cuya raíz ("argos") significa blanco. El diccionario de la Real Academia de la Lengua Española (RAE 2001), define arcilla como: "Tierra finamente dividida, constituida por agregados de silicatos de aluminio hidratados, que procede de la descomposición de minerales de aluminio, blanca cuando es pura y con coloraciones diversas según las impurezas que contiene". Profundizando en su concepto, encontramos dos criterios a tener en cuenta, uno granulométrico o textural, que define las arcillas como "partículas de dimensiones inferiores a 2 μm" y otro mineralógico que las define como "minerales estratificados o semi-estratificados hidratados" (Rautureau et al., 2004). El concepto de arcilla ha ido evolucionando a lo largo del tiempo. El tratado de Georg Bauer (al que se le conocía como Agrícola) "De Natura Fossilium" (1546) define a las arcillas como materiales finos, de comportamiento plástico, que se endurecen en el horno pero manteniendo su forma. Siglos después, Grim amplía el concepto definiéndolas como "sustancias terrosas y de grano fino, que presentan comportamiento plástico en presencia de agua, y que están formadas fundamentalmente por sílice, óxido de aluminio, agua y cantidades variables de hierro y metales alcalinos y alcalinotérreos" (Grim, 1968). Posteriormente, Bailey (Bailey, 1980) y Weaver (Weaver, 1989) manifestaron la dificultad que existe de combinar los requisitos granulométricos y mineralógicos en una misma definición de arcilla. La comisión de nomenclatura de la Asociación Internacional para el estudio de arcillas (AIPEA) y de la "Clay Mineral Society" (CMS) han definido a las arcillas como "un material natural, compuesto principalmente de minerales de pequeño tamaño de partícula (la mayor parte filosilicatos), que es generalmente plástico en presencia de una cantidad apropiada de agua, y que se endurece al secarse" (Guggenheim y Martin,

1995). Nótese que desde la definición dada por "Agrícola" hasta nuestros días, la noción y concepto de este material ha cambiado relativamente poco, y sigue siendo hoy día definido fundamentalmente por sus propiedades y no por su naturaleza.

Puesto que las arcillas están compuestas principalmente por un grupo de minerales denominados filosilicatos, muchos autores utilizan la denominación de "minerales de la arcilla" para referirse a los filosilicatos (Hurbult y Klein, 1991) y no resulta de extrañar que se solapen ambos términos. El Comité de Nomenclatura de la AIPEA utiliza el término de "minerales de la arcilla" tanto para referirse a los filosilicatos como a otros materiales presentes en fases minoritarias y coparticipes en las propiedades fisicoquímicas de la arcilla. Tales minerales se denominan "fases asociadas a los minerales de la arcilla" e incluyen el cuarzo, feldespato, calcita y dolomita.

I.3.2. FILOSILICATOS

El término filosilicato deriva de la palabra griega *phullon*, hoja, y de la latina *silex*, sílice. Éstos minerales están constituidos esencialmente por estratos tetraédricos y octaédricos, dispuestos regularmente el uno del otro a lo largo del eje *c* (Figura I.15). Los estratos tetraédricos están formados por tetraedros de SiO_4^{4-}, en los que un átomo de Si se encuentra en el centro, equidistante de cuatro vértices de O (o grupos OH) (coordinación tetraédrica). Los tetraedros están dispuestos en anillos concatenados de seis unidades, en el que cada uno comparte tres de sus cuatros vértices. Estos anillos se repiten indefinidamente, dando lugar a la unidad $Si_2O_5^{2-}$ (Figura I.16a). La fórmula mineral del estrato tetraédrico se completa con grupos OH localizados en el centro de la mayor parte de los anillos para dar $Si_2O_5(OH)^{3-}$ (Figura I.16b). Los O no compartidos, que constituyen los vértices de los tetraedros están orientados todos en la misma dirección y la base de todos los tetraedros dispuestas en el mismo plano (Figura I.16c).

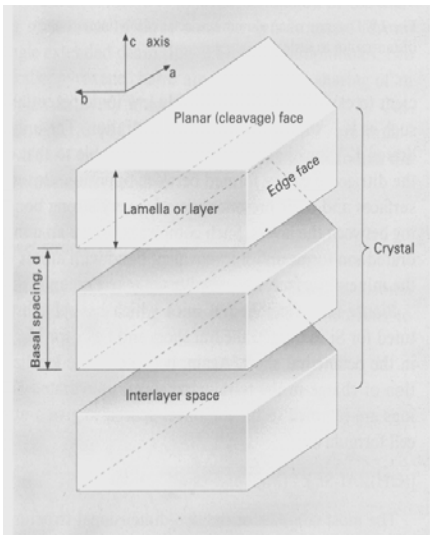

Terminología:

- **Plano de átomos** (O, OH, Si).
- **Estrato**: combinación de planos individuales de átomos (ej. estrato tetraédrico).
- **Lámina o Paquete**: combinación de estratos (ej. lamina TO, estrato tetraédrico y octaédrico consecutivos).
- **Cristal**: combinación de paquetes o láminas.
- **Interlámina**: espacio entre dos láminas sucesivas. Puede ser ocupado por agua, iones, moléculas orgánicas.
- **Espacio basal (d)**: parámetro característico de los fillosilicatos que deriva de la repetición de los planos de átomos a distancia regular en los cristales. Se considera constituido por la suma del paquete y la interlámina.

Figura I.15. Estructura general de los filosilicatos.

Para cada capa o estrato tetraédrico, podemos distinguir por tanto tres planos sucesivos de átomos: un plano de O, representado por las bases de los tetraedros; un plano de átomos de Si (en el que cada Si se encuentra en el punto de conjunción de tres O), y un plano de grupos hidroxilos, en el cual cada OH se encuentra en el ápice del tetraedro, directamente por encima de los átomos de Si (Grim, 1968).

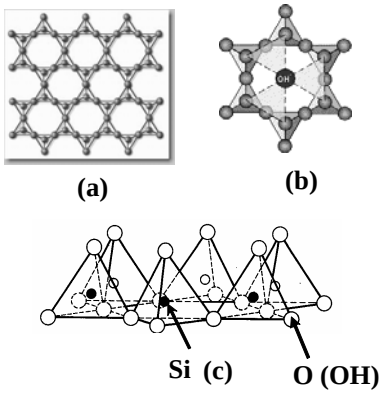

Figura I.16. Estrato tetraédrico.

Algunos átomos de O apicales y los grupos OH del estrato tetraédrico pueden unirse a cationes metálicos (Al^{3+}, Fe^{2+}, Fe^{3+}, Mg^{2+}) en coordinación octaédrica (equidistante de

O u OH). El estrato octaédrico está formado de modo que se encuentra constituido por dos planos de átomos de O u OH (Figura I.17).

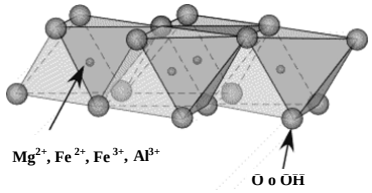

Figura I.17. Estrato octaédrico.

Con cationes divalentes (Mg^{2+}, Fe^{2+}) el estrato octaédrico asume la estructura de la brucita [$Mg(OH)_2$], mientras que con cationes trivalentes (Al^{3+}, Fe^{3+}) la de la gibbsita [$Al(OH)_3$]. En el primer caso, el catión ocupa todas las posiciones octaédricas disponibles (3/3) (filosilicatos trioctaédricos), mientras que en el segundo las posiciones ocupadas son sólo 2 de 3 (filosilicatos dioctaédricos).

Los estratos tetraédricos (T) y octaédricos (O) se asocian para formar paquetes estructurales, que pueden ser eléctricamente neutros o presentar una carga negativa, compensada por cationes no coordinados que se localizan en el espacio interlaminar.

Los principales criterios de clasificación para los filosilicatos (recomendados por la AIPEA) se basan en el tipo de apilamiento, tipo de catión en el estrato octaédrico, carga neta del paquete estructural y tipo de catión (moléculas o agua) en el espacio interlaminar. Según estos criterios, se clasifican de acuerdo a los tipos recogidos en la Tabla I.2.

Como sustancias naturales, las arcillas nunca están constituidas por un solo mineral. La denominación de la arcilla puede hacerse empleando en nombre del mineral mayoritario en ella (criterio seguido en el ámbito de la mineralogía) o con un nombre que informe de su calidad farmacéutica (criterio de Farmacopea), aunque en ambos casos no hay que perder de vista tanto la fase mineral mayoritaria en la sustancia como las fases asociadas (López Galindo et al., 2007). Con esta premisa, usaremos por sencillez la denominación arcilla cuando no sea necesario especificar más la composición o calidad de la sustancia en cuestión.

Tabla I.2. Clasificación de los filosilicatos de acuerdo con la AIPEA.

Tipo	Material interlaminar	Grupo	Subgrupo	Mineral (ejemplos)	Formula mineralógica
1:1	Ninguno o agua	Serpentina-Kaolinita (x ≡ 0)	Serpentinas	Crisotilo	$Al_2Si_2O_5(OH)_4$
			Kaolin	Kaolinita, Halloysita	$Mg_3Si_2O_5(OH)_4$
	Ninguno	Talco-Pirofilita (x ≡ 0)	Talco	Talco	$Mg_3Si_4O_{10}(OH)_2$
			Pirofilita	Pirofilita	$Al_2Si_4O_{10}(OH)_2$
2:1	Cationes hidratados intercambiables	Esmectita (x ≡ 0.2-0.6)	Saponita	Saponita, Hectorita	$Ca_{0.25}Si_4$ $(Mg_{2.5})Li_{0.5})O_{10}(OH)_2nH_2O$
			Montmorillonita	Montmorillonita, Nontronita	$(Na,Ca)(Al,Mg)_2(Si_4O_{10})(OH)_2nH_2O$
		Vermiculita (x ≡ 0.6-0.9)	Vermiculitas dioctaédricas	Vermiculitas dioctaédricas	
			Vermiculitas trioctaédricas	Vermiculitas trioctaédricas	$Ca_{0.65}(Si_{2.86}Al_{1.14})(Mg_{2.83}Al_{0.15}Fe_{0.01})O_{10}(OH)_2nH_2O$
	Cationes no hidratados	Mica (x ≡ 0.5-1)	Micas dioctaédricas	Moscovita, Paragonita	$KAl_2(Al, Si_3O_{10})(OH)_2$
			Micas trioctaédricas	Biotita, Lepiolita	$K(Fe,Mg)_3(Al,Si_3)O_{10}(OH)_2$
		Mica frágil (x ≡ 2)	Micas frágiles dioctaédricas	Margarita	$Ca(Si_2Al_2)Al_2O_{10}(OH)_2$
			Micas frágiles trioctaédricas	Clintonita	$Ca(Mg,Al)_3(Al_3Si)O_{10}(OH)_2$
	Hidróxidos	Clorita x variable	Cloritas Dioactaédricas	Donbassita	$Al_2(Al_{2.33})(Si_3AlO_{10})_4(OH)_8$
			Cloritas Di, Trioctaedricas	Cookeita	Li, $Al_4(Si_3Al)O_{10}(OH)_8$
			Cloritas Trioctaedricas	Clinochloro	$(Fe,Mg,Al)_6(Si, Al)_4O_{10}(OH)_8Si_{12}O_{30}$
	Ninguno	Sepiolita-Palygorskita (x variable)	Sepiolitas	Sepiolita	$Mg_8(OH)_4(OH_2)8H_2O$
			Palygorskitas	Palygorskita	$(Mg,Fe,Al)_5Si_8O_{20}(OH)_2(OH_2)4H_2O$

X = carga por unidad de fórmula

Las arcillas (en particular la caolinita, talco, esmectitas y las arcillas fibrosas) son excipientes de uso común en la formulación de formas farmacéuticas (sólidas, líquidas y semisólidas) para uso tópico y sistémico (López-Galindo et al., 2007; Viseras et al., 2007). Además son usadas como antiácidos y antidiarreicos en muchas especialidades publicitarias (Braun, 1994). Entre las esmectitas se utilizan la saponita y la montmorillonita, las cuales en el campo farmacéutico son conocidas como "bentonitas".

Las monografías de éstos materiales están incluidas en las principales farmacopeas En la Tabla I.3 se señalan las arcillas utilizadas en el campo farmacéutico, con sus respectivas denominaciones farmacéuticas, químicas y algunos de los nombres comunes más frecuentes. Se debe considerar algunas discrepancias entre la denominación mineralógica y la farmacéutica (López Galindo et al., 2007; Rowe et al., 2013). No obstante, por lo que se refiere a esta Tesis, basta señalar que una muestra de arcilla constituida principalmente por montmorillonita se denomina Bentonita en el ámbito farmacéutico.

Tabla I.3. Denominaciones de los minerales de la arcilla usados en el campo farmacéutico.

Especie Mineral	Formula molecular teórica	Nombre farmacéutico		Nombre químico (nº de CAS)	Nombre común
		EP	USP		
Caolinita	$Al_2H_4O_9Si_2$	Caolín, Heavy	Kaolin	Silicato de aluminio hidratado (1332-58-7)	Arcilla china, *Bolus Alba*
Talco	$Mg_6(Si_2O_5)_4(OH)_4$	Talco		Talco (14807-96-6)	Piedra-jabón, esteatita, polvo de talco
Montmorillonita	$(Na,K,Mg)_{0.33}(Al,Mg)_2Si_4O_8(OH)_2 \cdot nH_2O$	Bentonita		Bentonita (1302-78-9)	Jabón mineral, Taylorita, Wilkinita, Veegum®HS, Albagel®, Coloide Mineral
			Bentonita Purificada	Bentonita purificada (1302-78-9)	
Saponita	$MgAl_2(SiO_4)_2$	Silicato Aluminico Magnésico	Silicato Magnésico Alumínico	Silicato de Al y Mg(12511-31-8), Silicato de Mg y Al (1327-43-1)	Veegum®R-K-HV-F, Carrisorb®, Gelsorb®, Complejo coloideal
Hectorita*	$(Na)_{0.3}(Li,Mg)_3Si_4O_{10}(F,OH)_2$	Hectorita		Hectorita (12173-47-6)	Hectabrite, Laponite
Palygorskita	$MgAl_2O_8Si_2$		Atapulgita y Atapulgita Coloidal Activada	Atapulgita (12174-11-7)	Attapulgita, Attasorb®, Pharmasorb®
Sepiolita	$2Mg_2O.3SiO_2.X\ H_2O$	Trisilicato magnésico y Silicato Magnésico		Trisilicato de Mg hidrato (14987-04-3) Silicato de Mg (1343-88-0)	Acido silícico, Sal de Mg hidrato, Parasepiolita, Espuma de mar, Talco plastico

*La hectorita no tiene monografía en ninguna farmacopea, pero aparece recogida en la última edición del Handbook of Pharmaceutical Excipients (Rowe et al., 2013).

I.3.3. ESMECTITAS

El término ESMECTITAS se refiere a un grupo de filosilicatos, anteriormente conocido como "montmorillonita". La nueva denominación fue introducida por la AIPEA para resolver la ambigüedad del término montmorillonita, que era usado para indicar tanto el nombre del grupo, como el de las especies minerales individuales dentro del grupo (Brindley y Pedro, 1976). En el campo farmacéutico se distinguen la montmorillonita ("bentonita" en las principales Farmacopeas) y la saponita (silicato de Al y Mg o silicato de Mg y Al). En las esmectitas, los vértices de los tetraedros están todos orientados hacia el centro del paquete T/O/T, donde se unen a los grupos hidroxilos del estrato octaédrico, de modo que los grupos OH están compartidos por los dos estratos y en la interlámina aparecen cationes intercambiables, para neutralizar la carga negativa del paquete (Figura I.18).

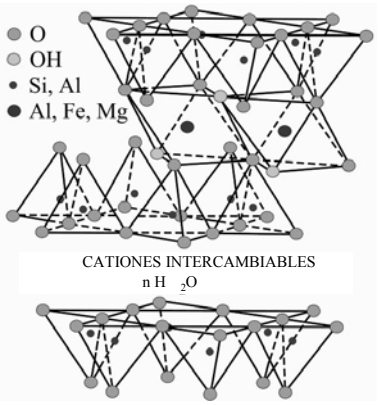

Figura I.18. Estructura de las esmectitas.

Una característica común de todas las esmectitas son las sustituciones isomórficas (cambio de un átomo con otro de similares dimensiones sin modificar la estructura cristalina) de los átomos de Si y Al en los estratos tetraédricos y octaédricos. En particular en los estratos tetraédricos el Si^{4+} puede estar sustituido por Al^{3+} (o más raramente por P^{3+}), mientras que para Al^{3+} en coordinación octaédrica son posibles las sustituciones con Mg^{2+} y/o Fe^{3+}, Zn^{2+}, Ni^{2+}, Li^{+}, etc. Como resultado de las distintas posibilidades aparecen minerales con composición y propiedades distintas. En la Tabla I.4 se muestran las formulas de algunas esmectitas, y sus respectivas denominaciones.

Tabla I.4. Formulas moleculares de algunas esmectitas.

	Dioctaédricas
Montmorillonita	$(OH)_4Si_8(Al_{3.34}Mg_{0.66})O_{20}$
Beidellita	$(OH)_4Si_8(Al_{6.34}Mg_{1.66})Al_{4.34}O_{20}$
Nontronita	$(OH)_4(Si_{7.34}Al_{0.66})Fe^{3+}_{4.34}O_{20}$
	Trioctaédricas
Hectorita	$(OH)_4Si_8(Mg_{5.34}Li_{0.66})O_{20}$
Saponita	$(OH)_4(Si_{7.34}Al_{0.66})Mg_6O_{20}$

La sustitución de Si^{4+} y Al^{3+} con átomos de valencia inferiores genera la deficiencia de carga en la red cristalina, y como resultado una carga negativa neta de los paquetes T/O/T (aproximadamente 0,2-0,6 por unidad de fórmula). El tipo de catión que viene retenido en la interlámina para compensar la carga negativa influye en el contenido de agua interlaminar y por lo tanto también en la dimensión del espacio basal (d_{001}) de la esmectita. En ausencia de moléculas de agua o de otras moléculas polares en el espacio interlaminar, el espacio basal de la montmorillonita mide alrededor de 0,94 nm (Fornes y Paul, 2003). En las esmectitas que contienen cationes divalentes (predominantemente Mg^{2+} o Ca^{2+}) la presencia de dos moléculas de agua interlaminares da como resultado un espacio basal entorno a 1,4-1,5 nm, mientras que las esmectitas con cationes monovalentes (Na^{+}) y una sola molécula de agua el espacio basal es de alrededor de 1,2 nm, siendo 0,96 nm en el caso de la montmorillonita sódica anhidra (Van Olphen, 1963). Mientras el espacio interlaminar de la montmorillonita es un parámetro cristalográfico bien definido, las dimensiones laterales de las láminas no lo son, dado que dependen de las condiciones en las que han crecido en los procesos geológicos que las han formado. El área de la lámina, A, y su raíz cuadrada viene por tanto normalizada respecto al espesor (t) (Figura I.19). Puesto que t es aproximadamente 1 nm, la Figura I.6 muestra que la dimensión lateral más probable en el rango de 100-200 nm.

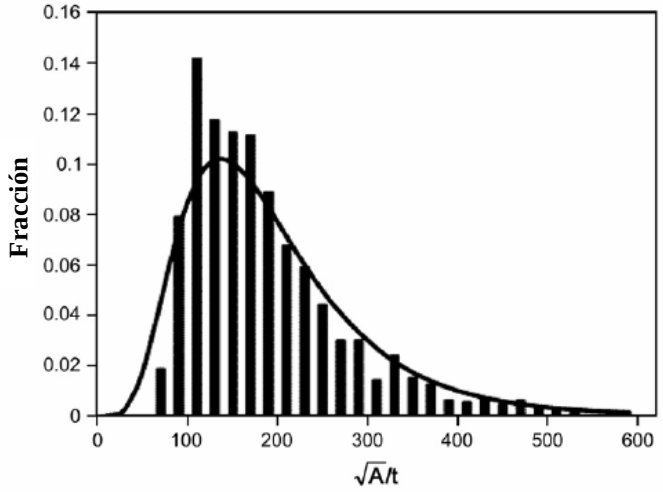

Figura I.19. Distribución de la dimensión lateral de la lámina en la montmorillonita sódica nativa (modificada de Ploehn y Liu, 2006).

La formula de la montmorillonita es $(Si_{7.8}\,Al_{0.2})_{IV}(Al_{3.4}Mg_{0.6})_{VI}O_{20}(OH)_4$ con sustitución de Si^{4+} por Al^{3+} en la capa tetraédrica y de Al^{3+} por Mg^{2+} en la octaédrica. Su composición teórica es SiO_2, 66.7%, Al_2O_3, 28.3%, H_2O, 5%. La carga neta de la capa de montmorillonita es: [7.8(+4)]+[0.2(+3)]+[3.4 (+3)]+[0.6(+2)]+[20(-2)]+[4(-1)]= -0.8 carga/celda unidad. El resultado neto es negativo y es equilibrado por cationes intercambiables presentes en las interláminas, así como alrededor de sus bordes (Bhattacharyya y Gupta, 2008).

Como resultado de la presencia de cationes interlaminares, la montmorillonita se comporta como un intercambiador de cationes, que pueden ser fármacos básicos en solución. Junto con este mecanismo principal, otros posibles mecanismos de interacción son descritos en la Tabla I.5.

Tabla I.5. Interacciones entre arcillas y componentes orgánicos (Aguzzi et al., 2007).

Mecanismo	Ejemplos de minerales	Grupos funcionales orgánicos
Interacciones hidrofóbicas (van der Waals)	Caolinita, esmectitas	Sin carga, no polares (ej: aromáticos)
Puentes de hidrógeno	Caolinita	Aminas, carbonilos, carboxilos
Protonación	Bordes de aluminiosilicato, óxidos de Fe y Al, alofano, imogolita	Aminas, carbonilos, carboxilato, heterociclo con N
Intercambio catiónico (sitios cargados permanentes)	Esmectita, vermiculita, ilita	Aminas, heterociclo con N
Sitios cargados pH-dependiente (intercambio aniónico) frecuentemente)	Bordes de aluminiosilicato, óxidos de Fe y al., alofano, imogolita	Carboxilatos, aminas, anillo NH, heterocíclico de N
Enlaces catiónicos	Esmectitas, vermiculita, ilita	Carboxilatos, aminas, carbonilo, OH

La interacción de la montmorillonita con un fármaco protonado permite obtener un complejo susceptible de ser empleado en liberación modificada (Aguzzi et al., 2007) (Figura I.20*)*.

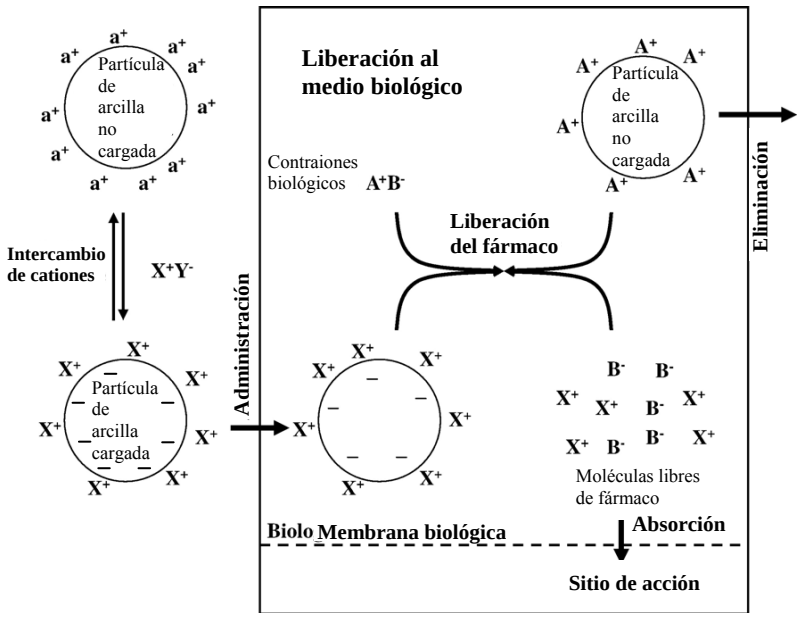

Figura I.20. Idealización de la formación de complejos fármaco-arcilla y mecanismos de liberación de fármacos (carga de la superficie de la arcilla (-), compensación de cationes (a^+), fármaco catiónico (X^+), fármaco asociado a aniones (Y^-), contra-iones in vivo (A^+), aniones asociados a los contra-iones (B^-) (modificada de Aguzzi et al., 2007).

En virtud de sus interacciones con fármacos de distinta naturaleza, la montmorillonita ha sido usada para el desarrollo de sistemas de liberación controlada y sitio específica de fármacos, aumento de la solubilidad del principio activo y de su estabilidad (Aguzzi et al., 2007).

I.3.4. MONTMORILLONITA EN LIBERACIÓN MODIFICADA

En los cinco años que han pasado desde que en 2007 el grupo de investigación en cuyo seno he realizado la tesis doctoral publicase una revisión titulada "Use of clays as drug delivery systems: Possibilities and limitations" (Aguzzi et al., 2007), esta ha recibido 120 citas (una media de 25 citas anuales). Una actualización de ese artículo de revisión llevada a cabo en 2010 con el título "Current challenges in clay minerals for drug delivery" ha sido citada otras 24 veces (Viseras et al., 2010). A la vista de estos datos, parece claro que el empleo de montmorillonita y otros minerales de la arcilla en el

desarrollo de sistemas de liberación modificada de fármacos goza de plena salud y es un área de interés científico. Los artículos que han citado estas dos revisiones aparecen listados en el Anexo I de la tesis.

La montmorillonita, que había sido y sigue siendo usada como excipiente en formas farmacéuticas convencionales (disgregante de comprimidos y viscosizante en suspensiones), recibe en la última década especial atención como excipiente de formas farmacéuticas de liberación modificada, en virtud de sus propiedades. En particular resultan de interés su capacidad para retener principios activos por distintos mecanismos, su capacidad de hinchamiento en agua y su tamaño coloidal. La utilidad de las interacciones entre este excipiente y las moléculas de fármaco permite desarrollar sistemas de liberación prolongada, retardada y sitio específica, así como aumentar la velocidad de disolución en ocasiones o la estabilidad del principio activo (Aguzzi et al., 2007).

En la segunda revisión a la que anteriormente hacía referencia, y en la que tuve el honor de participar como coautora, se actualizaban los empleos de las arcillas en liberación modificada y se abordaban nuevas áreas de interés (Viseras et al., 2010). En particular, junto con la interacción de los filosilicatos naturales y/o sintéticos o modificados con principios activos, se consideraba su interacción con otros excipientes, en particular poliméricos, para constituir híbridos de interés en liberación modificada. Este aspecto entronca directamente con el tema de mi tesis doctoral. La formación de sistemas híbridos polímero/arcilla para la liberación modificada de fármacos y en concreto de nanocomposites polímero/arcilla fue revisada por nuestro grupo de investigación en el artículo “Biopolymer–clay nanocomposites for controlled drug delivery” (Viseras et al., 2008a) y a partir de ella se ha abordado en el primer apartado de esta introducción de tesis.

I.4. OXITETRACICLINA

La oxitetraciclina clorhidrato (Figura I.21) es un antibiótico semisintético de amplio espectro dentro de la familia de las tetraciclinas, producido a partir de cultivos de *Streptomyces aureofaciens, Streptomyces rimosus* y *Streptomyces viridofaciens*. Es una sustancia cristalina, inodora, de sabor amargo y color amarrillo y presenta características físicas, químicas y farmacológicas comunes a otras moléculas de ésta clase química (Dollery, 1999; Katzung, 1997; Sun, 2004).

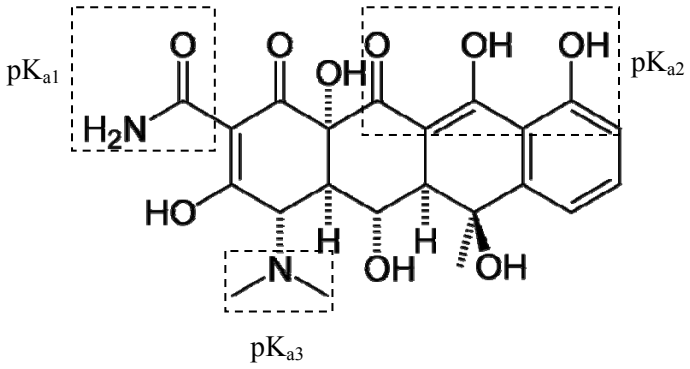

Figura I.20. Estructura química de la oxitetraciclina.

Posee carácter anfótero con un punto isoeléctrico alrededor de 5. Las principales propiedades físico-químicas se muestran en la Tabla I.6, dónde se observa que la oxitetraciclina presenta tres valores de pK_a que corresponden a los grupos indicados en la Figura I.10.

Tabla I.6. Propiedades físico-químicas de la oxitetraciclina (de Oleszczuk y Xing, 2011).

	S	pK_a			PM	Log K_{ow}
		pK_{a1}	pK_{a2}	pK_{a3}		
Oxitetraciclina	121	3.27	7.32	9.11	460.4	- 2.078

S= solubilidad (mg L^{-1}), PM=peso molecular (g mol^{-1}), Log K_{ow}= coeficiente de partición octanol-agua

En medio ácido diluido la oxitetraciclina clorhidrato sufre una reacción de deshidratación y se degrada a anidrositetraciclina; el medio ácido también promueve la epimerización del presente grupo dimetilamino en el C_4, reacción que convierte el compuesto de partida en la 4-epiositetraciclina (De Liguoro et al., 2003). Todos estos

productos de degradación son inactivos como antibacterianos. Es capaz de formar fácilmente sales cristalinas tanto con ácidos como con bases fuertes (gracias al carácter anfótero). Los grupos ácidos son capaces de formar sales para la quelación con iones metálicos polivalentes (Fe^{2+}, Al^{3+}, Ca^{2+}, Mg^{2+}), dando lugar a quelatos, insolubles a pH neutro.

La oxitetraciclina es un antibiótico de amplio espectro. Posee actividad bacteriostática contra numerosas bacterias gram-positivas y gram-negativas, incluyendo algunos anaerobios y microorganismos patógenos resistentes a agentes antimicrobianos capaces de inhibir la síntesis de la pared celular (Chopra et al., 2001). Es activa frente a rickettsia, clamidia, micoplasmas y algunos protozoos, como por ejemplo las amebas. Su mecanismo de acción implica la entrada de la oxitetraciclina en los microorganismos por transporte activo y difusión pasiva, para una vez dentro unirse a la subunidad 30s de los ribosomas bacterianos causando el bloqueo del enlace del aminoacil-tRNA al sitio receptor en el complejo ARN_m-ribosoma. Como consecuencia, se bloquea la adición de nuevos aminoácidos a la cadena peptídica naciente, con inhibición de la síntesis proteica. Las células de los mamíferos carecen del sistema de transporte activo de la oxitetraciclina y por tanto, en los seres humanos, el bloqueo de la síntesis proteica se produce sólo en presencia de elevadas concentraciones de fármaco. Entre las bacterias gram-negativas (*Pseudomonas*, *Proteus* y coliformes) existen tipos altamente resistentes, para las cuales la oxitetraciclina ha perdido utilidad. Debido al uso indiscriminado, la resistencia está aumentando también para las especies que en un principio eran altamente sensibles (como por ejemplo pneumococos). Los mecanismos de resistencia principales son los siguientes: (a) carecer de un mecanismo de transporte activo a través de la membrana celular, lo que provoca una reducción de la acumulación intracelular de fármaco; (b) síntesis de proteínas que interfieren con la unión de la oxitetraciclina a los ribosomas; (c) inactivación enzimática.

Cuando se administra por vía oral, la oxitetraciclina es absorbida irregularmente en el tracto gastrointestinal y una parte del fármaco queda en el lumen intestinal donde modifica la flora intestinal, siendo excretada con las heces. Un porcentaje que varía en el intervalo 60-80% se absorbe, principalmente en la parte superior del intestino delgado. La absorción aumenta en ayunas y disminuye por quelación con cationes bivalentes o con Al^{3+} presentes en la leche y antiácidos. Una vez en el torrente circulatorio, el 40-80% de la oxitetraciclina absorbida es ligada a proteínas plasmáticas.

Por vía oral con dosis de 500 mg cada 6 horas, se producen niveles plasmáticos de 4-6 μg/mL. La oxitetraciclina se distribuye ampliamente en los tejidos y fluidos corporales con excepción del líquido cefalorraquídeo. Atraviesa la placenta, pudiendo llegar al feto y es excretada con la leche. Por otra parte, por quelación con el calcio, la oxitetraciclina se deposita en los huesos en crecimiento y en los dientes de los niños, causando decoloración y displasia en el esmalte. Un tratamiento prolongado puede conducir a deformidades e inhibición del crecimiento óseo si se administra a niños menores de 8 años. La oxitetraciclina se excreta mayormente por la bilis y la orina, no obstante un porcentaje entre el 10 y el 40% se puede excretar con las heces. A través de la circulación enterohepática una parte del fármaco excretado en la bilis es reabsorbido.

La oxitetraciclina es usada como fármaco de primera elección en infecciones de *mycoplasma pneumonae*, clamidias, rickettsias y algunas espiroquetas. Puede ser usada para la profilaxis de la malaria, a dosis bajas en la terapia oral para el acné, tratamiento de úlceras duodenales y gástricas causadas por *Helicobacter pylori*, infecciones de las vías aéreas y oftálmicas, enfermedades de transmisión sexual, prevención de diarrea del viajero, shigelosis, cólera, brucelosis y borelosis. La oxitetraciclina por su amplio espectro, también ha sido ampliamente utilizada en veterinaria en los países en vía de desarrollo para el tratamiento y la prevención de infecciones bacterianas (Pérez-Silva et al., 2012), así como en alimentación animal para promover el crecimiento, contribuyendo a un aumento de la difusión de la resistencia al fármaco (Sponza et al., 2012).

Los efectos colaterales son causados por toxicidad directa del fármaco o por alteraciones de la flora bacteriana. A menudo causa nauseas, vómitos y diarrea por irritación local del tracto intestinal. Puede alterar la función hepática, especialmente durante el embarazo o si el paciente presenta insuficiencia hepática o la dosis administrada es elevada. La administración concomitante con diuréticos puede promover la retención de compuestos del nitrógeno y agravar la azoemia. La oxitetraciclina puede causar tromboflebitis si se administra por vía intravenosa, por lo que se prefiere la vía oral. La administración intramuscular es dolorosa debido probablemente a la formación de complejos insolubles. Otro efecto colateral es la fototoxicidad: ya que la oxitetraciclina absorbe luz en el visible pudiendo generar radicales libres por lo que individuos particularmente sensibles (en particular personas con piel clara) pueden desarrollar eritemas graves después de la exposición solar.

CAPÍTULO II.

Objetivo y plan de trabajo

II. 1- Objetivo

La oxitetraciclina es un antibiótico de amplio espectro con actividad bacteriostática. Su absorción en el tracto gastrointestinal es incompleta. Como resultado, son necesarias altas dosis para obtener concentraciones plasmáticas efectivas por vía oral para el tratamiento de infecciones sistémicas, y una elevada fracción de la dosis administrada es excretada inalterada en las heces. La baja biodisponibilidad oral de la oxitetraciclina es debida al efecto limitante de su absorción inducido por la glicoproteina P (Schrickx et al., 2007). Una estrategia útil para aumentar su biodisponibilidad es el desarrollo de un nanocomposite que actúe como nanotransportador aumentando la permeabilidad del fármaco y con ella su biodisponibilidad, reduciendo la interacción entre el fármaco y la glicoproteina P, ya que la absorción del fármaco transportado en el nanocomposite tendría lugar principalmente por transcritosis.

Con estas premisas, conocidas las propiedades del quitosano y de la montmorillonita para formar nanocomposites con capacidad para retener y liberar fármacos, se planteó el desarrollo de nanocomposites con estos excipientes y su dosificación con oxitetraciclina, determinando las propiedades biofarmacéuticas de los nanocomposites cargados mediante el empleo de células Caco-2, que permiten reproducir las condiciones de la barrera intestinal. Asimismo, y dado que los transportadores nanotecnológicos se consideran, en el ámbito de los medicamentos basados en nanotecnología, como sistemas que deben demostrar su seguridad, con independencia de los componentes usados en su desarrollo (http://www.emea.eu.int/htms/human/itf/itfguide.htm), se realizaron estudios de citotoxicidad específicos con los nanocomposites obtenidos.

Los objetivos específicos de la tesis son:

1. Actualizar el conocimiento sobre el empleo de los excipientes empleados en esta tesis para el desarrollo de nanocomposites con propiedades mejoradas respecto a las de los componentes por separado.
2. Preparar nanocomposites con quitosano y montmorillonita.
3. Caracterizar los nanocomposites obtenidos incluyendo su estructura, mecanismos de interacción y propiedades que determinan su eficacia como sistemas para transporte de fármacos, en particular mediante estudios de mucoadhesión.

4. Determinar la seguridad de empleo de los nanocomposites de quitosano y montmorillonita mediante estudios de citotoxicidad.
5. Dosificar los nanocomposites con oxitetraciclina, valorando la cantidad de fármaco retenido y el mecanismo de interacción.
6. Caracterizar los complejos oxitetraciclina-nanocomposite, incluyendo estudios de permeabilidad con células Caco-2 para evaluar su eficacia como sistemas capaces de mejorar el perfil biofarmacéutico del fármaco.
7. Determinar la seguridad de empleo de los complejos oxitetraciclina-nanocomposite mediante estudios de citotoxicidad.

II. 2- Plan de trabajo

De acuerdo con los objetivos citados con anterioridad, el plan de trabajo de la tesis doctoral se organizó en los siguientes apartados, correspondientes a capítulos en esta memoria de tesis:

Capítulo III. El empleo como excipientes farmacéuticos de los excipientes usados en esta tesis en aplicaciones convencionales es sobradamente conocido. No obstante, su uso en el desarrollo de sistemas híbridos de tipo nanocomposite que presenten propiedades significativamente mejoradas respecto de los componentes por separado requiere de una revisión y actualización de los conocimientos que consideramos el primer paso del método científico para el desarrollo galénico de estos sistemas nanotecnológicos de interés farmacéutico. En este apartado de la tesis se da cumplimento al primer objetivo planteado.

Viseras, C., Cerezo, P., Sanchez, R., Salcedo, I. y Aguzzi, C. (2010). Current challenges in clay minerals for drug delivery. Appl. Clay Sci. 48, 291–295.

Capítulo IV. En este capítulo se aborda el objetivo 2 de la tesis. En concreto se puso a punto el método de obtención de los nanocomposites de quitosano y montmorillonita mediante estudios de adsorción. En el artículo publicado junto con los estudios propiamente dirigidos a la obtención de nanocomposites de quitosano y montmorillonita,

se abordaban estudios con otros silicatos, incluyendo un polimorfo de la caolinita (halloysita) y su dosificación con ácido 5 amino salicílico, que no obstante no son parte de los objetivos propiamente dichos de esta tesis doctoral.

Aguzzi, C., Capra; P., Bonferoni, C., Cerezo, P., Salcedo, I., Sánchez, R., Caramella, C. y Viseras, C. (2010). Chitosan–silicate biocomposites to be used in modified drug release of 5-aminosalicylic acid (5-ASA). Appl. Clay Sci. 50, 106–111.

Capítulo V. En este capítulo se abordan los objetivos 3 y 4 de la tesis doctoral. En concreto, estudian las propiedades de los nanocomposites de quitosano y montmorillonita que determinan su eficacia en la mejora de la biodisponibilidad de fármacos (mucoadhesión) y seguridad de empleo (citotoxicidad).

Salcedo, I., Aguzzi, C., Sandri, G., Bonferoni, M.C., Mori, M., Cerezo, P., Sánchez, R., Viseras, C. y Caramella, C. (2012). In vitro biocompatibility and mucoadhesion of montmorillonite chitosan nanocomposite: A new drug delivery. Appl. Clay Sci. 55, 131–137.

Capítulo VI. Este capítulo se centra en los objetivos 5, 6 y 7 de la tesis doctoral. En el se lleva a cabo la dosificación de los nanocomposites de quitosano y montmorillonita con el antibiótico, la caracterización de la interacción de los componentes y los estudios de permeabilidad en células Caco-2 (eficacia) y citotoxicidad (seguridad).

Salcedo, I., Sandri, G., Aguzzi, C., Bonferoni, M.C., Cerezo, P., Viseras, C. y Caramella, C. Permeability of oxytetracycline from chitosan-montmorillonite nanocomposites. (En preparación).

CAPÍTULO III.

Current challenges in clay minerals for drug delivery

A B S T R A C T

This study reviews current challenges of clay minerals for drug delivery. Clay minerals are widely used in conventional pharmaceutical dosage forms both as excipients and active agents. Clay minerals may interact with drug molecules, but also with inactive components of medicinal products such as polymers. On the basis of these interactions, clay minerals and their modified forms can be effectively used to modify drug delivery systems. In this research area, recent advances include the use of montmorillonite and saponite to retain drug molecules and control their release. Synthetic analogues such as Laponite and layered double hydroxides are also being used for biopharmaceutical and technological purposes. Another interesting strategy is the preparation of composites with clay mineral particles in polymeric matrices to obtain different systems (films, nanoparticles, hydrogels, matrices…) with improved pharmaceutical properties compared to the single components.

III.1- INTRODUCTION

Clays and clay minerals play an important role in the field of health products. They can be considered as raw pharmaceutical materials that once evaluated and/or modified to fulfil regulatory pharmacopoeial requirements may achieve the status of pharmaceutical substances suitable for use in the manufacture of medicinal products (López-Galindo et al., 2007). The progression from raw material, to pharmaceutical grade substance, and finally to pharmaceutical forms suitable for administration to the body is achieved first through general pharmaceutical operations to adjust the material grade, and then by specific pharmaceutical operations leading to the final dosage form (Figure III.1).

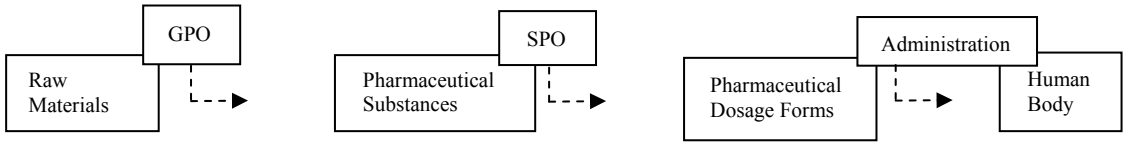

Figure III.1. Phases in the manufacture of medicinal products from raw materials (GPO: general pharmaceutical operations; SPO: specific pharmaceutical operations).

Consequently, clay minerals are fundamental components in several medicinal products, where they are used as excipients and fulfil some technological function (López-Galindo and Viseras, 2004). Table 1 shows the administration routes and dosage forms of clay minerals used as excipient in currently commercialized pharmaceutical products in the USA (FDA, 2009).

Table III.1. Inactive clay/clay mineral ingredients in pharmaceutical dosage forms (FDA, 2009).

Clay/clay mineral	Route of administration	Dosage form
Talc	Oral	Solid (conventional and modified release capsules and tablets, chewable tablets and granules) Liquid (drops, mucilage, solutions, elixir, suspensions and syrups)
Activated Attapulgite Bentonite	Buccal Sublingual Topical Rectal Oral Oral	Chewing gums and tablets Tablets Lotions, ointments and powders Tablets Powder Solid (capsules and tablets)
Magnesium Aluminium Silicate (MAS)	Topical Transdermal Rectal Vaginal Oral	Lotions, powders and suspensions Films and patches Suspensions Ovules Solid (conventional and modified tablets, granules, capsules, chewable tablets and powders)
Magnesium trisilicate Kaolin	Topical Rectal Vaginal Oral Oral Topical	Liquid (drops, suspensions and syrups) Emulsions, creams, lotions and suspensions Suspensions Ointments Conventional, modified and chewable tablets Solid (conventional and modified tablets and capsules, powders) Liquid (syrups) Controlled release films

*Magnesium trisilicate is the pharmaceutical denomination of sepiolite

Clay minerals are also used in pharmacy because of their biological activity, that is, as active substances or drugs (López-Galindo and Viseras, 2004). Pharmacological functions of clay minerals as active substances are summarized in Table III.2. As observed, clay minerals are mainly used in the treatment of gastrointestinal and topical diseases.

Table III.2. Therapeutic uses of clays/clay minerals (modified from López-Galindo and Viseras, 2004).

Clay/clay mineral	**Kaolin**	**Bentonite and MAS**	**Talc**	**Attapulgite and magnesium Trisilicate***
Therapeutic use	Antidiarrhoeal Gastrointestinal protector Anti-inflammatory Antacid Homeophatic product	Antidiarrhoeal Gastrointestinal protector Antipruritic Antacid	Anti-haemorrhoids Anti-rubbing Pleurodesis	Antidiarrhoeal Antacid

*Magnesium trisilicate is the pharmaceutical denomination of sepiolite

III.2- THE NEED FOR MODIFIED DRUG DELIVERY SYSTEMS

Besides these classic pharmaceutical uses, clay minerals may be effectively used in the development of new drug delivery systems (DDS). Strictly speaking, all pharmaceutical dosage forms are DDS, as they are used to administer drugs meant to reach the site of action and maintain a certain concentration during treatment. However, the ultimate therapeutic effect of a pharmaceutical treatment will depend on several factors (Figure III. 2).

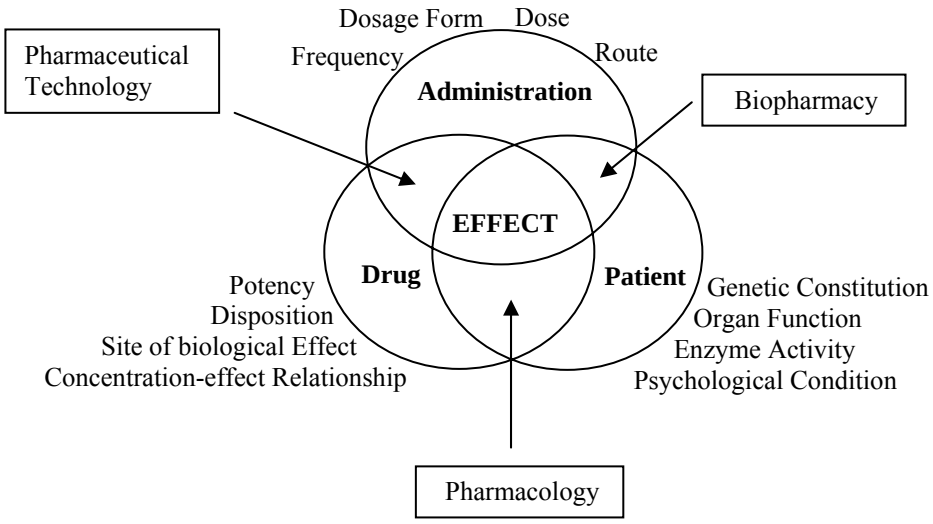

Figure III.2. Pharmaceutical treatment: determining elements (drug, administration and patient), study areas (Pharmacology, Pharmaceutical Technology and Biopharmacy) and variables affecting the final therapeutic effect.

Some concern the drug itself, such as potency, disposition (distribution and elimination) in the body, site of biological effect or concentration–effect relationship; others concern the patient, such as genetic constitution, organ function, and so on. A third group of factors concern pharmaceutical considerations such as optimal dosage forms and route of administration, frequency and dose of drug in the dosage forms, etc. Pharmacology studies the effect of a drug on a patient. Pharmaceutical technology works in the area between the drug and the dosage form, selecting and preparing the most adequate pharmaceutical product. Finally, biopharmacy studies the evolution of a dosage form (and the drug that it contains) after administration to the patient.

As might be expected, the intensity of the therapeutic effect will depend firstly on drug concentration at the site of action. Consequently, in drug therapy, it is very important to provide therapeutic levels of drug to the site of action (or at least in the blood) and maintain them during the treatment (Ding et al., 2002). Furthermore, it is desirable to minimize temporal variations in drug concentration by using some modified drug delivery system to avoid periods of overdosing or underdosing (Directive 75/318/EEC, 1992). As Fig. 3 shows, there is a direct relationship between drug release from the DDS and drug concentration in plasma.

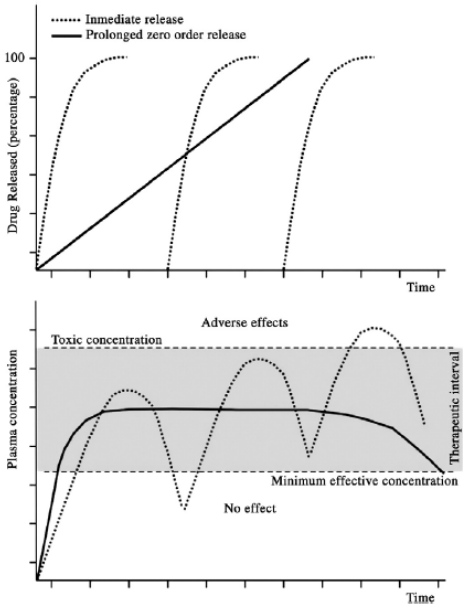

Figure III.3. Correlation between drug release profiles and plasma concentrations.

Consequently, pharmaceutical products evolve through modification of drug delivery systems (MDDS). The modifications involve changes in the rate and/or the time of release and/or the site of release, compared to conventional pharmaceutical dosage forms. These changes are achievable by several possible mechanisms, including modifications in pharmaceutical formulations and/or method of preparation (EP 6.0 2008; USP 31, 2008). At the moment, there are several pharmaceutical products on the market that modify the release of the drug by one of these mechanisms. In almost all these new pharmaceutical products, new excipients with specific targets must be included, as for example decreasing or increasing dissolution rate, delaying drug release, targeting drug release (biopharmaceutical targets), prevention or reduction of side effects (pharmacological targets), taste masking or increasing stability (technological targets). Clay minerals as recognized pharmaceutical excipients may be used in these new pharmaceutical products.

III.3- RECENT ADVANCES OF CLAY MINERALS IN MODIFIED DRUG DELIVERY SYSTEMS

Clay minerals have been proposed as fundamental constituents of several MDDS, with different purposes and acting through various mechanisms (Aguzzi et al., 2007). At this new frontier in the development of pharmaceutical dosage forms, these uses of clay minerals are changing very quickly, and new applications and clay minerals are continuously being proposed. Since the fully comprehensive review published by Aguzzi et al. (2007), some interesting advances have emerged that will be discussed below.

III.3.1- CLAY MINERALS AND SYNTHETIC CLAY MINERALS

The most recent examples of clay minerals use in MDDS include ibuprofen release control by interaction with montmorillonite (Zheng et al., 2007) and intercalation of Donepezil, a well-known drug for Alzheimer's disease, in montmorillonite, saponite or Laponite (Park et al., 2008). These studies characterized the clay mineral–drug interaction products and then examined the drug release kinetics. In all cases, drug

release depended on the method of preparation of the interaction products, and was affected by changes in the pH of the dissolution medium. In the case of donezepil, biphasic release patterns were found, consisting of an initial burst effect followed by slow release of the drug. Other examples of drugs effectively carried by clay minerals include nicotine (Pongjanyakul et al., 2009) and timolol (Joshi et al., 2009). Nicotine, a volatile liquid widely used in smoking cessation therapy to relieve addiction symptoms, has been carried by magnesium aluminium silicate to reduce drug evaporation and modulate drug release behaviour (Pongjanyakul et al., 2009). The pH determined the amount of drug retained and the release patterns, and cation exchange seemed to be the principal interaction mechanism. Magnesium aluminium silicate is a pharmaceutical denomination of a natural clay material mainly consisting of montmorillonite and saponite (López-Galindo and Viseras, 2004). Timolol was loaded on montmorillonite, but the release of the drug did not reach 100%. This is one of the main problems to be avoided. A release of 100% dose for oral MDDS cannot last over 24 h and, ideally, should take place within the first 12 h (Directive 75/318/EEC, 1992). Magnesium aluminium silicate has been also used to retain propranolol (a β-blocking agent) and release patterns have been correlated to particle size, drug loading, and release medium (Rojtanatanya and Pongjanyakul, 2008). Other authors compare results from natural and synthetic silicates. For example, montmorillonite and a siliceous mesoporous synthetic material have been loaded with sertraline (an antidepressive drug). The resultant complexes showed very different release profiles because of their diverse interaction mechanisms, resulting in different therapeutic indications for each system (Nunes et al., 2007).

Layered double hydroxides (LDHs), also known as hydrotalcite like compounds, are layered solids with positively charged layers and charge-balancing anions in the interlayer space. Their cationic layered framework leads to safe accommodation of many biologically important molecules including genes or drugs (Choy et al., 2007). In recent years, layered double hydroxides with different cations in the layers and consequently diverse exchangeable characteristics have been used to obtain interaction products with several non-steroid anti-inflammatory drugs (mefenamic and meclofenamic acids and naproxen), leading to slow release profiles (Del Arco et al., 2007, 2009).

Drug release from MDDS must be carefully studied and if possible it is very interesting to determine the mechanism underlying the release kinetics. Frequently, drug molecules are retained by different mechanisms and consequently the kinetics of drug release are complex. For example, halloysite was used to retain mesalazine, an anti-inflammatory drug used in the treatment of inflammatory bowel disease (Viseras et al., 2008b, 2009). As a result of this interaction, drug molecules were included in both the clay mineral nanotubes and on the external surface of the clay mineral particles. Consequently, release kinetics was the sum of drug released from the surface of the particles and that retained in the tubes with a much slower release rate (Viseras, 2008).

III.3.2- CLAY MINERAL POLYMER COMPOSITES

A very interesting possibility is to use clay minerals polymer composites (CPC) to modify drug release. Several polymers are used in the modification of drug release, including hydrogels, soluble polymers, biodegradable and non-biodegradable hydrophobic polymers. Although clay mineral and polymers are frequently used in their pure form, a single polymer or clay mineral often does not meet all the requirements.

Preparation of CPC improves the properties of the single components; those of clay mineral particles alone (stability of clay mineral dispersions and changes in ion exchange behaviour) and, more frequently, those of the polymer (mechanical properties, swelling capacity, film forming abilities, rheological properties, bioadhesion or cellular uptake) (Viseras et al., 2008a; Meenach et al., 2009).

Recent examples of MDDS based on CPC include intercalation of montmorillonite particles in polylactic glycolic acid to obtain nanoparticles loaded with Docetaxel (an anticancer drug) (Si-Shen et al., 2009). The in vitro drug release profiles of these drug loaded nanoparticles showed prolonged release over 25 days. Moreover, the presence of a clay mineral enhanced cellular uptake efficiency of the nanoparticles by Caco-2 and HT-29 cells, prolonging the therapeutic effect of the drug. Campbell et al. (2008) prepared composites of a modified montmorillonite with poly(ethylene glycol) by hot melt extrusion for controlled release of paracetamol. The presence of clay mineral particles in the polymer matrix resulted in retarded drug diffusion and improved dissolution behaviour.

Sodium alginate and magnesium aluminium silicate were used to prepare films loaded with nicotine to be used in buccal release (Pongjanyakul and Suksri, 2009). CPC operated as microreservoirs in the films showing adhesion properties to mucosal membranes and allowing controlled release of the drug molecules. Composite films with the same components have also been used to coat tablets and control drug release (Pongjanyakul, 2009).

Electrostatic interaction between chitosan, a deacetylated derivative of chitin, consists of D-glucosamine and N-acetyl-D-glucosamine units, and magnesium aluminium silicate caused a change in flow behaviour and flocculation of the composite dispersions (Khunawattanakul, et al., 2008). Chitosan has also been used to prepare composites with montmorillonite for prolonged release and biomedical applications (Xiaoying et al., 2008). The resultant composites were added to calcium alginate solutions to obtain nanoparticles loaded with bovine serum albumin as protein model drug, combining the drug adsorption action and mucosa protection effect of the clay mineral with the mucoadhesive and permeability enhancing properties of the chitosan. Montmorillonite has also been used as additive to retard ibuprofen release from delivery systems prepared with lactic acid-grafted chitosan (Depan et al., 2009). More recently, composites of chitosan and montmorillonite have shown a synergic effect between the clay mineral and the polysaccharide regarding the ability to retain 5-aminosalicylic acid (an anti-inflammatory drug) but also in the control of drug release in acidic medium, when compared to interaction products prepared with the drug and the single components (Aguzzi et al., 2010).

III. 4- CONCLUDING REMARKS

Some “special” clay minerals are components of medicines, both as active and inactive ingredients, once processed to fulfill regulatory requirements. The particular properties of these pharmaceutical grade clay minerals can be also exploited in the development of new drug delivery systems, designed to provide therapeutic levels of drug to the site of action and maintain them throughout the treatment. In recent years, some interesting advances have been proposed by using natural, but also modified and synthetic phyllosilicates, on the basis of their interaction with drug molecules. Finally, composites prepared with different polymers and clay minerals are attracting great

attention in this pharmaceutical field because of their synergic characteristics regarding biopharmaceutical and technological features.

CAPÍTULO IV.

Chitosan–silicate biocomposites to be used in modified drug release of 5-aminosalicylic acid (5-ASA)

A B S T R A C T

Biocomposites of chitosan (CS) and montmorillonite (VHS) were prepared by solid–liquid interaction of the components. The resultant composites were characterized by thermal analysis and the cation exchange capacity of the clay mineral was compared to polysaccharide retention. The results showed that chitosan was effectively retained by montmorillonite particles through cation exchange.

IV.1- INTRODUCTION

Biopolymers and clay minerals are common ingredients in pharmaceutical products. Although they are frequently used in their pure form, a single polymer or clay mineral often does not meet all the requirements. A way to further extend their applications is to modify polymers by incorporation of inorganic fillers to obtain biocomposites with improved properties (Viseras et al., 2008a).

Recently, synthesis of micro and nanocomposites with clay minerals was proposed as a novel approach to modify some of the properties of polysaccharides, including swelling and water uptake (Pongjanyakul et al., 2005a), mechanical and thermal behaviour (Wang et al., 2005; Wu and Wu, 2006), rheology (Günister et al., 2007; Khunawattanakul et al., 2008) and bioadhesion (Pongjanyakul and Suksri, 2009).

Given these premises, we prepared and characterized composites of chitosan and pharmaceutical grade montmorillonite.

IV.2- MATERIALS AND METHODS

Biopolymer: chitosan base (CS) (average molar mass = 251000 g mol^{-1}) containing an average of 1559 glucosamine units (glucosamine molar mass = 161 g mol^{-1}), with 98% deacetylation purchased from Faravelli (I).

Clay mineral filler: pharmaceutical grade montmorillonite (Veegum HS©, VHS) was kindly gifted by Vanderbilt Company (USA).

IV.2.1- DETERMINATION OF THE CATION EXCHANGE CAPACITY (CEC) OF THE CLAY MINERAL

Clay mineral powder (1 g) was dispersed in 20 ml tetramethylammonium bromide (1 M) aqueous solution, in order to displace constituent cations. Dispersions were shaken overnight at 50 rpm in water bath at 25.0 ± 1.0 °C and then filtered. Supernatant was diluted to 100 ml with distilled water and dissolved cations were individually assayed by atomic absorption (Na^+, Ca^{2+}, Mg^{2+}) or atomic emission (K^+) spectroscopy (Perkin–Elmer spectrophotometer). CEC was calculated as the sum of exchangeable cations, expressed in meq/100 g dry clay mineral. The same solution, minus the clay mineral sample, was used for the blank. Each experiment was done in triplicate.

IV.2.2- CLAY MINERAL/CHITOSAN INTERACTION STUDIES

CS solutions (1% mass/vol) were prepared according to Darder et al. (2003, 2005), by adding the corresponding amount of polymer to an aqueous acetic acid solution 1% (v/v) and stirring for about 4 h. Different amounts of clay mineral powder (ranging from 75 mg to 2000 mg) were then dispersed in 40 ml of CS solution at 10000 rpm for 5 min (Ultraturrax T25, Janke and Kunkel GMBH and Co. KG, G). CS solution was previously adjusted to pH 5.0 with 1 M NaOH, in order to provide $-NH_3^+$ groups in the chitosan structure and to avoid any structural alteration of the clay mineral (Darder et al., 2003, 2005).

The resulting dispersions were shaken for 2 days in water bath at 25 °C ± 1.0°C and the solid phases were then recovered by filtration, washed with distilled water and oven-dried at 50°C for 24 h. The uptake of CS (mass/mass %) was determined by assaying the C content of the samples with a CHNS analyzer (FISONS EA 1108, Carlo Erba, I). Data were fitted according to the Langmuir equation to calculate the amount of CS retained by the clay mineral (monolayer adsorption capacity, n_m). Experiments were done in triplicate.

IV.2.3- THERMAL ANALYSIS

Differential scanning calorimetry of the samples was performed at 10°C/min in the 30–320 °C temperature range (DSC Mettler FP800, Mettler-Toledo GMBH, CH).

IV.3- RESULTS AND DISCUSSION

IV.3.1- CEC

Table IV.1 summarizes the composition of individual exchangeable cationic species of the clay mineral. The total cation exchange capacity was 142 meq/100 g. Exchangeable species were mainly Na^{+} and Ca^{2+}, with amounts reaching 71% and 24% of the total, respectively. The material may be considered as a "sodium montmorillonite", but the presence of a noticeable Ca^{2+} amount in the interlayer space must be taken into account.

Table IV.1. Amount of exchangeable cations (meq/100g) and CEC of VHS (mean values ± s.d.; n = 3).

Ca^{++}	Mg^{++}	K^{+}	Na^{+}	CEC
34.67 ± 0.393	1.78 ± 0.251	4.27 ± 0.234	101.35 ± 0.478	142.07

IV.3.2- CLAY MINERAL/CHITOSAN INTERACTION STUDIES

The interaction curve between VHS and CS followed the form of the Giles L3 type isotherm (Giles et al., 1974) (Fig. IV.1). At low concentrations it was convex in shape, with the amount of adsorbed polymer initially increasing until it reached a plateau, where monolayer coverage of CS over the homogenous clay mineral surface was assumed. At higher concentrations, the curve showed an inflection point where the shape changed from convex to concave and the amount retained further increased, almost certainly by precipitation of CS onto the clay mineral surface. Langmuir linearization of the isotherm allowed calculation of the average amount of CS retained by the clay mineral at the saturation point (n_m), resulting in 14.47 % (mass/mass) ± 3.054 (R^2 = 0.997). This value,

corresponding to 107.43 meq of CS/100 g dry clay mineral, was slightly lower than the CEC of VHS (142 meq/100 g), most probably due to the particularities of the organic cation. These results are also lower than those obtained by other authors working at higher temperatures (Darder et al., 2005). However, in the experimental conditions used, the uptake of chitosan in the interlayer space of the clay mineral via cation exchange was considered adequate to prepare interaction products with drug molecules.

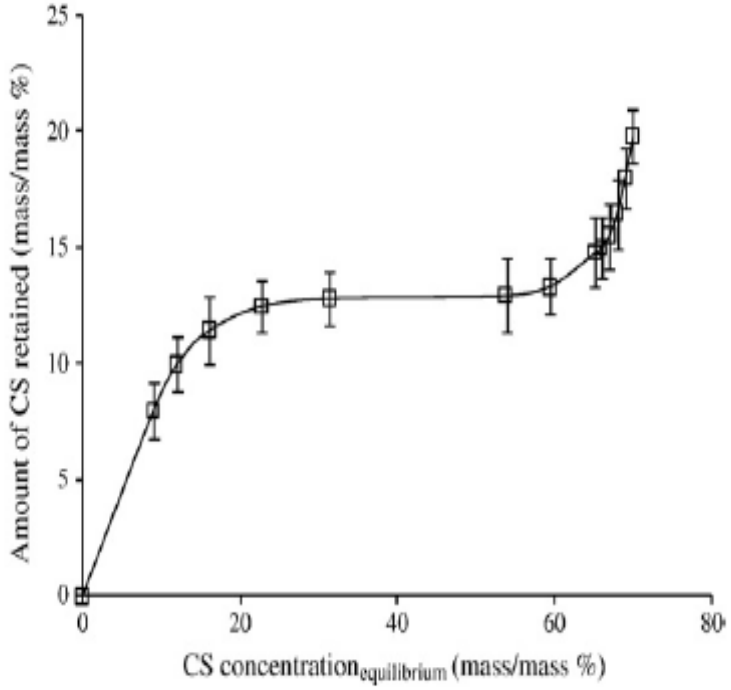

Figure IV.1. Interaction isotherm showing the amount of CS adsorbed on the clay mineral (mean values ± s.d.; n = 3).

IV.3.3- THERMAL ANALYSIS

Figure IV.2 shows the results of thermal characterization of the CS/VHS composites, and, for comparison purposes, it also includes DSC profiles of the single components and their physical mixtures at different wt/wt ratios. The calorimetric curve of CS showed a broad endothermic peak in the 60-150°C range, corresponding to polymer dehydration, followed by an exothermic phenomenon (around 220°C) due to the decomposition of the polymer chain. VHS showed a single band from 70 to 130°C, corresponding to the loss of free water at the clay mineral surface.

The DSC profiles of physical mixtures resembled those of their individual components. The decomposition peak of CS rose as the proportion of polymer in the mixtures

increased (C vs B). The presence of chitosan in the composites was confirmed by the slope increase in the curves at 200 °C - 220°C, corresponding to polymer decomposition.

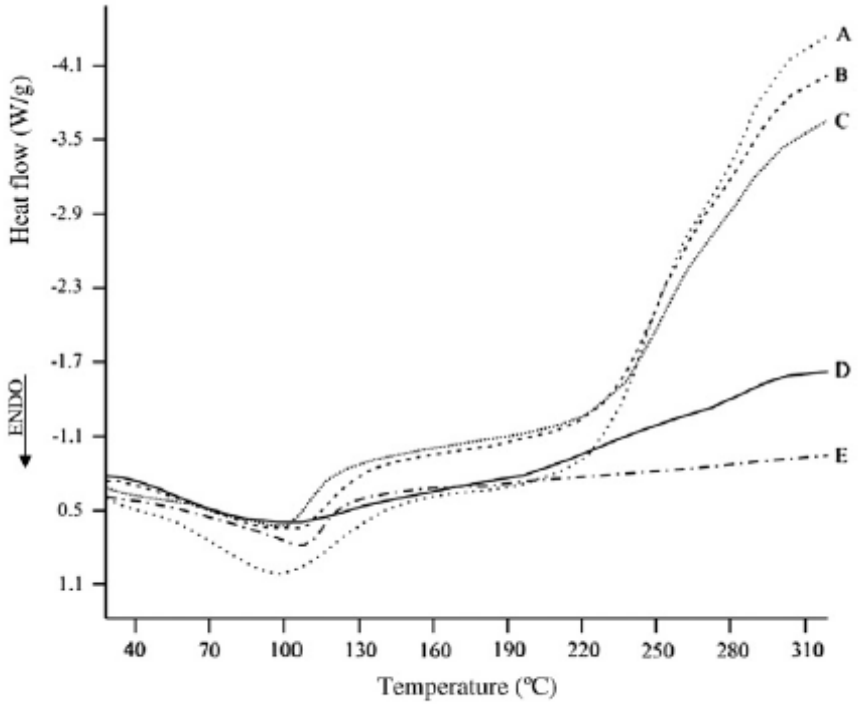

Figure IV.2. DSC curves of CS (A); Physical mixture CS:VHS 50;50 (B); Physical mixture CS:VHS 33:66 (C); composite CS:VHS 33:66 (D) and VHS (E).

IV.4- CONCLUSIONS

Composites of CS and VHS were prepared at 25°C by simple solid–liquid interaction. The results confirmed the effective complexation of CS by the clay mineral. The interaction mechanism involved interlayer exchange of the polymer with the exchangeable cations of the clay mineral, followed by precipitation of CS on VHS surfaces.

CAPÍTULO V.

In vitro biocompatibility and mucoadhesion of montmorillonite chitosan nanocomposite: A new drug delivery

A B S T R A C T

A "Clay Bio Polymer Nanocomposite" (CBPN) to be used in drug release was prepared by dispersion of montmorillonite (VHS) particles in chitosan (CS) solution. The obtained hybrid material was characterized for in vitro biocompatibility on Caco-2 cell cultures. Cytotoxicity and cell proliferation of the nanocomposite were tested, comparing results with free chitosan and montmorillonite. Cell proliferation was assessed both by WST-1 test and wound-healing measurements by means of Image Analysis Software. The last method is a proof of concept test that has the advantage of direct visualization and quantification of cell growth. Nanocomposite was also characterized for hydration (water uptake) pattern and mucoadhesive properties, which were considered as important features for the application of this material in modified release systems.

Results showed that the prepared CBPN showed good biocompatibility in the range 5–500 μg/ml, being also able to effectively stimulate cell proliferation. Moreover, nanocomposite possessed mucoadhesive properties combined with low solubility in acidic environment. We conclude that interaction between chitosan and montmorillonite produced a new biohybrid material that can be considered as promising candidate for modified drug delivery formulations.

V.1- INTRODUCTION

In the last decade, there has been growing interest in the development of nanocomposites between clay minerals and biopolymers for pharmaceutical applications (Viseras et al., 2008a, 2010). These hybrid materials can combine the properties of both components (inorganic and organic), such as swelling, water uptake, mechanical characteristics, thermal behavior, rheology and bioadhesion (Pongjanyakul et al., 2005a; Wu and Wu, 2006; Günister et al., 2007; Khunawattanakul et al., 2008; Pongjanyakul and Suksri, 2009, 2010). They could be formed from a variety of biopolymers and clay minerals. Among them, VHS/CS nanocomposites are receiving greater attention, especially for biomedical (tissue engineering) (Katti et al., 2008; Haroun et al., 2009;

Verma et al., 2010) and biopharmaceutical (modified release) (Wang et al., 2007; Wang et al., 2009; Khunawattanakul et al., 2010; Nanda et al., 2011) applications.

CS is a cationic copolymer formed by N-acetylglucosamine and Dglucosamine units, being obtained by the natural occurring polysaccharide chitin (Figure. V.1). It is widely used in pharmaceutical field, because of its suitable characteristics, including chemical safety, biodegradability, biocompatibility, antibacterial activity and mucoadhesive properties (Illum, 1998).

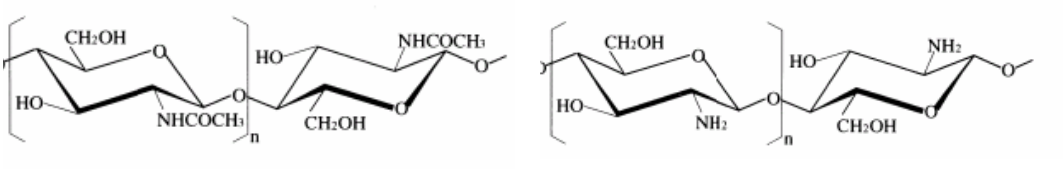

Figure V.1. Chemical structure of chitin (left) and CS (right).

VHS is a layered hydrated aluminium silicate whose unit cell is composed of one Al-octahedral sheet (O) sandwiched between two Si–tetrahedral sheets (T). It possesses a net negative charge due to isomorphous ionic substitutions in the T–O–T structure. This charge is compensated by interlayer hydrated cations, which can be exchanged by a variety of organic molecules (Bergaya et al., 2006; Aguzzi et al., 2007). In particular, CS chains have been described to intercalate with Na^+–montmorillonite, because of their hydrophilic and cationic character, giving hybrid nanocomposite materials with interesting properties (Darder et al., 2003). Other works showed that the concentration of the clay mineral is a critical parameter in VHS/CS nanocomposites to achieve materials with enhanced properties (mechanical, thermal and/or electro-stimuli response) in comparison with the pure components (Wang et al., 2005; Xu et al., 2006; Liu et al., 2007). For example, nanocomposite hydrogels containing 2% (wt/wt) of VHS showed improved release behavior of vitamin B12, compared with that of the pure CS (Liu et al., 2008). Ratio between VHS and CS was a crucial factor also in the case of nanocomposites prepared to control release of the chemotherapeutic agent doxorubicin (Yuan et al., 2010). pH dependent release profiles were found for these nanocomposites, which were described as promising supports for colonic prolonged drug delivery. The majority of the studies are devoted to the physicochemical and biopharmaceutical

characterisation of VHS/CS nanocomposites; however, their biocompatibility for drug release has been evaluated only by Depan et al. (2009).

In a previous work, a nanocomposite between CS and VHS was prepared by simple solid–liquid interaction; the effective polymer/clay mineral complexation was confirmed by thermal analysis and slower drug release was observed in comparison with CS and VHS alone (Aguzzi et al., 2010). In vitro biocompatibility was followed by cytotoxicity and cell proliferation in this paper, for further characterization. The effects of the nanocomposite were screened on Caco-2 cell cultures as a representative type of intestinal cells considering an oral administration and delivery. Cell proliferation was assayed by two different techniques: WST-1 test and wound-healing measurements. The last method has the advantage that allows a direct visualization of cell growth. Nanocomposites were also characterized for hydration (water uptake) pattern and mucoadhesive properties, which were considered as important features for the application of these materials in modified release systems.

V.2- MATERIALS AND METHODS

The polymer used was CS base with low viscosity* (12 mPa*s) and deacetylation degree of 98% (Giusto Faravelli, Italy) (*Viscosity measurements were performed on 1% (w/v) solutions in HCl 0.1 M at 90 1/s with rotational rheometer equipped with coaxial cylinders C14 (Bohlin CS, Bohlin Instrument Division, Metrics Group Ltd., Cirencester, UK). CS acetate was used as control in cell experiments. It was obtained by dissolving CS base in aqueous acetic acid (1 % vol/vol) and freeze drying (Edwards mod RV8) the polymer obtained solution. The clay mineral was a marketed pharmaceutical-grade montmorillonite (Veegum HS©), kindly gifted by Vanderbilt Company S.A. (USA).

CS and VHS powders were pulverized in a ball miller (IG.W2/E, Giuliani, Italy) and then sieved to separate a rigorous size fraction (45–75 μm) to limit variability of the data. The selected fraction was kept in a desiccator until required.

V.2.1- PREPARATION OF CHITOSAN/CLAY MINERAL NANOCOMPOSITE

VHS/CS nanocomposite was prepared following Aguzzi et al. (2010). Briefly, CS was dissolved in aqueous acetic acid (1 % vol/vol) at the concentration of 1 % (wt/vol). Then, VHS was added to the polymer solution in the wt:wt ratio (2:1 CS:VHS) corresponding to their maximum binding capacity, as calculated by interaction isotherms. Dispersion was stirred by a magnetic bar for 48 h at room temperature, washed with distilled water and then freeze dried. The product obtained was milled and sieved to select the size fraction between 45 and 75 μm.

V.2.2- WATER UPTAKE MEASUREMENTS

Water uptake experiments were carried out using a modified Enslin apparatus (Ferrari et al., 1991). Measurements were performed on 20 mg of nanocomposite, in acidic medium (0.1 M HCl) for 2000 s. For comparison, measurements were also performed on pure CS and clay mineral powders, at the same granulometric fraction as the nanocomposite. Powders were laid on dialysis membrane discs (cut off 14,000 Da), which were placed on the sample holder of the apparatus to retain dissolved CS molecules and avoid sample mass lost. Membranes alone were used for blank measurements. Six replicates were performed on each sample.

V.2.3- MUCOADHESION MEASUREMENTS

Mucoadhesive properties were investigated by TA-XT2 Plus Texture Analyser (Stable Micro Systems, Enco, Italy) using porcine gastric mucin (Type II) (Sigma, Italy) as biological substrate. 40 mg of samples were hydrated in pH 5.0 phosphate buffer (European Pharmacopeia (EP 6.0)) and then laid on a filter paper fixed with double sided adhesive tape on the bottom of the upper probe of the apparatus. 30 μl of an 8% (wt/wt) mucin dispersion in phosphate buffer pH 7 (EP 6.0) were applied on a filter paper disc (diameter = 10 mm), fixed in the lower probe of the apparatus and faced to

the sample. The upper probe with the sample was lowered at a speed of 1.0 mms^{-1} onto the surface of the lower probe and a downward force (preload) of 2500 mN was applied for 1 min to ensure intimate contact between the sample and the mucin dispersion and to allow the formation of the mucoadhesive joints. After a 1 min rest, the upper probe was moved upwards at a constant speed of 4.0 mms^{-1} until the complete separation of the two surfaces occurred. The detachment force (mN) and the adhesive work (calculated from the area under the force–distance curve, AUC (mN*s) were recorded and simultaneously collected on a personal computer (Texture Exponent Software 32, Stable Microsystem, Enco, Italy). Blank measurements were performed using phosphate buffer pH 7 instead of the mucin suspension.

The normalized mucoadhesion parameter (ΔAUC/AUC) was calculated according to the following equation (Ferrari et al., 1997):

$$\Delta AUC/AUC=(AUC_m-AUC_{blank})/AUC_{blank}$$

where AUC_m is the work of adhesion obtained in presence of mucin and AUC_{blank} is the work of adhesion obtained by the blank. Such normalization allowed comparing the mucoadhesive properties of samples characterised by different cohesive properties (viscosity) (Ferrari et al., 1997). Eight replicates were performed on each sample.

V.2.4- CELL CULTURES

Human colorectal adenocarcinoma cell lines (Caco-2) were obtained from the American Type Culture Collection (ATCC, USA). Cells were grown at 37 °C, 5 % CO_2 atmosphere (PBIinternational, Italy) in pH 7.4 Dulbecco's Modified Eagle's Medium (DMEM) (Lonza, Italy) containing 20 % vol/vol heat inactivated Fetal Bovine Serum (FBS) (Euroclone, Italy), penicillin (100 IU/ml), streptomycin (0.1 mg/ml) and 1 % vol/vol non essential aminoacids (Sigma Aldrich, Italy). The culture medium was changed twice weekly during maintenance.

V.2.4.1- CELL VIABILITY MEASUREMENTS

Cell viability was estimated by the (4-(3-(4-Iodophenyl)-2-(4-nitrophenyl)-2H-5-tetrazolio)-1,3-benzene disulfonate) (WST-1) assay (Roche Diagnostics GmbH, Roche Molecular Biochemicals, Bioidea, Italy). This reagent is metabolically reduced mainly by mitochondria in viable cells to a water soluble formazan product, allowing direct absorbance measures after experiments (Ishiyama et al., 1996).

Confluent Caco-2 cells (70 – 90 % confluence) were plated with the above described medium in 96-well plates (growth area 0,36 cm^2, Greineger Bio-one, PBI International, Italy) at a density of 1×10^5 cells/cm^2 and cultured for 24 h (37 °C, 5 % CO_2). Then, the medium was removed and 200 µl of nanocomposite dispersions at three different concentrations (5, 50, 500 µg/ml in medium without serum) were added to each well. For comparison, experiments were also done on CS and clay mineral alone, at the same concentrations as the nanocomposites (Table V.1).

TableV. I. Concentration of the samples for cell cultures studies.

Sample	Concentration (µg/ml)
CS/VHS	low: 5 medium: 50 high: 500
CS	low: 3.3 medium: 33.3 high: 333
VHS	low: 1.67 medium: 16.7 high: 167

Complete medium and Triton®X100 (Fluka, Italy) were used as positive and negative controls, respectively. The plates were then incubated (37°C, 5% CO_2) for different times, before being subjected to the WST-1 assay. The incubation time was 3 h for cytotoxicity and 24 h for cell proliferation assays. Subsequently, the medium was replaced by 100 µl of WST-1 10% v/v in HBSS ("Hanks' balanced salt solution") pH 7.4 and incubated for 3 h. At the end of the tests, the absorbance was assayed by using ELISA plate reader (iMark™ Microplate Absorbance Reader mod. 550, Bio-Rad, Italy) equipped with mechanical plate shaker at 450 nm wavelength with a reference wavelength of 650 nm. The data were expressed as the mean percentage of viable cells as compared to the respective control (untreated cultures).

V.2.4.2- WOUND-HEALING MEASUREMENTS

Wound-healing measurements were performed to directly evaluate cell proliferation. Experiments were carried out using a μ-Dish (Ibidi, Giardini, Italy) with an insert which delineates two distinct growth areas (growth area 2 × 0.22 cm^2) (Figure V.2). Caco-2 cells were seeded at 10^5 cells/cm^2 in each chamber (seeding volume of 70 μl) grown to confluence. After removal of the insert a cell free gap ("wound") (500 μm ± 50 μm) remained. Cells were put in contact with 500 μl of medium without serum containing nanocomposite (50 μg/ml), with corresponding concentrations of free CS and clay mineral. Dishes were re-incubated over a total period of 72 h. The growth of cells over each sample was investigated by taking photographs after fixed times (24, 48 and 72 h) using an inverted microscope (PBI international, Italy) at a magnification of 250× and the size of the gap between the chambers was taken as a measure of cell proliferation as a function of time. The digitalized images were elaborated by a suitable software (UTHSCSA Image Tool version 3.00, The University of Texas Health Science Center, USA), that allowed to measure the area left by the cell growth at each time.

The % of wound areas at different times were calculated considering 100 the mean area measured for each sample at time zero. At least three different pictures were analyzed for each sample and each time.

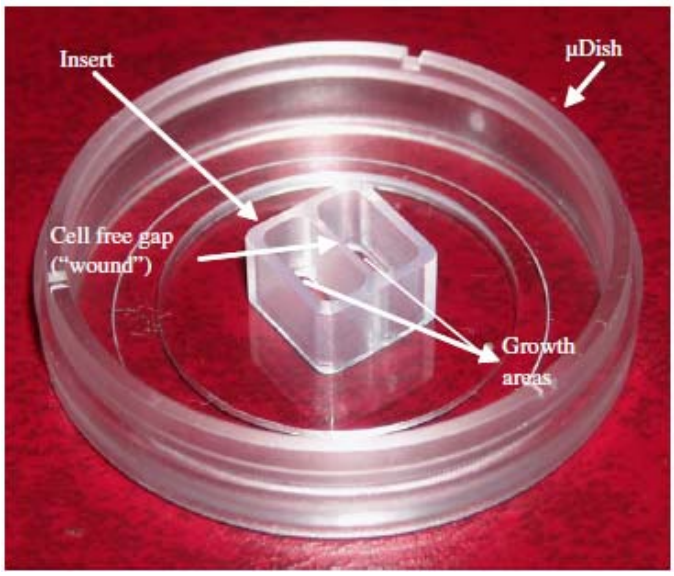

Figure V.2. Culture inserts used for wound-healing measurements.

V.2.4.3- STATISTICAL ANALYSIS

One-way analysis of variance (ANOVA) with the post hoc Sheffé test for multiple comparisons was performed using the software Siphar 4.0 (France). The comparison of two groups (t Student test) was performed with Statgraphics® 5.0 statistical package (Statistical Graphics Corporation, Rockville, MD, USA). Differences between groups were considered to be significant at a level of P less than 0.05.

V.3- RESULTS AND DISCUSSION

V.3.1- WATER UPTAKE MEASUREMENTS

Figure V.3 shows the water uptake profiles of nanocomposite (VHS/Ch) and free components (Ch base and VHS) in 0.1 M HCl. As observed the behaviour of the clay mineral was different from that of the pure polymer. VHS immediately levelled off in a plateau, whereas CS hydrated gradually, due to the progressive formation of the corresponding soluble hydrochloride salt in contact with the medium. After 20 min (1200 s) approximately, the polymer was fully hydrated and the total amount of medium absorbed was 11.5 g/g dry polymer, that is, significantly higher ($P < 0.001$, one-way ANOVA, post hoc Scheffé test) than the amount absorbed by the clay mineral. Nanocomposite achieved final amount absorbed of about 9 g/g. Data were normalized as a function of the actual amount of CS present in the VHS/Ch nanocomposite. The water uptake profile seemed have the same pattern of that of VHS, indicating that the solubility of the polymer in 0.1 M HCl was reduced by the presence of the clay mineral. Since drug release is strictly related with hydration, this result corroborated the hypothesis postulated in a previous work, where drug release from VHS/Ch nanocomposite in acidic medium was lower than the observed with CS alone (Aguzzi et al., 2010).

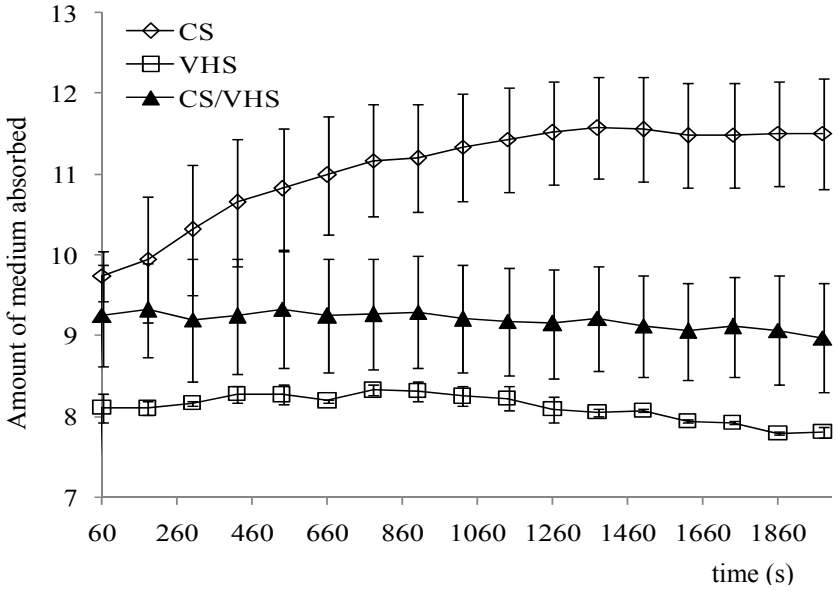

Figure V.3. Water uptake profiles of the samples in 0.1 M HCl (mean values ±s.e.; n=6).

V.3.2- MUCOADHESIVE PROPERTIES

Mucoadhesion measurements followed the trend CS > nanocomposite > clay mineral. CS was characterized by the highest mucoadhesive potential (2.75 ± 0.10). In fact it is known that CS possesses mucoadhesive properties, due to the presence of many amino groups in the polymer chains that form hydrogen bonds with glycoproteins in the mucus (Lim et al., 2000) and also ionic interactions between positively charged amino groups and negatively charged sialic acid residues of mucin. Clay mineral was also able to interact with the mucin, although the normalized mucoadhesion parameter (0.71 ± 0.03) was significantly lower compared with CS ($p < 0.001$, one-way ANOVA post hoc Scheffé test). Nanocomposite showed an intermediate behavior (0.85 ± 0.03). Probably, in the nanocomposite the mobility of the polymer chains was reduced by the interaction of the clay mineral, reducing contact/interpenetration with the substrate. A similar behavior was observed by other authors, studying bioadhesion of nanocomposite between alginate and other kind of layered clay mineral (Pongjanyakul and Suksri, 2009).

V.3.3- CELL VIABILITY

In Figure V.4a, cell viability over each sample after 3 h of incubation is given. At the concentrations studied, CS and nanocomposite did not significantly reduce cell viability compared with the blank (culture medium without serum), indicating good biocompatibility properties for these materials. However, in the case of clay mineral at high concentration a significant reduction of cell viability ($p < 0.001$, one-way ANOVA post hoc Scheffé test) was observed. This effect was observed by other authors: they suggested that high amounts of clay particles could block the most of the channels on cell membranes, causing the cell death (Wang et al., 2008).

Figure V.4b refers to cell viability obtained after 24 h of incubation with nanocomposite and pure components. For all the samples at all the concentrations considered the viability values were comparable or higher than that of the blank (culture medium without serum). In the case of Ch, viability increased progressively with increasing polymer concentration, compared to the blank. It is known that CS chains can enhance cell growth both because of their capacity to adhere to the (negatively charged) cell membranes (Wang et al., 2010) and their ability to bind serum factors, such as growth factors (Howling et al., 2001). Clay mineral also increased cell viability at low and intermediate concentrations, reaching values significantly ($p < 0.05$, one-way ANOVA post hoc Scheffé test) higher than the obtained with CS at the same concentration. It could be suggested that a limited amount of clay mineral particles might be engulfed by the cells through endocytosis, resulting in increased mitochondrial activity, rather than in effective cell proliferation activity (Lin et al., 2006; Wang et al., 2008). At higher concentrations, cell viability was reduced in line with the aforementioned observed results (Figure V.4a). The nanocomposite partially reflected the behaviour of the free components.

Cell viability increased with increasing nanocomposite concentration from low to intermediate level. However, at higher concentrations cell viability did not further increase, showing an intermediate value between CS and VHS.

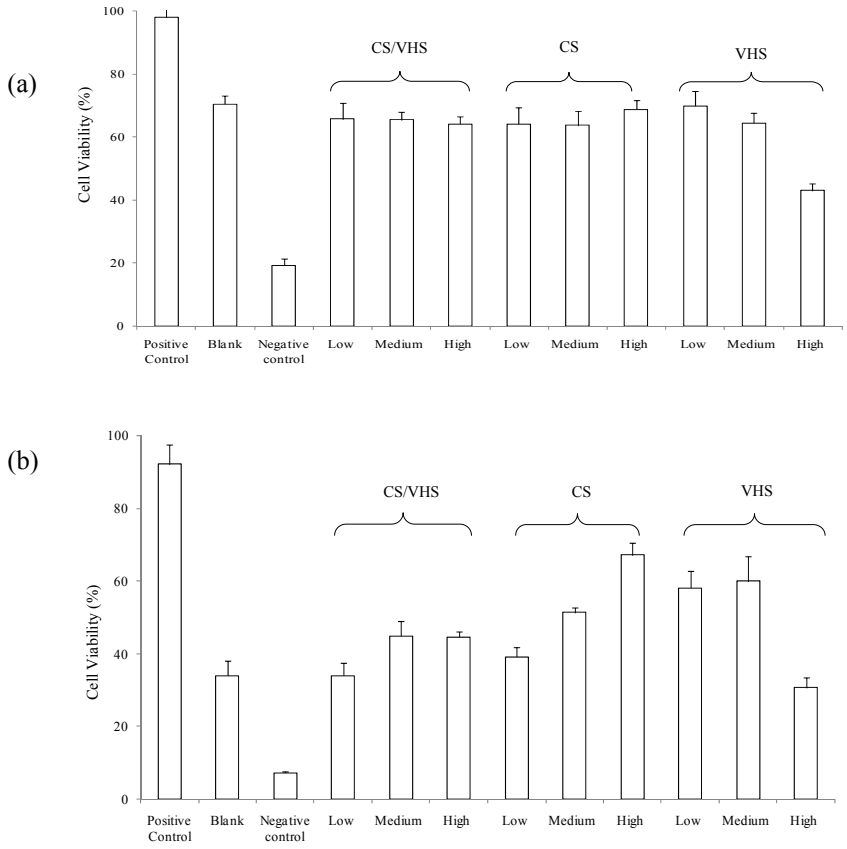

Figure V.4. Cell viability after 3 hours (a) and 24 h (b) of incubation with the samples studied. Positive control: untreated cells in complete medium; blank: untreated cells in medium without serum; negative control: Triton®X100 (Fluka, Milan, Italy) (mean values ± s.e.; n = 8). See Table V.1 for the meaning of the sample concentrations (low, medium, high) (mean values ± s.e.; n=8).

V.3.4- WOUND-HEALING MEASUREMENTS

Wound-healing measurements were done in order to verify the results of cell proliferation obtained by WST-1 test. These measurements allowed a direct observation of cell growth, excluding possible misunderstandings in the interpretation of WST-1 test. Experiments were performed on nanocomposite and free components at the intermediate concentration, where WST-1 test revealed an increase in cell proliferation for all the samples studied, compared with the blank.

In Figure V.5 photographs of cell cultures after different incubation times are given, showing the progression of the gap over each sample as a function of time. Results were expressed as average percentage of gap size after established times compared to time zero, as it is shown in Figure V.6. At time zero, gap's size was in all cases the maximum allowed (assumed 100 %). For each sample there was a significant total effect of time in

the reduction of wound area in the range 0-72 h ($p < 0.001$, one-way ANOVA). When comparison of two samples was performed (considering subsequent time intervals for each sample), in almost all cases the differences of area at different times were still significant at a 95 % level.

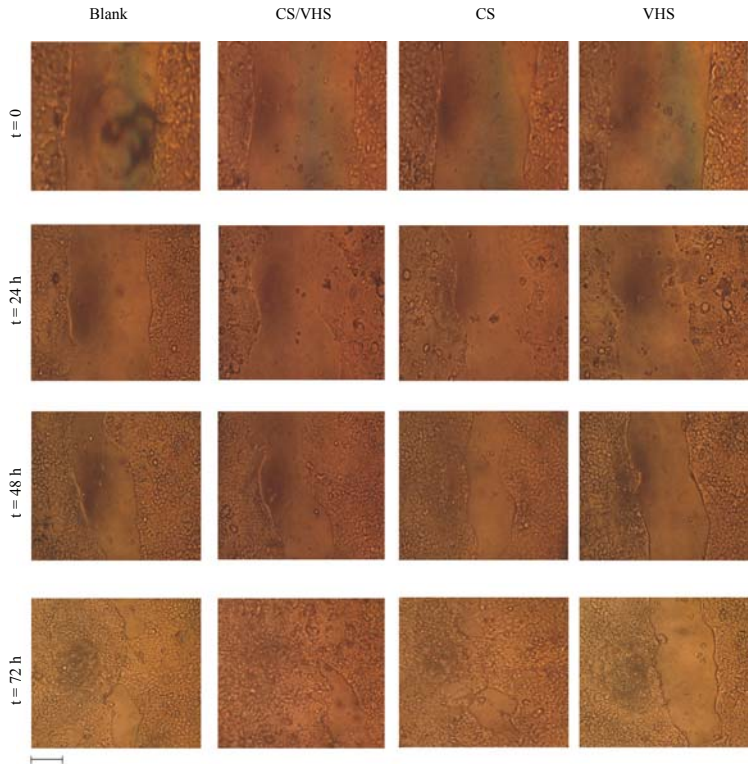

Figure V.5. Photographs of cell cultures from wound-healing test (bar is 200 μm).

The results of these comparisons are given in Table V.2, where the p values of statistical evaluation performed are reported.

Table V.2. P values obtained for two sample comparison of groups at different times (t Student).

Time (h)	Blank	CS/VHS	CS	VHS
0-24	0.013	0.003	0.008	0.063
24-48	0.118	< 0.001	0.003	0.053
48-72	0.037	0.004	0.019	0.032
0-48	0.004	< 0.001	< 0.001	0.011
0-72	< 0.001	< 0.001	< 0.001	0.003
24-72	0.007	< 0.001	< 0.001	0.002

p value considered significant below 0.05

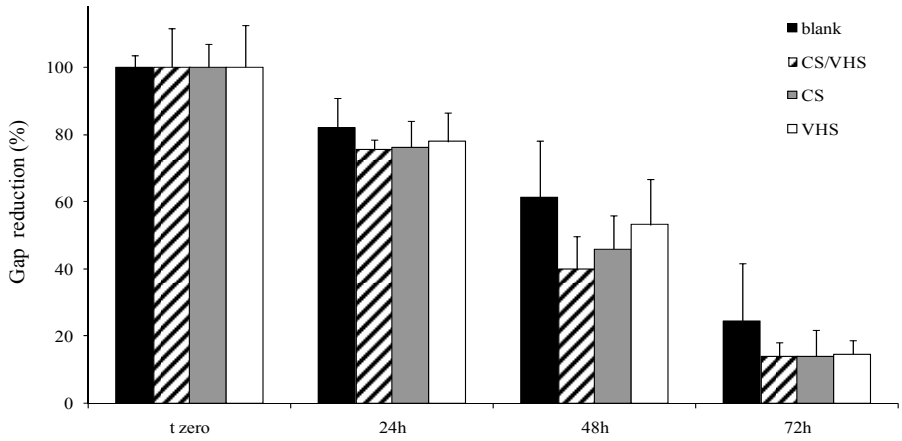

Figure V.7. Gap reduction after different incubation times (mean values ± s.e.; n = 4).

As for blank sample, the area reduction was not significant for the comparison between 24 and 48 h indicating a slow proliferation at early time. As for the VHS/CS nanocomposite and Ch, the area reduction was significant at all times, indicating a constant and progressive reduction of wound area, faster than that determined for blank sample. As for VHS sample, the reduction of the wound area was significant only between 48 and 72 h, indicating also in this case a slower proliferation as that of blank and corroborating that the previously observed augment in cell viability (WST-1 test at 24 h) might be due to an increase in mitochondrial activity, induced by the cellular uptake of the clay particles. It is known that in endocytosis processes, mitochondria provide the necessary energy (trapped in ATP) for vesicular transport and for the processing of lysosomal enzymes in the endoplasmic reticulum and Golgi apparatus (Nelson et al., 2008). These results indicated that the Caco-2 growth rate was predominantly enhanced by the nanocomposite and Ch. The observed area reduction also suggested an effective stimulation of cell growth by CS (as previously described in literature (Howling et al., 2001; Wang et al., 2008)) and nanocomposite. According to Lavie and Stotzky (1986) montmorillonite may develop London–van der Waals forces and hydrogen bonding with cells, promoting cell adhesion that, in nanocomposite, should allow CS to enhance cell growth. For each time there was not a significant effect of sample in the reduction of wound area (one-way ANOVA). When comparison of two samples was performed the only significant difference that could be evidenced was between blank and nanocomposite at 48 h ($p < 0.05$). At 24 h all samples presented an area of 80% with respect to the initial value, without significant differences between

samples (one-way ANOVA). At 48 h the wound area ranged between 40% (VHS/CS) and about 60% for blank with intermediate values for the other samples. After 72 h, in all cases the wound area was reduced to less than 20 % of the initial area.

V.4- CONCLUSIONS

According to the results, the prepared VHS/CS nanocomposite possessed mucoadhesive properties combined with lower hydration properties in acidic environment compared with pure CS. From cell cultures experiments, CS and nanocomposite showed good biocompatibility on Caco-2 cells in the concentration range studied (5-500 µg/ml). Nanocomposite and CS also exhibited a progressive reduction in wound area, indicating an effective stimulation of Caco-2 proliferation by these samples.

We conclude that a new biohybrid material was produced by interaction between CS and VHS, showing promising properties for pharmaceutical applications, especially for designing of modified drug delivery systems.

CAPÍTULO VI.

Permeability of oxytetracycline from chitosan-montmorillonite nanocomposites

ABSTRACT

The aim of the present paper was the development of a nanocomposite based on chitosan and montmorillonite to deliver oxytetracycline, improving its oral bioavailability. The nanocomposite was prepared by simple solid–liquid interaction and loaded with the drug. Then, it was characterized by X-Ray diffraction, thermal analysis, FTIR, zeta potential and particle size distribution. Cytotoxicity of the nanocomposite was also evaluated over Caco-2 cell cultures. Subsequently, drug permeation from the nanocomposite was also evaluated across cellular monolayers. The amount of drug permeated was determined and the monolayers were also analysed by means of confocal laser scanning microscopy (CLSM) to evaluate the eventual entrapment of drug into the Caco-2 cells.

VI.1- INTRODUCTION

Among the different advantages of nanocarriers in drug development, improvement of drug absorption is well described in literature (Ghaffarian et al., 2012). Transport of drugs across the intestinal epithelium occurs mainly by one or more of the following mechanisms: passive transcellular and paracellular difussion, carrier mediated transport and by transcytosis. Rapidly and completely absorbed drugs are generally transported by the passive transcellular route, whereas drugs that are slowly and incompletely passively absorbed are assumed to be transported in equal amounts by the paracellular and transcellular routes. However, in reality, the tight junctions which gate the entrance to the paracellular pathway restrict this transport. The low efficiency of the paracellular pathway has stimulated investigations into ways to enhance the permeability by this route. Many of these studies have been performed in monolayers of intestinal epithelial cells and have provided new insight into the regulation of tight junctions (the rate limiting barrier of the paracellular pathway).

Some hydrophilic drugs whose chemical structures mimic those of various nutrients can be transported across the intestinal epithelium by active, carrier-mediated transport. Often, transport is mediated partly by the carrier and partly by passive routes. Since carrier-mediated transport is saturable, the contribution of the passive route will increase

with increasing dose. If the drug has a low passive permeability, saturation of the carrier will result in a decreased absorbed fraction. This may occur either when the carrier is saturated by nutrients or at high dose levels of the drug. There are also active transporters such as P-glycoprotein (P-gp), which mediate drug transport in the serosal to mucosal direction. In this case, saturation of the carrier could result in an increase in the absorbed fraction of drug. The low capacity of the transcytosis route from the mucosal to the serosal side of the intestinal epithelium makes this route less attractive for the transport of drugs. It has therefore mainly been considered as a route for highly potent drugs (such as peptide antigens) which are excluded from the other transport pathways due to their size. Another disadvantage is that transport generally occurs in membrane vesicles which contain large amounts of proteolytic enzymes.

Oxytetracycline is frequently used for its extensive spectrum of antimicrobial activity. However, the antibiotic shows a low bioavailability following oral administration. Absorption of this drug from the gastrointestinal tract is incomplete, with major differences between species (Dyer, 1989; Mevius et al., 1986; Pijpers et al., 1991; Nielsen and Gyrd-Hansen, 1996). The low oral bioavailability of oxytetracycline poses the question to what extent P-gp expression in the intestines accounts for its limited absorption, as this would offer the possibility to improve the oral availability of the drug. It has been demonstrated that oxytetracycline is a substrate for the efflux transporter P-pg, being able to saturate the carrier (Schrickx and Fink-Gremmels, 2007).

Caco-2 cell line is an established model to investigate the mechanisms involved in the bioavailability after oral administration, as the cells grown as confluent monolayers, form tight junctions, and thus resemble the intestinal barrier (Calcagno et al., 2006). Depending on the chemical characteristics of the compound under consideration, passive diffusion and active transport, contributing to absorption and secretion through a Caco-2 cell monolayer, can be measured (Yamashita et al., 1997; Artursson et al., 2001). Consequently, Caco-2 mono layers have been used to study drug transport by all four routes. Caco-2 cell cultures are extensively used in studies aimed to evaluate both the permeability of drugs through the gastrointestinal wall and to evaluate cytotoxicity of the different components of a given formulation (Garcia-Casal et al., 2000). Caco-2 cells express morphological and biochemical characteristics similar to those of healthy human enterocytic cells, even if they are smaller than enterocytes (Pontier, 1998).

With this premises, aim of this paper was to asses the suitability of a chitosan-montmorillonite nanocomposite to improve oxytetracycline bioavailability. The nanocomposite was prepared following Salcedo et al. (2012), and Caco-2 cell model was used to evaluate the penetration enhancement properties of the nanocomposite towards the antibiotic. Cytotoxicity of the nanocomposite was also evaluated by using Neutral Red assay. The amount of drug permeated across the cellular substrates was determined and the monolayers were also analysed by means of Confocal Laser Scanning Microscopy (CLSM) to evaluate the eventual entrapment of drug into the Caco-2 cells.

VI.2- MATERIALS AND METHODS

Chitosan base (CS) with deacetylation degree of 98% and low viscosity (12 mPa*s) was used (Giusto Faravelli, Italy). CS was dissolved in aqueous acetic acid (1% v/v) and then freeze dried to obtained the corresponding acetate soluble salt (CSAc) to be used as control in sample characterisation. The clay mineral was a pharmaceutical-grade montmorillonite (Veegum HS© (VHS) kindly gifted by Vanderbilt Company S.A. (USA). The selected model drug was Oxytetracycline hydrochloride (OXT), purchased from Panreac (Spain), with pK_a 3.3, 7.3 and 9.1. Pentasodium trypolyphosphate (TPP) from Sigma Aldrich (Spain) was used as cross-linking agent.

VI.2.1- PREPARATION OF POLYMER/CLAY NANOCOMPOSITE

CS (2% w/v) and VHS (1% w/v) were dispersed under magnetic stirring in aqueous acetic acid (1% v/v) and then freeze dried to obtain dry polymer clay nanocomposite powder (PCNC) (Salcedo et al., 2012). The 2:1 CS:VHS w/w ratio was used in agreement to their previously calculated binding capacity (Aguzzi et al., 2010).

VI.2.2- PREPARATION OF DRUG-LOADED PCNC

To prepare dug loaded PCNC, CS and VHS were dispersed, at the same w/w % as described above, in acetic acid solution (1% v/v) containing 0.8 % (w/v) of OXT. 5%

(w/v) of TPP aqueous solution was then added to the dispersion to promote drug entrapment, by inducing ionotropic gelation the remaining free amino groups of CS. The resultant component concentrations in the final dispersion were the following: OXT (2% w/v), CS (0.7 % w/v), VHS (0.35% w/v) and TPP (1.125% w/v). The loaded PCNC was separated from the aqueous suspension by centrifugation at 10000 rpm for 10 min. The amount of free OXT was measured in the supernatant by UV spectroscopy at 270 nm. The OXT encapsulation efficiency (EE) of the process was calculated from equation [1], resulting in 15% (w/w) in presence of TPP *vs* 10% (w/w) in absence of ionotropic gelation of the polysaccharide chains.

EE = (Total amount of OXT - Free amount of OXT)/Total amount of OXT * 100 [1]

VI.2.3- THERMAL ANALYSIS

Thermogravimetric analysis (TGA) was carried out using a METTLER TOLEDO mod. TGA/DSC1 with FRS5 sensor and a microbalance (precision 0,1 µg) (Mettler-Toledo GMBH). The samples were heated under nitrogen atmosphere in the interval 30-400ºC at 10ºC/min.

VI.2.4. FTIR SPECTRA

FTIR spectra were recorded on a FTIR spectrophotometer (JASCO 6200, with software SPECTRA MANAGER v2). The FT-IR measurements of the samples were carried out in the transmission mode in the region from 600 cm^{-1} to 4000 cm^{-1} at 0.5 cm^{-1} resolution and using KBr pellets.

VI.2.5- ZETA POTENTIAL AND PARTICLE SIZE DISTRIBUTION

The zeta potential of sample suspensions (0.1 mg/ml) was measured using a laser Doppler electrophoresis analyzer (Zetasizer Model Nano ZS, Malvern Instruments Ltd. UK). The temperature of the samples was maintained at 25 ºC.

Granulometric distribution of the studied samples was studied by the laser diffraction method using a particle size analyser Mastersizer 2000 (Malvern Instruments Ltd. UK). Previously, the nanocomposite samples were sieved to separate the < 63 μm fraction.

VI.2.6- CYTOTOXICITY

Caco-2 cells were seeded in 96-well plates with area of 0.34 cm^2 at density of 10^5 cells per square centimetre. After 7 days, the growing cells are attached to the well bottom composed of a monolayer, and at the eighth day the experiments are performed. The toxicity study was performed using the neutral red (NR) assay (Tox Kit 4, Sigma-Aldrich, Milan, Italy), consisting in a vital dye able to penetrate into living cells. Each well bottom was washed with saline phosphate buffer (PBS) and 500 μl of each sample (diluted 1:1 with Hank's Balanced Salt Solution (HBSS; $CaCl_2$ anhydrous 140 mg/l, $MgCl_2$ $6H_2O$ 100 mg/l, $MgSO_4$ $7H_2O$ 100mg/l, KCl 400 mg/l, KH_2PO_4 60 mg/l, $NaHCO_3$ 350 mg/l, NaCl 8,000 mg/l, Na_2HPO_4 48 mg/l, D-glucose 1,000 mg/l, Phenol Red 10 mg/l; Sigma, Milan, Italy)) at pH 5.5 was put in contact with the cells (the same sample concentration and the same sample amount/area ratio were maintained as used in permeation experiment across Caco-2 cells). After 3 h, the samples were removed and the cell substrates washed with PBS. Two hundred microliters of NR solution (0.33 mg/ml in Dulbecco's Modified Eagle's Medium (DMEM)) was put in each well for either 1 or 2 h of contact time. Cell substrates were then washed with PBS to remove NR not entrapped in the cells, and the fixing medium (1% $CaCl_2$ and 0.5% formaldehyde aqueous solution) was added to fix the substrate. After removal of the fixing solution, a solubilizing solution (1% of acetic acid in ethanol) was added to the cell substrates to cause cell disruption and to release NR captured by viable cells. The NR solution absorbance was determined by means of a plate reader (Perkin Elmer, Milan, Italy) at wavelength of 490 nm. The absorbance read for each sample was compared with that of HBSS, negative control, that is not toxic and that was assumed to allow maximum cell viability (100%).

VI.2.7- PERMEABILITY STUDIES

The nanoparticle suspensions were diluted 1:1 using pH 5.5 HBSS and were subjected to permeability tests across Caco-2 cell monolayers. Caco-2 cells were seeded on tissue culture-treated polycarbonate filters (Figure VI.1) (area 113.1 mm^2; inner diameter 13.85 mm, pore size 0.4 μm) in 12-well plates (Greiner Bio-one, PBI international, Milan, Italy) at seeding density of 10^5 cells per square centimeter. DMEM (pH 7.40; Bioindustries, PBI international, Milan, Italy) supplemented with 10 % fetal bovine serum, benzylpenicillin G (160 U/ml), streptomycin sulfate (100 μg/ml; Bioindustries, PBI international, Milan, Italy) and nonessential amino acids (Sigma, Milan, Italy) was used as culture medium. Cell cultures were kept at 37 °C in an atmosphere of 95 % air and 5 % CO_2 and 95 % of relative humidity. Filters were used for transepithelial electrical resistance (TEER) measurements and transport experiments 21–23 days after seeding.

Five hundred microliters of the nanocomposite suspensions was diluted 1:1 in HBSS at pH 7.4 and were used as the apical (donor) phase of the monolayers. HBSS at pH 7.4 (2 ml) was used as the basolateral (receptor) phase and added to the basolateral side of the monolayers. At 0.5, 1.5, and 3 h, each filter and its mounting donor chamber filled with the apical phase were moved into a fresh basolateral (receptor) phase. During the experiments, the integrity of the monolayers was assessed by means of TEER measurements at fixed times using a Millicell ERS-meter (Millipore Corp., Bedford, MA, USA). OXT at the same concentration than that of nanocomposite was subjected to the same assay and used as control.

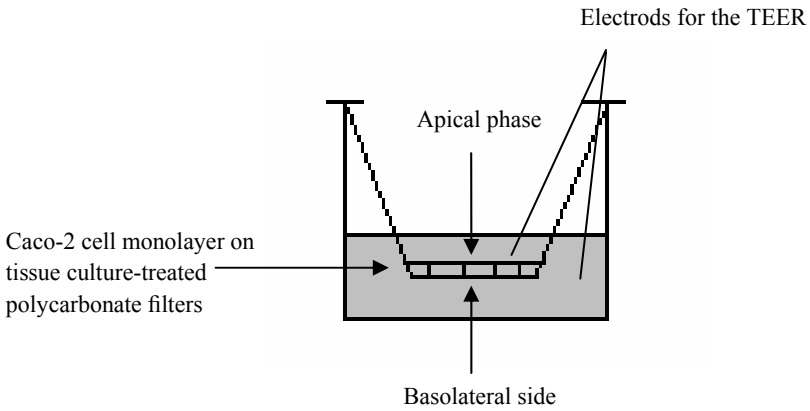

Figure V.1. Plate with tissue culture-treated polycarbonate filters for the TEER measurements.

VI.2.8- CLSM EVALUATION

Caco-2 cells grown on filters in 12-well plates and subjected to permeation/penetration measurements were analysed by using CLSM to visualize nanocomposites loaded with OXT eventually entrapped in the cells. The cell substrates were fixed in ethanol and dried overnight. Cell nuclei of cell substrates were stained by dipping the biological substrates into a solution (1:100 000) of Hoechst 33258 (Sigma, Milan, Italy). Each cell filter was mounted using PVA–DABCO, polyvinyl alcohol mounting medium with DABCO antifading (mixture of tris (hydroxymethyl) aminomethane/tris (hydroxymethyl) aminomethane hydrochloride, polyvinyl alcohol 22 000 Da, glycerol anhydrous and DABCO; BioChemika, Fluka, Milan, Italy) and covered with cover glass. A confocal microscope (Leica DM IRBE/Leica TCS SP2, Leica Microsystems, Milan, Italy) was used to observe the cellular uptake of nanocomposites at an excitation wavelength of 390 nm and an emission wavelength of 512 nm for OXT and at an excitation wavelength of 346 nm and an emission wavelength of 460 nm for Hoechst 33258. The acquired images were processed by means of specific software (Leica Microsystem, Milan, Italy).

VI.2.9- HPLC ASSAY OF OXYTETRACYCLINE

Drug assay was performed using an HPLC system (series 200, Perkin Elmer, S) equipped with binary pump, autosampler, column oven and UV–VIS spectrophotometer. The stationary phase was a column Kromasyl® C18, 5 μm, 250 X 4.6 mm (Teknokroma, S) and the mobile phase was a mixture of phosphoric acid (H_3PO_4 pH 2.3) and CH_3CN (76/24 vol/vol). The flow rate was set at 1 ml/min, the injection volume was 10 μl, the detector wavelength 365 nm and the run time 8 min. Data were recorded using TotalChrom WS 6.2 software package (Perkin Elmer, S). The method was linear ($y = 7*10^6x - 8532$) in the range from 0.01 to 0.1 mg/ml, with $R^2 = 0.9997$.

VI.3- RESULTS AND DISCUSSION

VI.3.1- XRPD

CSAc (chitosan acetate) showed the typical pattern of a low crystalline powder (Figure VI.2), with diffraction bands around 8 º, 11 º and 20 º 2θ. VHS pattern corresponds to that of a montmorillonite rich clay sample, as described in a previous work (Aguzzi et al., 2005). In the PCNC, the peak at 7.3 º 2θ of VHS (corresponding to the reflection of the d_{001} spacing of the clay mineral (12.0 Å)) moves to 6.7 º 2θ (13.2 Å). This expansion can be explained by the intercalation via cation exchange between the positively charged amino groups of the polysaccharide and the interlayer Na^+ associated to the clay mineral. In agreement with Darder et al. (2003), the d_{001} spacing of the PCNC corresponded to the intercalation of CS as a monolayer inside the montmorillonite interlayer.

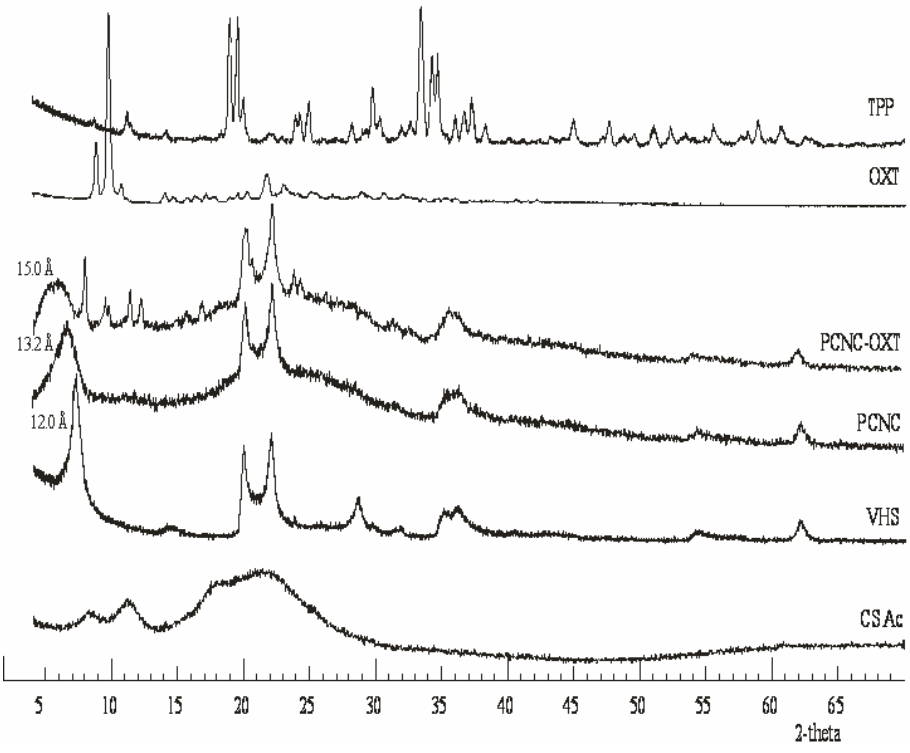

Figure VI.2. X-Ray diffraction patterns of the pure materials and nanocomposites.

XRPD patterns of OXT, TPP and drug-loaded PCNC are also included in Figure VI.2. OXT showed characteristics intense reflections at 9 º and 10 º 2θ (Kulshrestha et al., 2004), while various prominent crystalline peaks corresponding to a mixture of sodium

and potassium phosphates were observed in the case of TPP. As for loaded PCNC, the d-spacing (d_{001}) of the clay mineral further shifted to 15 Å, as a result of the intercalation of the drug molecules. Reflections corresponding to crystalline OXT and phosphates were also observed, indicating some degree of precipitation of the single constituents in the obtained nanocomposite.

VI.3.2- THERMOGRAVIMETRIC ANALYSIS

TGA curves of the samples are shown in Figure VI.3 CSAc showed three stages of weight loss with corresponding differential thermal analysis (DTA) peaks at 58.8ºC, 153.3 ºC and 292.6 ºC, respectively. The first stage occurred between 25ºC and 100ºC, being assigned to evaporation of absorbed water (11 % w/w). The second stage corresponds to the dehydration of polymer chains, occurring between 120 ºC and 250 ºC (17 % of weight loss).

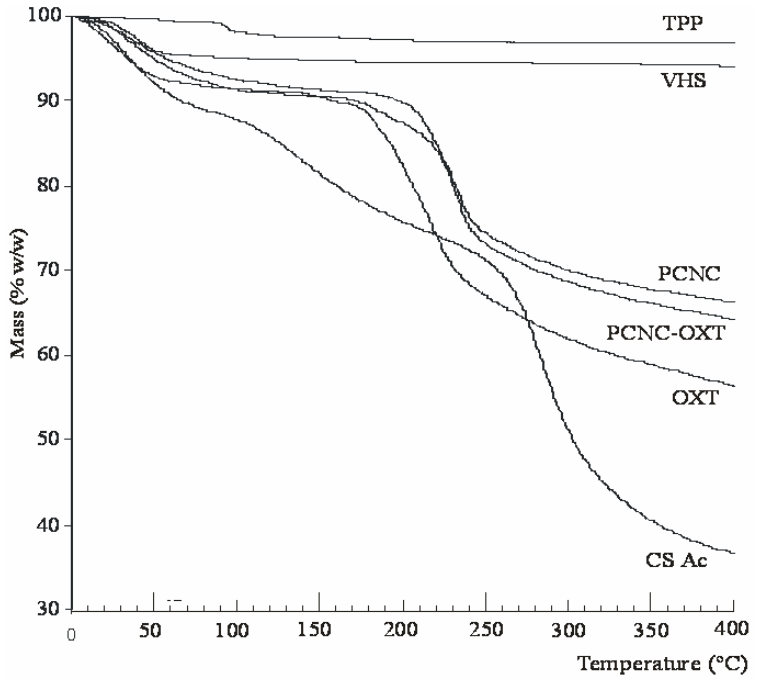

Figure VI.3. Thermogravimetric curves of the pure materials and nanocomposites.

Once dehydrated, the polymers chains undergo to the depolymerization and decomposition of the acetylated and deacetylated units (250- 350 ºC; 30 % w/w loss). Weight loss of VHS occurred in the interval between 25 ºC and 100 ºC (5 % w/w loss)

corresponding to loss of water moisture of external and interlayer clay surfaces. Above 100 ºC the clay did not show any other weight loss in the studied conditions. OXT showed a first weight loss below 100 ºC (DTA peak at 66.8 ºC) corresponding to free moisture (8 % w/w), followed by a second weight loss interval (180-260 ºC) ascribed to the degradation of the drug molecule.

In comparison with starting chitosan, TGA curve of PCNC did not show any weight loss in the interval 120-200 ºC. Only two weight loss steps were observed: the first one in the range 25-100 ºC, producing a mass loss of 6.5% (w/w), and the second between 200 and 300 ºC (DTA peak at 232.1 ºC), that can be assigned to dehydration, depolymerization and decomposition of the polymer chains. On the basis of these results, two important conclusions can be obtained. First of all, the amount of water retained by VHS increased (from 5 % to 6.5 %) as a result of the polymer chains intercalation, and finally, dehydration of chitosan was delayed up to 200 ºC, suggesting a higher thermal stability of the organic matter when intercalated into the clay mineral.

A similar behavior was observed for loaded PCNC, in which weight loss step (180-210 ºC) corresponding to the oxytetracycline degradation was also observed (DTA peak at 194.3 ºC).

VI.3.3- FTIR

FTIR spectra of CSAc showed a broad peak in the range of 3450–3100 cm^{-1}, assigned to stretching vibrations of O-H bonds, overlapping in the same region of a NH stretching (Figure VI.4). The peaks observed at 2944 cm^{-1} and 2890 cm^{-1} corresponded to C–H bonds and $–CH_3$ groups, respectively. Bending vibrations of $–CH_2$ (ν = 1380 cm^{-1}) and $–CH_3$ (ν = 1420 cm^{-1}) (Mano et al., 2003) were also observable. The 1645 cm^{-1} peak was associated to the vibration of carbonyl bonds of amide group CONH-R and the 1540 cm^{-1} peak corresponded to the bending vibrations of protonated amino groups ($–NH_3^+$) (Marchessault et al., 2006). Vibrations appearing in the interval 1160 cm^{-1} to 1000 cm^{-1} were ascribed to vibrations of –CO groups (Shigemasa et al., 1996; Nunthanid et al., 2001; Duarte et al., 2002; Xu et al., 2005). VHS spectrum showed a peak at 3640 cm^{-1}, ascribed to the stretching vibrations of interlayer O–H groups. The peak at 1658 cm^{-1} was attributed to the water molecules directly coordinated to the exchangeable cations of the clay. Stretching vibrations of Si–O bonds (ν = 997 cm^{-1}), as

well as bending vibrations of AlMgOH (ν = 798 cm^{-1}) and AlAlOH (ν =930 cm^{-1}) bonds were also clearly observed (Madejova et al., 1999). The frequency of the vibrational bands at 1540 cm^{-1} in the starting CSAc was shifted toward lower frequency in the nanocomposite (1520 cm^{-1}). This fact can be related to the electrostatic interaction between the protonated amine group and the negatively charged sites in the clay structure. The peak at 3640 cm^{-1} of interlayer O–H groups of VHS disappeared, confirming the intercalation via cation exchange of the polysaccharide in the clay interlayer. In the interval between 1030 cm^{-1} and 570 cm^{-1} overlapping of Si–O–Si absorbance band of VHS with C–O–C band of CSAc did not allow a clear description of the spectra, in line with other previous works (Paluszkiewicz et al., 2011).

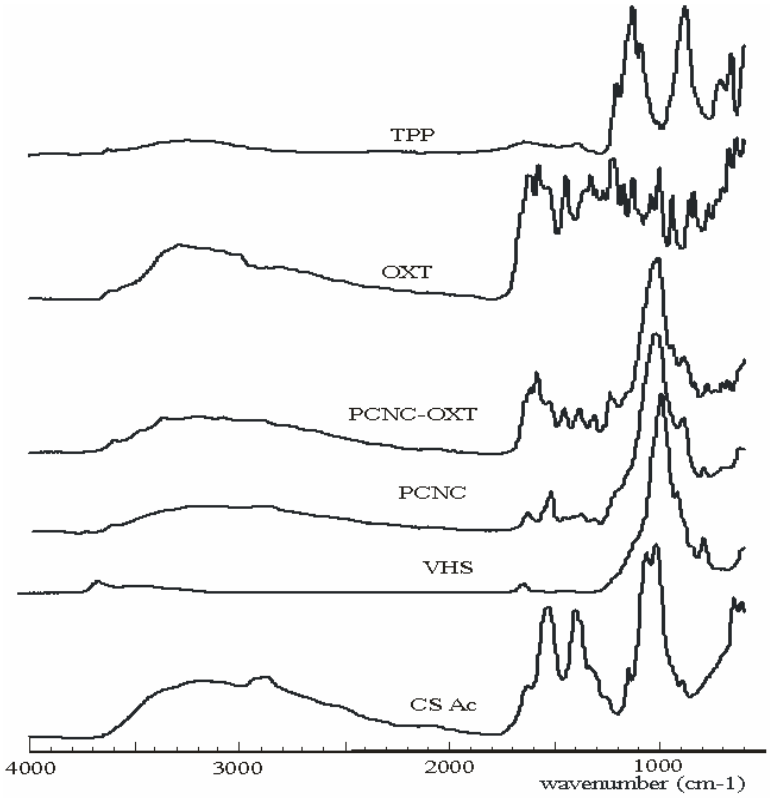

Figure VI.4. FTIR spectra of the pure materials and nanocomposites.

Loaded PCNC showed the typical peaks of oxytetracycline corresponding to amide I and II vibrations at 1630 cm^{-1} (amide I bands) and 1553 cm^{-1} (amide II bands). IR bands in the region 1400 - 600 cm^{-1} did not correspond to functional groups involved in possible drug-nanocomposite interactions and overlapped with TPP characteristic peaks

(1186 cm^{-1} (P=O stretching)), 1148 cm^{-1} (symmetric and antisymmetric stretching vibrations in PO_2 group), 1093 cm^{-1} (symmetric and antisymmetric stretching vibrations in PO_3 group), 912 cm^{-1} (antisymmetric stretching of the P-O-P bridge) (Corbridge et al., 1954; Gierszewska-Drużyńska et al., 2010). Papadimitriou et al. (2008) found that interaction of TPP with CS induced changes in the characteristic band of amide groups of the polymer in the region (1650 – 1600 cm^{-1}). Similar results were also obtained by Hua et al. (2010). These changes were not visible in our spectra because of overlapping of amide bands of CS with those of the drug.

VI.3.4- ZETA POTENTIAL AND PARTICLE SIZE DISTRIBUTION

Zeta potential of VHS was -45,1 mV (± 0.4 mV) corresponding to the negative charged clay particles. After intercalation of chitosan, the resulting nanocomposite particles showed positive values of zeta potential (35.1 mV ± 0.2 mV)), indicating that clay particles were covered by ionized CS molecules. This result corroborates the electrostatic interaction between CSAc and VHS. In fact, the nanocomposite structure resulted from a homogeneous dispersion of VHS particles in a chitosan matrix with intercalation of polysaccharide chains inside the phyllosilicate interlayer space. In the loaded PCNC, the measured zeta potential was 23.5 mV (± 0.6 mV). This decrease in zeta potential in comparison with the unloaded PCNC might be due to the partial anionic character of the exchanged drug molecule (pk_a 3.3; 7.3; 9.1).

In figure VI.5., particle size distribution of loaded PCNC is shown. Mode was 50 μm and resulting statistical diameter were 82.91 μm ($d_{0.9}$), 35.87 μm ($d_{0.5}$) and 8.98 μm ($d_{0.1}$).

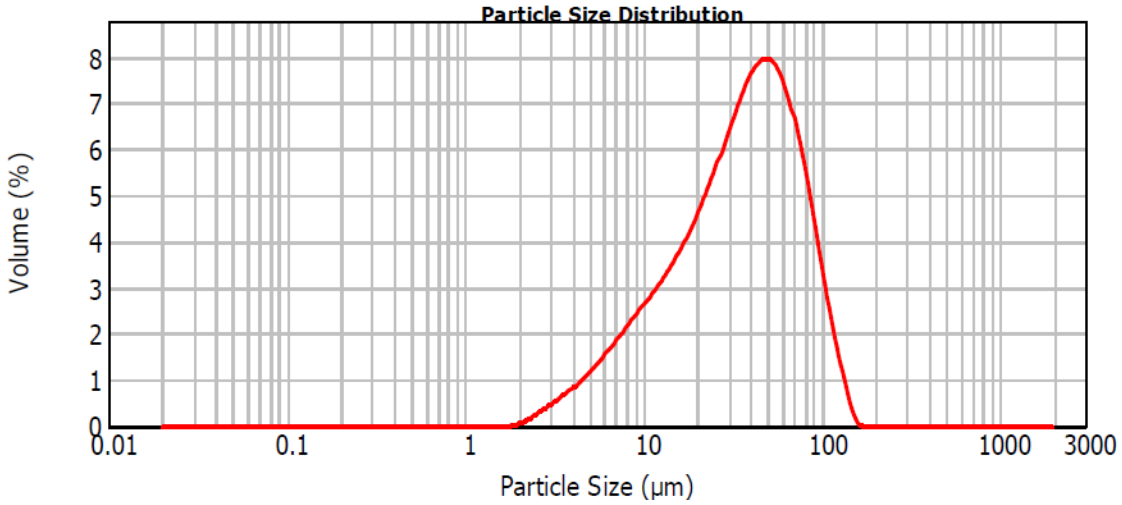

Figure VI.5. Granulometric distribution of loaded PCNC (< 63 µm sieve fraction).

It can be concluded that even if the interaction between the nanocomposite components (in particular, the intercalation of the polysaccharide chains into clay interlayers) are, as discussed previously, in the nanometer scale, the resulting particle size of the nanocomposites are in the micrometer scale.

VI.3.5- CYTOTOXICITY

In Figure VI.6. the results of cytotoxicity assay are reported. The viability was evaluated for the following samples: drug alone (OXT) at 0.075 and 0.0375 mg/ml; the corresponding loaded nanocomposites PCNC-OXT at 0.25 and 0.5 mg/ml and unloaded nanocomposites (PCNC) at 0.25 and 0.5 mg/ml. The nanocomposites crosslinked with TPP were also evaluated PCNC-TPP at 0.25 and 0.5 mg/ml.

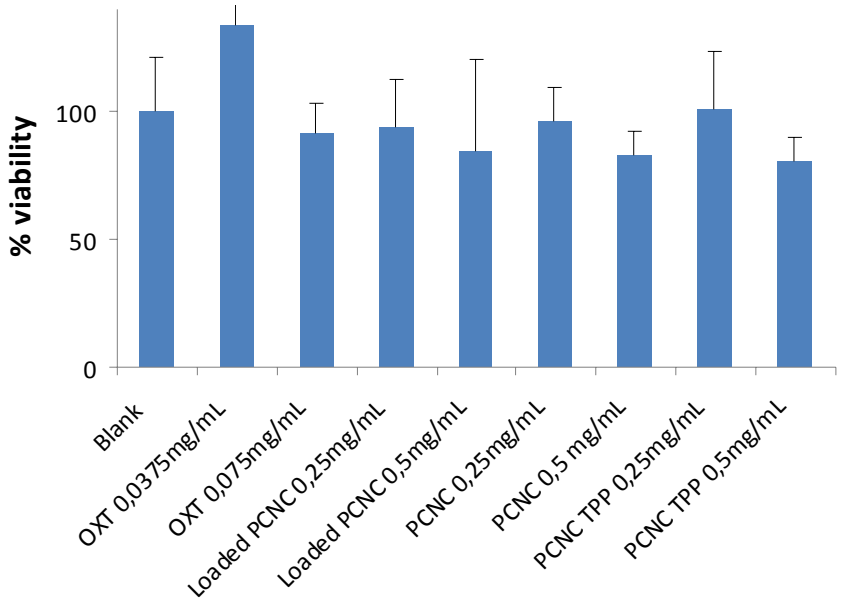

Figure VI.6. Caco-2 cell viability (%) after contact with OXT, PCNC, PCNC crosslinked with TPP, and loaded PCNC, at various concentrations (mean values ± sd; n=8).

All the samples resulted in % viability values close to 100%, to indicate good biocompatibility of the systems at the studied concentrations. This means that the montmorillonite and chitosan also combined to form nanocomposites are biocompatible as well as the nanocomposites crosslinked with TPP (in agreement with Salcedo et al. 2012). Moreover the OXT loading into the nanocarriers did not cause cytotoxic effect on Caco-2 cell line. Concentrations of nanocomposites that showed higher average values of cell viability (PCNC 0.25 mg/ml and OXT 0.0375 mg/ml) were selected for further characterization, in particular drug permeability.

VI.3.6- DRUG PERMEABILITY

Figure VI.7 shows the TEER % profiles as a function of time for nanocomposites at the concentration of 0.25 mg/ml and for OXT at the concentration equal to 0.0375 mg/ml. The TEER % profile of OXT was almost close the 100% for all the experiment time, to indicate that the substrates did not change the interconnections between cells due to the drug alone. As for the nanocomposite there was a moderate but significant decrease of the TEER % that reached the minimum value after three hours of contact time (the end

of the experiment). This decrease even if is quite limited could be due to the presence of chitosan in the nanocomposites which could interfere with the junctional proteins causing a widen of the paracellular route.

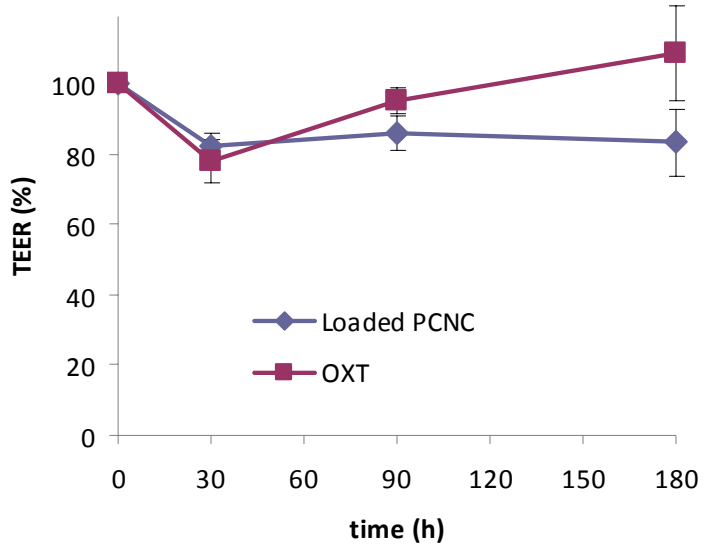

Figure VI.7. TEER % profiles of loaded PCNC (0.25 mg/ml) and OXT (0.0375 mg/ml) (mean values ± sd; n = 3).

Figure VI.8 shows the % of OXT permeated to the basolateral phase during the permeability experiments. Permeated amount was almost constant for the drug alone but increases for the nanocomposites. This probably means that OXT alone was subjected to P-gp action and the permeation was limited, while the nanocomposite could elude the P-gp efflux and consequently the amount of drug permeated to the basolateral phase increases with time.

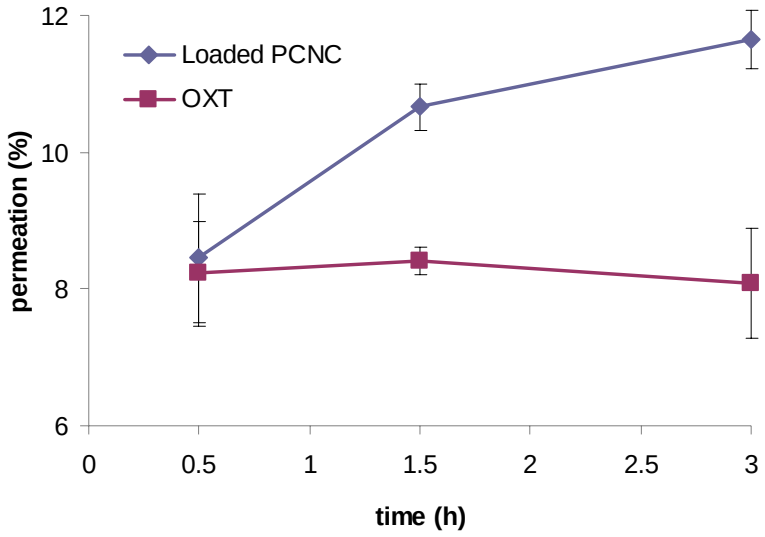

Figure VI.8. % profiles of drug permeated (mean values ± sd; n = 3).

VI.3.7- CLSM

To investigate the fate of OXT and the interaction with Caco-2 cell monolayers, CLSM analysis was performed on the substrates subjected to the permeability experiments. CLSM microphotographs obtained after 1.5 h (Figure VI.9.) and 3 h (Figure VI.10.) of contact time between Caco-2 substrates and either nanocomposite or drug alone showed the nuclei of the cells in blue and the nanocomposites loaded with oxytetracycline or the drug alone in light red. As both the contact time the OXT loaded nanocomposite were present in the cell substrates. In particular some particles are visible and in the z-projection it can be notice that the particles are into the depth of the cell substrate to indicate an actual internalization and not only a membrane interaction.

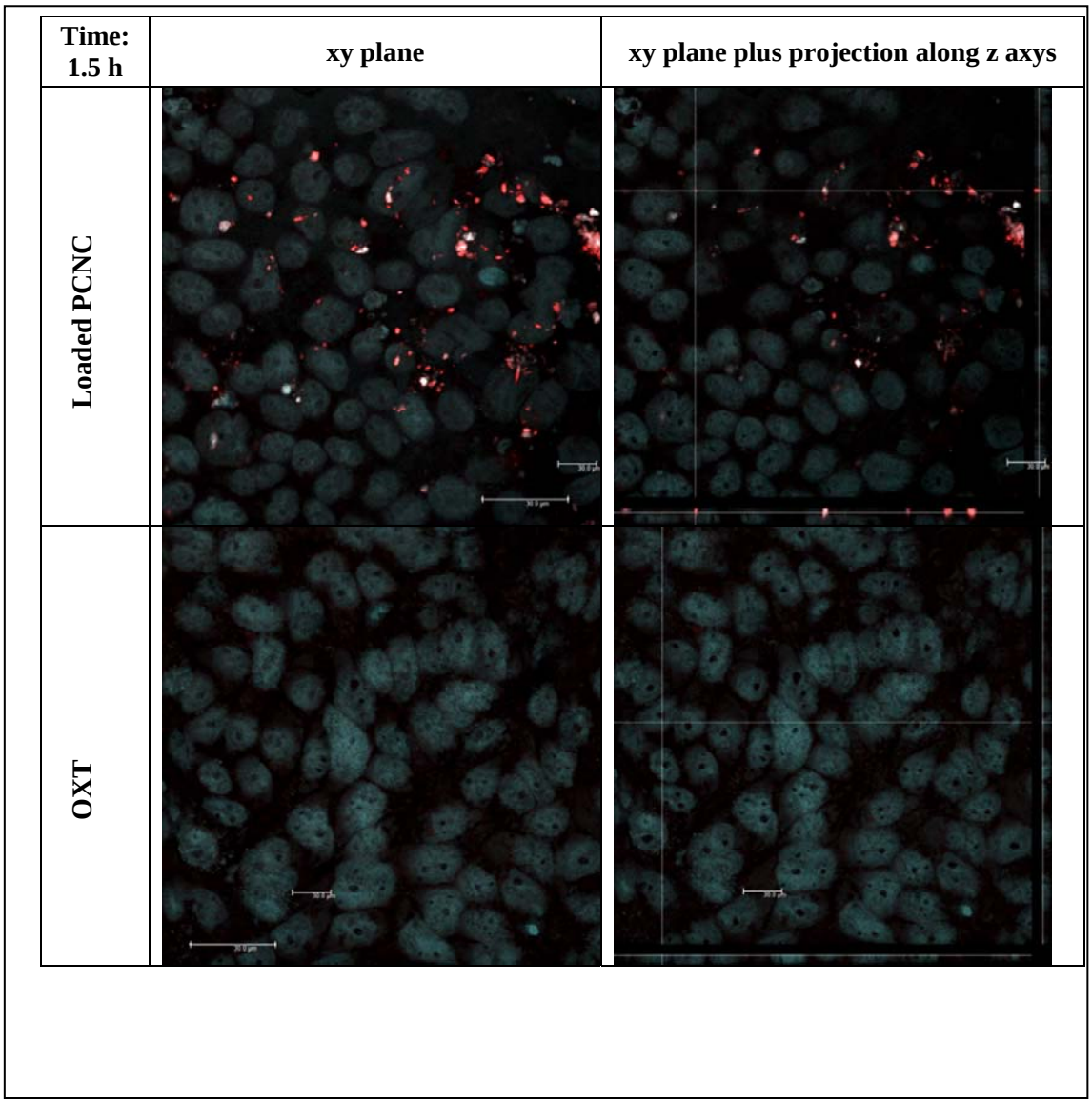

Figure VI.9. CLSM microphotographs of Caco-2 substrates treated with loaded PCNC or OXT for 1.5 h.

The nuclei were well defined without signal of apoptosis, to confirm the lack of cytotoxicity of the chitosan montmorillonite nanocomposite.

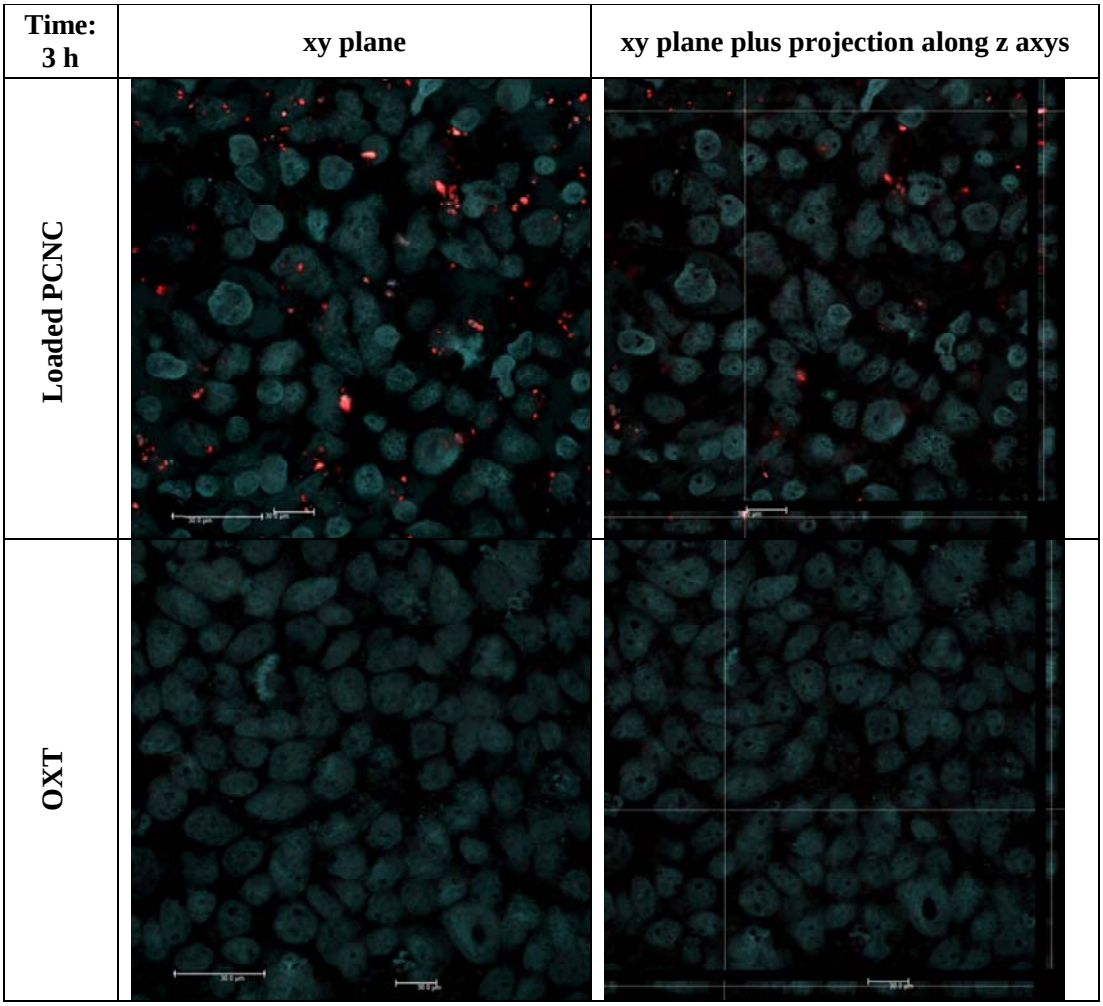

Figure VI.10. CLSM microphotographs of Caco-2 substrates treated with loaded PCNC or OXT for 3 h.

VI.4- CONCLUSIONS

It was possible to prepare a nanocomposite based on montmorillonite and chitosan and loaded with oxytetracycline, as confirmed by thermogravimetry and FTIR analysis. Such a system was characterized by good biocompatibility towards Caco-2 cells.

The nanocomposite slightly decreased the permeation rate of the drug in the first phase of the permeation assay, nevertheless the permeation was linear and proceeded all over the experiment time.

The CLSM analysis suggests that there was an interaction between the nanocomposites and the cell substrates thus causing the uptake of the nanocomposite into the cells.

Even if a limited enhancement of drug permeation was determined by the nanocomposites the mechanism of internalization/uptake should be a chance for the drug to elude the P-gp. This should be promising to obtain high bioavailability in vivo after oral administration of the drug.

CAPÍTULO VII.

Conclusiones

En esta Tesis doctoral se han desarrollado nanocomposites de quitosano y montmorillonita, evaluando su seguridad y eficacia como sistemas de transporte del antibiótico Oxitetraciclina. Fruto del trabajo desarrollado se han publicado (uno aún pendiente de publicación) cuatro artículos JCR situados entre los primeros de su categoría, en los que se abordan los objetivos planteados en la Tesis. En cada uno de ellos se dan conclusiones parciales que han quedado plasmadas en los capítulos anteriores. En el presente capítulo de conclusiones de esta memoria de Tesis doctoral se señalan aquellas que consideramos conclusiones generales a las que cabe llegar, que son las siguientes:

1. El quitosano es un polisacárido susceptible de ser empleado como matriz para la obtención de sistemas híbridos de tipo nanocomposite de interés farmacéutico, mediante la incorporación a escala nanométrica de partículas de montmorillonita.

2. La incorporación de montmorillonita a un gel de quitosano puede realizarse a temperatura ambiente y por interacción sólido-líquido, en la que a través de un mecanismo de intercambio catiónico se obtiene una estructura formada por la intercalación de cadenas de polímero en la interlámina del filosilicato.

3. La matriz polímerica resultante de la incorporación del filosilicato presenta propiedades diferenciadas, que incluyen cambios en el potencial electrocinético de las partículas de los componentes cuando forman el nanocomposite.

3. Los nanocomposites quitosano/montmorillonita obtenidos presentan propiedades mucoadhesivas de especial interés en sus aplicaciones como excipientes de liberación modificada.

4. Los nanocomposites quitosano/montmorillonita obtenidos presentan buena biocompatibilidad y estimulan la proliferación celular en cultivos de células Caco-2.

5. Los nanocomposites quitosano/montmorillonita obtenidos pueden actuar como soportes de oxitetraciclina dando lugar a complejos fármaco-nanoexcipiente con presencia del antibiótico a nivel de la interlámina del filosilicato.

6. Los nanocomposites cargados con oxitetraciclina no presentan citotoxicidad en las concentraciones ensayadas en cultivos de células Caco-2 y promueven la permeabilidad del fármaco, evitando el conocido efecto limitante de su biodisponibilidad inducido por la glicoproteina P.

Como corolario de la Tesis Doctoral puede inferirse que:

El desarrollo tecnológico centrado en la interacción a escala nanométrica de excipientes "clasicos", como la montmorillonita y el quitosano, puede conducir a la obtención de materiales novedosos susceptibles de empleo como excipientes de última generación con prometedoras funcionalidades de interés biofarmacéutico.

CAPÍTULO VII.

Bibliografía

Aguzzi C., Viseras C., Cerezo P., Rossi S., Ferrari F., López-Galindo A., Caramella C. (2005). Influence of dispersion conditions of two pharmaceutical grade clays on their interaction with some tetracyclines. Appl. Clay Sci. 30(2), 79-86.

Aguzzi C., Cerezo P., Viseras C., Caramella C. (2007). Use of clays as drug delivery systems: Possibilities and limitations. Appl. Clay Sci. 36(1-3), 22-36.

Aguzzi C., Capra P., Bonferoni C., Cerezo P., Salcedo I., Sánchez R., Caramella C., Viseras C. (2010). Chitosan-silicate biocomposites to be used in modified drug release of 5-aminosalicylic acid (5-ASA). Appl. Clay Sci. 50(1), 106-111.

Aiedeh K., Taha MO. (2001). Synthesis of iron-crosslinked chitosan succinate and iron-crosslinked hydroxamated chitosan succinate and their in vitro evaluation as potential matrix materials for oral theophylline sustained-release beads. Eur. J. Pharm. Sci. 13(2), 159-168.

Aimin C., Chunlin H., Juliang B., Tinyin Z., Zhichao D. (1999). Antibiotic loaded chitosan bar. An in vitro, in vivo study of a possible treatment for osteomyelitis. Clin. Orthop. Relat. Res. 366, 239-247.

Alexandre M., Dubois P. (2000). Polymer-layered silicate nanocomposites: preparation, properties and uses of a new class of materials. Mater. Sci. Eng. R. 28, 1-63.

An J., Dultz S. (2007). Adsorption of tannic acid on chitosan-montmorillonite as a function of pH and surface charge properties. Appl. Clay Sci. 36(4), 256-264.

Arizmendi-Morquecho A., Chávez-Valdez A., Navarro CH., Moreno KJ. (2013). Performance evaluation of chitosan/hydroxyapatite composite coating on ultrahigh molecular weight polyethylene. Polym. Test. 32(1), 32-37.

Artursson P., Palm K., Luthman K. (2001). Caco-2 monolayers in experimental and theoretical predictions of drug transport. Adv. Drug Deliv. Rev. 46(1-3), 27-43.

Aspden T., Illum L., Skaugrud O. (1997). The effect of chronic nasal application of chitosan solutions on cilia beat frequency in guinea pigs. Int. J. Pharm. 153(2), 137-146.

Azab AK., Doviner V., Orkin B., Kleinstern J., Srebnik M., Nissan A., Rubinstein A. (2007). Biocompatibility evaluation of crosslinked chitosan hydrogels after subcutaneous and intraperitoneal implantation in the rat. J. Biomed. Mater. Res. A. 83(2), 414-422.

Bailey, SW. (1980). Summary of recommendation of AIPEA. Nomenclature Committee. Clays and Clay Minerals. 28, 73-78.

Baxter A., Dillon M., Taylor KDA., Roberts GAF. (1992). Improved method for i.r. determination of the degree of *N*-acetylation of chitosan. Int. J. Biol. Macromol. 14(3), 166-169.

Bergaya F., Theng BKG., Lagaly G. (2006). Handbook of Clay Science. Elsevier, Amsterdam.

Bernkop-Schnürch A., Dünnhaupt S. (2012). Chitosan-based drug delivery systems. Eur. J. Pharm. Biopharm. 81(3), 463-469.

Beyer G. (2002). Nanocomposites: a new class of flame retardants for polymers. Plast. Addit. Compound. 4(10), 22-27.

Bharadwaj RK. (2001). Modeling the barrier properties of polymer-layered silicate nanocomposites. Macromolecules. 34(26), 9189-9192.
Bhattacharyya KG., Gupta SS. (2008). Adsorption of a few heavy metals on natural and modified kaolinite and montmorillonite: a review. Adv. Colloid Interfac. Sci. 140(2), 114-131.

Bhise K., Dhumal R., Paradkar A., Kadam S. (2008). Effect of drying methods on swelling, erosion and drug release from chitosan–naproxen sodium complexes. AAPS Pharm. Sci. Tech. 9(1), 1-12.

Biswas M., Sinha Ray S. (2001). Recent progress in synthesis and evaluation of polymer-montmorillonite nanocomposites. Adv. Polym. Sci. 155, 167-221.

Bivas-Benita M., Laloup M., Versteyhe S., Dewit J., De Braekeleer J., Jongert E. (2003). Generation of Toxoplasma gondii GRA1 protein and DNA vaccine loaded chitosan particles: preparation, characterization and preliminary in vivo studies. Int. J. Pharm. 266(1-2), 17-27.

Borchard G., Lueßen HL., de Boer AG., Verhoef JC., Lehr C. (1996). The potential of mucoadhesive polymers in enhancing intestinal peptide drug absorption. III: Effects of chitosan-glutamate and carbomer on epithelial tight junctions in vitro. J. Control. Release. 39, 131-138.

Bowler P., Duerden B., Armstrong D. (2001). Wound microbiology and associated approaches to wound management. Clin. Microbiol. Rev. 14(2), 244-269.

Braun DB. (1994). Antidiarrheal products. In: Braun DB. (Ed.), Over the Counter Pharmaceutical Formulations. Noyes Publications, New Jersey, USA, pp. 61-71.

Bravo-Osuna I., Vauthier C., Farabollini A., Palmieri GF., Ponche G. (2007). Mucoadhesion mechanism of chitosan and thiolated chitosan-poly (isobutyl cyanoacrylate) core-shell nanoparticles. Biomaterials. 28, 2233-2243.

Brindley GW., Pedro G. (1972). Report of the AIPEA Nomenclature Committee, AIPEA Newsletter Nº. 7, pp. 8-13.

Burnside SD., Giannelis EP. (1995). Synthesis and properties of new poly(dimethylsiloxane) nanocomposites. Chem. Mater. 7(9), 1597-600.

Calcagno AM., Ludwig JA., Fostel JM., Gottesman MM., Ambudkar SV. (2006). Comparison of drug transporter levels in normal colon, colon cancer, and Caco-2 cells: impact on drug disposition and discovery. Mol. Pharm. 3(1), 87-93.

Calvo P., Vila-Jato JL., Alonso MJ. (1997). Evaluation of cationic polymer-coated nanocapsules as ocular drug carriers. Int. J. Pharm. 153(1), 41-50.

Campbell K., Craig DQM., McNallyt T. (2008). Poly(ethylene glycol) layered silicate nanocomposites for retarded drug release prepared by hot-melt extrusion. Int. J. Pharm. 363(1-3), 126-131.

Cao F., Wang Y., Ping Q., Liao Z. (2011). Zn-Al-NO_3-layered double hydroxides with intercalated diclofenac for ocular delivery. Int. J. Pharm. 404(1-2), 250-256.

Carreño-Gómez B., Duncan R. (1997). Evaluation of the biological properties of soluble chitosan and chitosan microspheres. Int. J. Pharm. 148(2), 231-240.

Celis R., Adelino MA., Hermosin MC., Cornejo J. (2012). Montmorillonite–chitosan bionanocomposites as adsorbents of the herbicide clopyralid in aqueous solution and soil/water suspensions. J. Hazard. Mater. 209-210, 67-76.

Chae SY., Jang MK., Nah JW. (2005). Influence of molecular weight on oral absorption of water soluble chitosans. J. Control. Release. 102(2), 383-394.

Chandy T., Sharma CP. (1990). Chitosan as a biomaterial. Artif. Cells Artif. Organs. 18(1), 1-24.

Chatelet C., Damour O., Domard A. (2001). Influence of the degree of acetylation on some biological properties of chitosan films. Biomaterials. 22(3), 261-268.

Chatterjee S., Lee MW., Woo SH. (2010). Adsorption of Congo red by chitosan hydrogel beads impregnated with carbon nanotubes. Bioresour. Technol. 101(6), 1800-1806.

Chen SC., Wu YC., Mi FL., Lin YH., Lin CY., Hsing WS. (2008). A novel pH sensitive hydrogel composed of N,O-carboxymethyl chitosan and alginate crosslinked by genipine for protein drug delivery. J. Control. Release. 96(2), 245-52.

Chieruzzi M., Miliozzi A., Kenny JM. (2013). Effects of the nanoparticles on the thermal expansion and mechanical properties of unsaturated polyester/clay nanocomposites. Compos. Part. A Appl. Sci. Manuf. 45, 44-48.

Chin IJ., Thurn-Albrecht T., Kim HC., Russell TP., Wang J. (2001). On exfoliation of montmorillonite in epoxy. Polymer. 42(13), 5947-5952.

Cho JW., Paul DR. (2001). Nylon 6 nanocomposites by melt compounding. Polymer. 42(3), 1083-1094.

Chopra I., Roberts M. (2001). Tetracycline antibiotics: mode of action, applications, molecular biology and epidemiology of bacterial resistance. Microbiol. Mol. Biol. Rev. 65(2), 232-260.

Chourasia MK., Jain SK. (2004). Polysaccharides for colon targeted drug delivery. Drug. Deliv. 11(2), 129-148.

Choy JH., Choi SJ., Oh JM., Park T. (2007). Clay minerals and layered double hydroxides for novel biological applications. Appl. Clay Sci. 36(1-3), 122–132.

Chrissafis K., Bikiaris D. (2011). Can nanoparticles really enhance thermal stability of polymers Part I: An overview on thermal decomposition of addition polymers. Thermochim. Acta. 523(1-2), 1-24.

Chung YC., Chen CY. (2008). Antibacterial characteristics and activity of acid-soluble chitosan. Bioresour. Technol. 99(8), 2806-2814.

Cojocariu A., Profire L., Aflori M., Vasile C. (2012). In vitro drug release from chitosan/Cloisite 15A hydrogels. Appl. Clay Sci. 57, 1-9.

Corbridge DEC., Lowe EJ. (1954). The infrared spectra of some inorganic phosphorus compounds. J. Chem. Soc. 493-502.

Cushen M., Kerry J., Morris M., Cruz-Romero M., Cummins E. (2012). Nanotechnologies in the food industry and recent developments, risks and regulation. Trends Food Sci. Tech. 24(1), 30-46.

Dabrowski F., Lebras M., Bourbigot S., Gilman JW., Kashiwagi T. (1999). PA-6 montmorillonite nanocomposite in intumescent fire retarded EVA. Proceedings of the Eurofillers'99, Lyon-Villeurbanne, France.

Darder M., Colilla M., Ruiz-Hitzky E. (2003). Biopolymer–clay nanocomposites based on chitosan intercalated in montmorillonite. Chem. Mater. 15(20), 3774-3780.

Darder M., Colilla M., Ruiz-Hitzky E. (2005). Chitosan–clay nanocomposites: application as electrochemical sensors. Appl. Clay Sci. 28(1-4), 199-208.

De Campos AM., Sanchez A., Alonso MJ. (2001). Chitosan nanoparticles: a new vehicle for the improvement of the delivery of drugs to the ocular surface. Application to cyclosporin A. Int. J. Pharm. 224(1-2), 159-168.

De Liguoro M., Cibin V., Capolongo F., Halling-Sorensen B., Montesissa C. (2003). Use of oxytetracycline and tylosin in intensive calf farming: evaluation of transfer to manure and soil. Chemosphere. 52(1), 203-212.

De Sousa Rodrigues LA., Figueiras A., Veiga F., De Freitas RM., Nunes Livio CC., Da Silva Leite CM., Da Silva Leite CM. (2013). The systems containing clays and clay minerals from modified drug release: a review. Colloids Surf. B Biointerfaces. 103, 642-651.

Del Arco M., Fernández A., Martín C., Rives V. (2007). Intercalation of mefenamic and meclofenamic acid anions in hydrotalcite-like matrixes. Appl. Clay Sci. 36(1-3), 133-140.

Del Arco M., Fernández A., Martín C., Rives V. (2009). Release studies of different NSAIDs encapsulated in Mg, Al, Fe-hydrotalcites. Appl. Clay Sci. 42, 538–544.

Dennis HR., Hunter DL., Chang D., Kim S., White JL., Cho JW., Paul DR. (2001). Effect of melt processing conditions on the extent of exfoliation in organoclay-based nanocomposites. Polymer. 42(23), 9513-9522.

Depan D., Kumar AP., Singh RP. (2009). Cell proliferation and controlled drug release studies of nanohybrids based on chitosan-g-lactic acid and montmorillonite. Acta Biomater. 5(1), 93-100.

Des Rieux A., Fievez V., Garinot M., Schneider YJ., Preat V. (2006). Nanoparticles as potential oral delivery systems of proteins and vaccines: a mechanistic approach. J. Control. Release. 116(1), 1-27.

Des Rieux A., Fievez V., Theate I., Mast J., Preat V., Schneider YJ. (2007). An improved in vitro model of human intestinal follicle-associated epithelium to study nanoparticle transport by M cells. Eur. J. Pharm. Sci. 30(5), 380-391.

Devadasu VR., Bhardwaj V., Kumar MNVR. (2013). Can Controversial Nanotechnology Promise Drug Delivery?. Chem. Rev. 113, 1686-1735.

Díaz Crespín G. (2002). Caracterización de quitina y quitosano obtenidos a partir de exoesqueletos de camarón. Ph.D. Thesis, University of Salvador, Salvador, America.

Ding X., Alani AWG., Robinson JR. (2002). Extended-release and targeted drug delivery systems. In: Troy, DB. (Ed.), Remington: The Science and Practice of Pharmacy, 21st Edition. Lippincott Williams & Wilkins, USA, pp. 939–964. Chap. 47.

Directive 75/318/EEC. (1992). Quality of Prolonged Release Oral Solid Dosage Forms, European Directorate for Medicinal Products (EMEA). November.

Dodane V., Khan MA., Merwin JR. (1999). Effect of chitosan on epithelial permeability and structure. Int. J. Pharm. 182(1), 21-32.

Dollery C. (1999). Tetracicline hydrochloride (2nd ed). Therapeutic Drugs, Churchill Livingstone, London, pp. T66-T69.

Dong YI., Feng SS. (2005). Poly(d,l-lactide-co-glycolide)/montmorillonite nanoparticles for oral delivery of anticancer drugs. Biomaterials. 26(30), 6068-6076.

Dornish M., Hagen A., Hansson E., Pecheur C., Verdier F., Skaugrad O. (1997). Safety of protasan: ultrapure chitosan salts for biomedical and pharmaceutical use. In: Domard A., Roberts G., Varum K. (Eds.), Advances of Chitin Sci., vol II. Jaques Andre, Lyon, France, pp. 694-670.

Duarte ML., Ferreira MC., Marvao MR., Rocha J. (2002). An optimised method to determine the degree of acetylation of chitin and chitosan by FTIR spectroscopy. Int. J. Biol. Macromol. 31(1-3), 1-8.

Duceppe N., Tabrizian M. (2010). Advances in using chitosan-based nanoparticles for in vitro and in vivo drug and gene delivery. Expert Opin. Drug Deliv. 7(10), 1191-1207.

Dyer, DC. (1989). Pharmacokinetics of oxytetracycline in the turkey: evaluation of biliary and urinary excretion. Am. J. Vet. Res. 50(4), 522-524.

El-Kamel A., Sokar M., Naggar V., Al Gamal S. (2002). Chitosan and sodium alginate based bioadhesive vaginal tablets. AAPS J. 4(4), 224-230.

El-Leithy ES., Shaker DS., Ghorab MK., Abdel-Rashid RS. (2010). Evaluation of mucoadhesive hydrogels loaded with diclofenac sodium–chitosan microspheres for rectal administration. AAPS Pharm. Sci. Tech. 11(4), 1695-16702.

El-Sherif H., El-Masry M. (2011). Superabsorbent nanocomposite hydrogels based on intercalation of chitosan into activated bentonite. Polymer Bull. 66(6), 721-734.

EP 6.0. (2008). European Pharmacopoeia Sixth Edition. Directorate for the Quality of Medicines of the Councile of Europe, Strasbourg (F).

FDA. (2009). Inactive ingredients database for approved drug products. FDA/Center for Drug Evaluation and Research. Office of Generic Drugs. Division of Labeling and Program Support. Database Last Updated: July 10. http://www.fda.gov/Drugs/InformationOnDrugs/.

Felt O., Buri P., Gurny R. (1998). Chitosan: a unique polysaccharide for drug delivery. Drug Dev. Ind. Pharm. 24(11), 979-993.

Feng SS., Mei L., Anitha P., Gan CW., Zhou W. (2009). Poly(lactide)-vitamin E derivative/montmorillonite nanoparticle formulations for the oral delivery of Docetaxel. Biomaterials. 30, 3297-3306.

Fernández-Urrusuno R., Calvo P., Remuñán-López C., Vila-Jato JL., Alonso MJ. (1999). Enhancement of nasal absorption of insulin using chitosan nanoparticles. Pharm. Res. 16(10), 1576-1581.

Ferrari F., Rossi S., Bertoni M., Caramella C., Geddo M. (1991). Modelling of water penetration into fast disintegrating tablets. STP Pharma Sci. 1(2), 137-144.

Ferrari F., Rossi S., Martini A., Muggetti L., De Ponti R., Caramella C. (1997). Technological induction of mucoadhesive properties on waxy starches by grinding. Eur. J. Pharm. Sci. 5(5), 277-285.

Fisher A., Watling M., Smith A., Knight A. (2010). Pharmacokinetic comparisons of three nasal fentanyl formulations; pectin, chitosan and chitosan–poloxamer 188. Int. J. Clin. Pharmacol. Ther. 48(2), 138-145.

Flood E., Block S., Hall M., Rousculp M., Divino V., Toback S., Mahadevia P. (2010). Children's perceptions of influenza illness and preferences for influenza vaccine. J. Pediatr. Health Care. 25(3), 171-179.

Fornes TD., Yoon PJ., Keskkula H., Paul DR. (2001). Nylon 6 nanocomposites: the effect of matrix molecular weight. Polymer. 42(25), 9929-9940.

Fornes TD., Paul DR. (2003). Modeling properties of nylon 6/clay nanocomposites using composite theories. Polymer. 44(17), 4993-5013.

Forsgren J., Jamstorp E., Bredenberg S., Engqvist H., Stromme M. (2010). A ceramic drug delivery vehicle for oral administration of highly potent opioids. J. Pharm. Sci. 99(1), 219-226.

Fredrickson GH., Bicerano J. (1999). Barrier properties of oriented disk composites. J. Chem. Phis. 110(4), 2181-2188.

Fukushima K., Wu MH., Bocchini S., Rasyida A., Yang MC. (2012a). PBAT based nanocomposites for medical and industrial applications. Mater. Sci. Eng. C Mater. Biol. Appl. 32(6), 1331-1351.

Fukushima K., Tabuani D., Camino G. (2012b). Poly(lactic acid)/clay nanocomposites: effect of nature and content of clay on morphology, thermal and thermo-mechanical properties. Mater. Sci. Eng. C Mater. Biol. 32(7), 1790-1795.

Futalan CM., Kan CC., Dalida ML. (2011). Comparative and competitive adsorption of copper, lead, and nickel using chitosan immobilized on bentonite. Carbohyd. Polym. 83(2), 528-536.

Gades MD., Stern JS. (2003). Chitosan supplementation and fecal fat excretion in men. Obesity Res. 11(5), 683-688.

García-Casal MN., Leets I., Layrisse M. (2000). β-carotene and inhibitors of iron absorption modify iron uptake by Caco-2 cells. J. Nutr. 130(1), 5-9.

Genta I., Conti B., Perugini P., Pavanetto F., Spadaro A., Puglisi G. (1997). Bioadhesive microspheres for ophthalmic administration of acyclovir. J. Pharm. Pharmacol. 49(8), 737-742.

Germershaus O., Mao SR., Sitterberg J., Bakowsky U., Kissel T. (2008). Gene delivery using chitosan, trimethyl chitosan or polyethylenglycol-graft-trimethyl chitosan block copolymers: establishment of structure–activity relationships in vitro. J. Control. Release. 125(2), 145-154.

Ghaffarian R., Bhowmick T., Muro S. (2012). Transport of nanocarriers across gastrointestinal epithelial cells by a new transcellular route induced by targeting ICAM-1. J. Control. Release. 163(1), 25-33.

Giannelis EP. (1996). Polymer layered silicate nanocomposites. Adv. Mater. 8(1), 29-35.

Giannelis EP. (1998). Polymer-layered silicate nanocomposites: synthesis, properties and applications. Appl. Organomet. Chem. 12(10-11), 675-680.

Gierszewska-Drużyńska M., Ostrowska-Czubenko J. (2010).The effect of ionic crosslinking on thermal properties of hydrogel chitosan membranes. In: Jaworska MM. (Ed.), Progress on Chemistry and Application of Chitin and Its Derivates, vol. XV, Polish Chitin Society, Łódź, pp. 25-32.

Giles CH., Smith D., Huitson A. (1974). A general treatment and classification of the solute adsorption isotherm. I. Theoretical. J. Colloid Interface Sci. 47(3), 755–765.

Gilman JW., Kashiwagi T., Brown JET., Lomakin S. (1998a). Flammability studies of polymer layered silicate nanocomposites. In: Kigler HS., Rasmussen LA., Pilato LA., Tolle TB (Eds), Materials and Process Affordability keys to the Future. 43rd International Society for the Advancement of Material and Process Engineering (SAMPE) Symposium and Exhibition, Covina, California, pp. 1053-1066.

Gilman JW., Kashiwagi T., Giannelis EP., Manias E., Lomakin S., Lichtenhan JD., Jones P. (1998b). Radiative gasification and vinyl polymer flammability. In: Camino G., Bourbigot S., Delobel R. (Eds), Fire Retardancy of polymers: The Use of Intumescence Cambridge: The Royal Society of Chemistry. 6th European Meeting. (FRPM'97). Proceedings, Lille, France, pp. 203-221.

Gilman JW. (1999). Flammability and thermal stability studies of polymer layered silicate (clay) nanocomposites. App. Clay Sci. 15(1-2), 31-49.

Gilman JW., Jackson CL., Morgan AB., Harris R., Manias E., Giannelis EP., Wuthenow M., Hilton D., Phillips SH. (2000). Flammability properties of polymer-layered silicate nanocomposites. Propylene and polystyrene nanocomposites. Chem. Mater. 12, 1866-1873.

Grim RE. (1968). Structure of the clays minerals. In: Emery KO., Engel AE., Krauskopf K., Murray B., Siever R. (Eds.), Clay Mineralogy, 2nd Edition. McGraw-Hill International Series in the Earth and Planetary Sciences, New York, USA, pp.70-77. Chap. 4.

Guggenheim S., Martin RT. (1995). Definition of clay mineral: Joint Report of the AIPEA Nomenclature and CMS Nomenclature Committees. Clays and Clay Minerals. 43(2), 255-256.

Günister E., Pestreli D., Ünlü CH., Atıcı O., Güngör N., (2007). Synthesis and characterization of chitosan–MMT bionanocomposite systems. Carbohydr. Polym. 67(3), 358-365.

Gupta H., Velpandian T., Jain S. (2010). Ion- and pH-activated novel in-situ gel system for sustained ocular drug delivery. J. Drug Targeting. 18(7), 499-505.

Gupta S., Vyas SP. (2010). Carbopol/chitosan based pH triggered in situ gelling system for ocular delivery of timolol maleate. Sci. Pharm. 78(4), 959-976.

Ha J., Xanthos M. (2011). Drug release characteristics from nanoclay hybrids and their dispersions in organic polymers. Int. J. Pharm. 414(1-2), 321-331.

Haffejee N., Du Plessis J., Muller D.G., Schultz C., Kotzé A.F. Goosen, C. (2001). Intranasal toxicity of selected absorption enhancers. Pharmazie. 56(11), 882-888.

Haroun AA., Gamal-Eldeen A., Harding DRK. (2009). Preparation, characterization and in vitro biological study of biomimetic three-dimensional gelatin–montmorillonite/cellulose scaffold for tissue engineering. J. Mater. Sci. Mate. Med. 20(12), 2527-2540.

Hasegawa H., Ichinoche T., Tamura S., Kurata T. (2007). Development of a mucosal vaccine for influenza viruses: preparation for a potential influenza pandemic. Exp. Rev. Vacc. 6(2), 193-201.

He P., Davis SS., Illum L. (1998). In vitro evaluation of the mucoadhesive properties of chitosan microspheres. Int. J. Pharm. 166(1), 75-88.

Hirano S., Itakura C., Seino H., Akiyama Y., Nonaka I., Kanbara N., Kawakami T. (1990). Chitosan as an ingredient for domestic animal feeds. J. Agric. Food chem. 38, 1214-1217.
Howling GI., Dettmar PW., Goddard PA., Hampson FC., Dornish M., Wood EJ. (2001). The effect of chitin and chitosan on the proliferation of human skin fibroblasts and keranocytes in vitro. Biomaterials. 22(22), 2959-2966.

Hua S., Yang H., Wang W., Wang A. (2010). Controlled release of ofloxacin from chitosan–montmorillonite hydrogel. Appl. Clay Sci. 50(1), 112-117.

Huang D., Wang W., Xu J., Wang A. (2012). Mechanical and water resistance properties of chitosan/poly(vinyl alcohol) films reinforced with attapulgite dispersed by high-pressure homogenization. Chem. Eng. J. 210, 166-172.

Hurlbut CS., Klein C. (1991). Manual de mineralogía de Dana, Reverté, Barcelona, pp. 418-431.

Hussain F., Hojjati MJ., Okamoto M., Gorga RE. (2006). Review article: polymer-matrix nanocomposites, processing, manufacturing, and application: an overview. J. Compos. Mater. 40(17), 1511-1575.

Illum L. (1998). Chitosan and its use as a pharmaceutical excipient. Pharm. Res. 15(9), 1326-1331.

Ishihara M., Nakanishi K., Ono K., Sato M., Kikuchi M., Saito Y., Yura H., Matsui T., Hattori H., Uenoyama M., Kurita A. (2002). Photocrosslinkable chitosan as a dressing for wound occlusion and accelerator in healing process. Biomaterials. 23(3), 833-840.

Ishiyama M., Tominada H., Shiga M., Sasamoto K., Ohkura Y., Ueno K. (1996). The combined assay of cell viability and in vitro toxicity with a high water-soluble tetrasolium salt, neutral red and crystal violet. Biol. Pharm. Bull. 19, 1518-1520.

Jabbal-Gill I., Fisher AN., Rappuoli R., Davis SS., Illum L. (1998). Stimulation of mucosal and systemic antibody responses against *Bordetella pertussis* filamentous haemagglutinin and recombinant pertussis toxin after nasal administration with chitosan in mice. Vaccine. 16(20), 2039-2046.

Jiang HL., Kim YK., Lee SM., Park MR., Kim EM., Jin YM., Arote R., Jeong HJ., Song SC., Cho MH., Cho CS. (2010). Galactosylated chitosan-g-PEI/DNA complexes-loaded poly(organophosphazene) hydrogel as a hepatocyte targeting gene delivery system. Arch. Pharm. Res. 33(4), 551-556.

Jintapattanakit A., Junyaprasert VB., Kissel T. (2009). The role of mucoadhesion of trimethyl chitosan and PEGylated trimethyl chitosan nanocomplexes in insulin uptake. J. Pharm. Sci. 98(12), 4818-4830.

Joshi GV., Kevadiyaa BD., Patel HA., Bajaj HC., Jasrab RV. (2009). Montmorillonite as a drug delivery system: intercalation and in vitro release of timolol maleate. Int. J. Pharm. 374(1-2), 53-57.

Kabiri K., Mirzadeh H., Zohuriaan-Mehr MJ. (2007). Highly rapid preparation of a bio-modified nanoclay with chitosan. Iran. Polym. J. 16(3), 147-151.

Kamiyama K., Onishi H., Machida Y. (1999). Biodisposition characteristics of N-succinyl-chitosan and glycol-chitosan in normal and tumor-bearing mice. Biol. Pharm. Bull. 22(2), 179-186.

Kashiwagi T., Harris RH Jr., Zhang X., Briber RM., Cipriano BH., Ragharan SR., Awad WH., Shields JR. (2004). Flame retardant mechanism of polyamide 6-clay nanocomposites. Polymer. 45, 881-891.

Katti KS., Katti DR., Dash R. (2008). Synthesis and characterization of a novel chitosan/ montmorillonite/hydroxyapatite nanonanocomposite for bone tissue engineering. Biomed. Mater. 3 034122 (12 pp).

Katzung BG. (1997). Cloramfenicolo e tetracicline. Farmacologia generale e clínica. Piccin, Padova, pp. 751-757. Chap. 44.

Kawasumi M. (2004). The discovery of polymer-clay hybrids. J. Polym. Sci. Part. A Polym. Chem. 42(4), 819-824.

Kevadiya BD., Patel HA., Joshi GV., Abdi SHR., Bajaj HC. (2011). Montmorillonite-alginate composites as a drug delivery system: intercalation and in vitro release of diclofenac sodium. Indian J. Pharm. Sci. 72(6), 732-737.

Khunawattanakul W., Puttipipatkhachorn S., Rades T., Pongjanyakul T. (2008). Chitosan-magnesium aluminum silicate composite dispersions: characterization of rheology, flocculate size and zeta potential. Int. J. Pharm. 351(1-2), 227-235.

Khunawattanakul W., Puttipipatkhachorn S., Rades T., Pongjanyakul T. (2010). Chitosan-magnesium aluminum silicate nanocompositefilms: physicochemical characterization and drug permeability. Int. J. Pharmaceut. 393(1-2), 219-229.

Khunawattanakul W., Puttipipatkhachorn S., Rades T., Pongjanyakul T. (2011). Novel chitosan-magnesium aluminum silicate nanocomposite film coatings for modified-release tablets. Int. J. Pharm. 407(1-2), 132-141.

Kim CM., Lee DH., Hoffmann B., Kressler J., Stoppelmann G. (2001). Influence of nanofillers on the deformation process in layered silicate/polyamide-12 nanocomposites. Polymer. 42(3), 1095-1100.

Kockisch S., Rees GD., Young SA., Tsibouklis J., Smart JD. Polymeric microspheres for drug delivery to the oral cavity: an in vitro evaluation of mucoadhesive potential. J. Pharm. Sci. 92(8), 1614-1623.

Kojima Y., Usuki A., Kawasumi M., Okada A., Kurauchi T., Kamigaito O. (1993). Synthesis of nylon 6–clay hybrid by montmorillonite intercalated with ϵ-caprolactam. J. Polym. Sci. Part. A Polym. Chem. 31(4), 983-986.

Kotzé AF., Lueßen HL., de Leeuw BJ., De Boer BG., Coos Verhoef J., Junginger HE. (1998). Comparison of the effect of different chitosan salts and N-trimethyl chitosan chloride on the permeability of intestinal epithelial cells (Caco-2). J. Control. Release. 51(1), 35-46.

Krishnamoorti R. (2007). Strategies for Dispersing Nanoparticles in Polymers. MRS Bull. 32(4), 341-347.

Kulshrestra P., Rossman F., Giese JR., Aga DS. (2004). Investigating the molecular interactions of oxytetracycline in clay and organic matter: insights on factors affecting its mobility in soil. Environ. Sci. Technol. 38(15), 4097-4105.

Lange J., Wyser Y. (2003). Recent innovations in barrier technologies for plastic packaging, a review. Packag. Technol. Sci. 16(4), 149-158.

Lavie S., Stotzky G. (1986). Adhesion of the clay minerals montmorillonite, kaolinite, and attapulgite reduces respiration of histoplasma capsule. Appl. Environ. Microbiol. 51, 65-73.

LeBaron PC., Wang Z., Pinnavaia TJ. (1999). Polymer layered silicate nanocomposites: an overview. Appl. Clay Sci. 15(1-2), 11-29.

Lee KY., Ha WS., Park WH. (1995). Blood compatibility and biodegradability of partially N-acylated chitosan derivatives. Biomaterials. 16(16), 1211-1216.

Lee SR., Park HM., Lim H., Kang T., Li X., Cho WJ., Ha CH. (2002). Microstructure, tensile properties, and biodegradability of aliphatic polyester/clay nanocomposites. Polymer. 43(8), 2495-2500.

Lee KY., Shibutani M., Takagi H., Arimura T., Takigami S., Uneyama C., Kato N., Hirose M. (2004). Subchronic toxicity study of dietary N-acetylglucosamine in F344 rats. Food Chem. Tox. 42(4), 687-695.

Lee WF., Chen YJ. (2004). Effect of bentonite on the physical properties and drug release behavior of poly(AA-*co*-PEGMEA)/bentonite nanocomposite hydrogels for mucoadhesive. J. Appl. Polym. Sci. 91(5), 2934-2941.

Lehr C., Bouwstra JA., Schacht EH., Junginger HE. (1992). In vitro evaluation of mucoadhesive properties of chitosan and some other natural polymers. Int. J. Pharm. 78(1-3), 43-48.

Lertsutthiwong P., Noomun K., Khunthon S., Limpanart S. (2012). Influence of chitosan characteristics on the properties of biopolymeric chitosan–montmorillonite. Prog. Nat. Sci. 22(5), 502-508.

Li W., Xu R., Zheng L., Du J., Zhu Y., Huang R., Deng H. (2012). LBL structured chitosan-layered silicate intercalated composites based fibrous mats for protein delivery. Carbohydr. Polym. 90, 1650-1663.

Lim ST., Martin GP., Berry DJ., Brown MB. (2000). Preparation and evaluation of the in vitro drug release properties and mucoadhesion of novel microspheres of hyaluronic acid and chitosan. J. Control. Release. 66(2-3), 281-292.

Lin FH., Chen CH., Cheng WTK., Kuo TF. (2006). Modified montmorillonite as vector for gene delivery. Biomaterials. 27(17), 3333-3338.

Liu KH., Liu TY., Chen SY., Liu DM. (2007). Effect of clay content on electrostimulus deformation and volume recovery behavior of a clay–chitosan hybrid nanocomposite. Acta Biomater. 3(6), 919-926.

Liu KH., Liu TY., Chen SY., Liu DM. (2008). Drug release behavior of chitosan–montmorillonite nanocomposite hydrogels following electrostimulation. Acta Biomater. 4(4), 1038-1045.

López-Galindo A., Viseras C. (2004). Pharmaceutical and cosmetic applications of clays. In: Wypych F., Satyanarayana KG. (Eds.), Clay Surfaces: Fundamentals and Applications. Elsevier, Armsterdam, pp. 267-289.

López-Galindo A., Viseras C., Cerezo P. (2007). Compositional, technical and safety specifications of clays to be used as pharmaceutical and cosmetic products. Appl. Clay Sci. 36(1-3), 51-63.

López-Galindo A., Viseras C., Aguzzi C., Cerezo P. (2011). Pharmaceutical and cosmetic uses of fibrous clays; In: Galán E., Singer A. (Eds.), Developments in clay science. Elsevier, Amsterdam, pp. 299-324. Chap. 13.

Lueßen HL., de Leeuw BJ., Langemeÿer MWE., de Boer AG., Verhoef JC., Junginger HE. (1996). Mucoadhesive polymers in peroral peptide drug delivery. VI. Carbomer and chitosan improve the intestinal absorption of the peptide drug buserelin in vivo. Pharm. Res. 13(11), 1668-1672.

MacLaughlin FC., Mumper RJ., Wang J., Tagliaferri JM., Gill I., Hinchcliffe M., Rolland AP. (1998). Chitosan and depolymerized chitosan oligomers as condensing carriers for in vivo plasmid delivery. J. Control. Release. 56(1–3), 259-272.

Macleod GS., Fell JT., Collett JH., Sharma HL., Smith AM. (1999). Selective drug delivery to the colon using pectin:chitosan:hydroxypropyl methylcellulose film coated tablets. Int. J. Pharm. 187(2), 251–257.

Madejova J., Arvaiova B., Komadel P. (1999). FTIR spectroscopic characterization of thermally treated Cu_2^+, Cd_2^+ and Li^+ montmorillonites. Spectrochim. Acta Part. A. 55, 2467-2476.

Mahmoudian S., Wahit MU., Ismail AF., Yussuf AA. (2012). Preparation of regenerated cellulose/montmorillonite nanocomposite films via ionic liquids. Carbohyd. Polym. 88(4), 1251-1257.

Mai YW., Yu ZZ. (2006). Polymer nanocomposites CRC. In: Mai YW., Yu ZZ. (Eds.), Polymer Nanocomposites. Woodhead Publishing Ltd, Cambridge, UK, p.594.

Maiti P., Batt CA., Giannelis EP. (2003). Renewable plastics: synthesis and properties of PHB nanocomposites. J. Macromol. Sci. Rev. 88, 58-59.

Majithiya RJ., Ramchandra RS. (2005). Chitosan-based mucoadhesive microspheres of clarithromycin as a delivery system for antibiotic to stomach. Curr. Drug Deliv. 2(3), 235-242.

Mano JF., Koniarova D., Reis RL. (2003). Thermal properties of thermoplastic starch/synthetic polymer blends with potential biomedical applicability. J. Mater. Sci.: Mater. Med. 14(2), 127-135.

Marchessault, RH., Ravenelle, F., Zhu, XX. (2006). Polysaccharides for drug delivery and pharmaceutical applications. American Chemical Society.

Martin JE., Patil AJ., Butler MF., Mann S. (2011). Guest-molecule-directed assembly of mesostructured nanocomposite polymer/organoclay hydrogels. Adv. Funct. Mater. 21(4), 674-681.

Meenach SA., Anderson KW., Hilt JZ. (2009). Hydrogel nanocomposites: biomedical applications, biocompatibility, and toxicity analysis. In: Webster, TJ. (Ed.), Safety of Nanoparticles: From Manufacturing to Medical Applications. Springer Science + Business Media, New York, pp. 1–27. Chap. 7.

Messersmith PB., Giannelis EP. (1995). Sinthesis and barrier properties of poly(ε-caprolactone)-layered silicate nanocomposites. J. Polym. Sci. Part. A: Polym. Chem. 33(7), 1047-1057.

Mevius DJ., Vellenga L., Breukink HJ., Nouws JF. (1986). Pharmacokinetics and renal clearence of oxytetracycline in pigelets following intravenous and oral administration. Vet. Quarterly. 8(4), 274-284.

Morimoto M., Hiroyuki S., Shigemasa Y. (2002). Control of functions of chitin and chitosan by chemical modification. Trends Glycosci. Blycotechnol. 14(78), 205-222.

Murata JI., Ohya Y., Ouchi T. (1997). Design of quaternary chitosan conjugate having antennary galactose residues as a gene delivery tool. Carbohydr. Polym. 32(2), 105-109.

Muzzarelli RAA., Boudrant J., Meyer D., Manno N., Demarchis M., Paoletti MG. (2012). Current views on fungal chitin/chitosan, human chitinases, food preservation, glucans, pectins and inulin: A tribute to Henri Braconnot, precursor of the carbohydrate polymers science, on the chitin bicentennial. Carbohydr. Polym. 87(2), 995-1012.

Najafi N., Heuzey MC., Carreau PJ. (2012). Polylactide (PLA)-clay nanocomposites prepared by melt compounding in the presence of a chain extender. Compos. Sci. Technol. 72(5), 608-615.

Naguib HF., Aziz MSA., Sherif SM., Saad GR. (2012). Thermal properties of biodegradable poly(PHB/PCL-PEG-PCL) urethanes nanocomposites using clay/poly(ε-caprolactone) nanohybrid based masterbatch. Appl. Clay Sci. 57, 55-63.

Naito Y., Tago K., Nagata T., Furuya M., Seki T., Kato H., Morimura T., Ohara N. (2007). A 90-day ad libitum administration toxicity study of oligoglucosamine in F344 rats. Food Chem. Tox. 45(9), 1575-1587.

Nanda R., Sasmal A., Nayak PL. (2011). Preparation and characterization of chitosan-polylactide composites blended with Cloisite 30B for control release of the anticancer drug paclitaxel. Carbohydr. Polym. 83, 988-994.

Needleman IG., Smales FC. (1995). In vitro assessment of bioadhesion for periodontal and buccal drug delivery. Biomaterials. 16(8), 617-624.

Nelson DL., Lehinger AL., Cox, MM. (2008). Principles of Biochemistry, 5th ed. Freeman, New York.

Nielsen P., Gyrd-Hansen N. (1996). Bioavailability of oxytetracycline, tetracycline and chlortetracycline after oral administration to fed and fasted pigs. J. Vet. Pharmacol. Ther. 19(4), 305-311.

NIH (National Institute of Health). (2006). NIH Roadmap for Medical Research: Nanomedicine, https://commonfund.nih.gov/nanomedicine/.

Nordtveit RJ., Varum KM., Smidsrod O. (1996). Degradation of partially N-acetylated chitosans with hen egg white and human lysozyme. Carbohydr. Polym. 29(2), 163-167.

Nunes CD., Vaz PD., Fernandes AC., Ferreira P., Roma CC., Calhorda MJ. (2007). Loading and delivery of sertraline using inorganic micro and mesoporous materials. Eur. J. Pharm. Biopharm. 66, 357-365.

Nunthanid J., Puttipipatkhachorn S., Yamamoto K., Peck GE. (2001). Physical properties and molecular behavior of chitosan films. Drug Dev. Ind. Pharm. 27(2), 143-157.

Okada A., Fukushim Y., Kawasumi M., Inagaki S., Usuki A., Sugiyama S., Kurauchi T., Kamigaito O. (1988). US Patent 4,739,007.

Okada A., Kawasumi M., Kojima Y., Kurauchi T., Kamigaito O. (1990). Synthesis and properties of nylon-6/clay hybrids. In: Schaefer DW., Mark JE. (Eds.), Polymers based molecular composites, vol. 171, MRS symposium proceedeings, Pittsburgh, pp. 45-50.

Oleszczuk P., Xing B. (2011). Influence of anionic, cationic and nonionic surfactants on adsorption and desorption of oxytetracycline by ultrasonically treated and non-treated multiwalled carbon nanotubes. Chemosphere. 85(8), 1312-1317.

Opanasopit P., Aumklad P., Kowapradit J., Ngawhiranpat T., Apirakaramwong A., Rojanarata T., Puttipipatkhachorn S. (2007). Effect of salt forms and molecular weight of chitosans on in vitro permeability enhancement in intestinal epithelial cells (Caco-2). Pharm. Dev. Technol. 12(5), 447-455.

Paluszkiewicz C., Stodolak E., Hasik M., Blazewicz M. (2011). FT-IR study of montmorillonite-chitosan nanocomposite materials. Spectrochim. Acta A: Mol. Biomol. Spectrosc. 79(4), 784-788.

Pandey K., Raghuntha REK., Pratheep KA., Singh RP. (2005). An overview on the degradability of polymer nanocomposites. Polym. Degrad. Stabil. 88(2), 234-250.

Papadimitriou S., Bikiaris D., Avgoustakis K., Karavas E., Georgarakis M. (2008). Chitosan nanoparticles loaded with dorzolamide and pramipexole. Carbohydr. Polym. 73(1), 44-54.

Paradossi G., Chiessi E., Venanzi M., Pispisa B., Palleschi A. (1992). Branched-chain analogues of linear polysaccharides: a spectroscopic and conformational investigation of chitosan derivatives. Int. J. Biol. Macromol. 14(2), 73-80.

Park JK., Choy YB., Oh JM., Kima JY., Hwanga SJ., Choy JH. (2008). Controlled release of donepezil intercalated in smectite clays. Int. J. Pharm. 359(1-2), 198-204.

Patel VR., Amiji MM. (1996). Preparation and characterization of freeze-dried chitosan-poly(ethylene oxide) hydrogels for site-specific antibiotic delivery in the stomach. Pharm. Res. 13(4), 588-593.

Paul DR., Robeson LM. (2008). Polymer nanotechnology: Nanocomposites. Polymer. 49, 3187-3204.

Pavlidou S., Papaspyrdes CD. (2008). A review on polymer-layered silicate nanocomposites. Prog. Polym. Sci. 33(12), 111-1198.

Peh K., Khan T., Ch'ng H. (2000). Mechanical, bioadhesive strength and biological evaluations of chitosan films for wound dressing. J. Pharm. Pharm. Sci. 3(3), 303-311.

Peng Y., Chen D., Ji J., Kong Y., Wan H., Yao C. (2012). Chitosan-modified palygorskite: Preparation, characterization and reactive dye removal. Appl. Clay Sci. 74, 81-86.

Peppas NA., Brannon-Peppas L., Buschow KHJ., Cahn RW., Flemings MC., Ilschner B., Kramer EJ., Mahajan S., Veyssière P. (Eds). (2001). Encyclopedia of Materials: Science and Technology, Elsevier, Amsterdam, pp. 2351-2355.

Pérez-Silva I., Rodríguez JA., Ramírez-Silva MT., Páez-Hernández ME. (2012). Determination of oxytetracycline in milk samples by polymer inclusion membrane separation coupled to high performance liquid chromatography. Anal. Chim. Acta. 718, 42-46.

Pijpers A., Schoevers EJ., Van Gogh H., Van Leengoed LA., Visser IJ., Van Miert AS., Verheijden JH. (1991). The influence of disease on feed and water consumption and on pharmacokinetics of orally administered oxytetracycline in pigs. J. Anim. Sci. 69(7), 3947-2954.

Pinnavaia TJ., Beall GW. (Eds). (2000). Polymer-clay nanocomposites. Wiley Series in Polymer Science, Australia.

Pongjanyakul T., Priprem A., Puttipipatkhachorn S. (2005a). Investigation of novel alginate−magnesium aluminum silicate microcomposite films for modified-release tablets. J. Control. Release. 107(2), 343-356.

Pongjanyakul T., Proprem A., Puttipipatkhachorn S. (2005b). Influence of magnesium aluminium silicate on rheological, release and permeation characteristics of diclofenac sodium aqueous gels in-vitro. J. Pharm. Pharmacol. 57(4), 429-434.

Pongjanyakul T., Puttipipatkhachorn S. (2007). Alginate-magnesium aluminum silicate films: effect of plasticizers on film properties, drug permeation and drug release from coated tablets. Int. J. Pharm. 333(1-2), 34-44.

Pongjanyakul T. (2009). Alginate-magnesium aluminum silicate films: importance of alginate block structures. Int. J. Pharm. 365, 100-108.

Pongjanyakul T., Suksri H. (2009). Alginate–magnesium aluminum silicate films for buccal delivery of nicotine. Colloids Surf. B Biointerfaces. 74(1), 103-113.

Pongjanyakul T., Khunawattanakul W., Puttipipatkhachorn S. (2009). Physicochemical characterizations and release studies of nicotine–magnesium aluminum silicate complexes. Appl. Clay Sci. 44(3-4), 242-250.

Pongjanyakul T., Suksri H. (2010). Nicotine-loaded sodium alginate–magnesium aluminum silicate (SA–MAS) films: importance of SA–MAS ratio. Carbohydr. Polym. 80(4), 1018-1027.

Pongjanyakul T., Rongthong T. (2010). Enhanced entrapment efficiency and modulated drug release of alginate beads loaded with drug-clay intercalated complexes as microreservoirs. Carbohydr. Polym. 81(2), 409-419.

Pontier D., Balagué C., Roby D. (1998). The hypersensitive response. A programmed cell death associated with plant resistance. La réponse hypersensible. Un cas de mort cellulaire programmée associée à la résistance des plantes. Comptes Rendus de l'Académie des Sciences (Series III) Sciences de la Vie. 321(9), 721-734.

Porter D., Metcalfe E., Thomas MJK. (2000). Nanocomposite fire retardants: a review. Fire Mater. 24(1), 45-52.

Prabaharan M., Mano JF. (2005). Chitosan-based particles as controlled drug delivery systems. Drug Deliv. 12(1), 41-57.

Pradosh RD., Rudra MN., Anamika B., Nayak PI. (2011). Gelatin blended with nanoparticle cloisite30B (Mt) for control drug delivery of anticancer drug paclitaxel. International Research Journal of Biochemistry and Bioinformatics. 1(2), 35-42.

Preston CML., Amarasinghe G., Hopewell JL., Shanks RA., Mathys Z. (2004). Evaluation of polar ethylene copolymers as fire retardant nanocomposite matrices. Polym. Degrad. Stabil. 84(3), 533-544.

Punitha S., Girish Y. (2010). Polymers in mucoadhesive buccal drug delivery system: a review. Int. J. Res. Pharm. Sci. 1(2), 170-186.

Qian Y., Liu W., Park YT., Lindsay CI., Rafael C., Christopher WM., Andreas S. (2012). Modification with tertiary amine catalysts improves vermiculite dispersion in polyurethane via in situ intercalative polymerization. Polymer. 53(22), 5060-5068.

RAE. (2001). Diccionario de la Real Academia Española, 22 edición.

Rao SB., Sharma CP. (1997). Use of chitosan as a biomaterial: studies on its safety and hemostatic potential. J. Biomed. Mater. Res. 34(1), 21-28.

Rautureau M., Caillère S., Hénin S. (2004). Utilisation de l'argile au cours des âges (2nd ed.). Les Argiles, France.

Raymond L., Morin FG., Marchessault RH. (1993). Degree of deacetylation of chitosan using conductometric titration and solid-state NMR. Carbohydr. Res. 246(1), 331-336.

Richardson SW., Kolbe HJ., Duncan R. (1999). Potential of low molecular mass chitosan as a DNA delivery system: biocompatibility, body distribution and ability to complex and protect DNA. Int. J. Pharm. 178(2), 231-243.

Rillosi M., Buckton G. (1995). Modelling mucoadhesion by use of surface energy terms obtained from the lewis acid–lewis Base Approach. II. Studies on anionic, cationic, and unionisable polymers. Pharm. Res. 12(5), 669-675.

Rojtanatanya S., Pongjanyakul T. (2008). Propranolol–magnesium aluminum silicate complex dispersions and particles: characterization and factors influencing drug release. Int. J. Pharm. 383(1–2), 106-115.

Roy K., Mao HQ., Leong KW. (1997). DNA-chitosan nanospheres: transfection efficiency and cellular uptake. Proc. Int. Symp. Control. Rel. Bioact. Mater. 24, 673-674.

Rowe RC., Sheskey PJ., Quinn ME. (2009). Handbook of pharmaceutical excipients. Pharmaceutical Press, London, Chicago.

Salcedo I., Aguzzi C., Sandri G., Bonferoni MC., Mori M., Cerezo P., Sánchez R., Viseras C. Caramella C. (2012). In vitro biocompatibility and mucoadhesion of montmorillonite chitosan nanocomposite: A new drug delivery. Appl. Clay Sci. 55, 131-137.

Sandri G., Rossi S., Ferrari F., Bonferoni MC., Muzzarelli C., Caramella C. (2004). Assessment of chitosan derivatives as buccal and vaginal penetration enhancers. Eur. J. Pharm. Sci. 21(2-3), 351-359.

Sandri G., Bonferoni MC., Rossi S., Ferrari F., Gibin S., Zambito Y., Colo GD., Caramella C. (2007). Nanoparticles based on N-trimethylchitosan: evaluation of absorption properties using in vitro (Caco-2 cells) and ex vivo (excised rat jejunum) models. Eur. J. Pharm. Biopharm. 65(1), 68-67.

Scarfato P., Di Maio L., Fariello ML., Russo P., Incarnato L. (2012). Preparation and evaluation of polymer/clay nanocomposite surface treatments for concrete durability enhancement. Cement. Concrete Comp. 34(3), 297-305.

Schipper NGM., Vårum KM., Artursson P. (1996). Chitosans as absorption enhancers for poorly absorbable drugs. 1: influence of molecular weight and degree of acetylation on drug transport across human intestinal epithelial (Caco-2) cells. Pharm. Res. 13(11), 1686-1692.

Schipper NGM., Olsson S., Hoogstraate JA., deBoer AG., Vårum KM.,. Artursson P. (1997). Chitosans as absorption enhancers for poorly absorbable drugs. 2: mechanism of absorption enhancement. Pharm. Res. 14, 923-929.

Schrickx J., Fink-Gremmels J. (2007). P-glycoprotein-mediated transport of oxytetracycline in the Caco-2 cell model. J. Vet. Pharmacol. Ther. 30(1), 25-31.

Shaikh S., Birdi A., Qutubuddin S., Lakatosh E., Baskaran H. (2007). Controlled release in transdermal pressure sensitive adhesives using organosilicate nanocomposites. Ann. Biomed. Eng. 35, 2130-2137.

Shavi G., Nayak U., Reddy M., Karthik A., Deshpande P., Kumar A., Udupa N. (2011). Sustained release optimized formulation of anastrozole-loaded chitosan microspheres: in vitro and in vivo evaluation. J. Mater. Sci. Mater. Med. 22(4), 865-878.

Shigemasa Y., Matsuura H., Sashiwa H., Saimoto H. (1996). Evaluation of different absorbance ratios from infrared spectroscopy for analyzing the degree of deacetylation in chitin. Int. J. Biol. Macromol. 18(3), 237-242.

Shimoda J., Onishi H., Machida Y. (2001). Bioadhesive characteristics of chitosan microspheres to the mucosa of rat small intestine. Drug Dev. Ind. Pharm. 27(6), 567-576.

Sieval AB., Thanou M., Kotzé AF., Verhoef JC., Brussee J., Junginger HE. (1998). Preparation and NMR characterization of highly substituted N-trimethyl chitosan chloride. Carbohydr. Polym. 36(2), 157-165.

Silva GR., Ayres E., Orefice RL., Moura SA., Cara DC., Cunha Ada S. Jr. (2009). Controlled release of dexamethasone acetate from biodegradable and biocompatible polyurethane and polyurethane nanocomposite. J. Drug Target. 17(5), 374-383.

Silvestre C., Duraccio D., Cimmino S. (2011). Food packaging based on polymer nanomaterials. Prog. Polym. Sci. 36(12), 1766-1782.

Sinha Ray S., Yamada K., Okamoto M., Ueda K. (2002). New polylactide/layred silicate nanocomposite: a novel biodegradable material. Nano Lett. 2(10), 1093-1096.

Sinha Ray S., Okamoto M. (2003). Polymer/layered silicate nanocomposites: a review from preparation to processing. Prog. Polym. Sci. 28(11), 1539-1641.

Sinha Ray S., Yamada K., Okamoto M., Ogami A., Ueda K. (2003a). New polylactide/ layered silicate nanocomposites. 3. High performance biodegradable materials. Chem. Mater. 15(7), 1456-1465.

Sinha Ray S., Yamada K., Okamoto M., Fujimoto Y., Ogami A., Ueda K. (2003b). New polylactide/layered silicate nanocomposites. 5. Designing of materials with desired properties. Polymer. 44 (21), 6633-6646.

Sinha Ray S., Bousmina M. (2005). Biodegradable polymers and their layered silicate nanocomposites: In greening the 21st century materials world. Prog. Mater. Sci. 50(8), 962-1079.

Sinha VR., Singla AK., Wadhawan S., Kaushik R., Kumria R., Bansal K., Dhawan S. (2004). Chitosan microspheres as a potential carrier for drugs. Int. J. Pharm. 274, 1-33.

Si-Shen F., Lin M., Panneerselvan A., Cheewee G., Zhou W. (2009). Poly(lactide)-vitamin E derivative/montmorillonite nanoparticle formulations for the oral delivery of Docetaxel. Biomaterials. 30(19), 3297-3306.

Soane RJ., Frier M., Perkins AC., Jones NS., Davis SS., Illum L. (1999). Evaluation of the clearance characteristics of bioadhesive systems in humans. Int. J. Pharm. 178(1), 55-65.

Solomon MJ., Almusallam AS., Seefeldt KF., Somwangthanaroj A., Varadan P. (2001). Rheology of polypropylene/clay hybrid materials. Macromolecules. 34(6), 1864-1872.

Sonia TA., Sharma CP. (2011). Chitosan and its Derivatives for drug delivery perspective. Adv. Polym. Sci. 243, 23–54.

Sponza DT., Celebi H. (2012). Removal of oxytetracycline (OTC) in a synthetic pharmaceutical waste water by a sequential anaerobic multichamber bed reactor (AMCBR)/completely stirred tank reactor (CSTR) system: biodegradation and inhibition kinetics. Bioresour. Tech. 104, 100-110.

Sudarshan NR., Hoover DG., Knorr D. (1992). Antibacterial action of chitosan. Food Biotechnol. 6(3), 257-272.

Sun XX., Zhang X., Aboul-Enein HY. (2004). Construction and characterization of potentiometric sensor for the determination of oxytetracycline hydrochloride. Il Farmaco. 59(4), 307-314.

Sun B., Ranganathan B., Feng SS. (2008). Multifunctional poly(d,l-lactide-co-glycolide)/montmorillonite (PLGA/MMT) nanoparticles decorated by Trastuzumab for targeted chemotherapy of breast cancer. Biomaterials 29(4), 475-486.

Sun W., Mao S., Wang Y., Junyaprasert VB., Zhang T., Na L., Wang J. (2010). Bioadhesion and oral absorption of enoxaparin nanocomplexes. Int. J. Pharm. 386(1-2), 275–281.

Tai Q., Yuen RKK., Song L., Hu Y. (2012). A novel polymeric flame retardant and exfoliated clay nanocomposites: Preparation and properties. Chem. Eng. J. 183, 542-549.

Takahashi T., Yamada Y., Kataoka K., Nagasaki YJ. (2005). Preparation of a novel PEG–clay hybrid as a DDS material: dispersion stability and sustained release profiles. J. Control. Rel. 107(3), 408-416.

Tammaro L., Russo G., Vittoria V. (2009). Encapsulation of diclofenac molecules into poly(epsilon-caprolactone) electrospun fibers for delivery protection. J. Nanomater. 1-8.

Tapan Kumar G., Amrita T., Amit A., Ajazuddin, Hemant B., Dulal Krishna T. (2012). Modified chitosan hydrogels as drug delivery and tissue engineering systems: present status and applications. Acta Pharm. Sinic. B. 2(5), 439-449.

Tapia C., Corbalán V., Costa E., Gai MN., Yazdani-Pedram M. (2005). Study of the release mechanism of diltiazem hydrochloride from matrices based on chitosan-alginate and chitosan-carrageenan mixtures. Biomacromolecules. 6(5), 2389-2395.

Tapola NS., Lyyra ML., Kolehmainen RM., Sarkkinen ES., Schauss AG. (2008). Safety aspects and cholesterol-lowering efficacy of chitosan tablets. J. Am. Coll. Nutr. 27(1), 22-30.

Tetto JA., Steeves DM., Welsh EA., Powell BE. (1999). Biodegradable poly(ε-caprolactone)/clay nanocomposites. ANTEC'99, 1628-1632.

Thakral NK., Ray AR., Majumdar DK. (2010). Eudragit S-100 entrapped chitosan microspheres of valdecoxib for colon cancer. J. Mater. Sci. Mater. Med. 21(9), 2691-2699.

Thein-Han WW., Stevens WF. (2004). Transdermal delivery controlled by a chitosan membrane. Drug Dev. Ind. Pharm. 30(4), 397-404.

Tomihata K., Ikada Y. (1997). In vitro and in vivo degradation of films of chitin and its deacetylated derivatives. Biomaterials. 18(7), 567-575.

Tozaki H., Komoike J., Tada C., Maruyama T., Terabe A., Suzuki T., Yamamoto A., Muranishi S. (1997). Chitosan capsules for colon-specific drug delivery: improvement of insulin absorption from the rat colon. J. Pharm. Sci. 86(9), 1016-1021.

Tozaki H., Fujita T., Odoriba T., Terabe A., Suzuki T., Tanaka C., Okabe S., Shoo Muranishi S., Yamamoto A. (1999). Colon specific delivery of R68070, a new thromboxane synthase inhibitor, using chitosan capsules: therapeutic effect against 2, 4, 6,-trinitrobenzene sulphonic acid-induced ulcerative colitis in rats. Life Sci. 64, 1155-1162.

USP 31. (2008). United States Pharmacopoeia 31 and National Formulary 28, US Pharmacopoeial Convention, Rockville, MD (USA).

Vaia RA., Price G., Ruth PN., Nguyen HT., Lichtenhan J. (1999). Polymer/layered silicate nanocomposites as high performance ablative materials. Appl. Clay Sci. 15(1-2), 67-92.
Van der Lubben IM., Verhoef JC., Borchard G., Junginger HE. (2001). Chitosan for mucosal vaccination. Adv. Drug. Deliv. Rev. 52(2), 139-144.

Van der Merwe SM., Verhoef JC., Verheijden JHM. (2004). Trimethylated chitosan as polymeric absorption enhancer for improved peroral delivery of peptide drugs. Eur. J. Pharm. Biopharm. 58(2), 225-235.

VandeVord PJ., Matthew HW., Desilva SP., Mayton L., Wu B., Wooley PH. (2002). Evaluation of the biocompatibility of a chitosan scaffold in mice. J. Biomed. Mater. Res. 59(3), 585-590.

Van Olphen H. (1963). An introduction to clay colloid chemistry. Interscience, New York.

Vasishtha N., Barlow D., Beashear JG., Rastellini C. (1997). Alginate-chitosan biomatrices for islet cell encapsulation. Proc. Int. Symp. Control. Rel. Bioact. Mater. 24, 1013-1014.

Verma D., Katti KS., Katti DR. (2010). Osteoblast adhesion, proliferation and growth on polyelectrolyte complex–hydroxyapatite nanocomposites. Philosophical transactions. Series A, Mathematical, physical, and engineering sciences. 368, 2083-2097.

Viseras C., Aguzzi C., Cerezo P., López-Galindo A. (2007). Uses of clay minerals in semisolid health care and therapeutic products. Appl. Clay Sci. 36(1-3), 37-50.

Viseras M.T. (2008). Desarrollo galénico de preparados obtenidos por interacción del ácido 5 amino salicílico con haloysita. Ph.D. Thesis, University of Granada, Granada, Spain.

Viseras C., Aguzzi C., Cerezo P., Bedmar MC. (2008a). Biopolymer-clay nanocomposites for controlled drug delivery. Mater. Sci. Technol. 24(9), 1020-1026.

Viseras MT., Aguzzi C., Cerezo P., Viseras C., Valenzuela C. (2008b). Equilibrium and kinetics of 5-aminosalicylic acid adsorption by halloysite. Microporous Mesoporous Mat. 108, 112-116.

Viseras MT., Aguzzi C., Cerezo P., Cultrone G., Viseras C. (2009). Supramolecular structure of 5-aminosalycilic acid/halloysite composites. J. Microencapsul. 26(3), 279-286.

Viseras C., Cerezo P., Sanchez R., Salcedo I., Aguzzi C. (2010). Current challenges in clay minerals for drug delivery. Appl. Clay Sci. 48(3), 291-295.

Viyoch J., Sudedmark T., Srema W., Suwonkrua W. (2005). Development of hydrogel patch for controlled release of alpha-hydroxy acid contained in tamarind fruit pulp extract. Int. J. Cosmet. Sci. 27(2), 89-99.

Wang S., Shen L., Tong YJ., Chen L., Phang IY., Lim PQ., Liu TX. (2005). Biopolymer chitosan/montmorillonite nanonanonanocomposites: preparation and characterization. Polym. Degrad. Stabil. 90, 123-131.

Wang X., Du Y., Luo J., Lin B., Kennedy JF. (2007). Chitosan/organic rectorite nanocomposite films: structure, characteristic and drug delivery behavior. Carbohydr. Polym. 69, 41-49.

Wang X., Du Y., Luo J. (2008). Biopolymer/montmorillonite nanocomposite: preparation, drug-controlled release property and cytotoxicity. Nanotechnology. 19(6), 1-7.

Wang Q., Zhang J., Wang A. (2009). Preparation and characterization of a novel pH sensitive chitosan-g-poly(acrylic acid)/attapulgite/sodium alginate nanocomposite hydrogel bead for controlled release of diclofenac sodium. Carbohydr. Polym. 78, 731-737.

Wang X., Liu B., Ren J., Liu C., Wang X., Wu J., Sun R. (2010). Preparation and characterization of new quaternized carboxymethyl chitosan/rectorite nanonanocomposite. Nanonanocomposites Science and Technology. 70(7), 1161-1167.

Ward CJ., Song S., Davis EW. (2010). Controlled release of tetracycline-HCl from halloysite-polymer composite films. J. Nanosci. Nanotechnol. 10(10), 6641-6649.

Weaver CE. (1989). Clays, muds and shales. Elsevier, Amsterdam, Holland, p. 819.

Werle M., Bernkop-Schnürch A. (2008). Thiolated chitosans: useful excipients for oral drug delivery. J. Pharm. Pharmacol. 60(3), 273-281.

Wu TM., Wu CY. (2006). Biodegradable poly(lactic acid)/chitosan-modified montmorillonite nanocomposites: preparation and characterization. Polym. Degrad. Stabil. 91, 2198-2204.

Xiaoying W., Yumin D., Jiwen L. (2008). Biopolymer/montmorillonite nanocomposite: preparation, drug-controlled release property and cytotoxicity. Nanotechnology. 19(6), 1-7.

Xie Y., Zhou NJ., Gong YF., Chen J., Zhou XJ., Lu NH., Wang CW. (2007). Th immune response induced by *H. pylori* therapeutic vaccine with chitosan as adjuvant. J. Gastroenterol. Hepatol. 22(S2), A239.

Xu R., Manias E., Snejder AJ., Runt J. (2001). New biomedical poly(urethane urea)-layered silicate nanocomposite. Macromolecules. 34, 337-339.

Xu Y., Kim K., Hanna M., Nag D. (2005). Chitosan–starch composite film: preparation and characterization. Ind. Crop. Prod. 21(2), 185-192.

Xu Y., Ren X., Milford A. (2006). Chitosan/clay nanonanocomposite film preparation and characterization. J. Appl. Polym. Sci. 99(4), 1684-1691.

Yano K., Usuki A., Kurauchi T., Kamigaito O. (1993). Synthesis and properties of polymide-clay hybrid. J. Polym. Sci. Part. A: Polym. Chem. 31(10), 2493-2498.

Yamashita S., Tanaka Y., Endoh Y., Taki Y., Sakane T., Nadai T., Sezaki H. (1997). Analysis of drug permeation across Caco-2 monolayer: implication for predicting in vivo drug absorption. Pharm. Res. 14(4), 486-491.

Yariv S., Cross H. (2002). Organo-clay complexes and interactions. Marcel Dekker, New York.

Yilmaz O., Cheabururu CN., Gulumser G., Cornelia V. (2011). Rheological behaviour of acrylate/ montmorillonite nanocomposite latexes and their application in leather finishing as binders. Prog. Org. Coat. 70(1), 52-58.

Ylitalo R., Lehtinen S., Wuolijoki E., Ylitalo P., Lehtimaki T. (2002). Cholesterol-lowering properties and safety of chitosan. Arzneimittelforschung. 52(1), 1-7.

Yuan Q., Shah J., Hein S., Misra RDK. (2010). Controlled and extended drug release behavior of chitosan-based nanoparticle carrier. Acta Biomater. 6(3), 1140-1148.

Zhao X., Yin L., Ding J., Tang C., Gu S., Yin C., Mao Y. (2010). Thiolated trimethyl chitosan nanocomplexes as gene carriers with high in vitro and in vivo transfection efficiency. J. Control. Release 144(1), 46-54.

Zheng JP., Luan L., Wang HY., Xi LF., Yao KD. (2007). Study on ibuprofen/montmorillonite intercalation composites as drug release system. Appl. Clay Sci. 36(4), 297-301.

Zhou HY., Chen XG., Zhang WF. (2007). In vitro and in vivo evaluation of mucoadhesiveness of chitosan/cellulose acetate multimicrospheres. J. Biomed. Mater. Res. A. 83(4), 1146-1153.

Zhu J., Uhl FM., Morgan AB., Wilkie CA. (2001). Studies on the mechanism by which the formation of nanocomposites enhances thermal stability. Chem. Mater. 13(12), 4649-4654.

ANEXO I

ARTÍCULOS CIENTÍFICOS QUE HAN CITADO LA REVISIÓN:

Aguzzi C., Cerezo P., Viseras C., Caramella C. Use of clays as drug delivery systems: Possibilities and limitations. (2007). Applied Clay Science, (1-3) 22-36.

Scopus: EXPORT DATE: 29 May 2013

Zhu, S., Peng, H., Chen, J., Li, H., Cao, Y., Yang, Y., Feng, Z. Intercalation behavior of poly(ethylene glycol) in organically modified montmorillonite. (2013). Applied Surface Science, 276, pp. 502-511.

Lambert, J.-F., Bergaya, F. Smectite-polymer nanocomposites. (2013). Developments in Clay Science, 5, pp. 679-706.

Aguzzi, C., Viseras, C., Cerezo, P., Salcedo, I., Sánchez-Espejo, R., Valenzuela, C. Release kinetics of 5-aminosalicylic acid from halloysite. (2013). Colloids and Surfaces B: Biointerfaces, 105, pp. 75-80.

Hu, C.H., Xiao, K., Song, J., Luan, Z.S.Effects of zinc oxide supported on zeolite on growth performance, intestinal microflora and permeability, and cytokines expression of weaned pigs. (2013). Animal Feed Science and Technology, 181 (1-4), pp. 65-71.

Seema, Datta, M.MMT-PLGA nanocomposites as an oral and controlled release carrier for 5 - Fluorouracil: A novel approach. (2013). International Journal of Pharmacy and Pharmaceutical Sciences, 5 (2), pp. 332-341.

Oh, Y.-J., Choi, G., Choy, Y.B., Park, J.W., Park, J.H., Lee, H.J., Yoon, Y.J., Chang, H.C., Choy, J.-H. Aripiprazole-montmorillonite: A new organic-inorganic nanohybrid material for biomedical applications. (2013). Chemistry - A European Journal, 19 (15), pp. 4869-4875.

Yu, D., Lin, Z., Li, Y. Octadecenylsuccinic anhydride pickering emulsion stabilized by γ-methacryloxy propyl trimethoxysilane grafted montmorillonite. (2013). Colloids and Surfaces A: Physicochemical and Engineering Aspects, 422, pp. 100-109.

Kiparissides, C., Kammona, O. Nanoscale carriers for targeted delivery of drugs and therapeutic biomolecules. (2013). Canadian Journal of Chemical Engineering, 91 (4), pp. 638-651.

Conterosito, E., Van Beek, W., Palin, L., Croce, G., Perioli, L., Viterbo, D., Gatti, G., Milanesio, M. Development of a fast and clean intercalation method for organic molecules into layered double hydroxides. (2013). Crystal Growth and Design, 13 (3), pp. 1162-1169.

Rodrigues, L.A.D.S., Figueiras, A., Veiga, F., de Freitas, R.M., Nunes, L.C.C., da Silva Filho, E.C., da Silva Leite, C.M. The systems containing clays and clay minerals from modified drug release: A review. (2013). Colloids and Surfaces B: Biointerfaces, 103, pp. 642-651.

Chung, J.H.-Yu., Simmons, A., Zeng, Q., Poole-Warren, L.A. Effects of drug chemistry on the dispersion and release behaviour of polyurethane organosilicate nanocomposites. (2013) European Polymer Journal, 49 (3), pp. 652-663.

Yang, Q., Ren, X.-F.Use of nano-oxide materials as anti-diarrhea agents in piglets. (2013) World Chinese Journal of Digestology, 21 (1), pp. 71-74.

Tămăşan, M., Radu, T., Simon, V. Spectroscopic characterisation and in vitro behaviour of kaolinite polyvinyl alcohol nanocomposite. (2013). Applied Clay Science, 72, pp. 147-154.

Nagy, K., Bíró, G., Berkesi, O., Benczédi, D., Ouali, L., Dékány, I. Intercalation of lecithins for preparation of layered nanohybrid materials and adsorption of limonene. (2013). Applied Clay Science, 72, pp. 155-162.

Valarezo, E., Tammaro, L., González, S., Malagón, O., Vittoria, V. Fabrication and sustained release properties of poly(ε-caprolactone) electrospun fibers loaded with layered double hydroxide nanoparticles intercalated with amoxicillin. (2013). Applied Clay Science, 72, pp. 104-109.

Rossi, D., Jobstraibizer, P.G., Bosco, C.D., Bettero, A. A combined chemico-mineralogical and tensiometric approach for evaluation of Euganean Thermal Mud (ETM) quality. (2013). Journal of Adhesion Science and Technology, 27 (1), pp. 30-45.

Hu, C.H., Qian, Z.C., Song, J., Luan, Z.S., Zuo, A.Y. Effects of zinc oxide-montmorillonite hybrid on growth performance, intestinal structure, and function of broiler chicken. (2013). Poultry Science, 92 (1), pp. 143-150. Cited 1 time.

Rabello De Castro, F., Lau Lam, Y., Hawrylak Herbst, M., MacIel Pereira, M., Crispim Da Silva, T., Homs, N., Ramirez De La Piscina, P. VO2+ reaction with hydrotalcite and hydrotalcite-derived oxide: The effect of the vanadium loading on the structure of catalyst precursors and on the vanadium species. (2013). European Journal of Inorganic Chemistry, (2), pp. 241-247.

Parolo, M.E., Avena, M.J., Savini, M.C., Baschini, M.T., Nicotra, V. Adsorption and circular dichroism of tetracycline on sodium and calcium-montmorillonites. (2013). Colloids and Surfaces A: Physicochemical and Engineering Aspects, 417, pp. 57-64.

Krajišnik, D., Daković, A., Malenović, A., Djekić, L., Kragović, M., Dobričić, V., Milić, J. An investigation of diclofenac sodium release from cetylpyridinium chloride-modified natural zeolite as a pharmaceutical excipient. (2013). Microporous and Mesoporous Materials, 167, pp. 94-101.

Chen, M., Le, D.Q.S., Hein, S., Li, P., Nygaard, J.V., Kassem, M., Kjems, J., Besenbacher, F., Bünger, C. Fabrication and characterization of a rapid prototyped tissue engineering scaffold with embedded multicomponent matrix for controlled drug release. (2012). International Journal of Nanomedicine, 7, pp. 4285-4297.

Giri, T.K., Thakur, D., Alexander, A., Ajazuddin, Badwaik, H., Tripathi, D.K. Alginate based hydrogel as a potential biopolymeric carrier for drug delivery and cell delivery systems: Present status and applications. (2012). Current Drug Delivery, 9 (6), pp. 539-555.

Perioli, L., Pagano, C. Inorganic matrices: An answer to low drug solubility problem. (2012). Expert Opinion on Drug Delivery, 9 (12), pp. 1559-1572.

Reger, M., Sekine, T., Hoffmann, H. Pickering emulsions stabilized by amphiphile covered clays. (2012). Colloids and Surfaces A: Physicochemical and Engineering Aspects, 413, pp. 25-32. Cited 1 time.

Hu, C., Song, J., You, Z., Luan, Z., Li, W. Zinc oxide-montmorillonite hybrid influences diarrhea, intestinal mucosal integrity, and digestive enzyme activity in weaned pigs. (2012). Biological Trace Element Research, 149 (2), pp. 190-196. Cited 5 times.

Teixeira-Neto, Ã.A., Izumi, C.M.S., Temperini, M.L.A., Ferreira, A.M.D.C., Constantino, V.R.L. Hybrid materials based on smectite clays and nutraceutical anthocyanins from the Açaí fruit. (2012). European Journal of Inorganic Chemistry, (32), pp. 5411-5420.

Wang, L., Guo, W., Zhao, Y. Preparation and characterization of cefradine /montmorillionite composites. (2012). Advanced Materials Research, 560-561, pp. 434-437.

Yun, J., Oh, A.-R., Im, J.S., Kim, H.-I., Lee, Y.-S. Control of drug release behavior of pH-responsive PVA/PAAc hydrogel by surface modification with oxyfluorination. (2012). Macromolecular Research, 20 (10), pp. 1029-1036.

Da Nóbrega, G.Â..S., Navarro, M.V.M., De Lima E Moura, T.A., Soares, D., Costa, J.A.F., Lavor, E.P., Santiago, R.H.N. Classification of pharmaceutical solid excipients using self-organizing maps. (2012). Lecture Notes in Computer Science (including subseries Lecture Notes in Artificial Intelligence and Lecture Notes in Bioinformatics), 7435 LNCS, pp. 707-716.

Salahuddin, N., Kenawy, E.-R., Abdeen, R. Polyoxypropylene-montmorillonite nanocomposites for drug-delivery vehicles: Preparation and characterization. (2012). Journal of Applied Polymer Science, 125 (SUPPL. 1), pp. E157-E166. Cited 1 time.

Anirudhan, T.S., Sandeep, S. Synthesis, characterization, cellular uptake and cytotoxicity of a multi-functional magnetic nanocomposite for the targeted delivery and controlled release of doxorubicin to cancer cells. (2012). Journal of Materials Chemistry, 22 (25), pp. 12888-12899. Cited 2 times.

El Kadib, A., Bousmina, M. Chitosan bio-based organic-inorganic hybrid aerogel microspheres. (2012). Chemistry - A European Journal, 18 (27), pp. 8264-8277. Cited 1 time.

Su, D., Wang, C., Cai, S., Mu, C., Li, D., Lin, W. Influence of palygorskite on the structure and thermal stability of collagen. (2012). Applied Clay Science, 62-63, pp. 41-46. Cited 1 time.

Chakraborti, M., Jackson, J.K., Plackett, D., Gilchrist, S.E., Burt, H.M. The application of layered double hydroxide clay (LDH)-poly(lactide-co- glycolic acid) (PLGA) film composites for the controlled release of antibiotics. (2012). Journal of Materials Science: Materials in Medicine, 23 (7), pp. 1705-1713.

Wang, Q., Wang, W., Wu, J., Wang, A. Effect of attapulgite contents on release behaviors of a pH sensitive carboxymethyl cellulose-g-poly(acrylic acid)/attapulgite/sodium alginate composite hydrogel bead containing diclofenac. (2012). Journal of Applied Polymer Science, 124 (6), pp. 4424-4432. Cited 1 time.

Lee, J.H., Jung, D.-Y. Highly oriented nanoplates of layered double hydroxides as an ultra slow release system. (2012). Chemical Communications, 48 (45), pp. 5641-5643. Cited 1 time.

Heinz, H. Clay minerals for nanocomposites and biotechnology: Surface modification, dynamics and responses to stimuli. (2012). Clay Minerals, 47 (2), pp. 205-230. Cited 2 times.

Acchar, W., Da Costa, A.C.S., De Lima E Moura, T.F.A., Barreto, L. Study of attapulgite for human health. (2012). TMS Annual Meeting, pp. 169-173.

Betsiou, M., Bantsis, G., Zoi, I., Sikalidis, C. Adsorption and release of gemcitabine hydrochloride and oxaliplatin by hydroxyapatite. (2012). Ceramics International, 38 (4), pp. 2719-2724. Cited 1 time.

Baek, M., Lee, J.-A., Choi, S.-J. Toxicological effects of a cationic clay, montmorillonite in vitro and in vivo. (2012). Molecular and Cellular Toxicology, 8 (1), pp. 95-101. Cited 2 times.

Ma, Z., Wang, J., Gao, X., Ding, T., Qin, Y. Application of halloysite nanotubes. (2012). Progress in Chemistry, 24 (2), pp. 275-283.

Reger, M., Hoffmann, H. Hydrophobin coated boehmite nanoparticles stabilizing oil in water emulsions. (2012). Journal of Colloid and Interface Science, 368 (1), pp. 378-386. Cited 2 times.

Hsu, S.-H., Wang, M.-C., Lin, J.-J. Biocompatibility and antimicrobial evaluation of montmorillonite/chitosan nanocomposites. (2012). Applied Clay Science, 56, pp. 53-62. Cited 5 times.

Joshi, G.V., Kevadiya, B.D., Mody, H.M., Bajaj, H.C. Confinement and controlled release of quinine on chitosan-montmorillonite bionanocomposites. (2012). Journal of Polymer Science, Part A: Polymer Chemistry, 50 (3), pp. 423-430. Cited 1 time.

Salcedo, I., Aguzzi, C., Sandri, G., Bonferoni, M.C., Mori, M., Cerezo, P., Sánchez, R., Viseras, C., Caramella, C. In vitro biocompatibility and mucoadhesion of montmorillonite chitosan nanocomposite: A new drug delivery. (2012). Applied Clay Science, 55, pp. 131-137. Cited 7 times.

Anirudhan, T.S., Sandeep, S. Synthesis and characterization of a novel pH-controllable composite hydrogel for anticancer drug delivery. (2011). New Journal of Chemistry, 35 (12), pp. 2869-2876. Cited 3 times.

Sommer, A.E., Fetter, G., Bosch, P., Novelo, O. Protein template effect on hydrotalcite morphology. (2011). Polymers for Advanced Technologies, 22 (12), pp. 2638-2642. Cited 1 time.

Pinto, F.C.H., Silva-Cunha, A., Pianetti, G.A., Ayres, E., Oréfice, R.L., Da Silva, G.R. Montmorillonite clay-based polyurethane nanocomposite as local triamcinolone acetonide delivery system. (2011). Journal of Nanomaterials, 2011, art. no. 528628, . Cited 1 time.

El-Din, H.M.N., El-Naggar, A.W.M. Characterization of gamma irradiated concentrated aqueous solutions of chitosan/sodium alginate blends and their drug uptake-release characters. (2011). Journal of Applied Polymer Science, 122 (4), pp. 2383-2390.

Tabak, A., Yilmaz, N., Eren, E., Caglar, B., Afsin, B., Sarihan, A. Structural analysis of naproxen-intercalated bentonite (Unye). (2011). Chemical Engineering Journal, 174 (1), pp. 281-288. Cited 4 times.

Chandrasekaran, G., Han, H.-K., Kim, G.-J., Shin, H.-J. Antimicrobial activity of delaminated aminopropyl functionalized magnesium phyllosilicates. (2011). Applied Clay Science, 53 (4), pp. 729-736. Cited 1 time.

Chakraborti, M., Jackson, J.K., Plackett, D., Brunette, D.M., Burt, H.M. Drug intercalation in layered double hydroxide clay: Application in the development of a nanocomposite film for guided tissue regeneration. (2011). International Journal of Pharmaceutics, 416 (1), pp. 305-313. Cited 8 times.

Vaiana, C.A., Leonard, M.K., Drummy, L.F., Singh, K.M., Bubulya, A., Vaia, R.A., Naik, R.R., Kadakia, M.P. Epidermal growth factor: Layered silicate nanocomposites for tissue regeneration. (2011). Biomacromolecules, 12 (9), pp. 3139-3146. Cited 3 times.

Iliescu, R.I., Andronescu, E., Ghițulică, C.D., Berger, D., Ficai, A. Montmorillonite-alginate nanocomposite beads as drug carrier for oral administration of carboplatin-preparation and characterization. (2011). UPB Scientific Bulletin, Series B: Chemistry and Materials Science, 73 (3), pp. 3-16.

Jun, J.Y., Nguyen, H.H., Paik, S.-Y.-R., Chun, H.S., Kang, B.-C., Ko, S. Preparation of size-controlled bovine serum albumin (BSA) nanoparticles by a modified desolvation method. (2011). Food Chemistry, 127 (4), pp. 1892-1898. Cited 6 times.

Dawson, J.I., Kanczler, J.M., Yang, X.B., Attard, G.S., Oreffo, R.O.C. Clay gels for the delivery of regenerative microenvironments. (2011). Advanced Materials, 23 (29), pp. 3304-3308. Cited 2 times.

Ha, J.U., Xanthos, M. Drug release characteristics from nanoclay hybrids and their dispersions in organic polymers. (2011). International Journal of Pharmaceutics, 414 (1-2), pp. 321-331. Cited 6 times.

Joshi, G.V., Pawar, R.R., Kevadiya, B.D., Bajaj, H.C. Mesoporous synthetic hectorites: A versatile layered host with drug delivery application. (2011). Microporous and Mesoporous Materials, 142 (2-3), pp. 542-548. Cited 5 times.

Cattaneo, A.S., Bracco, S., Comotti, A., Galimberti, M., Sozzani, P., Eckert, H. Structural characterization of pristine and modified fluoromica using multinuclear solid-state NMR. (2011). Journal of Physical Chemistry C, 115 (25), pp. 12517-12529. Cited 5 times.

Xu, J.-F., Liang, Y.-Y., Ma, N., Chen, L.-K., Li, Y., Du, P.-Y. Preparation of 0.85 nm hydrated kaolinite by direct displacement intercalation. (2011). Chinese Journal of Inorganic Chemistry, 27 (6), pp. 1121-1127. Cited 1 time.

Chung, J.H.-Y., Simmons, A., Poole-Warren, L.A. Non-degradable polymer nanocomposites for drug delivery. (2011). Expert Opinion on Drug Delivery, 8 (6), pp. 765-778.

Iliescu, R.I., Andronescu, E., Voicu, G., Ficai, A., Covaliu, C.I. Hybrid materials based on montmorillonite and citostatic drugs: Preparation and characterization. (2011). Applied Clay Science, 52 (1-2), pp. 62-68. Cited 8 times.

Hosseinzadeh, H. Preparation of pH-sensitive carrageenan-g-poly (acrylic acid)/bentonite composite hydrogel for 5-fluorouracil controlled release in colon. (2011). Research Journal of Pharmaceutical, Biological and Chemical Sciences, 2 (2), pp. 446-456.

Inayat, A., Klumpp, M., Schwieger, W. The urea method for the direct synthesis of ZnAl layered double hydroxides with nitrate as the interlayer anion. (2011). Applied Clay Science, 51 (4), pp. 452-459. Cited 7 times.

Gamiz, E., Parraga, J., Sanchez-Marantildn, M., Melgosa, M., Fernandez-Gonzalez, M.V., Delgado, R. Is the Pharmacopoeia test a good estimator of the organic impurities in kaolin?. (2011). Applied Clay Science, 51 (4), pp. 431-437.

Krajišnik, D., Daković, A., Milojević, M., Malenović, A., Kragović, M., Bogdanović, D.B., Dondur, V., Milić, J. Properties of diclofenac sodium sorption onto natural zeolite modified with cetylpyridinium chloride. (2011). Colloids and Surfaces B: Biointerfaces, 83 (1), pp. 165-172. Cited 3 times.

Liu, Q., Liu, Y., Xiang, S., Mo, X., Su, S., Zhang, J. Apoptosis and cytotoxicity of oligo(styrene-co-acrylonitrile)-modified montmorillonite. (2011). Applied Clay Science, 51 (3), pp. 214-219. Cited 1 time.

Choi, G., Lee, J.-H., Oh, Y.-J., Choy, Y.B., Park, M.C., Chang, H.C., Choy, J.-H. Inorganic-polymer nanohybrid carrier for delivery of a poorly-soluble drug, ursodeoxycholic acid. (2010). International Journal of Pharmaceutics, 402 (1-2), pp. 117-122. Cited 10 times.

Rytwo, G., Mendelovits, A., Eliyahu, D., Pitcovski, J., Aizenshtein, E. Adsoption of two vaccine-related proteins to montmorillonite and organo-montmorillonite. (2010). Applied Clay Science, 50 (4), pp. 569-575. Cited 1 time.

Tămăşan, M., Vulpoi, A., Vanea, E., Simon, V. Textural properties of the medical Algo clay as influenced by calcinations. (2010). Applied Clay Science, 50 (3), pp. 418-422. Cited 6 times.

Han, S., Li, G.-J., Li, N., Yan, S.-Q. In-Situ preparation and characterization of magnetic attapulgite. (2010). Xiandai Huagong/Modern Chemical Industry, 30 (10), pp. 46-48.

Ward, C.J., Song, S., Davis, E.W. Controlled release of tetracycline-HCl from halloysite-polymer composite films. (2010). Journal of Nanoscience and Nanotechnology, 10 (10), pp. 6641-6649. Cited 3 times.

Joshi, G.V., Kevadiya, B.D., Bajaj, H.C. Controlled release formulation of ranitidine-containing montmorillonite and Eudragit® E-100. (2010). Drug Development and Industrial Pharmacy, 36 (9), pp. 1046-1053. Cited 3 times.

Hua, S., Yang, H., Wang, W., Wang, A. Controlled release of ofloxacin from chitosan-montmorillonite hydrogel. (2010). Applied Clay Science, 50 (1), pp. 112-117. Cited 17 times.

Hua, S., Yang, H., Wang, A. A pH-sensitive nanocomposite microsphere based on chitosan and montmorillonite with in vitro reduction of the burst release effect. (2010). Drug Development and Industrial Pharmacy, 36 (9), pp. 1106-1114. Cited 3 times.

Joshi, G.V., Kevadiya, B.D., Bajaj, H.C. Design and evaluation of controlled drug delivery system of buspirone using inorganic layered clay mineral. (2010). Microporous and Mesoporous Materials, 132 (3), pp. 526-530. Cited 7 times.

Kevadiya, B.D., Joshi, G.V., Patel, H.A., Ingole, P.G., Mody, H.M., Bajaj, H.C. Montmorillonite-Alginate nanocomposites as a drug delivery system: Intercalation and in vitro release of vitamin B1 and vitamin B 6. (2010). Journal of Biomaterials Applications, 25 (2), pp. 161-177. Cited 3 times.

Parolo, M.E., Avena, M.J., Pettinari, G., Zajonkovsky, I., Valles, J.M., Baschini, M.T. Antimicrobial properties of tetracycline and minocycline-montmorillonites. (2010). Applied Clay Science, 49 (3), pp. 194-199. Cited 7 times.

Pongjanyakul, T., Suksri, H. Nicotine-loaded sodium alginate-magnesium aluminum silicate (SA-MAS) films: Importance of SA-MAS ratio. (2010). Carbohydrate Polymers, 80 (4), pp. 1018-1027. Cited 3 times.

Zhou, W.Y., Rabie, A.B.M., Wong, R.W.K., Tang, B. Nanocoating of montmorillonite/Mg-β-tricalcium phosphate on orthodontic titanium miniscrews. (2010). INEC 2010 - 2010 3rd International Nanoelectronics Conference, Proceedings, art. no. 5425193, pp. 817-818.

Lakshmi, M.S., Sriranjani, M., Bakrudeen, H.B., Kannan, A.S., Mandal, A.B., Reddy, B.S.R. Carvedilol/montmorillonite: Processing, characterization and release studies. (2010). Applied Clay Science, 48 (4), pp. 589-593. Cited 4 times.

Viseras, C., Cerezo, P., Sanchez, R., Salcedo, I., Aguzzi, C. Current challenges in clay minerals for drug delivery. (2010). Applied Clay Science, 48 (3), pp. 291-295. Cited 24 times.

Wang, Q., Xie, X., Zhang, X., Zhang, J., Wang, A. Preparation and swelling properties of pH-sensitive composite hydrogel beads based on chitosan-g-poly (acrylic acid)/vermiculite and sodium alginate for diclofenac controlled release. (2010). International Journal of Biological Macromolecules, 46 (3), pp. 356-362. Cited 23 times.

Xu, D., Zhou, N.-L., Fang, S., Meng, N., Zhang, J., Mo, H., Shen, J. Synchronicity of a controlled drug release system. (2010). Gongneng Cailiao/Journal of Functional Materials, 41 (3), pp. 425-427.

Yuan, Q., Shah, J., Hein, S., Misra, R.D.K. Controlled and extended drug release behavior of chitosan-based nanoparticle carrier. (2010). Acta Biomaterialia, 6 (3), pp. 1140-1148. Cited 28 times.

Wang, X., Strand, S.P., Du, Y., Vårum, K.M. Chitosan-DNA-rectorite nanocomposites: Effect of chitosan chain length and glycosylation. (2010). Carbohydrate Polymers, 79 (3), pp. 590-596. Cited 8 times.

Wang, F., Hui, H., Barnes, T.J., Barnett, C., Prestidge, C.A. Oxidized mesoporous silicon microparticles for improved oral delivery of poorly soluble drugs. (2010). Molecular Pharmaceutics, 7 (1), pp. 227-236. Cited 40 times.

Rojtanatanya, S., Pongjanyakul, T. Propranolol-magnesium aluminum silicate complex dispersions and particles: Characterization and factors influencing drug release. (2010). International Journal of Pharmaceutics, 383 (1-2), pp. 106-115. Cited 8 times.

Wang, X., Tang, Y., Li, Y., Zhu, Z., Du, Y. The rheological behaviour and drug-delivery property of chitosan/rectorite nanocomposites. (2010). Journal of Biomaterials Science, Polymer Edition, 21 (2), pp. 171-184. Cited 7 times.

Wang, Q., Zhang, J., Wang, A. Preparation and characterization of a novel pH-sensitive chitosan-g-poly (acrylic acid)/attapulgite/sodium alginate composite hydrogel bead for controlled release of diclofenac sodium. (2009). Carbohydrate Polymers, 78 (4), pp. 731-737. Cited 43 times.

Xiaoying, W., Yumin, D., Runcang, S., Lu, L. Chitosan-based layered silicate nanocomposites. (2009). Progress in Chemistry, 21 (7-8), pp. 1507-1514. Cited 2 times.

Kudaibergenova, B.M. Immobilization of alchidine on the physical polymer-clay composite gels. (2009). Journal of the Chemical Society of Pakistan, 31 (5), pp. 785-789.

Carretero, M.I., Pozo, M. Clay and non-clay minerals in the pharmaceutical industry. Part I. Excipients and medical applications. (2009). Applied Clay Science, 46 (1), pp. 73-80. Cited 21 times.

Joshi, G.V., Patel, H.A., Bajaj, H.C., Jasra, R.V. Intercalation and controlled release of vitamin B6 from montmorillonite - Vitamin B6 hybrid. (2009). Colloid and Polymer Science, 287 (9), pp. 1071-1076. Cited 11 times.

Teixeira-Neto, E., Teixeira-Neto, A.A. Chemical modification of clays: Scientific and technological chalenges for obtaining new value added products [Modificaçao quimica de argilas: desafios cientificos e tecnologicos para obtençao de novos produtos com maior valor agregado]. (2009). Quimica Nova, 32 (3), pp. 809-817. Cited 10 times.

Joshi, G.V., Patel, H.A., Kevadiya, B.D., Bajaj, H.C. Montmorillonite intercalated with vitamin B1 as drug carrier. (2009). Applied Clay Science, 45 (4), pp. 248-253. Cited 31 times.

Viçosa, A.L., Gomes, A.C.O., Soares, B.G., Paranhos, C.M. Effect of sepiolite on the physical properties and swelling behavior of rifampicin-loaded nanocomposite hydrogels. (2009). Express Polymer Letters, 3 (8), pp. 518-524. Cited 5 times.

Rice, Z., Bergkvist, M. Adsorption characteristics of a cationic porphyrin on nanoclay at various pH. (2009). Journal of Colloid and Interface Science, 335 (2), pp. 189-195. Cited 3 times.

Nieddu, E., Mazzucco, L., Gentile, P., Benko, T., Balbo, V., Mandrile, R., Ciardelli, G. Preparation and biodegradation of clay composites of PLA. (2009). Reactive and Functional Polymers, 69 (6), pp. 371-379. Cited 23 times.

Seki, Y., Yurdakoç, K. Equilibrium, kinetics and thermodynamic aspects of Promethazine hydrochloride sorption by iron rich smectite. (2009). Colloids and Surfaces A: Physicochemical and Engineering Aspects, 340 (1-3), pp. 143-148. Cited 8 times.

Guillot, S., Bergaya, F., de Azevedo, C., Warmont, F., Tranchant, J.-F. Internally structured pickering emulsions stabilized by clay mineral particles. (2009). Journal of Colloid and Interface Science, 333 (2), pp. 563-569. Cited 19 times.

Pongjanyakul, T., Khunawattanakul, W., Puttipipatkhachorn, S. Physicochemical characterizations and release studies of nicotine-magnesium aluminum silicate complexes. (2009). Applied Clay Science, 44 (3-4), pp. 242-250. Cited 12 times.

Viseras, M.-T., Aguzzi, C., Cerezo, P., Cultrone, G., Viseras, C. Supramolecular structure of 5-aminosalycilic acid/halloysite composites. (2009). Journal of Microencapsulation, 26 (3), pp. 279-286. Cited 8 times.

Suter, J.L., Anderson, R.L., Christopher Greenwell, H., Coveney, P.V. Recent advances in large-scale atomistic and coarse-grained molecular dynamics simulation of clay minerals. (2009). Journal of Materials Chemistry, 19 (17), pp. 2482-2493. Cited 21 times.

Wang, H., Sheng, X., Lin, P., Chu, C., Dong, Y. Preparation and performance of magnetic palygorskite particles by in situ synthesis method. (2009). Kuei Suan Jen Hsueh Pao/ Journal of the Chinese Ceramic Society, 37 (4), pp. 506-511. Cited 1 time.

Peterson, L.W., McKenna, C.E. Prodrug approaches to improving the oral absorption of antiviral nucleotide analogues. (2009). Expert Opinion on Drug Delivery, 6 (4), pp. 405-420. Cited 18 times.

Del Arco, M., Fernández, A., Martín, C., Rives, V. Release studies of different NSAIDs encapsulated in Mg,Al,Fe-hydrotalcites. (2009). Applied Clay Science, 42 (3-4), pp. 538-544. Cited 28 times.

Srivastava, R., Fujita, S., Arai, M. Synthesis and adsorption properties of smectite-like materials prepared using ionic liquids. (2009). Applied Clay Science, 43 (1), pp. 1-8. Cited 4 times.

Kiparissides, C., Kammona, O. Nanotechnology advances in controlled drug delivery systems. (2008). Physica Status Solidi (C) Current Topics in Solid State Physics, 5 (12), pp. 3828-3833. Cited 4 times.

Bonina, F.P., Giannossi, M.L., Medici, L., Puglia, C., Summa, V., Tateo, F. Diclofenac-hydrotalcite: In vitro and in vivo release experiments. (2008). Applied Clay Science, 41 (3-4), pp. 165-171. Cited 10 times.

Viseras, C., Aguzzi, C., Cerezo, P., Bedmar, M.C. Biopolymer-clay nanocomposites for controlled drug delivery. (2008). Materials Science and Technology, 24 (9), pp. 1020-1026. Cited 28 times.

Suksri, H., Pongjanyakul, T. Interaction of nicotine with magnesium aluminum silicate at different pHs: Characterization of flocculate size, zeta potential and nicotine adsorption behaviour. (2008). Colloids and Surfaces B: Biointerfaces, 65 (1), pp. 54-60. Cited 17 times.

Elbokl, T.A., Detellier, C. Intercalation of cyclic imides in kaolinite. (2008). Journal of Colloid and Interface Science, 323 (2), pp. 338-348. Cited 28 times.

Parolo, M.E., Savini, M.C., Vallés, J.M., Baschini, M.T., Avena, M.J. Tetracycline adsorption on montmorillonite: pH and ionic strength effects. (2008). Applied Clay Science, 40 (1-4), pp. 179-186. Cited 43 times.

Bisio, C., Gatti, G., Boccaleri, E., Marchese, L., Bertinetti, L., Coluccia, S. On the acidity of saponite materials: A combined HRTEM, FTIR, and solid-state NMR study. (2008). Langmuir, 24 (6), pp. 2808-2819. Cited 17 times.

Magaña, S.M., Quintana, P., Aguilar, D.H., Toledo, J.A., Ángeles-Chávez, C., Cortés, M.A., León, L., Freile-Pelegrín, Y., López, T., Sánchez, R.M.T. Antibacterial activity of montmorillonites modified with silver. (2008). Journal of Molecular Catalysis A: Chemical, 281 (1-2), pp. 192-199. Cited 58 times.

Wang, X., Du, Y., Luo, J. Biopolymer/montmorillonite nanocomposite: Preparation, drug-controlled release property and cytotoxicity. (2008). Nanotechnology, 19 (6), art. no. 065707, . Cited 49 times.

Viseras, M.T., Aguzzi, C., Cerezo, P., Viseras, C., Valenzuela, C. Equilibrium and kinetics of 5-aminosalicylic acid adsorption by halloysite. (2008). Microporous and Mesoporous Materials, 108 (1-3), pp. 112-116. Cited 27 times.

Isabel Carretero, M., Lagaly, G. Clays and health: An introduction. (2007). Applied Clay Science, 36 (1-3), pp. 1-3. Cited 5 times.

López-Galindo, A., Viseras, C., Cerezo, P. Compositional, technical and safety specifications of clays to be used as pharmaceutical and cosmetic products. (2007). Applied Clay Science, 36 (1-3), pp. 51-63. Cited 40 times.

ARTÍCULOS CIENTÍFICOS QUE HAN CITADO LA REVISIÓN:

Viseras C., Cerezo P., Sanchez R., Salcedo I., Aguzzi C. Current challenges in clay minerals for drug delivery. (2010). Applied Clay Science, (3) 291-295.

Scopus: EXPORT DATE:29 May 2013

Aguzzi, C., Viseras, C., Cerezo, P., Salcedo, I., Sánchez-Espejo, R., Valenzuela, C. Release kinetics of 5-aminosalicylic acid from halloysite. (2013). Colloids and Surfaces B: Biointerfaces, 105, pp. 75-80.

Wang, S., Wu, Y., Guo, R., Huang, Y., Wen, S., Shen, M., Wang, J., Shi, X. Laponite nanodisks as an efficient platform for doxorubicin delivery to cancer cells. (2013). Langmuir, 29 (16), pp. 5030-5036 begin_of_the_skype_highlighting GRATIS 5030-5036 end_of_the_skype_highlighting.

Galán-Jiménez, M.C., Mishael, Y.-G., Nir, S., Morillo, E., Undabeytia, T. Factors Affecting the Design of Slow Release Formulations of Herbicides Based on Clay-Surfactant Systems. A Methodological Approach. (2013). PLoS ONE, 8 (3), art. no. e59060,.

Wang, Y., Shang, D., Niu, Z. Removal of heavy metals by poly(vinyl pyrrolidone)/laponite nanocomposite hydrogels. (2013). Advanced Materials Research, 631-632, pp. 291-297.

Mahdavi, F., Rashid, S.A., Yusop, M.K. Application of urea-intercalated kaolinite for controlled release fertilizer. (2012). Jurnal Teknologi (Sciences and Engineering), 59 (SUPPL.3), pp. 71-74.

Wang, S., Zheng, F., Huang, Y., Fang, Y., Shen, M., Zhu, M., Shi, X. Encapsulation of amoxicillin within laponite-doped poly(lactic-co-glycolic acid) nanofibers: Preparation, characterization, and antibacterial activity. (2012). ACS Applied Materials and Interfaces, 4 (11), pp. 6393-6401. Cited 1 time.

Teixeira-Neto, Ã.A., Izumi, C.M.S., Temperini, M.L.A., Ferreira, A.M.D.C., Constantino, V.R.L. Hybrid materials based on smectite clays and nutraceutical anthocyanins from the Açaí fruit. (2012). European Journal of Inorganic Chemistry, (32), pp. 5411-5420.

Gu, Q., Sun, Y., Chu, N., Ma, S., Jia, Z., Yang, X. Intercalation of amino acids into Eu 3+-doped layered gadolinium hydroxide and quenching of Eu 3+ luminescence. (2012). European Journal of Inorganic Chemistry, (28), pp. 4407-4412.

Da Nóbrega, G.Â..S., Navarro, M.V.M., De Lima E Moura, T.A., Soares, D., Costa, J.A.F., Lavor, E.P., Santiago, R.H.N. Classification of pharmaceutical solid excipients using self-organizing maps. (2012). Lecture Notes in Computer Science (including subseries Lecture Notes in Artificial Intelligence and Lecture Notes in Bioinformatics), 7435 LNCS, pp. 707-716.

Chakraborti, M., Jackson, J.K., Plackett, D., Gilchrist, S.E., Burt, H.M. The application of layered double hydroxide clay (LDH)-poly(lactide-co- glycolic acid) (PLGA) film composites for the controlled release of antibiotics. (2012). Journal of Materials Science: Materials in Medicine, 23 (7), pp. 1705-1713.

Angadi, S.C., Manjeshwar, L.S., Aminabhavi, T.M. Novel composite blend microbeads of sodium alginate coated with chitosan for controlled release of amoxicillin. (2012). International Journal of Biological Macromolecules, 51 (1-2), pp. 45-55.

Wang, Q., Wang, W., Wu, J., Wang, A. Effect of attapulgite contents on release behaviors of a pH sensitive carboxymethyl cellulose-g-poly(acrylic acid)/attapulgite/sodium alginate composite hydrogel bead containing diclofenac. (2012). Journal of Applied Polymer Science, 124 (6), pp. 4424-4432. Cited 1 time.

Salcedo, I., Aguzzi, C., Sandri, G., Bonferoni, M.C., Mori, M., Cerezo, P., Sánchez, R., Viseras, C., Caramella, C. In vitro biocompatibility and mucoadhesion of montmorillonite chitosan nanocomposite: A new drug delivery. (2012). Applied Clay Science, 55, pp. 131-137. Cited 7 times.

Papoulis, D. Clay-based nanocomposites possibilities and limitations. (2011). AIP Conference Proceedings, 1389, pp. 1450-1453.

Iliescu, R.I., Andronescu, E., Ghițulică, C.D., Berger, D., Ficai, A. Montmorillonite-alginate nanocomposite beads as drug carrier for oral administration of carboplatin-preparation and characterization. (2011). UPB Scientific Bulletin, Series B: Chemistry and Materials Science, 73 (3), pp. 3-16.

Han, H.-K., Lee, Y.-C., Lee, M.-Y., Patil, A.J., Shin, H.-J. Magnesium and calcium organophyllosilicates: Synthesis and in vitro cytotoxicity study. (2011). ACS Applied Materials and Interfaces, 3 (7), pp. 2564-2572. Cited 7 times.

Yang, H., Hua, S., Wang, W., Wang, A. Composite hydrogel beads based on chitosan and laponite: Preparation, swelling, and drug release behaviour. (2011). Iranian Polymer Journal (English Edition), 20 (6), pp. 479-490. Cited 5 times.

Li, Y., MacIel, D., Tomás, H., Rodrigues, J., Ma, H., Shi, X. PH sensitive Laponite/alginate hybrid hydrogels: Swelling behaviour and release mechanism. (2011). Soft Matter, 7 (13), pp. 6231-6238. Cited 10 times.

Finocchio, E., Baccini, I., Cristiani, C., Dotelli, G., Gallo Stampino, P., Zampori, L. Hybrid organo-inorganic clay with nonionic interlayers. Mid- and near-IR spectroscopic studies. (2011). Journal of Physical Chemistry A, 115 (26), pp. 7484-7493. Cited 3 times.

Chen, Y., Zhou, S., Li, F., Wei, J., Dai, Y., Chen, Y. Fluorescence of Mg-Al-Eu ternary layered double hydroxide sensitivity to phenylalanine. (2011). Journal of Fluorescence, 21 (4), pp. 1677-1682. Cited 4 times.

Iliescu, R.I., Andronescu, E., Voicu, G., Ficai, A., Covaliu, C.I. Hybrid materials based on montmorillonite and citostatic drugs: Preparation and characterization. (2011). Applied Clay Science, 52 (1-2), pp. 62-68. Cited 8 times.

Abu-Jdayil, B. Rheology of sodium and calcium bentonite-water dispersions: Effect of electrolytes and aging time. (2011). International Journal of Mineral Processing, 98 (3-4), pp. 208-213. Cited 3 times.

Wan, C., Chen, B. Synthesis and characterization of biomimetic hydroxyapatite/sepiolite nanocomposites. (2011). Nanoscale, 3 (2), pp. 693-700. Cited 10 times.

Ruiz-Hitzky, E., Aranda, P., Darder, M., Ogawa, M. Hybrid and biohybrid silicate based materials: Molecular vs. block-assembling bottom-up processes. (2011). Chemical Society Reviews, 40 (2), pp. 801-828. Cited 27 times.

Applied Clay Science 48 (2010) 291–295

Contents lists available at ScienceDirect

Applied Clay Science

journal homepage: www.elsevier.com/locate/clay

Review Article

Current challenges in clay minerals for drug delivery

C. Viseras [a,b,*], P. Cerezo [a], R. Sanchez [a], I. Salcedo [a], C. Aguzzi [a]

[a] Department of Pharmacy and Pharmaceutical Technology, University of Granada, Spain
[b] Andalussian Institute of Earth Sciences, CSIC, Spain

ARTICLE INFO

Article history:
Received 26 October 2009
Received in revised form 16 January 2010
Accepted 18 January 2010
Available online 1 February 2010

Keywords:
Clay minerals
Clay polymer composites
Pharmaceutical dosage forms
Modified drug release

ABSTRACT

This study reviews current challenges of clay minerals for drug delivery. Clay minerals are widely used in conventional pharmaceutical dosage forms both as excipients and active agents. Clay minerals may interact with drug molecules, but also with inactive components of medicinal products such as polymers. On the basis of these interactions, clay minerals and their modified forms can be effectively used to modify drug delivery systems. In this research area, recent advances include the use of montmorillonite and saponite to retain drug molecules and control their release. Synthetic analogues such as Laponite and layered double hydroxides are also being used for biopharmaceutical and technological purposes. Another interesting strategy is the preparation of composites with clay mineral particles in polymeric matrices to obtain different systems (films, nanoparticles, hydrogels, matrices…) with improved pharmaceutical properties compared to the single components.

1. Introduction

Clays and clay minerals play an important role in the field of health products. They can be considered as raw pharmaceutical materials that once evaluated and/or modified to fulfill regulatory pharmacopoeial requirements may achieve the status of pharmaceutical substances suitable for use in the manufacture of medicinal products (López-Galindo et al., 2007). The progression from raw material, to pharmaceutical grade substance, and finally to pharmaceutical forms suitable for administration to the body is achieved first through general pharmaceutical operations to adjust the material grade, and then by specific pharmaceutical operations leading to the final dosage form (Fig. 1).

Consequently, clay minerals are fundamental components in several medicinal products, where they are used as excipients and fulfill some technological function (López-Galindo and Viseras, 2004). Table 1 shows the administration routes and dosage forms of clay minerals used as excipient in currently commercialized pharmaceutical products in the USA (FDA, 2009). Clay minerals are also used in pharmacy because of their biological activity, that is, as active substances or drugs (López-Galindo and Viseras, 2004). Pharmacological functions of clay minerals as active substances are summarized in Table 2. As observed, clay minerals are mainly used in the treatment of gastrointestinal and topical diseases.

2. The need for modified drug delivery systems

Besides these classic pharmaceutical uses, clay minerals may be effectively used in the development of new drug delivery systems (DDS). Strictly speaking, all pharmaceutical dosage forms are DDS, as they are used to administer drugs meant to reach the site of action and maintain a certain concentration during treatment. However, the ultimate therapeutic effect of a pharmaceutical treatment will depend on several factors (Fig. 2). Some concern the drug itself, such as potency, disposition (distribution and elimination) in the body, site of biological effect or concentration–effect relationship; others concern the patient, such as genetic constitution, organ function, and so on. A third group of factors concern pharmaceutical considerations such as optimal dosage forms and route of administration, frequency and dose of drug in the dosage forms, etc. Pharmacology studies the effect of a drug on a patient. Pharmaceutical technology works in the area between the drug and the dosage form, selecting and preparing the most adequate pharmaceutical product. Finally, biopharmacy studies the evolution of a dosage form (and the drug that it contains) after administration to the patient.

As might be expected, the intensity of the therapeutic effect will depend firstly on drug concentration at the site of action. Consequently, in drug therapy, it is very important to provide therapeutic levels of drug to the site of action (or at least in the blood) and maintain them during the treatment (Ding et al., 2002). Furthermore, it is desirable to minimize temporal variations in drug concentration by using some modified drug delivery system to avoid periods of overdosing or underdosing (Directive 75/318/EEC, 1992). As Fig. 3 shows, there is a direct relationship between drug release from the DDS and drug concentration in plasma.

* Corresponding author. Departamento de Farmacia y Tecnología Farmacéutica, Universidad de Granada, Facultad de Farmacia, Campus de Cartuja, s/n, 18071 Granada, Spain. Tel.: +34 958 249551; fax: +34 958 248958.
E-mail address: cviseras@ugr.es (C. Viseras).

0169-1317/$ – see front matter © 2010 Elsevier B.V. All rights reserved.
doi:10.1016/j.clay.2010.01.007

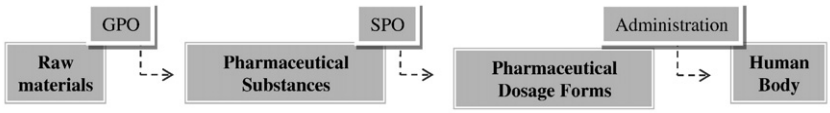

Fig. 1. Phases in the manufacture of medicinal products from raw materials (GPO: general pharmaceutical operations; SPO: specific pharmaceutical operations).

Consequently, pharmaceutical products evolve through modification of drug delivery systems (MDDS). The modifications involve changes in the rate and/or the time of release and/or the site of release, compared to conventional pharmaceutical dosage forms. These changes are achievable by several possible mechanisms, including modifications in pharmaceutical formulations and/or method of preparation (EP 6.0, 2008; USP 31, 2008). At the moment, there are several pharmaceutical products on the market that modify the release of the drug by one of these mechanisms. In almost all these new pharmaceutical products, new excipients with specific targets must be included, as for example decreasing or increasing dissolution rate, delaying drug release, targeting drug release (biopharmaceutical targets), prevention or reduction of side effects (pharmacological targets), taste masking or increasing stability (technological targets). Clay minerals as recognized pharmaceutical excipients may be used in these new pharmaceutical products.

3. Recent advances of clay minerals in modified drug delivery systems

Clay minerals have been proposed as fundamental constituents of several MDDS, with different purposes and acting through various mechanisms (Aguzzi et al., 2007). At this new frontier in the development of pharmaceutical dosage forms, these uses of clay minerals are changing very quickly, and new applications and clay minerals are continuously being proposed. Since the fully comprehensive review published by Aguzzi et al. (2007), some interesting advances have emerged that will be discussed below.

3.1. Clay minerals and synthetic clay minerals

The most recent examples of clay minerals use in MDDS include ibuprofen release control by interaction with montmorillonite (Zheng et al., 2007) and intercalation of Donepezil, a well-known drug for Alzheimer's disease, in montmorillonite, saponite or Laponite (Park et al., 2008). These studies characterized the clay mineral–drug interaction products and then examined the drug release kinetics. In all cases, drug release depended on the method of preparation of the interaction products, and was affected by changes in the pH of the dissolution medium. In the case of donezepil, biphasic release patterns were found, consisting of an initial burst effect followed by slow release of the drug. Other examples of drugs effectively carried by clay minerals include nicotine (Pongjanyakul et al., 2009) and timolol (Joshi et al., 2009). Nicotine, a volatile liquid widely used in smoking cessation therapy to relieve addiction symptoms, has been carried by magnesium aluminium silicate to reduce drug evaporation and modulate drug release behaviour (Pongjanyakul et al., 2009). The pH determined the amount of drug retained and the release patterns, and cation exchange seemed to be the principal interaction mechanism. Magnesium aluminium silicate is a pharmaceutical denomination of a natural clay material mainly consisting of montmorillonite and saponite (López-Galindo and Viseras, 2004). Timolol was loaded on montmorillonite, but the release of the drug did not reach 100%. This is one of the main problems to be avoided. A release of 100% dose for oral MDDS cannot last over 24 h and, ideally, should take place within the first 12 h (Directive 75/318/EEC, 1992).

Magnesium aluminium silicate has been also used to retain propranolol (a β-blocking agent) and release patterns have been correlated to particle size, drug loading, and release medium (Rojtanatanya and Pongjanyakul, 2008). Other authors compare results from natural and synthetic silicates. For example, montmorillonite and a siliceous mesoporous synthetic material have been loaded with sertraline (an antidepressive drug). The resultant complexes showed very different release profiles because of their diverse interaction mechanisms, resulting in different therapeutic indications for each system (Nunes et al., 2007).

Table 1
Inactive clay/clay mineral ingredients in pharmaceutical dosage forms (FDA, 2009).

Clay/clay mineral (USA pharmacopoeial name)	Route of administration	Dosage form
Talc	Oral	Solid (conventional and modified release capsules and tablets, chewable tablets, and granules) Liquid (drops, mucilage, solutions, elixir, suspensions, and syrup)
	Buccal	Chewing gums and tablets
	Sublingual	Tablets
	Topical	Lotions, ointments, and powders
	Rectal	Tablets
Activated Attapulgite	Oral	Powder
Bentonite	Oral	Solid (capsules and tablets) Liquid (suspensions)
	Topical	Lotions, powders, and suspensions
	Transdermal	Films and patches
	Rectal	Suspensions
	Vaginal	Ovules
Magnesium Aluminum Silicate (MAS)	Oral	Solid (conventional and modified tablets, granules, capsules, chewable tablets, and powders) Liquid (drops, suspensions, and syrups)
	Topical	Emulsions, creams, lotions, and suspensions
	Rectal	Suspensions
	Vaginal	Ointments
Magnesium trisilicate*	Oral	Conventional, modified and chewable tablets
Kaolin	Oral	Solid (conventional and modified tablets and capsules, powders) Liquid (syrups)
	Topical	Controlled release films

* Magnesium trisilicate is the pharmaceutical denomination of sepiolite.

Table 2
Therapeutic uses of clays/clay minerals (modified from López-Galindo and Viseras, 2004).

Clay/clay mineral (pharmaceutical names)	Kaolin	Bentonite and MAS	Talc	Attapulgite and magnesium Trisilicate*
Therapeutic use	Antidiarrhoeal Gastrointestinal protector Anti-inflammatory Antacid Homeopathic product	Antidiarrhoeal Gastrointestinal protector Antipruritic Antacid	Anti-haemorrhoids Anti-rubbing Pleurodesis	Antidiarrhoeal Antacid

* Magnesium trisilicate is the pharmaceutical denomination of sepiolite.

Layered double hydroxides (LDHs), also known as hydrotalcite like compounds, are layered solids with positively charged layers and charge-balancing anions in the interlayer space. Their cationic layered framework leads to safe accommodation of many biologically important molecules including genes or drugs (Choy et al., 2007). In recent years, layered double hydroxides with different cations in the layers and consequently diverse exchangeable characteristics have been used to obtain interaction products with several non-steroid anti-inflammatory drugs (mefenamic and meclofenamic acids and naproxen), leading to slow release profiles (Del Arco et al., 2007, 2009).

Drug release from MDDS must be carefully studied and if possible it is very interesting to determine the mechanism underlying the release kinetics. Frequently, drug molecules are retained by different mechanisms and consequently the kinetics of drug release are complex. For example, halloysite was used to retain mesalazine, an anti-inflammatory drug used in the treatment of inflammatory bowel disease (Viseras et al., 2008a, 2009). As a result of this interaction, drug molecules were included in both the clay mineral nanotubes and on the external surface of the clay mineral particles. Consequently, release kinetics was the sum of drug released from the surface of the particles and that retained in the tubes with a much slower release rate (Viseras, 2008).

3.2. Clay mineral polymer composites

A very interesting possibility is to use clay minerals polymer composites (CPC) to modify drug release. Several polymers are used in the modification of drug release, including hydrogels, soluble polymers, biodegradable and non-biodegradable hydrophobic polymers. Although clay mineral and polymers are frequently used in their pure form, a single polymer or clay mineral often does not meet all the requirements. Preparation of CPC improves the properties of the single components; those of clay mineral particles alone (stability of clay mineral dispersions and changes in ion exchange behaviour) and, more frequently, those of the polymer (mechanical properties, swelling capacity, film forming abilities, rheological properties, bioadhesion or cellular uptake) (Viseras et al., 2008b; Meenach et al., 2009).

Recent examples of MDDS based on CPC include intercalation of montmorillonite particles in polylactic glycolic acid to obtain nanoparticles loaded with Docetaxel (an anticancer drug) (Si-Shen et al., 2009). The in vitro drug release profiles of these drug loaded nanoparticles showed prolonged release over 25 days. Moreover, the presence of a clay mineral enhanced cellular uptake efficiency of the nanoparticles by Caco-2 and HT-29 cells, prolonging the therapeutic effect of the drug. Campbell et al. (2008) prepared composites of a modified montmorillonite with poly(ethylene glycol) by hot melt extrusion for controlled release of paracetamol. The presence of clay mineral particles in the polymer matrix resulted in retarded drug diffusion and improved dissolution behaviour.

Sodium alginate and magnesium aluminium silicate were used to prepare films loaded with nicotine to be used in buccal release (Pongjanyakul and Suksri, 2009). CPC operated as microreservoirs in the films showing adhesion properties to mucosal membranes and

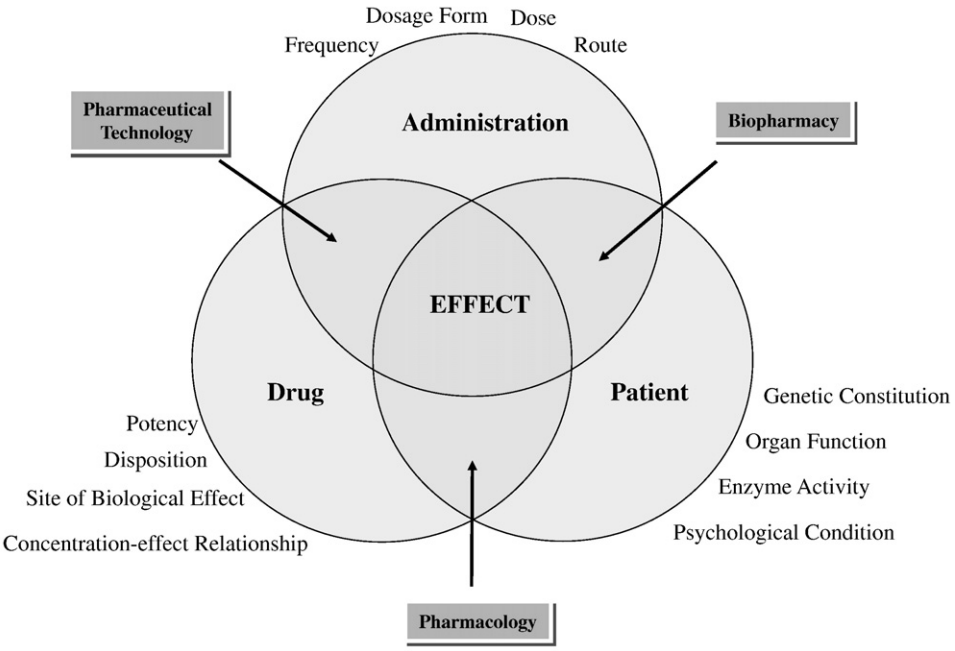

Fig. 2. Pharmaceutical treatment: determining elements (drug, administration and patient), study areas (Pharmacology, Pharmaceutical Technology and Biopharmacy) and variables affecting the final therapeutic effect.

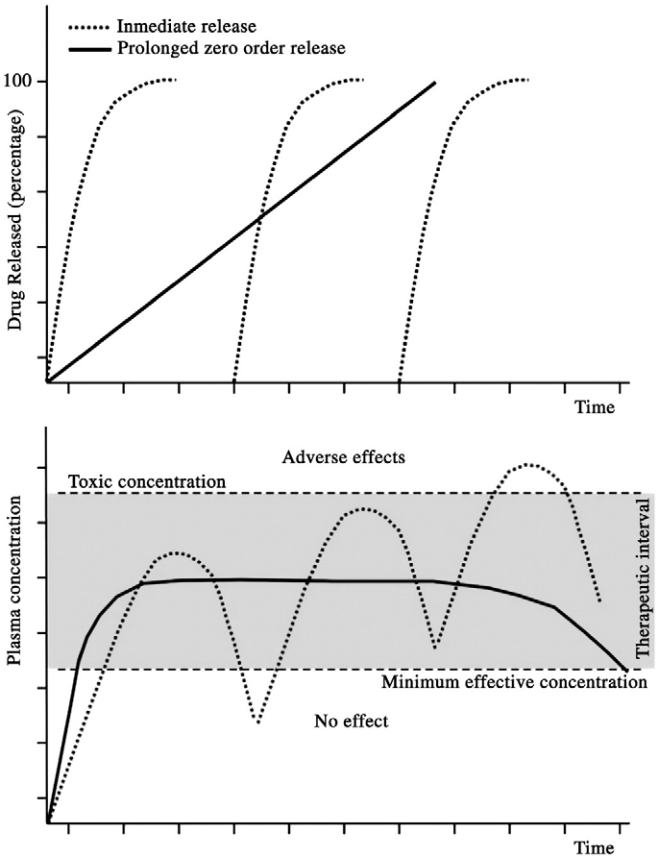

Fig. 3. Correlation between drug release profiles and plasma concentrations.

allowing controlled release of the drug molecules. Composite films with the same components have also been used to coat tablets and control drug release (Pongjanyakul, 2009).

Electrostatic interaction between chitosan, a deacetylated derivative of chitin, consists of D-glucosamine and N-acetyl-D-glucosamine units, and magnesium aluminium silicate caused a change in flow behaviour and flocculation of the composite dispersions (Khunawattanakul, et al., 2008). Chitosan has also been used to prepare composites with montmorillonite for prolonged release and biomedical applications (Xiaoying et al., 2008). The resultant composites were added to calcium alginate solutions to obtain nanoparticles loaded with bovine serum albumin as protein model drug, combining the drug adsorption action and mucosa protection effect of the clay mineral with the mucoadhesive and permeability enhancing properties of the chitosan. Montmorillonite has also been used as additive to retard ibuprofen release from delivery systems prepared with lactic acid-grafted chitosan (Depan et al., 2009). More recently, composites of chitosan and montmorillonite have shown a synergic effect between the clay mineral and the polysaccharide regarding the ability to retain 5-aminosalicylic acid (an anti-inflammatory drug) but also in the control of drug release in acidic medium, when compared to interaction products prepared with the drug and the single components (Aguzzi et al., 2009).

4. Concluding remarks

Some "special" clay minerals are components of medicines, both as active and inactive ingredients, once processed to fulfill regulatory requirements. The particular properties of these pharmaceutical grade clay minerals can be also exploited in the development of new drug delivery systems, designed to provide therapeutic levels of drug to the site of action and maintain them throughout the treatment. In recent years, some interesting advances have been proposed by using natural, but also modified and synthetic phyllosilicates, on the basis of their interaction with drug molecules. Finally, composites prepared with different polymers and clay minerals are attracting great attention in this pharmaceutical field because of their synergic characteristics regarding biopharmaceutical and technological features.

Acknowledgements

We thank Prof. Ian MacCandless (Department of English Philology, University of Granada, Spain) for assisting us with the English version of the text.

References

Aguzzi, C., Cerezo, P., Viseras, C., Caramella, C., 2007. Use of clays as drug delivery systems: possibilities and limitations. Appl. Clay Sci. 36, 22–36.
Aguzzi, C., Capra, P., Bonferoni, C., Cerezo, P., Caramella, C., Viseras, C., 2009. Chitosan-silicate biocomposites for colonic delivery of 5-aminosalicylic acid (5-ASA). In: Fiore, S., Belviso, C., Giannossi, M.L. (Eds.), Micro et Nano: Scientiae Mare Magnum, vol. II. 14th Int. Clay Conf., Castellaneta M., Italy, p. 275.
Campbell, K., Craig, D.Q.M., McNallya, T., 2008. Poly(ethylene glycol) layered silicate nanocomposites for retarded drug release prepared by hot-melt extrusion. Int. J. Pharm. 363, 126–131.
Choy, J.-H., Choi, S.-J., Oh, J.-M., Park, T., 2007. Clay minerals and layered double hydroxides for novel biological applications. Appl. Clay Sci. 36, 122–132.
Del Arco, M., Fernández, A., Martín, C., Rives, V., 2007. Intercalation of mefenamic and meclofenamic acid anions in hydrotalcite-like matrixes. Appl. Clay Sci. 36, 133–140.
Del Arco, M., Fernández, A., Martín, C., Rives, V., 2009. Release studies of different NSAIDs encapsulated in Mg, Al, Fe-hydrotalcites. Appl. Clay Sci. 42, 538–544.
Depan, D., Kumar, A.P., Singh, R.P., 2009. Cell proliferation and controlled drug release studies of nanohybrids based on chitosan-g-lactic acid and montmorillonite. Acta Biomater. 5, 93–100.
Ding, X., Alani, A.W.G., Robinson, J.R., 2002. Extended-release and targeted drug delivery systems, In: Troy, D.B. (Ed.), Remington: The Science and Practice of Pharmacy, 21st Edition. Lippincott Williams & Wilkins, USA, pp. 939–964. Chap. 47.
Directive 75/318/EEC, 1992. Quality of Prolonged Release Oral Solid Dosage Forms, European Directorate for Medicinal Products (EMEA). November.
EP 6.0, 2008. European Pharmacopoeia Sixth Edition. Directorate for the Quality of Medicines of the Councile of Europe, Strasbourg (F).
FDA, 2009. Inactive ingredients database for approved drug products. FDA/Center for Drug Evaluation and Research. Office of Generic Drugs. Division of Labeling and Program Support. Database Last Updated: July 10, 2009. http://www.fda.gov/Drugs/InformationOnDrugs/.
Joshi, G.V., Kevadiyaa, B.D., Patel, H.A., Bajaj, H.C., Jasrab, R.V., 2009. Montmorillonite as a drug delivery system: Intercalation and in vitro release of timolol maleate. Int. J. Pharm. 374, 53–57.
Khunawattanakul, W., Puttipipatkhachorn, S., Rades, T., Pongjanyakul, T., 2008. Chitosan–magnesium aluminum silicate composite dispersions: Characterization of rheology, flocculate size and zeta potential. Int. J. Pharm. 351, 227–235.
López-Galindo, A., Viseras, C., 2004. Pharmaceutical and cosmetic applications of clays. In: Wypych, F., Satyanarayana, K.G. (Eds.), Clay Surfaces: Fundamentals and Applications. Elsevier, Armsterdam, pp. 267–289.
López-Galindo, A., Viseras, C., Cerezo, P., 2007. Compositional, technical and safety specifications of clays to be used as pharmaceutical and cosmetic products. Appl. Clay Sci. 36, 51–63.
Meenach, S.A., Anderson, K.W., Hilt, J.Z., 2009. Hydrogel nanocomposites: biomedical applications, biocompatibility, and toxicity analysis. In: Webster, T.J. (Ed.), Safety of Nanoparticles: From Manufacturing to Medical Applications. Springer Science+Business Media, New York, pp. 1–27. Chap. 7.
Nunes, C.D., Vaz, P.D., Fernandes, A.C., Ferreira, P., Roma, C.C., Calhorda, M.J., 2007. Loading and delivery of sertraline using inorganic micro and mesoporous materials. Eur. J. Pharm. Biopharm. 66, 357–365.
Park, J.K., Choy, Y.B., Oh, J.-M., Kima, J.Y., Hwanga, S.-J., Choy, J.-H., 2008. Controlled release of donepezil intercalated in smectite clays. Int. J. Pharm. 359, 198–204.
Pongjanyakul, T., 2009. Alginate–magnesium aluminum silicate films: importance of alginate block structures. Int. J. Pharm. 365, 100–108.
Pongjanyakul, T., Suksri, H., 2009. Alginate–magnesium aluminum silicate films for buccal delivery of nicotine. Colloids Surf. B Biointerfaces 74 (1), 103–113.
Pongjanyakul, T., Khunawattanakul, W., Puttipipatkhachorn, S., 2009. Physicochemical characterizations and release studies of nicotine–magnesium aluminum silicate complexes. Appl. Clay Sci. 44, 242–250.
Rojtanatanya, S., Pongjanyakul, T., 2008. Propranolol–magnesium aluminum silicate complex dispersions and particles: characterization and factors influencing drug release. Int. J. Pharm. 383 (1–2), 106–115.
Si-Shen, F., Lin, M., Panneerselvan, A., Chee Wee, G., Zhou, W., 2009. Poly(lactide)-vitamin E derivative/montmorillonite nanoparticle formulations for the oral delivery of Docetaxel. Biomaterials 30, 3297–3306.
USP 31, 2008. United States Pharmacopoeia 31 and National Formulary 28, US Pharmacopoeial Convention, Rockville, MD (USA).

Viseras, M.T., 2008. Desarrollo galénico de preparados obtenidos por interacción del ácido 5 amino salicílico con haloysita. Ph.D. Thesis, University of Granada, Granada, Spain.
Viseras, M.T., Aguzzi, C., Cerezo, P., Viseras, C., Valenzuela, C., 2008a. Equilibrium and kinetics of 5-aminosalicylic acid adsorption by halloysite. Microporous Mesoporous Mat. 108, 112–116.
Viseras, C., Aguzzi, C., Cerezo, P., Bedmar, M.C., 2008b. Biopolymer–clay nanocomposites for controlled drug delivery. Mater. Sci. Technol. 24, 1020–1026.
Viseras, M.T., Aguzzi, C., Cerezo, P., Cultrone, G., Viseras, C., 2009. Supramolecular structure of 5-aminosalycilic acid/halloysite composites. J. Microencapsul. 26, 279–286.
Xiaoying, W., Yumin, D., Jiwen, L., 2008. Biopolymer/montmorillonite nanocomposite: preparation, drug-controlled release property and cytotoxicity. Nanotechnology 19, 1–7.
Zheng, J.P., Luan, L., Wang, H.Y., Xi, L.F., Yao, K.D., 2007. Study on ibuprofen/montmorillonite intercalation composites as drug release system. Appl. Clay Sci. 36, 297–301.

Applied Clay Science 50 (2010) 106–111

Contents lists available at ScienceDirect

Applied Clay Science

journal homepage: www.elsevier.com/locate/clay

Chitosan–silicate biocomposites to be used in modified drug release of 5-aminosalicylic acid (5-ASA)

C. Aguzzi [a], P. Capra [b], C. Bonferoni [b], P. Cerezo [a], I. Salcedo [a], R. Sánchez [a], C. Caramella [b], C. Viseras [a,c,*]

[a] Department of Pharmacy and Pharmaceutical Technology, School of Pharmacy, University of Granada, Spain
[b] Department of Pharmaceutical Chemistry, School of Pharmacy, University of Pavia, Italy
[c] Andalusian Institute of Earth Sciences, CSIC, Granada, Spain

ARTICLE INFO

Article history:
Received 22 September 2009
Received in revised form 29 June 2010
Accepted 12 July 2010
Available online 23 July 2010

Keywords:
Montmorillonite
Chitosan
Biocomposites
5-amino salicylic acid
Drug release

ABSTRACT

Biocomposites of chitosan (CS) and montmorillonite (VHS) were prepared by solid–liquid interaction of the components. The resultant composites were characterized by thermal analysis and the cation exchange capacity of the clay mineral was compared to polysaccharide retention. The composites were loaded with 5-amino salicylic acid (5-ASA), comparing the drug loading capacity and drug release behavior with those of the interaction products prepared with the drug and chitosan or montmorillonite alone. The results showed that chitosan was effectively retained by montmorillonite particles through cation exchange. In comparison with interaction products prepared using the drug and the individual components, there was a synergic effect between the clay mineral and the polysaccharide regarding both their ability to retain drug molecules, and also the control of drug release in acidic medium. In particular, the 5-ASA/CS/VHS composites showed higher drug loading and slower drug release compared to both 5-ASA/VHS and 5-ASA/CS interaction products, with almost linear release profile throughout test. According to the results, biocomposites of chitosan and montmorillonite were promising supports for modified formulations of 5-amino salicylic acid.

1. Introduction

Biopolymers and clay minerals are common ingredients in pharmaceutical products. Although they are frequently used in their pure form, a single polymer or clay mineral often does not meet all the requirements. A way to further extend their applications is to modify polymers by incorporation of inorganic fillers to obtain biocomposites with improved properties (Viseras et al., 2008).

5-ASA (Fig. 1) has been extensively used for the long-term maintenance therapy of Crohn's disease and ulcerative colitis (Dollery, 1991). It is an amphoteric molecule with pH-dependent aqueous solubility. According to the pK_a values of the carboxyl and amino groups (2.30 and 5.69, respectively), solubility of 5-ASA increases at pH<2 and pH>5.5 and is reduced in the 2–5.5 pH interval (French and Mauger, 1993).

Numerous in vitro studies found that the beneficial effects of 5-ASA were related to its anti-inflammatory and anti-oxidant properties within the inflamed gut (Clemett and Markham, 2000). In order to maximize the efficacy of the drug and avoid adverse effects associated with systemic absorption (Novis et al., 1988; Sachedina et al., 1989; Isaacs and Murphy, 1990), target release of 5-ASA to the site of action (small bowel and/or colon) would be desirable. However, the drug is quickly absorbed in the upper gastrointestinal tract and the amount reaching the colon is fairly reduced (Crotty and Jewel, 1992). Hence, many approaches aimed at delivery of 5-ASA to the colon, including prodrugs (Baron et al., 1962; Chan et al., 1983; Wadworth and Fitton, 1991), time-dependent approaches based on the gastrointestinal (GI) transit time (Hardy et al., 1993), pH-dependent approaches utilizing the changes in pH along the GI tract (Dew et al., 1982; Rudolph et al., 2001), pH- and time-dependent systems (Gupta et al., 2001), pressure dependent systems relying on the strong peristaltic waves in the colon (Muraoka et al., 1998) and biodegradable polymers which exploit metabolism by the colonic microflora to release the drug (Davaran et al., 1999). Among these strategies, the use of bacterial degradable polymers, such as polysaccharides, seems to be a more site specific approach for colonic drug delivery (Sinha and Kumria, 2001). In particular, chitosan is a non-toxic, biodegradable and biocompatible (Illum, 1998) polycationic polysaccharide that has been extensively used for drug release into the colon (Zhang and Neau, 2002; Chourasia and Jain, 2003; Friend, 2005). However, due to its high solubility and swelling properties in acidic media, chitosan alone is unable to prevent the release of drugs from dosage forms during their transit through the stomach and the small intestine. To avoid such problems, pH-dependent coating (Tozaki et al., 1997; Lorenzo-Lamosa et al., 1998; Varshosaz et al.,

* Corresponding author. Departamento de Farmacia y Tecnología Farmacéutica, Facultad de Farmacia — Universidad de Granada, Campus de Cartuja, s/n, 18071 Granada, Spain. Tel.: +34 58 249551; fax: +34 58 248958.
E-mail address: cviseras@ugr.es (C. Viseras).

0169-1317/$ – see front matter © 2010 Elsevier B.V. All rights reserved.
doi:10.1016/j.clay.2010.07.011

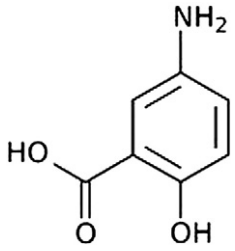

Fig. 1. Structure of 5-ASA.

2006; Nunthanid et al., 2009), cross-linking (Zhang et al., 2002) and grafting with other polymers (Meshali and Gabr, 1993; MacLeod et al., 1999; Takeuchi et al., 2000; Hiorth et al., 2003) have been studied as useful strategies.

Recently, synthesis of micro and nanocomposites with clay minerals was proposed as a novel approach to modify some of the properties of polysaccharides, including swelling and water uptake (Pongjanyakul et al., 2005), mechanical and thermal behavior (Wang et al., 2005; Wu and Wu, 2006), rheology (Günister et al., 2007; Khunawattanakul et al., 2008) and bioadhesion (Pongjanyakul and Suksri, 2009).

Given these premises, we prepared and characterized composites of chitosan and pharmaceutical grade montmorillonite, which we then loaded with 5-ASA. The resultant loaded composites were tested to assess their possibilities in modified release formulations by performing preliminary release studies.

2. Materials and methods

Drug: 5-ASA (Sigma, S). *Biopolymer*: chitosan base (CS) (average molar mass = 251 000 g mol^{-1}) containing an average of 1559 glucosamine units (glucosamine molar mass = 161 g mol^{-1}), with 98% deacetylation purchased from Faravelli (I). *Clay mineral filler*: pharmaceutical grade montmorillonite (Veegum HS©, VHS) was kindly gifted by Vanderbilt Company (USA).

Analytical grade reagents (glacial acetic acid, sodium hydroxide, hydrochloric acid 37% mass/mass) and acetonitrile HPLC grade were purchased from Panreac Química Sau (S) and used as received.

2.1. Determination of the Cation Exchange Capacity (CEC) of the clay mineral

Clay mineral powder (1 g) was dispersed in 20 ml tetramethylammonium bromide (1 M) aqueous solution, in order to displace constituent cations. Dispersions were shaken overnight at 50 rpm in water bath at 25.0 ± 1.0 °C and then filtered. Supernatant was diluted to 100 ml with distilled water and dissolved cations were individually assayed by atomic absorption (Na^+, Ca^{2+}, Mg^{2+}) or atomic emission (K^+) spectroscopy (Perkin–Elmer spectrophotometer). CEC was calculated as the sum of exchangeable cations, expressed in meq/100 g dry clay mineral. The same solution, minus the clay mineral sample, was used for the blank. Each experiment was done in triplicate.

2.2. Clay mineral/chitosan interaction studies

CS solutions (1% mass/vol) were prepared according to Darder et al. (2003, 2005), by adding the corresponding amount of polymer to an aqueous acetic acid solution 1% (v/v) and stirring for about 4 h. Different amounts of clay mineral powder (ranging from 75 mg to 2000 mg) were then dispersed in 40 ml of CS solution at 10000 rpm for 5 min (Ultraturrax T25, Janke and Kunkel GMBH and Co. KG, G). CS solution was previously adjusted to pH 5.0 with 1 M NaOH, in order to provide $-NH_3^+$ groups in the chitosan structure and to avoid any structural alteration of the clay mineral (Darder et al., 2003, 2005). The resulting dispersions were shaken for 2 days in water bath at 25 °C ± 1.0 °C and the solid phases were then recovered by filtration, washed with distilled water and oven-dried at 50 °C for 24 h.

The uptake of CS (mass/mass%) was determined by assaying the C-content of the samples with a CHNS analyzer (FISONS EA 1108, Carlo Erba, I). Data were fitted according to the Langmuir equation to calculate the amount of CS retained by the clay mineral (monolayer adsorption capacity, n_m). Experiments were done in triplicate.

2.3. Drug loading

Dialysis tubing cellulose membranes (average flat width 25 mm; cut off 12 400) (Sigma, S) were hydrated following the preparation procedure provided by the manufacturer. The membranes were then filled with 20 ml of CS:VHS dispersions in mass:mass ratio corresponding to the monolayer binding capacity, as calculated from interaction studies. The filled membranes were put in amber glass flasks with 200 ml of 500 ppm 5-ASA solution (in aqueous acetic acid 1% vol/vol) and stirred by a magnetic bar for 48 h at room temperature. CS and drug solutions were previously adjusted to pH 5.0 with 1 M NaOH.

Initial and final drug concentrations were assessed by HPLC in order to calculate the amounts of drug adsorbed at equilibrium. At the end of the experiment, membranes were emptied for freeze drying of the dispersions in order to obtain solid samples (5-ASA/CS/VHS drug loaded composites). Binary interaction products (5-ASA/CS and 5-ASA/VHS) were also prepared for comparison purposes. Each experiment was done in triplicate.

2.4. Drug assay

Drug assay was performed using an HPLC system (series 200, Perkin–Elmer, S) equipped with quaternary pump, autosampler, column oven and UV–VIS diode–array spectrophotometer. The stationary phase was a column Kromasyl® C18, 5 μm, 250 X 4.6 mm (Teknokroma, S) and the mobile phase was a mixture of H_20 and CH_3CN (78/22 vol/vol) and acetic acid 0.5% (vol/vol) (Cendrowska et al., 1990). The flow rate was set at 1 ml/min, the injection volume was 20 μl, the detector wavelength 300 nm and the run time 5 min. Data were recorded using TotalChrom WS 6.2 software package (Perkin–Elmer, S). The method was validated in acetic acid 1% v/v and HCl 0.1 M by determining in both cases the analytical (linearity, detection limit, quantification limit, repeatability, accuracy) and system suitability (column efficiency, tailing factor) parameters, according to both international (ICH, 1995) and pharmacopoeial (USP 32, 2009) indications.

2.5. Thermal analysis

Differential scanning calorimetry of the samples was performed at 10 °C/min in the 30–320 °C temperature range (DSC Mettler FP800, Mettler-Toledo GMBH, CH).

2.6. Intrinsic dissolution studies

250 mg of 5-ASA/VHS, 5-ASA/CS and 5-ASA/CS/VHS composites were compressed in a Perkin–Elmer hydraulic press (Specac, S) equipped with flat 10 mm punches at 5 T for 3 min. The resultant matrices were coated, except for one face (0.785 cm^2 area), with a water insoluble polymer (cellulose acetate propionate 15% mass/vol in acetone), in order to maintain constant surface area during tests. Matrices were then glued (uncoated face up) to an inert disc to be maintained at the bottom of the vessels. Experiments were carried out for 2 h in a USP apparatus 2 (Sotax AT7, S) at 50 rpm, 37 °C and 600 ml of medium (HCl 0.1 M) previously degassed under vacuum. At

established time intervals, samples of dissolution medium (2 ml) were withdrawn, filtered through 0.45 μm Millipore® (S) membranes and analyzed via HPLC for drug content. The data (mg released/cm^2) were normalized according to the different dose of drug in the composites. The drug release rate was expressed as mg released per unit of time and area (mg/min/cm^2) by linear fitting of the experimental points (mg released/cm^2) as a function of time in the time interval 0–20 min (linear portion of the curves). Each experiment was done in triplicate. Some tablets, prepared as described, but uncoated, were hydrated for 2 h in HCl 0.1 M without agitation, so that some photographs could be taken.

2.7. Statistical analysis

One-way analysis of variance (ANOVA) with the post hoc Sheffé test for multiple comparisons was performed using Siphar 4.0 software (F). Differences between groups were considered to be significant at a level of $P<0.05$.

3. Results and discussion

3.1. CEC

Table 1 summarizes the composition of individual exchangeable cationic species of the clay mineral. The total cation exchange capacity was 142 meq/100 g. Exchangeable species were mainly Na^+ and Ca^{2+}, with amounts reaching 71% and 24% of the total, respectively. The material may be considered as a "sodium montmorillonite", but the presence of a noticeable Ca^{2+} amount in the interlayer space must be taken into account.

3.2. Clay mineral/chitosan interaction studies

The interaction curve between VHS and CS followed the form of the Giles L3 type isotherm (Giles et al., 1974) (Fig. 2). At low concentrations it was convex in shape, with the amount of adsorbed polymer initially increasing until it reached a plateau, where monolayer coverage of CS over the homogenous clay mineral surface was assumed. At higher concentrations, the curve showed an inflection point where the shape changed from convex to concave and the amount retained further increased, almost certainly by precipitation of CS onto the clay mineral surface. Langmuir linearization of the isotherm allowed calculation of the average amount of CS retained by the clay mineral at the saturation point (n_m), resulting in 14.47% (mass/mass) ± 3.054 ($R^2 = 0.997$). This value, corresponding to 107.43 meq of CS/100 g dry clay mineral, was slightly lower than the CEC of VHS (142 meq/100 g), most probably due to the particularities of the organic cation. These results are also lower than those obtained by other authors working at higher temperatures (Darder et al., 2005). However, in the experimental conditions used, the uptake of chitosan in the interlayer space of the clay mineral via cation exchange was considered adequate to prepare interaction products with the drug.

3.3. Drug assay

Detector response was linear in the 10–50 μg/ml range (five data points, replicated three times, were considered) in both media tested (acetic acid 1% vol/vol and HCl 0.1 M). The related linearity equations were $y = 17653x + 11529$ ($R^2 = 0.9994$) in acetic acid and $y = 18278x + 16119$ ($R^2 = 0.9997$) in HCl.

Table 1
Amount of exchangeable cations (meq/100 g) and CEC of VHS (mean values ± s.d.; $n = 3$).

Ca^{++}	Mg^{++}	K^+	Na^+	CEC
34.67 ± 0.393	1.78 ± 0.251	4.27 ± 0.234	101.35 ± 0.478	142.07

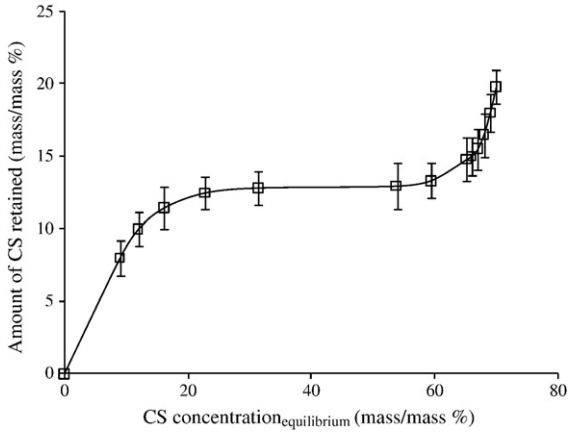

Fig. 2. Interaction isotherm showing the amount of CS adsorbed on the clay mineral (mean values ± s.d.; $n = 3$).

Table 2 summarizes analytical and suitability parameters calculated according to ICH and USP recommendations. The slope of the curves obtained by plotting log of drug concentration *vs* log of peak area ("log–log slope") fulfilled ICH recommendations (0.95–1.05 accepted interval). The limit of detection (LD) and the limit of quantification (LQ), determined from the signal-to-noise ratio, were respectively 1 μg/ml and 5 μg/ml in both media. Repeatability (variation within-day) of peak area (A) and retention time (t_R), expressed as relative standard deviation (S_R) and assessed using 9 determinations (3 concentrations/3 replicates each) of 5-ASA standard solutions covering the linearity range, was <1% for all samples tested. The column efficiency, expressed as the number of theoretical plates (N), was about 8000. The tailing factor (T) was about 1, indicating that suitable peak symmetry was reached under the experimental conditions in both media. Finally, accuracy, evaluated as the amount of 5-ASA recovered (mass/mass%) from samples prepared by adding known amounts of drug to known volume of blank solutions, was satisfactory (>97%) in all cases.

3.4. Drug loading

The amount of 5-ASA bound to VHS in the drug/clay mineral interaction product was about 10% (mass/mass) of the initial drug concentration (500 ppm), whereas, in the case of chitosan, the amount bound was slightly greater (14% (mass/mass); $P<0.05$). It was probable that, under the experimental conditions of the interaction (pH 5), the negative surface charge of the clay mineral partially rejected the drug, whose molecules were dissolved at a pH very close to anionic dissociation (French and Mauger, 1993). In the composites, with a combination of chitosan and clay mineral, a synergic effect took place as shown by the significant increase in the amount of 5-ASA loaded (23% mass/mass; $P<0.001$) in comparison with the binary systems (drug/clay mineral and drug/polymer).

Table 2
Parameters of the analytic method used for drug assay in both media studied.

Parameter		Medium	
		Acetic acid (1% v/v)	HCl 0.1 M
Log–log slope		0.97	0.96
LD (μg/ml)		1	1
LQ (μg/ml)		5	5
Repeatability (SR) (%)	Peak area (A)	0.89	0.22
	t_R	0.03	0.08
Accuracy (recovery, %)		97.8–99.2	98.5–99.9
Column efficiency (N)		≅8000	≅8000
Tailing factor (T)		1.12	0.9

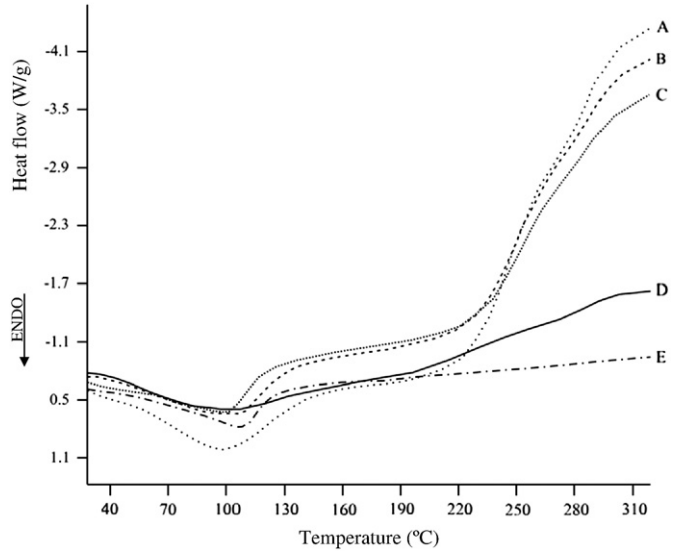

Fig. 3. DSC curves of CS (A); Physical mixture CS:VHS 50:50 (B); Physical mixture CS:VHS 33:66 (C); composite CS:VHS 33:66 (D) and VHS (E).

3.5. Thermal analysis

Fig. 3 shows the results of thermal characterization of the CS/VHS composites, and, for comparison purposes, it also includes DSC profiles of the single components and their physical mixtures at different wt/wt ratios. The calorimetric curve of CS showed a broad endothermic peak in the 60–150 °C range, corresponding to polymer dehydration, followed by an exothermic phenomenon (around 220 °C) due to the decomposition of the polymer chain. VHS showed a single band from 70 to 130 °C, corresponding to the loss of free water at the clay mineral surface.

The DSC profiles of physical mixtures resembled those of their individual components. The decomposition peak of CS rose as the proportion of polymer in the mixtures increased (C *vs* B). The presence of chitosan in the composites was confirmed by the slope increase in the curves at 200 °C-220 °C, corresponding to polymer decomposition.

Fig. 4 shows the results of thermal characterization of the 5-ASA/CS/VHS composites. The fusion peak of 5-ASA around 280 °C disappeared in

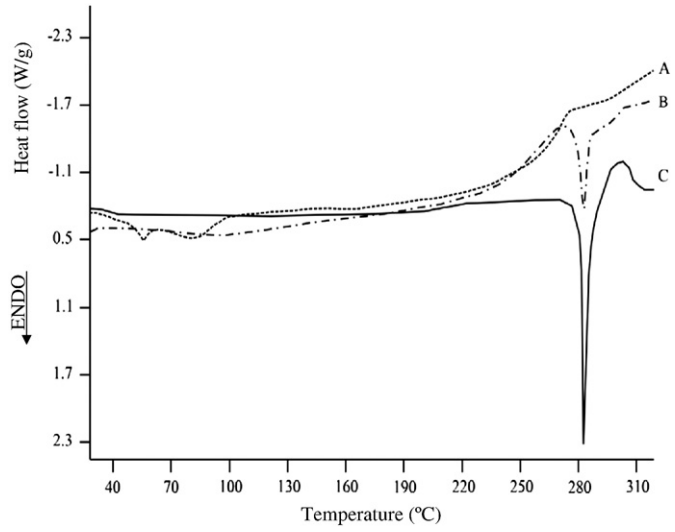

Fig. 4. DSC curves of loaded composite (5-ASA:CS:VHS) (A), corresponding physical mixture (B) and 5-ASA (C).

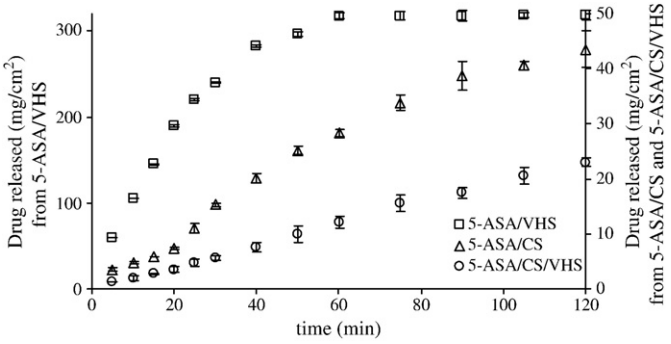

Fig. 5. Drug release profiles from the composite and interaction products in HCl 0.1 M (mean values ± s.d.; $n = 3$).

the composite (A), whereas it was presented in the corresponding physical mixture (B).

3.6. Intrinsic dissolution studies

Fig. 5 shows the release curves (mg released/cm^2 *vs* time) obtained from the interaction products (5-ASA/CS and 5-ASA/VHS) and composites (5-ASA/CS/VHS). The release profile of 5-ASA/VHS exhibited high initial burst effect and drug release was rapidly completed, because the matrices disintegrated in contact with the dissolution medium. 5-ASA/CS interaction products showed an almost linear release profile for the first 20 min of the test, after which progressive dissolution of the polymer in the medium lead to a drastic increase in the slope of the release profile, which became sigmoid, making it impossible to estimate with sufficient precision the rate of release of the drug by linear regression of the curve. In the composites the amount of drug released was slower compared both to 5-ASA/VHS and 5-ASA/CS interaction products, with an almost linear release profile throughout the entire test. The estimated values of intrinsic dissolution rate of the studied samples were in line with the release curves, following the trend 5-ASA/VHS > 5-ASA/CS > 5-ASA/CS/VHS (Table 3). 5-ASA/VHS matrices disintegrated very quickly and 5-ASA/CS matrices dissolved in acidic media in a short time, due to high solubility of the polymer in this medium. On the contrary, for the composites, the presence of chitosan prevented the disintegration of the matrix (Fig. 6). Moreover, the presence of the clay mineral reduced hydration of chitosan resulting in slower drug release compared to the polymer alone.

4. Conclusions

Composites of CS and VHS were prepared at 25 °C by simple solid–liquid interaction. The results confirmed the effective complexation of CS by the clay mineral. The interaction mechanism involved interlayer exchange of the polymer with the exchangeable cations of the clay mineral, followed by precipitation of CS on VHS surfaces. According to the loading results, there was a synergic effect between CS and VHS resulting in higher incorporation of 5-ASA in comparison to retention by free polysaccharide or clay mineral alone. Finally, in the composites drug release in acidic medium was slower compared both to 5-ASA/VHS and 5-ASA/CS interaction products, with an almost linear release profile throughout the test, suggesting encouraging possibilities as

Table 3
Intrinsic dissolution rate of the composite and interaction products (mean values ± s.d.; $n = 3$).

Composite	Release rate (mg/cm^2 min)	R^2
5-ASA/CS	0.247 ± 0.0157	0.9900
5-ASA/VHS	8.626 ± 0.0579	0.9990
5-ASA/CS/VHS	0.152 ± 0.0265	0.9970

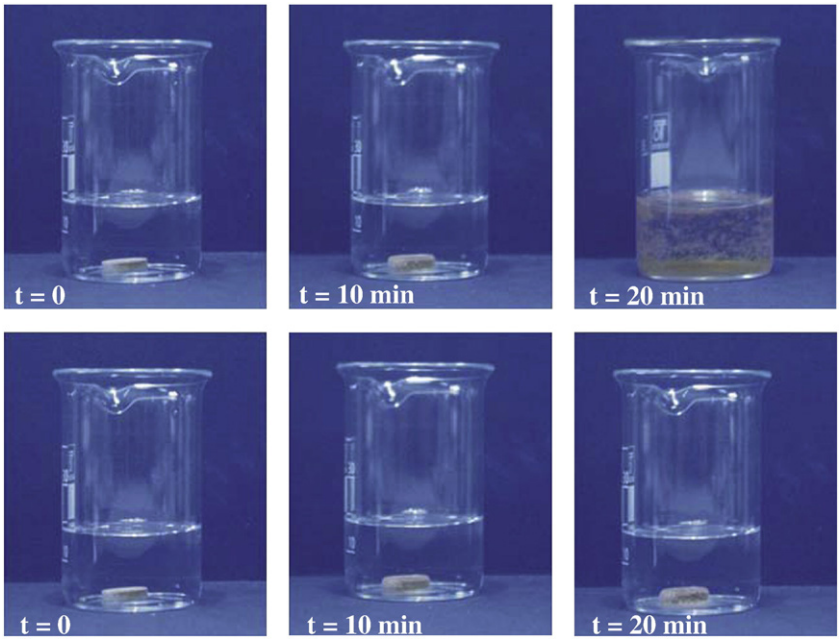

Fig. 6. Photographs of drug/clay mineral (top) and drug/chitosan–clay mineral (bottom) matrices in acidic medium at different hydration time intervals.

supports in modified release formulations. Further studies will attempt to fully characterize and improve these systems to verify their possibilities in modified drug delivery.

Acknowledgements

This research was financially supported by Research Project MAT2006-05231 (MEC, Spain). We thank Prof. Ian MacCandless (Department of English Philology, University of Granada, S) for assisting us with the English version of the text.

References

Baron, J.H., Connell, A.M., Lennard-Jones, J.E., Jones, F.A., 1962. Sulphasalazine and salicylazosulphadimidine in ulcerative colitis. Lancet 1, 1094–1096.
Cendrowska, I., Drewnowska, M., Grzeszkiewicz, A., Butkierwicz, K., 1990. Investigation of the stability of 5-aminosalicylic acid in tablets and suppositories by high-performance liquid chromatography. J. Chromatogr. 509, 195–199.
Chan, R.P., Pope, D.J., Gilbert, A.P., Sacra, P.J., Baron, J.H., Lennard-Jones, J.E., 1983. Studies of two novel sulfasalazine analogs, ipsalazide and balsalazide. Dig. Dis. Sci. 28, 609–615.
Chourasia, M.K., Jain, S.K., 2003. Pharmaceutical approaches to colon targeted drug delivery systems. J. Pharm. Pharmaceut. Sci. 6 (1), 33–66.
Clemett, D., Markham, A., 2000. Prolonged-release mesalazine. A review of its therapeutic potential in ulcerative colitis and Crohn's disease. Drugs 59 (4), 929–956.
Crotty, B., Jewel, J.P., 1992. Drug therapy of ulcerative colitis. Br. J. Clin. Pharmacol. 34, 189–198.
Darder, M., Colilla, M., Ruiz-Hitzky, E., 2003. Biopolymer — clay nanocomposites based on chitosan intercalated in montmorillonite. Chem. Mater. 15 (20), 3774–3780.
Darder, M., Colilla, M., Ruiz-Hitzky, E., 2005. Chitosan–clay nanocomposites: application as electrochemical sensors. Appl. Clay Sci. 28, 199–208.
Davaran, S., Hanaee, J., Khosravi, A., 1999. Release of 5-amino salicylic acid from acrylic type polymeric prodrugs designed for colon-specific drug delivery. J. Control. Release 58, 279–287.
Dew, M.J., Hughes, P.J., Lee, M.G., Evans, B.K., Rhodes, J., 1982. An oral preparation to release drugs in the human colon. Br. J. Clin. Pharmacol. 14, 405–408.
Dollery, C., 1991. Mesalazine. In: Sir Dollery, C. (Ed.), Therapeutic Drugs, vol. 1. Churchill Livingstone, London.
French, D.L., Mauger, J.W., 1993. Evaluation of the physicochemical properties and dissolution characteristics of mesalamine: relevance to controlled intestinal drug delivery. Pharm. Res. 10 (9), 1285–1289.
Friend, D.R., 2005. New oral delivery systems for treatment of inflammatory bowel disease. Adv. Drug Deliver. Rev. 57, 247–265.
Giles, C.H., Smith, D., Huitson, A., 1974. A general treatment and classification of the solute adsorption isotherm. I. Theoretical. J. Colloid Interface Sci. 47 (3), 755–765.
Günister, E., Pestreli, D., Ünlü, C.H., Atıcı, O., Güngör, N., 2007. Synthesis and characterization of chitosan–MMT biocomposite systems. Carbohydr. Polym. 67, 358–365.
Gupta, V.S., Beckert, T.E., Price, J.C., 2001. A novel pH- and time-based multi-unit potential colonic drug delivery system. I. Development. Int. J. Pharm. 213, 83–91.
Hardy, J.G., Harvey, W.J., Sparrow, R.A., Marshall, G.B., Steed, K.P., Macarios, M., Wilding, I.R., 1993. Localization of drug release sites from an oral sustained-release formulation of 5-ASA (Pentasa) in the gastrointestinal tract using gamma scintigraphy. J. Clin. Pharmacol. 33, 712–718.
Hiorth, M., Tho, I., Sande, S.A., 2003. The formation and permeability of drugs across free pectin and chitosan films prepared by a spraying method. Eur. J. Pharm. Biopharm. 56, 175–182.
ICH, 1995. International Conference on Harmonization of Technical Requirements for the Registration of Pharmaceuticals for Human Use. Validation of analytical procedures, Ginevra (CH).
Illum, L., 1998. Chitosan and its use as a pharmaceutical excipient. Pharm. Res. 15, 1326–1331.
Isaacs, K.L., Murphy, D., 1990. Pancreatitis after rectal administration of 5-aminosalicylic acid. J. Clin. Gastroenterol. 12, 198–199.
Khunawattanakul, W., Puttipipatkhachorn, S., Rades, T., Pongjanyakul, T., 2008. Chitosan–magnesium aluminum silicate composite dispersions: characterization of rheology, flocculate size and zeta potential. Int. J. Pharm. 351, 227–235.
Lorenzo-Lamosa, M.L., Remuñan-López, C., Vila-Jato, J.L., Alonso, M.J., 1998. Design of microencapsulated chitosan microspheres for colonic drug delivery. J. Control. Release 52, 109–118.
Macleod, G.S., Collett, J.H., Fell, J.T., 1999. The potential use of mixed films of pectin, chitosan and HPMC for bimodal drug release. J. Control. Release 58, 303–310.
Meshali, M.M., Gabr, K.E., 1993. Effect of interpolymer complex-formation of chitosan with pectin or acacia on the release behavior of chlorpromazine HCl. Int. J. Pharm. 89, 177–181.
Muraoka, M., Kimura, G., Zhaopeng, H., Takada, K., 1998. Ulcerative colitis colon delivery of 5-aminosalicylic acid. Nippon Rinsho. Jpn. J. Clin. Med. 56, 788–794.
Novis, B.H., Korsets, Z., Chen, P., 1988. Nephrotic syndrome after treatment with 5-aminosalicylic acid. Br. Med. J. 296, 1442.
Nunthanid, J., Luangtana-anan, M., Sriamornsak, P., Limmatvapirat, S., Huanbutta, K., Puttipipatkhachorn, S., 2009. Use of spray-dried chitosan acetate and ethylcellulose as compression coats for colonic drug delivery: effect of swelling on triggering in vitro drug release. Eur. J. Pharm. Biopharm. 71, 356–361.
Pongjanyakul, T., Suksri, H., 2009. Alginate–magnesium aluminum silicate films for buccal delivery of nicotine. Colloids Surf. B Biointerfaces 74, 103–113.
Pongjanyakul, T., Priprem, A., Puttipipatkhachorn, S., 2005. Investigation of novel alginate-magnesium aluminum silicate microcomposite films for modified-release tablets. J. Control. Release 107, 343–356.
Rudolph, M.W., Kleina, S., Beckertb, T.E., Petereitb, H.-U., Dressman, J.B., 2001. A new 5-aminosalicylic acid multi-unit dosage form for the therapy of ulcerative colitis. Eur. J. Pharm. Biopharm. 51, 183–190.
Sachedina, B., Saibil, F., Cohen, L.B., Whitley, J., 1989. Acute pancreatitis due to 5-amminosalicylate. Ann. Intern. Med. 110, 490–492.
Sinha, V.R., Kumria, R., 2001. Polysaccharides in colon-specific drug delivery. Int. J. Pharm. 224, 19–38.
Takeuchi, H., Yasuji, T., Yamamoto, H., Kawashima, Y., 2000. Spray-dried lactose composite particles containing an ion complex of alginate–chitosan for designing a

dry-coated tablet having a time-controlled releasing function. Pharm. Res. 17 (1), 94–99.
Tozaki, H., Komoike, J., Tada, C., Maruyama, T., Terabe, A., Suzuki, T., Yamamoto, A., Muranishi, S., 1997. Chitosan capsules for colon-specific drug delivery: improvement of insulin absorption from the rat colon. J. Pharm. Sci. 86, 1016–1021.
USP 32, 2009. United States Pharmacopoeia 32 and National Formulary 29. US Pharmacopoeial Convention, Rockville, MD (USA.
Varshosaz, J., Jaffarian Dehkordi, A., Golafshan, S., 2006. Colon-specific delivery of mesalazine chitosan microspheres. J. Microencapsul. 23 (3), 329–339.
Viseras, C., Aguzzi, C., Cerezo, P., Bedmar, M.C., 2008. Biopolymer-clay nanocomposites for controlled drug delivery. Mater. Sci. Technol. 24 (9), 1020–1026.
Wadworth, A.N., Fitton, A., 1991. Olsalazine. A review of its pharmacodynamic and pharmacokinetic properties, and therapeutic potential in inflammatory bowel disease. Drugs 41, 647–664.
Wang, S.F., Shen, L., Tong, Y.J., Chen, L., Phang, I.Y., Lim, P.Q., Liu, T.X., 2005. Biopolymer chitosan/montmorillonite nanocomposites: preparation and characterization. Polym. Degrad. Stab. 90, 123–131.
Wu, T.-M., Wu, C.-Y., 2006. Biodegradable poly (lactic acid)/chitosan-modified montmorillonite nanocomposites: preparation and characterization. Polym. Degrad. Stab. 91, 2198–2204.
Zhang, H.S., Neau, H., 2002. In vitro degradation of chitosan by bacterial enzymes from rat cecal and colonic contents. Biomaterials 23, 2761–2766.
Zhang, H., Alsarra, I.A., Neau, S.H., 2002. An in vitro evaluation of a chitosan-containing multiparticulate system for macromolecule delivery to the colon. Int. J. Pharm. 239, 197–205.

Applied Clay Science 55 (2012) 131–137

Contents lists available at SciVerse ScienceDirect

Applied Clay Science

journal homepage: www.elsevier.com/locate/clay

In vitro biocompatibility and mucoadhesion of montmorillonite chitosan nanocomposite: A new drug delivery

Inmaculada Salcedo [a], Carola Aguzzi [a,*], Giuseppina Sandri [b], Maria C. Bonferoni [b], Michela Mori [b], Pilar Cerezo [a], Rita Sánchez [a], César Viseras [a,c], Carla Caramella [b]

[a] Department of Pharmacy and Pharmaceutical Technology, School of Pharmacy, University of Granada, Campus of Cartuja, 18071 s/n, Granada, Spain
[b] Department of Pharmaceutical Sciences, School of Pharmacy, University of Pavia, viale Taramelli 12, 27100, Pavia, Italy
[c] Andalusian Institute of Earth Sciences, CSIC-University of Granada, School of sciences, Campus of Fuentenueva, 18002 s/n, Granada, Spain

ARTICLE INFO

Article history:
Received 4 February 2011
Received in revised form 20 July 2011
Accepted 8 November 2011
Available online 3 December 2011

Keywords:
Montmorillonite
Chitosan
Nanonanocomposites
Cell proliferation
Wound healing
Biocompatibility

ABSTRACT

A "Clay Bio Polymer Nanocomposite" (CBPN) to be used in drug release was prepared by dispersion of montmorillonite (Mt) particles in chitosan (Ch) solution. The obtained hybrid material was characterized for in vitro biocompatibility on Caco-2 cell cultures. Cytotoxicity and cell proliferation of the nanocomposite were tested, comparing results with free Ch and Mt. Cell proliferation was assessed both by WST-1 test and wound-healing measurements by means of Image Analysis Software. The last method is a proof of concept test that has the advantage of direct visualization and quantification of cell growth. Nanocomposite was also characterized for hydration (water uptake) pattern and mucoadhesive properties, which were considered as important features for the application of this material in modified release systems.
Results showed that the prepared CBPN showed good biocompatibility in the range 5–500 μg/ml, being also able to effectively stimulate cell proliferation. Moreover, nanocomposite possessed mucoadhesive properties combined with low solubility in acidic environment. We conclude that interaction between Ch and Mt produced a new biohybrid material that can be considered as promising candidate for modified drug delivery formulations.

1. Introduction

In the last decade, there has been growing interest in the development of nanocomposites between clay minerals and biopolymers for pharmaceutical applications (Viseras et al., 2008, 2010). These hybrid materials can combine the properties of both components (inorganic and organic), such as swelling, water uptake, mechanical characteristics, thermal behavior, rheology and bioadhesion (Pongjanyakul et al., 2005; Wu and Wu, 2006; Günister et al., 2007; Khunawattanakul et al., 2008; Pongjanyakul and Suksri, 2009, 2010). They could be formed from a variety of biopolymers and clay minerals. Among them, Mt/ch nanocomposites are receiving greater attention, especially for biomedical (tissue engineering) (Katti et al., 2008; Haroun et al., 2009; Verma et al., 2010) and biopharmaceutical (modified release) (Wang et al., 2007; Wang et al., 2009; Khunawattanakul et al., 2010; Nanda et al., 2011) applications.

Ch is a cationic copolymer formed by N-acetylglucosamine and D-glucosamine units, being obtained by the natural occurring polysaccharide chitin (Fig. 1). It is widely used in pharmaceutical field, because of its suitable characteristics, including chemical safety, biodegradability, biocompatibility, antibacterial activity and mucoadhesive properties (Illum, 1998).

Mt is a layered hydrated aluminum silicate whose unit cell is composed of one Al-octahedral sheet (O) sandwiched between two Si–tetrahedral sheets (T). It possesses a net negative charge due to isomorphous ionic substitutions in the T–O–T structure. This charge is compensated by interlayer hydrated cations, which can be exchanged by a variety of organic molecules (Bergaya et al., 2006; Aguzzi et al., 2007). In particular, ch chains have been described to intercalate with Na^+–Mt, because of their hydrophilic and cationic character, giving hybrid nanocomposite materials with interesting properties (Darder et al., 2003). Other works showed that the concentration of the clay mineral is a critical parameter in Mt/ch nanocomposites to achieve materials with enhanced properties (mechanical, thermal and/or electro-stimuli response) in comparison with the pure components (Wang et al., 2005; Xu et al., 2006; Liu et al., 2007). For example, nanocomposite hydrogels containing 2% (wt/wt) of Mt showed improved release behavior of vitamin B_{12}, compared with that of the pure Ch (Liu et al., 2008). Ratio between Mt and Ch was a crucial factor also in the case of nanocomposites prepared to control release of the chemotherapeutic agent doxorubicin (Yuan et al., 2010). pH-dependent release profiles were found for these nanocomposites, which were described as promising supports for colonic prolonged

* Corresponding author at: Departamento de Farmacia y Tecnología Farmacéutica, Facultad de Farmacia, Universidad de Granada, Campus de Cartuja, s/n, 18071 Granada, Spain. Tel.: +34 58 249551; fax: +34 58 248958.
E-mail address: carola@ugr.es (C. Aguzzi).

0169-1317/$ – see front matter © 2011 Elsevier B.V. All rights reserved.
doi:10.1016/j.clay.2011.11.006

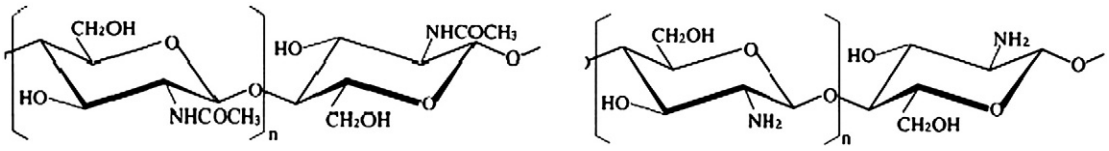

Fig. 1. Chemical structure of chitin (left) and Ch (right).

drug delivery. The majority of the studies are devoted to the physicochemical and biopharmaceutical characterisation of Mt/ch nanocomposites; however, their biocompatibility for drug release has been evaluated only by Depan et al. (2009).

In a previous work, a nanocomposite between Ch and Mt was prepared by simple solid–liquid interaction; the effective polymer/clay mineral complexation was confirmed by thermal analysis and slower drug release was observed in comparison with Ch and Mt alone (Aguzzi et al., 2010). In vitro biocompatibility was followed by cytotoxicity and cell proliferation in this paper, for further characterization. The effects of the nanocomposite were screened on Caco-2 cell cultures as a representative type of intestinal cells considering an oral administration and delivery. Cell proliferation was assayed by two different techniques: WST-1 test and wound-healing measurements. The last method has the advantage that allows a direct visualization of cell growth. Nanocomposites were also characterized for hydration (water uptake) pattern and mucoadhesive properties, which were considered as important features for the application of these materials in modified release systems.

2. Materials and methods

The polymer used was Ch base with low viscosity* (12 mPa *s) and deacetylation degree of 98% (Giusto Faravelli, Italy) (*Viscosity measurements were performed on 1% (w/v) solutions in HCl 0.1M at 90 1/s with rotational rheometer equipped with coaxial cylinders C14 (Bohlin CS, Bohlin Instrument Division, Metrics Group Ltd., Cirencester, UK). Ch acetate was used as control in cell experiments. It was obtained by dissolving Ch base in aqueous acetic acid (1% vol/vol) and freeze drying (Edwards mod RV8) the polymer obtained solution.

The clay mineral was a marketed pharmaceutical-grade Mt (Veegum HS©), kindly gifted by Vanderbilt Company S.A. (USA).

Ch and Mt powders were pulverized in a ball miller (IG.W2/E, Giuliani, Italy) and then sieved to separate a rigorous size fraction (45–75 μm) to limit variability of the data. The selected fraction was kept in a desiccator until required.

2.1. Preparation of chitosan/clay mineral nanocomposite

Mt/ch nanocomposite was prepared following Aguzzi et al. (2010). Briefly, Ch was dissolved in aqueous acetic acid (1% vol/vol) at the concentration of 1% (wt/vol). Then, Mt was added to the polymer solution in the wt:wt ratio (2:1 Ch:Mt) corresponding to their maximum binding capacity, as calculated by interaction isotherms. Dispersion was stirred by a magnetic bar for 48 h at room temperature, washed with distilled water and then freeze dried. The product obtained was milled and sieved to select the size fraction between 45 and 75 μm.

2.2. Water uptake measurements

Water uptake experiments were carried out using a modified Enslin apparatus (Ferrari et al., 1991). Measurements were performed on 20 mg of nanocomposite, in acidic medium (0.1 M HCl) for 2000 s. For comparison, measurements were also performed on pure Ch and clay mineral powders, at the same granulometric fraction as the nanocomposite. Powders were laid on dialysis membrane discs (cut off 14,000 Da), which were placed on the sample holder of the apparatus to retain dissolved Ch molecules and avoid sample mass lost. Membranes alone were used for blank measurements. Six replicates were performed on each sample.

2.3. Mucoadhesion measurements

Mucoadhesive properties were investigated by TA-XT2 Plus Texture Analyser (Stable Micro Systems, Enco, Italy) using porcine gastric mucin (Type II) (Sigma, Italy) as biological substrate. 40 mg of samples were hydrated in pH 5.0 phosphate buffer (European Pharmacopeia (EP) 6.0) and then laid on a filter paper fixed with double sided adhesive tape on the bottom of the upper probe of the apparatus. 30 μl of an 8% (wt/wt) mucin dispersion in phosphate buffer pH 7 (EP 6.0) were applied on a filter paper disc (diameter = 10 mm), fixed in the lower probe of the apparatus and faced to the sample. The upper probe with the sample was lowered at a speed of 1.0 mms^{-1} onto the surface of the lower probe and a downward force (preload) of 2500 mN was applied for 1 min to ensure intimate contact between the sample and the mucin dispersion and to allow the formation of the mucoadhesive joints. After a 1 min rest, the upper probe was moved upwards at a constant speed of 4.0 mms^{-1} until the complete separation of the two surfaces occurred. The detachment force (mN) and the adhesive work (calculated from the area under the force–distance curve, AUC ($mN*s$) were recorded and simultaneously collected on a personal computer (Texture Exponent Software 32, Stable Microsystem, Enco, Italy). Blank measurements were performed using phosphate buffer pH 7 instead of the mucin suspension.

The normalized mucoadhesion parameter (ΔAUC/AUC) was calculated according to the following equation (Ferrari et al., 1997):

$$\Delta AUC/AUC = (AUC_m - AUC_{blank})/AUC_{blank}$$

where AUC_m is the work of adhesion obtained in presence of mucin and AUC_{blank} is the work of adhesion obtained by the blank. Such normalization allowed comparing the mucoadhesive properties of samples characterised by different cohesive properties (viscosity) (Ferrari et al., 1997). Eight replicates were performed on each sample.

2.4. Cell cultures

Human colorectal adenocarcinoma cell lines (Caco-2) were obtained from the American Type Culture Collection (ATCC, USA). Cells were grown at 37 °C, 5% CO_2 atmosphere (PBIinternational, Italy) in pH 7.4 Dulbecco's Modified Eagle's Medium (DMEM) (Lonza, Italy) containing 20% vol/vol heat inactivated Fetal Bovine Serum (FBS) (Euroclone, Italy), penicillin (100 IU/ml), streptomycin (0.1 mg/ml) and 1% vol/vol non essential aminoacids (Sigma Aldrich, Italy). The culture medium was changed twice weekly during maintenance.

2.4.1. Cell viability measurements

Cell viability was estimated by the (4-(3-(4-Iodophenyl)-2-(4-nitrophenyl)-2H-5-tetrazolio)-1,3-benzene disulfonate) (WST-1) assay (Roche Diagnostics GmbH, Roche Molecular Biochemicals, Bioidea, Italy). This reagent is metabolically reduced mainly by mitochondria in viable cells to a water soluble formazan product, allowing direct absorbance measures after experiments (Ishiyama et al., 1996).

Confluent Caco-2 cells (70–90% confluence) were plated with the above described medium in 96-well plates (growth area 0,36 cm^2, Greineger Bio-one, PBI International, Italy) at a density of 1×10^5 cells/cm^2 and cultured for 24 h (37 °C, 5% CO_2). Then, the medium was removed and 200 μl of nanocomposite dispersions at three different concentrations (5, 50, 500 μg/ml in medium without serum) were added to each well. For comparison, experiments were also done on Ch and clay mineral alone, at the same concentrations as the nanocomposites (Table 1). Complete medium and Triton®X100 (Fluka, Italy) were used as positive and negative controls, respectively.

The plates were then incubated (37 °C, 5% CO_2) for different times, before being subjected to the WST-1 assay. The incubation time was 3 h for cytotoxicity and 24 h for cell proliferation assays. Subsequently, the medium was replaced by 100 μl of WST-1 10% v/v in HBSS ("Hanks' balanced salt solution") pH 7.4 and incubated for 3 h. At the end of the tests, the absorbance was assayed by using ELISA plate reader (iMark™ Microplate Absorbance Reader mod. 550, Bio-Rad, Italy) equipped with mechanical plate shaker at 450 nm wavelength with a reference wavelength of 650 nm. The data were expressed as the mean percentage of viable cells as compared to the respective control (untreated cultures).

2.4.2. Wound-healing measurements

Wound-healing measurements were performed to directly evaluate cell proliferation. Experiments were carried out using a μ-Dish (Ibidi, Giardini, Italy) with an insert which delineates two distinct growth areas (growth area 2×0.22 cm^2) (Fig. 2). Caco-2 cells were seeded at 10^5 cells/cm^2 in each chamber (seeding volume of 70 μl) grown to confluence. After removal of the insert a cell free gap ("wound") (500 μm ± 50 μm) remained. Cells were put in contact with 500 μl of medium without serum containing nanocomposite (50 μg/ml), with corresponding concentrations of free Ch and clay mineral. Dishes were re-incubated over a total period of 72 h. The growth of cells over each sample was investigated by taking photographs after fixed times (24, 48 and 72 h) using an inverted microscope (PBIinternational, Italy) at a magnification of 250× and the size of the gap between the chambers was taken as a measure of cell proliferation as a function of time. The digitalized images were elaborated by a suitable software (UTHSCSA Image Tool version 3.00, The University of Texas Health Science Center, USA), that allowed to measure the area left by the cell growth at each time. The % of wound areas at different times were calculated considering 100 the mean area measured for each sample at time zero. At least three different pictures were analyzed for each sample and each time.

2.4.3. Statistical analysis

One-way analysis of variance (ANOVA) with the post hoc Sheffé test for multiple comparisons was performed using the software Siphar 4.0 (France). The comparison of two groups (t Student test) was performed with Statgraphics® 5.0 statistical package (Statistical Graphics Corporation, Rockville, MD, USA). Differences between groups were considered to be significant at a level of P less than 0.05.

Table 1
Concentration of the samples for cell cultures studies.

Sample	Concentration (μg/ml)
Mt/ch	Low: 5 Medium: 50 High: 500
Ch	Low: 3.3 Medium: 33.3 High: 333
Mt	Low: 1.67 Medium: 16.7 High: 167

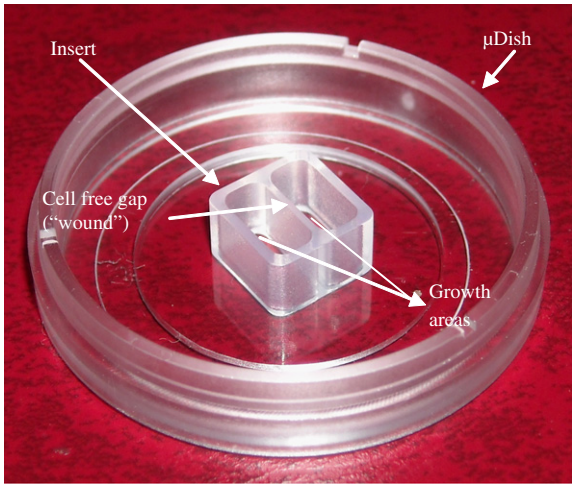

Fig. 2. Culture inserts used for wound-healing measurements.

3. Results and discussion

3.1. Water uptake measurements

Fig. 3 shows the water uptake profiles of nanocomposite (Mt/ch) and free components (Ch base and Mt) in 0.1 M HCl. As observed the behavior of the clay mineral was different from that of the pure polymer. Mt immediately levelled off in a plateau, whereas Ch hydrated gradually, due to the progressive formation of the corresponding soluble hydrochloride salt in contact with the medium. After 20 min (1200 s) approximately, the polymer was fully hydrated and the total amount of medium absorbed was 11.5 g/g dry polymer, that is, significantly higher ($P<0.001$, one-way ANOVA, post hoc Scheffé test) than the amount absorbed by the clay mineral. Nanocomposite achieved final amount absorbed of about 9 g/g. Data were normalized as a function of the actual amount of Ch present in the Mt/ch nanocomposite. The water uptake profile seemed have the same pattern of that of Mt, indicating that the solubility of the polymer in 0.1 M HCl was reduced by the presence of the clay mineral. Since drug release is strictly related with hydration, this result corroborated the hypothesis postulated in a previous work, where drug release from Mt/ch nanocomposite in acidic medium was lower than the observed with Ch alone (Aguzzi et al., 2010).

3.2. Mucoadhesive properties

Mucoadhesion measurements followed the trend Ch > nanocomposite > clay mineral. Ch was characterized by the highest

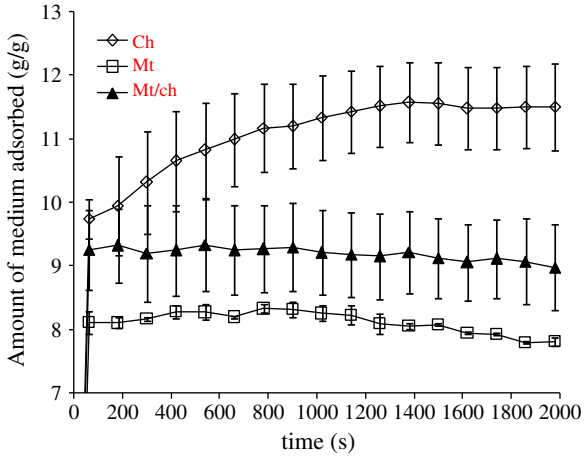

Fig. 3. Water uptake profiles of the samples in 0.1 M HCl (mean values ± s.e.; n = 6).

mucoadhesive potential (2.75 ± 0.10). In fact it is known that Ch possesses mucoadhesive properties, due to the presence of many amino groups in the polymer chains that form hydrogen bonds with glycoproteins in the mucus (Lim et al., 2000) and also ionic interactions between positively charged animogroups and negatively charged sialic acid residues of mucin. Clay mineral was also able to interact with the mucin, although the normalized mucoadhesion parameter (0.71 ± 0.03) was significantly lower compared with Ch ($p<0.001$, one-way ANOVA post hoc Scheffé test). Nanocomposite showed an intermediate behavior (0.85 ± 0.03). Probably, in the nanocomposite the mobility of the polymer chains was reduced by the interaction of the clay mineral, reducing contact/interpenetration with the substrate. A similar behavior was observed by other authors, studying bioadhesion of nanocomposite between alginate and other kind of layered clay mineral (Pongjanyakul and Suksri, 2009).

3.3. Cell viability

In Fig. 4a, cell viability over each sample after 3 h of incubation is given. At the concentrations studied, Ch and nanocomposite did not significantly reduce cell viability compared with the blank (culture medium without serum), indicating good biocompatibility properties for these materials. However, in the case of clay mineral at high concentration a significant reduction of cell viability ($p<0.001$, one-way ANOVA post hoc Scheffé test) was observed. This effect was observed by other authors: they suggested that high amounts of clay particles could block the most of the channels on cell membranes, causing the cell death (Wang et al., 2008).

Fig. 4b refers to cell viability obtained after 24 h of incubation with nanocomposite and pure components. For all the samples at all the concentrations considered the viability values were comparable or higher than that of the blank (culture medium without serum). In the case of Ch, viability increased progressively with increasing polymer concentration, compared to the blank. It is known that Ch chains can enhance cell growth both because of their capacity to adhere to the (negatively charged) cell membranes (Wang et al., 2010) and their ability to bind serum factors, such as growth factors (Howling et al., 2001). Clay mineral also increased cell viability at low and intermediate concentrations, reaching values significantly ($p<0.05$, one-way ANOVA post hoc Scheffé test) higher than the obtained with Ch at the same concentration. It could be suggested that a limited

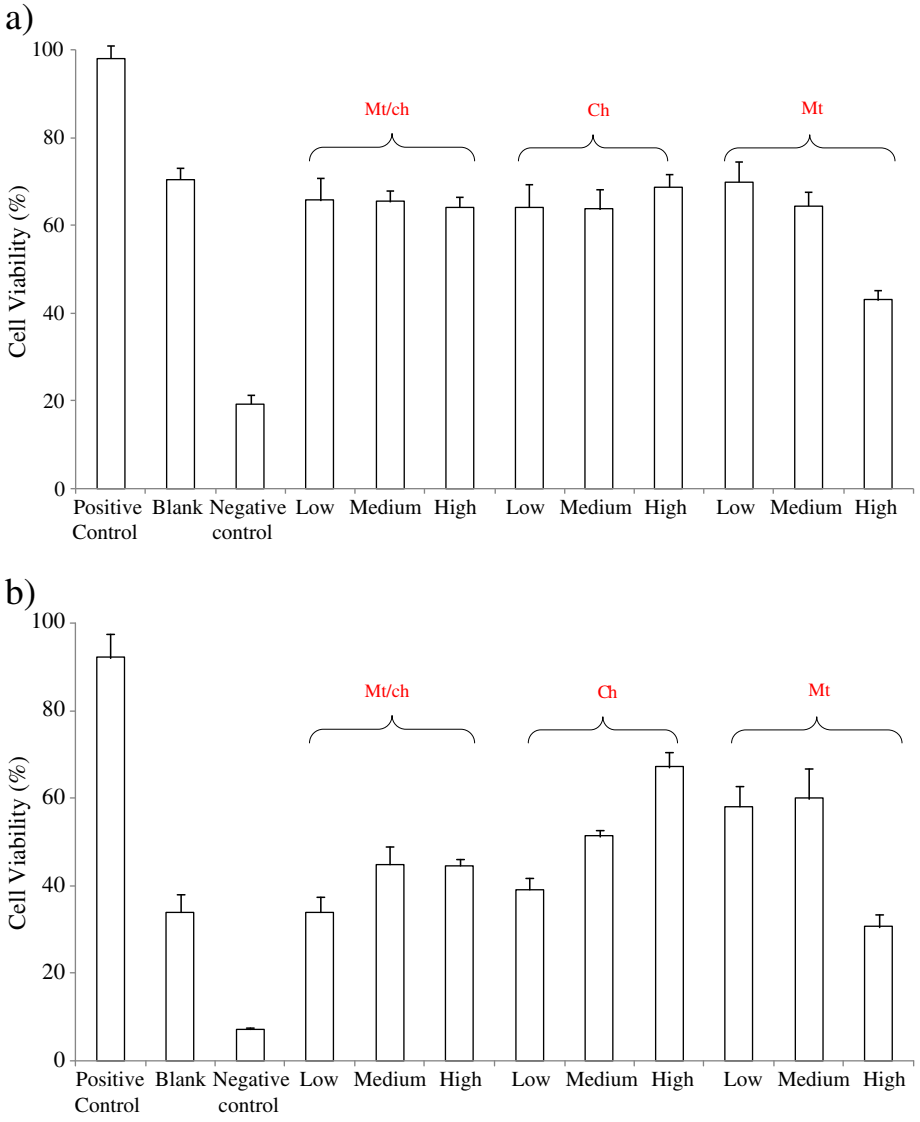

Fig. 4. Cell viability after 3 h (a) and 24 h (b) of incubation with the samples studied. Positive control: untreated cells in complete medium; blank: untreated cells in medium without serum; negative control: Triton®X100 (Fluka, Italy). See Table 1 for the meaning of the sample concentrations (low, medium, high) (mean values ± s.e.; n = 8).

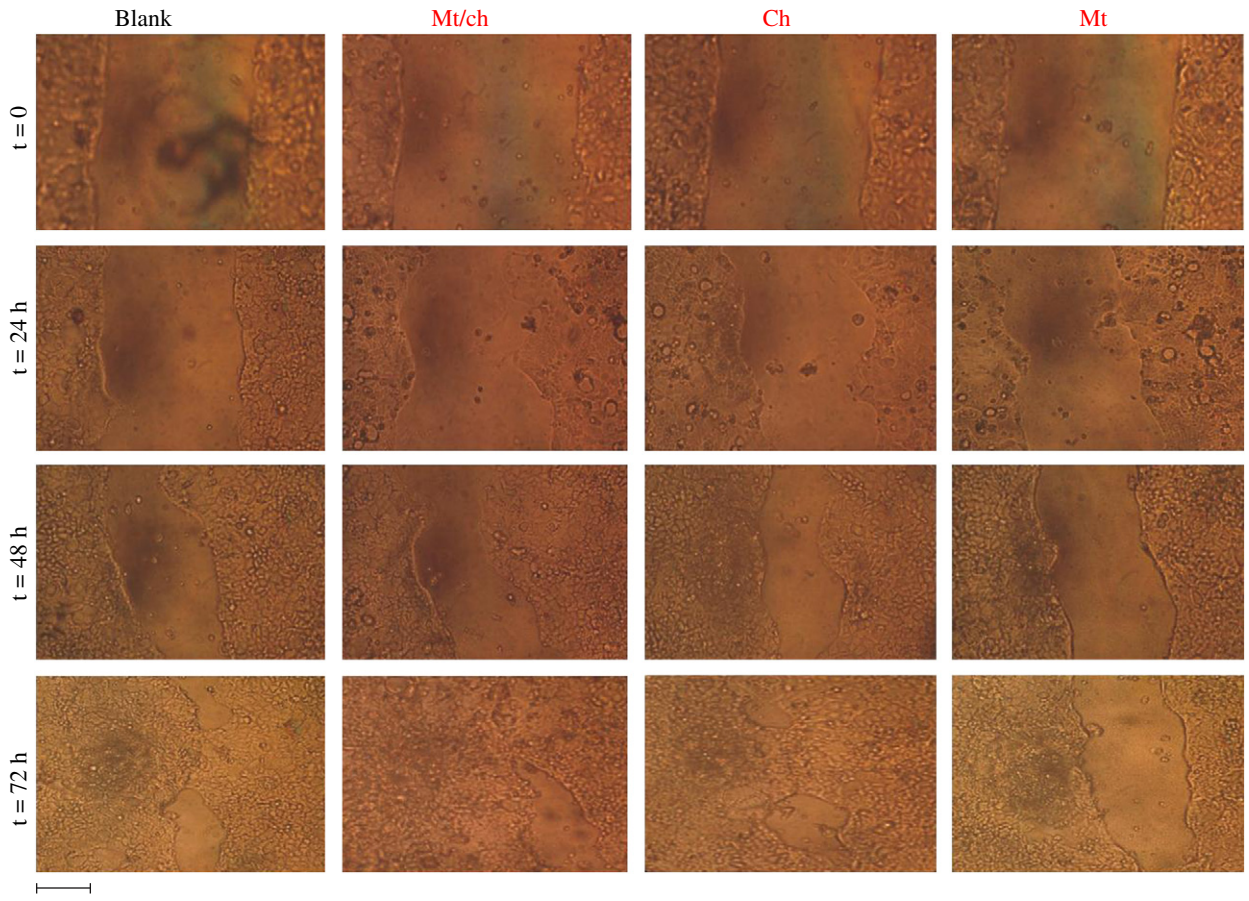

Fig. 5. Photographs of cell cultures from wound-healing test (bar is 200 μm).

amount of clay mineral particles might be engulfed by the cells through endocytosis, resulting in increased mitochondrial activity, rather than in effective cell proliferation activity (Lin et al., 2006; Wang et al., 2008). At higher concentrations, cell viability was reduced in line with the aforementioned observed results (Fig. 4a). The nanocomposite partially reflected the behavior of the free components. Cell viability increased with increasing nanocomposite concentration from low to intermediate level. However, at higher concentrations cell viability did not further increase, showing an intermediate value between Ch and Mt.

3.4. Wound-healing measurements

Wound-healing measurements were done in order to verify the results of cell proliferation obtained by WST-1 test. These measurements allowed a direct observation of cell growth, excluding possible misunderstandings in the interpretation of WST-1 test. Experiments were performed on nanocomposite and free components at the intermediate concentration, where WST-1 test revealed an increase in cell proliferation for all the samples studied, compared with the blank.

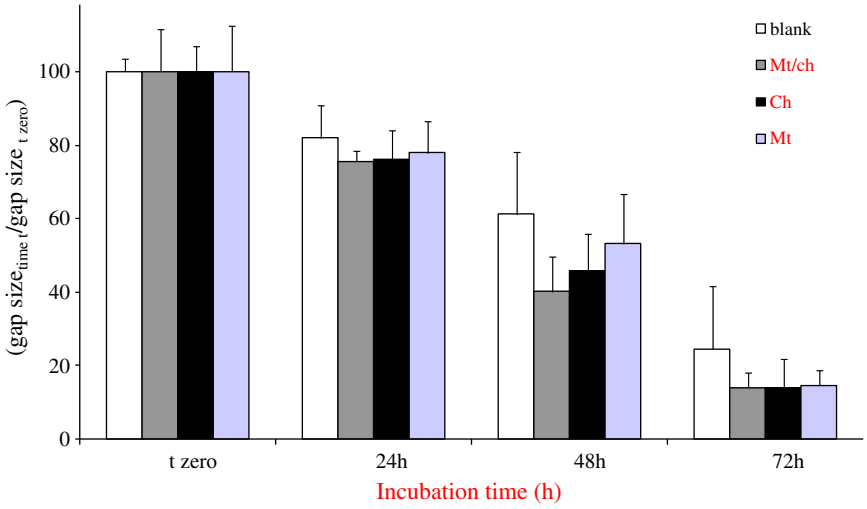

Fig. 6. Gap reduction after different incubation times (mean values ± s.e.; n = 3–5).

In Fig. 5 photographs of cell cultures after different incubation times are given, showing the progression of the gap over each sample as a function of time. Results were expressed as average percentage of gap size after established times compared to time zero, as it is shown in Fig. 6. At time zero, gap's size was in all cases the maximum allowed (assumed 100%). For each sample there was a significant total effect of time in the reduction of wound area in the range 0–72 h ($p<0.001$, one-way ANOVA). When comparison of two samples was performed (considering subsequent time intervals for each sample), in almost all cases the differences of area at different times were still significant at a 95% level. The results of these comparisons are given in Table 2, where the p values of statistical evaluation performed are reported. As for blank sample, the area reduction was not significant for the comparison between 24 and 48 h indicating a slow proliferation at early time. As for the Mt/ch nanocomposite and Ch, the area reduction was significant at all times, indicating a constant and progressive reduction of wound area, faster than that determined for blank sample. As for Mt sample, the reduction of the wound area was significant only between 48 and 72 h, indicating also in this case a slower proliferation as that of blank and corroborating that the previously observed augment in cell viability (WST-1 test at 24 h) might be due to an increase in mitochondrial activity, induced by the cellular uptake of the clay particles. It is known that in endocytosis processes, mitochondria provide the necessary energy (trapped in ATP) for vesicular transport and for the processing of lysosomal enzymes in the endoplasmic reticulum and Golgi apparatus (Nelson et al., 2008).

These results indicated that the Caco-2 growth rate was predominantly enhanced by the nanocomposite and Ch. The observed area reduction also suggested an effective stimulation of cell growth by Ch (as previously described in literature (Howling et al., 2001; Wang et al., 2008)) and nanocomposite. According to Lavie and Stotzky (1986) montmorillonite may develop London–van der Waals forces and hydrogen bonding with cells, promoting cell adhesion that, in nanocomposite, should allow Ch to enhance cell growth.

For each time there was not a significant effect of sample in the reduction of wound area (one-way ANOVA). When comparison of two samples was performed the only significant difference that could be evidenced was between blank and nanocomposite at 48 h ($p<0.05$). At 24 h all samples presented an area of 80% with respect to the initial value, without significant differences between samples (one-way ANOVA). At 48 h the wound area ranged between 40% (Mt/ch) and about 60% for blank with intermediate values for the other samples. After 72 h, in all cases the wound area was reduced to less than 20% of the initial area.

4. Conclusions

According to the results, the prepared Mt/ch nanocomposite possessed mucoadhesive properties combined with lower hydration properties in acidic environment compared with pure Ch.

From cell cultures experiments, Ch and nanocomposite showed good biocompatibility on Caco-2 cells in the concentration range studied (5–500 μg/ml). Nanocomposite and Ch also exhibited a progressive reduction in wound area, indicating an effective stimulation of Caco-2 proliferation by these samples.

We conclude that a new biohybrid material was produced by interaction between Ch and Mt, showing promising properties for pharmaceutical applications, especially for designing of modified drug delivery systems.

Table 2
p value obtained for two sample comparison of groups at different times (t Student).

Time (h)	Blank	Mt/ch	Ch	Mt
0–24	0.013	0.003	0.008	0.063
24–48	0.118	<0.001	0.003	0.053
48–72	0.037	0.004	0.019	0.032
0–48	0.004	<0.001	<0.001	0.011
0–72	<0.001	<0.001	<0.001	0.003
24–72	0.007	<0.001	<0.001	0.002

p value considered significant below 0.05.

Acknowledgments

The authors wish to thank the “Abroad Mobility Stage “José Castillejo” for young phDs” for financially supporting the work through the “National Programme of Mobility of Human Resources and Research” (Spain).

References

Aguzzi, C., Cerezo, P., Viseras, C., Caramella, C., 2007. Use of clays as drug delivery systems: possibilities and limitations. Appl. Clay Sci. 36, 22–36.
Aguzzi, C., Capra, P., Bonferoni, C., Cerezo, P., Salcedo, I., Sánchez, R., Caramella, C., Viseras, C., 2010. Chitosan silicate bionanonanocomposites for colonic delivery of 5-aminosalicylic acid (5-ASA). Appl. Clay Sci. 50, 106–111.
Bergaya, F., Theng, B.K.G., Lagaly, G., 2006. Handbook of Clay Science. Elsevier, Amsterdam.
Darder, M., Colilla, M., Ruiz-Hitzky, E., 2003. Biopolymer–clay nanonanonanocomposites based on chitosan intercalated in montmorillonite. Chem. Mater. 15 (20), 3774–3780.
Depan, D., Kumar, A.P., Singh, R.P., 2009. Cell proliferation and controlled drug release studies of nanohybrids based on chitosan-g-lactic acid and montmorillonite. Acta Biomater. 5, 93–100.
Ferrari, F., Rossi, S., Bertoni, M., Caramella, C., Geddo, M., 1991. Modelling of water penetration into fast disintegrating tablets. STP Pharma Sci. 1 (2), 137–144.
Ferrari, F., Rossi, S., Martini, A., Muggetti, L., De Ponti, R., Caramella, C., 1997. Technological induction of mucoadhesive properties on waxy starches by grinding. Eur. J. Pharm. Sci. 5, 277–285.
Günister, E., Pestreli, D., Ünlü, C.H., Atıcı, O., Güngör, N., 2007. Synthesis and characterization of chitosan–MMT bionanocomposite systems. Carbohydr. Polym. 67, 358–365.
Haroun, A.A., Gamal-Eldeen, A., Harding, D.R.K., 2009. Preparation, characterization and in vitro biological study of biomimetic three-dimensional gelatin–montmorillonite/cellulose scaffold for tissue engineering. J. Mater. Sci. Mate. Med. 20, 2527–2540.
Howling, G.I., Dettmar, P.W., Goddard, P.A., Hampson, F.C., Dornish, M., Wood, E.J., 2001. The effect of chitin and chitosan on the proliferation of human skin fibroblasts and keranocytes in vitro. Biomaterials 22, 2959–2966.
Illum, L., 1998. Chitosan and its use as a pharmaceutical excipient. Pharm. Res. 15, 1326–1331.
Ishiyama, M., Tominada, H., Shiga, M., Sasamoto, K., Ohkura, Y., Ueno, K., 1996. The combined assay of cell viability and in vitro toxicity with a high water-soluble tetrasolium salt, neutral red and crystal violet. Biol. Pharm. Bull. 19, 1518–1520.
Katti, K.S., Katti, D.R., Dash, R., 2008. Synthesis and characterization of a novel chitosan/montmorillonite/hydroxyapatite nanonanocomposite for bone tissue engineering. Biomed. Mater. 3 034122 (12 pp).
Khunawattanakul, W., Puttipipatkhachorn, S., Rades, T., Pongjanyakul, T., 2008. Chitosan–magnesium aluminum silicate nanocomposite dispersions: characterization of rheology, flocculate size and zeta potential. Int. J. Pharm. 351, 227–235.
Khunawattanakul, W., Puttipipatkhachorn, S., Rades, T., Pongjanyakul, T., 2010. Chitosan-magnesium aluminium silicate nanonanocomposite films: physicochemical characterization and drug permeability. Int. J. Pharm. 393, 219–229.
Lavie, S., Stotzky, G., 1986. Adhesion of the clay minerals montmorillonite, kaolinite, and attapulgite reduces respiration of histoplasma capsule. Appl. Environ. Microbiol. 51, 65–73.
Lim, S.T., Martin, G.P., Berry, D.J., Brown, M.B., 2000. Preparation and evaluation of the in vitro drug release properties and mucoadhesion of novel microspheres of hyaluronic acid and chitosan. J. Control. Release 66, 281–292.
Lin, F.-H., Chen, C.-H., Cheng, W.T.K., Kuo, T.-F., 2006. Modified montmorillonite as vector for gene delivery. Biomaterials 27, 3333–3338.
Liu, K.-H., Liu, T.-Y., Chen, S.-Y., Liu, D.-M., 2007. Effect of clay content on electrostimulus deformation and volume recovery behavior of a clay–chitosan hybrid nanocomposite. Acta Biomater. 3, 919–926.
Liu, K.-H., Liu, T.-Y., Chen, S.-Y., Liu, D.-M., 2008. Drug release behavior of chitosan–montmorillonite nanonanocomposite hydrogels following electrostimulation. Acta Biomater. 4, 1038–1045.
Nanda, R., Sasmal, A., Nayak, P.L., 2011. Preparation and characterization of chitosan–polylactide nanonanocomposites blended with Cloisite 30B for control release of the anticancer drug paclitaxel. Carbohydr. Polym. 83, 988–994.
Nelson, D.L., Lehinger, A.L., Cox, M.M., 2008. Principles of Biochemistry, 5th ed. Freeman, New York.
Pongjanyakul, T., Priprem, A., Puttipipatkhachorn, S., 2005. Investigation of novel alginate-magnesium aluminum silicate micronanocomposite films for modified-release tablets. J. Control. Release 107, 343–356.

Pongjanyakul, T., Suksri, H., 2009. Alginate-magnesium aluminum silicate films for buccal delivery of nicotine. Colloids Surf. B Biointerfaces 74, 103–113.
Pongjanyakul, T., Suksri, H., 2010. Nicotine-loaded sodium alginate–magnesium aluminum silicate (SA–MAS) films: importance of SA–MAS ratio. Carbohydr. Polym. 80, 1018–1027.
Verma, D., Katti, K.S., Katti, D.R., 2010. Osteoblast adhesion, proliferation and growth on polyelectrolyte complex–hydroxyapatite nanonanonanocomposites. Phil. Trans. R Soc. A 368, 2083–2097.
Viseras, C., Aguzzi, C., Cerezo, P., Bedmar, M.C., 2008. Biopolymer–clay nanonanonanocomposites for controlled drug delivery. Mater. Sci. Technol. 24 (9), 1020–1026.
Viseras, C., Cerezo, P., Sanchez, R., Salcedo, I., Aguzzi, C., 2010. Current challenges in clay minerals for drug delivery. Appl. Clay Sci. 48, 291–295.
Wang, S., Shen, L., Tong, Y.J., Chen, L., Phang, I.Y., Lim, P.Q., Liu, T.X., 2005. Biopolymer chitosan/montmorillonite nanonanonanocomposites: preparation and characterization. Polym. Degrad. Stabil. 90, 123–131.
Wang, X., Du, Y., Luo, J., Lin, B., Kennedy, J.F., 2007. Chitosan/organic rectorite films: structure, characteristic and drug delivery behavior. Carbohydr. Polym. 69, 41–49.
Wang, X., Du, Y.M., Luo, J., 2008. Biopolymer/montmorillonite nanonanocomposite: preparation, drug-controlled release property and cytotoxicity. Nanotechnology 19 065707 (7 pp).
Wang, Q., Zhang, J., Wang, A., 2009. Preparation and characterization of a novel pH-sensitive chitosan-g-poly(acrylic acid)/attapulgite/sodium alginate nanocomposite hydrogel bead for controlled release of diclofenac sodium. Carbohydr. Polym. 78, 731–737.
Wang, X., Liu, B., Ren, J., Liu, C., Wang, X., Wu, J., Sun, R., 2010. Preparation and characterization of new quaternized carboxymethyl chitosan/rectorite nanonanocomposite. Nanonanocomposites Science and Technology 70, 1161–1167.
Wu, T.M., Wu, C.Y., 2006. Biodegradable poly(lactic acid)/chitosan-modified montmorillonite nanonanonanocomposites: preparation and characterization. Polym. Degrad. Stabil. 91, 2198–2204.
Xu, Y., Ren, X., Milford, A., 2006. Chitosan/clay nanonanocomposite film preparation and characterization. J. Appl. Polym. Sci. 99, 1684–1691.
Yuan, Q., Shah, J., Hein, S., Misra, R.D.K., 2010. Controlled and extended drug release behavior of chitosan-based nanoparticle carrier. Acta Biomater. 6, 1140–1148.